

Abu Zahrim Yaser *Editor*

# Advances in Waste Processing Technology

 Springer

# Advances in Waste Processing Technology

Abu Zahrim Yaser  
Editor

# Advances in Waste Processing Technology

 Springer

*Editor*

Abu Zahrim Yaser  
Faculty of Engineering  
Universiti Malaysia Sabah  
Kota Kinabalu, Sabah, Malaysia

ISBN 978-981-15-4820-8                      ISBN 978-981-15-4821-5 (eBook)  
<https://doi.org/10.1007/978-981-15-4821-5>

© Springer Nature Singapore Pte Ltd. 2020

This work is subject to copyright. All rights are reserved by the Publisher, whether the whole or part of the material is concerned, specifically the rights of translation, reprinting, reuse of illustrations, recitation, broadcasting, reproduction on microfilms or in any other physical way, and transmission or information storage and retrieval, electronic adaptation, computer software, or by similar or dissimilar methodology now known or hereafter developed.

The use of general descriptive names, registered names, trademarks, service marks, etc. in this publication does not imply, even in the absence of a specific statement, that such names are exempt from the relevant protective laws and regulations and therefore free for general use.

The publisher, the authors and the editors are safe to assume that the advice and information in this book are believed to be true and accurate at the date of publication. Neither the publisher nor the authors or the editors give a warranty, expressed or implied, with respect to the material contained herein or for any errors or omissions that may have been made. The publisher remains neutral with regard to jurisdictional claims in published maps and institutional affiliations.

This Springer imprint is published by the registered company Springer Nature Singapore Pte Ltd. The registered company address is: 152 Beach Road, #21-01/04 Gateway East, Singapore 189721, Singapore

*This book is dedicated to my beloved children: A'ishah, Anas and Asma. Your love and smile make me stronger.*

# Foreword

This book compiles the latest advances in technologies for liquid and solid waste treatments. Due to increasing development as well as human population, waste generation keeps increasing and waste characteristics have evolved to be more complex, involving many more manmade chemicals. Thus scientists and engineers face greater challenges to solve the escalating problems, while trying to accommodate solutions to global warming, circular economy, etc.

At this opportunity, I would like to congratulate Dr. Abu Zahrim as editor of this book, and the dedicated authors for the timely publishing the important findings on waste processing. Dr. Abu Zahrim was working with me on palm oil mill sludge processing and effluent treatment at the National University of Malaysia (UKM) from August 2000, before joining Universiti Malaysia Sabah (UMS) in April 2005, where he continued his research explorations.

Several types of liquid and solid wastes, typically found in Malaysia and Indonesia have been covered; they include those from agroindustries, petrochemical industry, and domestic wastes. These industries cover various domestic and export products, including those for automotive, electrical and electronics, pharmaceuticals and construction. Drastic economic development, coupled with rising commercialization and urbanisation in this region has resulted in large and increasing amounts of food wastes and other domestic wastes: an estimated 15,000 tons of food wastes are discarded daily in Malaysia, and this is an opportunity to produce useful resources from the large tonnage. Research would enable higher added value products to be produced from them, such as high value proteins.

Towards high value products or materials from wastes, several advanced topics have been discussed in this book, namely, genetic algorithm, nanofibre, micromixing, and microwave technology. These would hopefully be used in other areas in future. In complex systems, Genetic Algorithm (GA), has been shown to have great potential for finding effective solutions. Due to their effectiveness in

smaller sizes, nanofibre and micromixing are being studied in various waste processing applications. Apart from their effectiveness and lower costs, the above technologies will open up new opportunities when dealing with complex and more abundant wastes in the future, to convert them to useful raw materials and products.



Bangi, Malaysia

Prof. Emeritus Dr. Rakmi Abd. Rahman

# Acknowledgements

The editor gratefully acknowledges the following individuals for their time and efforts in assisting the editor with the reviewing of manuscript. This book would not have been possible without the commitment of the reviewers.

- Abdul Aziz Abdul Raman
- Ahmad Fatzilah Misman
- Ali Chekima
- Asmadi Ali
- Duduku Krisnaiah
- Faiezah Hashim
- Fazilah Ariffin
- Husnul Azan Tajarudin
- Juraidah Ahmad
- Khairul Fikri Tamrin
- Mohamed Hasnain Isa
- Mohd Rakib Mohd Rashid
- Muhammad Roil Bilad
- Norazwina Zainol
- Nur Izzi Md. Yusoff
- Nurzaida Zahari
- Yasmin Che Ani
- Zulsyazwan Ahmad Khushairi

Special thanks to the 26th Regional Symposium on Chemical Engineering (RSCE 2019) committee especially Prof. Ir. Dr. Mohd Azlan Hussain for suggesting few papers from the conference to be included in this book.



# Contents

<b>A Review of Enhanced Micromixing Techniques in Microfluidics for the Application in Wastewater Analysis</b> .....	1
F. Mahmud, K. F. Tamrin, and N. A. Sheikh	
<b>Conversion of Waste Transformer Oil into Grease</b> .....	23
N. Suhaila A. Japar, Mohd Aizudin Abd Aziz, and N. W. Abdu Rahman	
<b>Nanofiber-Immobilized <math>\beta</math>-Galactosidase for Dairy Waste Conversion into Galacto-Oligosaccharides</b> .....	37
Mailin Misson, Suryani Saallah, and Hu Zhang	
<b>Treatment of Petroleum-Based Industrial Wastewater Using Electrocoagulation Technology</b> .....	49
Faten Ahada Mohd Azli, Abdul Aziz Mohd Azoddein, Mazrul Nizam Abu Seman, Agus Sahar Abdul Hamid, Tahfiz Tajuddin, and Said Nurdin	
<b>Activated Carbon from Meranti Wood Sawdust Waste Prepared by Microwave Heating for Dye Removal</b> .....	61
Mohd Azmier Ahmad, Mohamad Firdaus Mohamad Yusop, and Soon Huat Tan	
<b>A Study on the Adsorption of 2,4,6, Trichlorophenol by Palm Kernel Cake</b> .....	89
Duduku Krishnaiah, Awang Bono, Collin G. Joseph, S. M. Anisuzzaman, and Lester Venantius	
<b>Development of Low-Cost Aerobic Bioreactor for Decentralized Greywater Treatment</b> .....	111
Asa Paramesti, Bimo Adiartha Damarjati, Adhika Widyaparaga, Deendarlianto, Aswati Mindaryani, Lisendra Marbelia, and Wiratni Budhijanto	

<b>Management of Biodegradable Plastic Waste: A Review</b> . . . . .	127
Sariah Saalah, Suryani Saallah, Mariani Rajin, and Abu Zahrim Yaser	
<b>Challenges and Current State-of-Art of the <i>Volvariella volvacea</i> Cultivation Using Agriculture Waste: A Brief Review</b> . . . . .	145
N. A. Umor, S. Abdullah, A. Mohamad, S. Ismail, S. I. Ismail, and A. Misran	
<b>Microbial Degradation of Hydrocarbons from Petrochemical Waste Using Food Waste Amendments</b> . . . . .	157
Fazilah Ariffin, Cheah Jin Min, Gan Sik Ze, Sabariah Yussof, and Noraznawati Ismail	
<b>Model Optimization Using Artificial Intelligence Algorithms for Biological Food Waste Degradation</b> . . . . .	173
Norazwina Zainol, Abdul Sahli Fakharudin, and Nor Ilyya Syahira Zulaidi	
<b>Anaerobic Digestion of Food Waste: The Effect of <i>Candida rugosa</i> Lipase Amount on the Digestive Activity</b> . . . . .	183
Mariani Rajin, Abu Zahrim Yaser, Sariah Saalah, Yogananthini Jagadeson, Siti Nazihah Ibrahim, and Muhammad Syah Azhar Mislahani	
<b>Recycled Materials and Warm Mix Asphalt Technology: A Green Approach in Pavement Modification</b> . . . . .	195
Lillian Gungat, Nurul Ariqah Ispal, Ng Chee Hiong, and Meor Othman Hamzah	

## About the Editor



**Abu Zahrim Yaser** is Associate Professor of Waste Processing Technology at Universiti Malaysia Sabah (UMS). He obtained his Ph.D. from Swansea University. Dr. Zahrim's has published 4 books, 16 book chapters, 34 journals and 50++ other publications. He was the Guest Editor for *Environmental Science and Pollution Research* special issue (Springer). The Elsevier (UK) has recognised him as the Outstanding Reviewer for the Journal of Environmental Chemical Engineering. Dr. Zahrim was a visiting scientist at the University of Hull. He is a member of Board of Engineers (Malaysia), IChemE and MyBIOGAS.

# A Review of Enhanced Micromixing Techniques in Microfluidics for the Application in Wastewater Analysis



F. Mahmud, K. F. Tamrin, and N. A. Sheikh

**Abstract** Owing to new methods in agriculture, modern techniques and innovations in domestic activities and mushroom industrialization, rigorous studies are required to understand the wastewater ingredients and their toxicities so that minimization of harmful effects can be achieved. Micromixers may provide insight for analysis in efficient and reliable water treatment methods. Due to the high interfacial-area-to-volume ratio of fluids in micromixers, the study of interaction/reaction between several mixtures and chemicals can be performed, for in-depth, microscale wastewater analysis. This involves various applications, including analysis of wastewater for monitoring and evaluation of heavy metal removal, diclofenac detection, consumption assessment of the illicit drug, tobacco, alcohol and cocaine within local communities and treatment of palm oil mill effluent. However, achieving adequate mixing performance is considerably difficult in microfluidic micromixer, as the flow is always associated with unfavourable laminar flow and dominated by molecular diffusion. As an effort to address the issue, active and passive mixing configurations have been proposed in previous studies. Active mixing mechanism operates on the basis of external energy input to actuate relevant actuators, to enhance mixing by stretching and folding of the fluid mixture by several modes such as pressure, thermal effect, magnetohydrodynamic, electrohydrodynamic, vibration, acoustic and micro-stirrer. Passive mixing mechanism can be categorized based on different fluid stream types which ascribe to geometric design modifications such as lamination, chaotic advection, droplet, collision of jets and special effects. In the prospect of reducing energy consumption, the passive flow driving mechanism does not require energy as it mostly depends on the effects of surface tension, capillary action and gravity rather than using powered syringe pumps.

---

F. Mahmud · K. F. Tamrin (✉)

Department of Mechanical and Manufacturing Engineering, Faculty of Engineering,  
Universiti Malaysia Sarawak (UNIMAS), 94300 Kota Samarahan, Sarawak, Malaysia  
e-mail: [tkfikri@unimas.my](mailto:tkfikri@unimas.my)

N. A. Sheikh

Department of Mechanical Engineering, Faculty of Engineering,  
International Islamic University, Islamabad, Pakistan

© Springer Nature Singapore Pte Ltd. 2020

A. Z. Yaser (ed.), *Advances in Waste Processing Technology*,  
[https://doi.org/10.1007/978-981-15-4821-5\\_1](https://doi.org/10.1007/978-981-15-4821-5_1)

**Keywords** Microfluidic · Wastewater · Processing · Measurement · Micromixer · Laser · Material

## 1 Introduction

The global demand for quality water, whether for purposes of drinking, sanitation, irrigation and industrial use, has been on a continuous rise, and there has been overwhelming concern in recent years about water treatment requiring the strictest standards. With rapid industrialization and modern methods of agricultural and domestic activities, the demand for water has increased tremendously, and this has resulted in the generation of large amounts of industrial wastewater (Gupta et al. 2009; Michael et al. 2013). Industrial wastewater has been under extensive research by the science community since it presents a serious danger to the aquatic, air and soil environment, especially with respect to the human and animal health. The industrial wastewater may contain heavy metals, oil emulsions, inorganic and organic compounds, which are difficult to remove either due to their solubility in water or owing to the presence of persistent and recalcitrant compounds (Xu et al. 2012; Boczkaj and Fernandes 2017). These chemicals enter the aquatic medium in several different ways, either dumped directly, such as industrial effluents, or from wastewater treatment plants that do not fulfil their obligations. They may also enter the water indirectly through the use of plant health products, such as biocides and fertilizers, in agriculture (Oller et al. 2011).

In an effort to combat the problem of water pollution, rapid and significant progresses in wastewater analysis utilizing microfluidics micromixer has been performed, involving the study of interaction/reaction between several mixtures and chemicals, for in-depth wastewater analysis. This involves various applications, including but not limited to the analysis of wastewater for monitoring and evaluation of illicit drug use (Zuccato et al. 2016; Tschärke et al. 2016; Bijlsma et al. 2016), diclofenac in wastewater (Schirmer et al. 2018) and alcohol, cocaine and (Rodríguez-Álvarez et al. 2015) tobacco (Castiglioni et al. 2015; Gartner 2015) consumption by local communities. Apart from these, pollutant removal has been demonstrated through mixing of several mixtures which leads to formation of coagulant, for instance, treatment of palm oil mill effluent via calcium lactate-polyacrylamide (Zahrim et al. 2014; Tamrin and Zahrim 2017) and water purification from heavy metals (Kou et al. 2009; Karvelas et al. 2019; Tang et al. 2016). Microfluidic micromixer implementation in these applications is expected to be able to overcome several shortcomings of the current methods, as the former leads to reduced reagent consumption, increased throughput, minimized operation complexity and maximized information extracted from the analysis due to noticeable increase in surface-area-to-volume ratio (Sivashankar et al. 2016). Previously, the evaluation used to concentrate mostly on the effect of individual substances, whereas researchers are now beginning to study and understand interactions in mixtures of these substances through microfluidics (Pérez et al. 2018; Wang et al. 2014; Martínez-Huitle and Panizza 2018).

Microfluidics is an emerging field in which fluid behaviours at microscale are studied. For the past few decades, the microfluidic system has become a major topic

of research due to its widespread application especially in several domains such as biomedical diagnostics, chemical analysis, drug development, precipitation and food industry (Lee et al. 2016) to name a few. The miniaturized characteristics of microfluidic devices have led to substantial cost reduction since these devices use a minimum amount of chemical reagents and simultaneously reduce overall process waste (Ward and Fan 2015). In addition, a noticeable increase in surface-area-to-volume ratio substantially reduces the sample volume and reagent consumption, increases throughput, minimizes operation complexity and maximizes information extracted from the analysis (Sivashankar et al. 2016).

Homogenous and rapid micromixing are important criteria for wastewater treatment (Karvelas et al. 2019; Parvizian et al. 2012; Izadi et al. 2019; Guha et al. 2017). Attaining sufficient mixing performance is considerably difficult as the flow is typically laminar, and mixing is dominated by molecular diffusion (Ward and Fan 2015; Fu et al. 2017). For this reason, the enhancement of micromixing through active and/or passive approaches is necessary. In particular, micromixer serves as a crucial component of many functional microfluidic devices. Fluid flow inside microfluidics is highly laminar ( $Re < 100$ ) due to the dominant viscous effect over inertial forces within the flow. Therefore, the mixing process inside the micromixer depends almost entirely on diffusion, which is slow and ineffective (Le The et al. 2015). Slow mixing rate between the reactants has become a critical challenge in this field and various types of mixer configurations and designs have been proposed to tackle this issue (You et al. 2015). This chapter discusses key methods that had been employed in the past to increase the efficiency of the micromixers.

## ***1.1 Mixing Mechanism***

Micromixers are one of the important components in microfluidic devices that are used in a wide range of applications. Since the channels are small in features, sizes and geometries, there are a number of dimensionless parameters that can be used to characterize fluid flow in microchannels such as Reynolds number, Peclet number, Schmidt number, Dean number and Poiseuille number. These dimensionless numbers are predominantly governed by viscous effect in the absence of turbulent fluctuations (Ta et al. 2015), placing a challenge for the researcher to address low mixing efficiency in this laminar regime since mixing depends solely on molecular diffusion (You et al. 2015; Ta et al. 2015). A number of studies have been conducted to promote efficient micromixing either actively and/or passively. Figure 1 shows an overview of mixing and flow driving mechanisms that can be employed to enhance micromixing performance. In the case of mixing mechanisms, active micromixing enhancement exploits external energy input to initiate extra fluidic motion for improving mixing efficiency. Therefore, additional external energy is required apart from the energy to drive the fluid into the device. Passive micromixer only depends on manipulation of microchannel geometry to increase contact surface area and residence time between

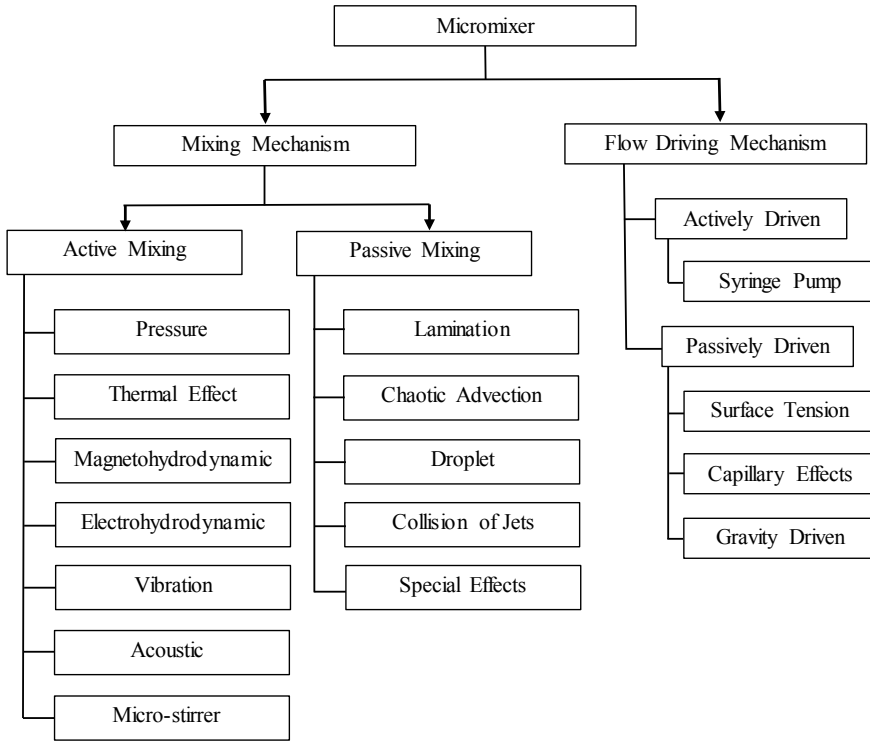


**Fig. 1** Overview of mixing principle and flow driving mechanisms for enhanced micromixing

mixing fluids. This type of mixing mechanism only requires energy to drive the mixing fluid.

### 1.1.1 Active Mixing

Low Reynolds number is typically experienced within the microfluidic due to the dominant viscous effect. To overcome this, the provision of external energy is used to achieve a relatively high mixing efficiency by stretching and folding of the fluid mixture (Kumar et al. 2011). This is often stated as active mixing. Active mixing can be classified into several actuating modes such as pressure, thermal effect, magneto-hydrodynamic, electrohydrodynamic, vibration, acoustic and microstirrer as shown in Fig. 1.

Shamsoddini (2018) investigated the influence of temperature ratio (thermal effect) on the mixing performance of a micromixer. The viscosity of the liquid was substantially reduced by increasing the temperature which in turn increases the molecular diffusion rate. As a result of reduced viscosity, this also promotes vortex

formation. Chen et al. (2016b) demonstrated the hydrodynamic effect of pressure disturbance on improving micromixing performance. Nouri et al. (2017) demonstrated the rapid mixing of deionized water and ferrofluid liquid using magnetohydrodynamic concept in Y-micromixer. It was found that magnetohydrodynamic (variation in magnetic field strength and flow rate) mixing significantly increases the mixing efficiency. However, mixing efficiency was found to reduce with the increase in flow rate. Kim et al. (2018a) studied the effects of electrodes configuration towards mixing performance of an electrohydrodynamic micromixer. Potential difference generated by the electrodes creates non-uniform flow of microparticles which favourably increases the mixing efficiency.

Liu et al. (2018) utilized piezoelectric transducers to induce high-frequency vibration in the flowing liquid. This resulted in the formation of vortex flow and active convection mixing. In a different study, Kim et al. (2018b) proposed low-powered acoustic micromixer consisting of voice coil attached at the bottom of a PDMS micromixer where maximum mixing efficiency was obtained at resonance frequency.

Jafarian et al. (2014) modelled active micromixer with different rotational arrangements and angular velocity of microstirrers to study the effect of these parameters towards mixing efficiency. The study shows that the rotational arrangement of microstirrers is a crucial parameter towards mixing performance. Furthermore, the mixing efficiency of the system can be increased by decreasing the inlet Reynolds number or increasing the angular velocity of the microstirrer. Of many active mixing mechanisms, stirrer type mixing provides the fastest, most efficient mixing with flexibility for many fluid types (Khozayem-Nezhad and Niazmand 2018). This corroborates well with finding reported by Jafarian et al. (2014), Ryu et al. (2011), Shamsoddini et al. (2016), and Park et al. (2008).

In short, mixing in active micromixer is much easier to control externally even though they are difficult to fabricate (Ward and Fan 2015). The system that utilizes active mixing principles have substantially higher mixing performance at the expense of complex and sophisticated design (Cortelezzi et al. 2017). For this reason, passive mixing mechanism is preferable for a wide variety of applications.

### 1.1.2 Passive Mixing

Fundamental concept behind passive micromixing is the enhancement of diffusive effect between fluids. In order to achieve this, the contact surface area between the mixing samples must be increased. Other than that, residence time or contact time between the fluids should be increased. One approach to increase the contact surface and residence time is by manipulating the microfluidic channels' geometry, pattern and surface (Ward and Fan 2015).

The most common design for micromixing is T- and Y-micromixers where two streams of fluid are brought together towards a single microchannel (Sarkar et al. 2014). Due to small Peclet number, the mixing primarily occurred due to molecular diffusion and is typically slow that requires a very long microchannel in the absence of thermal energy. On the other hand, parallel lamination was found to increase the



mixing efficiency (Capretto et al. 2011) where the main sample fluid will be split into several smaller microchannels and at certain point these fluids will be joined together to form laminated fluids with increased interface area. This mixing mechanism was also applied in a gradient reactor with network microchannels (Jeon et al. 2000). In addition, hydrodynamic focusing can be used to increase mixing efficiency. A smaller and thinner stream of sample fluid is supplied to the main channel where its mixing time is proportional to the focused stream width (Capretto et al. 2011; Lu et al. 2016; Jiang et al. 2013). This has led to a significant increase in mixing as the focused stream width is reduced. Split and recombine (also known as sequential lamination) micromixer uses a sequential process of splitting and recombination for several times to enhance mixing (Nimafar et al. 2012).

Chaotic advection is another alternative for enhancing micromixing. Compared to standard advection which occurs in horizontal direction, chaotic advection generally occurs in multiple directions generating transverse flow which causes rapid growth in the contact area between the mixing fluids. Appropriate geometrical manipulation can stretch, fold, break and split the laminar flow inside the microchannel. The most straightforward method to alter the flow direction and create recirculation inside the flow system is by introducing obstacles inside the microchannel (Chen and Zhao 2017; Heshmatnezhad et al. 2017). The whirl flow created by this method produces transversal mass flow which increases mixing efficiency. Three-dimensional serpentine (Chen et al. 2016b), zigzag (Ta et al. 2015), sequential logarithmic shape (Scherr et al. 2012) and sinusoidal shaped (Parsa et al. 2014) are some of the geometric manipulations that have been used to induce chaotic advection through the consecutive formation of Dean vortices. Dean vortices which comprise two tangentially opposite vortices are usually formed when the fluids pass through curved path (Shamloo et al. 2017). Furthermore, the abrupt changes in the shape of microchannel also promote faster mixing with transverse velocity component localized at certain channel walls (Capretto et al. 2011). Another effective method to increase mixing performance is by introducing patterns on the walls of the microchannels such as cylindrical grooves (Wang et al. 2012) and herringbone (Chen and Wang 2015). In one study, a standard T-shaped micromixer with straight microchannel requires two times longer mixing length compared to staggered herringbone micromixers (Capretto et al. 2011).

In addition to geometrical manipulation, mixing performance can be enhanced through the formation of droplets in a multi-phase flow. Due to the immiscibility of the droplet with surrounding fluids, the mixing reagent remains concentrated and localized inside their respective droplets (Ward and Fan 2015). Sakurai et al. (2018) utilized the immiscibility of the droplet injection frequency to generate disorder on the mixing interface. Collision of jets was applied in a chemical reactor to achieve a relatively high mixing efficiency as demonstrated by Gao et al. (2015). It was found this method provides a better mixing efficiency compared to conventional stirred tank. Xu and Chu (2015) utilized Coanda effect to enhance mixing in oscillating feedback micromixer. Table 1 summarizes different methods of active and passive micromixing.

**Table 1** Summary of mixing mechanisms

Type of mixing	Method		Description/example	Ref.
Active mixing	Pressure		Influence of artificial cilia actuation in microchannel towards micromixing	(Chen et al. 2016a)
	Thermal energy		Thermal effect on mixing rate in active micromixer with rotating stirrer	(Shamsoddini 2018)
	Magnetohydrodynamic		Rapid mixing of deionized water and Fe <sub>3</sub> O <sub>4</sub> ferrofluid assisted by magnetic field	(Nouri et al. 2017)
	Electrohydrodynamic		Influence of AC voltage induced coplanar meandering electrode towards mixing	(Sasaki et al. 2006)
	Vibration		Self-circulation micromixer integrated with high frequency vibration based on piezoelectric drive technology	(Liu et al. 2018)
	Acoustic		Mixing efficiency of electro-acoustic coupled micromixer	(Kim et al. 2018b)
	Microstirrer		Effects of disturbance induced by oscillating microstirrer	(Park et al. 2008)
Passive mixing	Lamination	Junction manipulation	Evaluation of mixing for different 1-1 and 1-2 microfluidic junctions	(Sarkar et al. 2014)
		Multiple parallel lamination	Gradient mixing inside network microchannel	(Jeon et al. 2000)

(continued)

**Table 1** (continued)

Type of mixing	Method		Description/example	Ref.
		Hydrodynamic focusing	Formation of organic nanoparticle by hydrodynamic focusing	(Jiang et al. 2013)
		Series (split and recombine)	Mixing enhancement of using H-shaped split and recombination microchannel	(Nimafar et al. 2012)
Chaotic advection		Obstacle	Layout design optimization employing obstacles in 3D passive micromixer	(Chen and Zhao 2017)
		Patterned wall	Mixing enhancement using fabricated cylindrical grooves in straight microchannel	(Wang et al. 2012)
		3D serpentine	Mixing performance in serpentine micromixer by experiment and numerical simulation	(Chen et al. 2016b)
		Zigzag	Effect of geometric parameters for trapezoidal-zigzag micromixer	(Ta et al. 2015)
	Droplet		Thrust of droplets into mixing interface in passive micromixer	(Sakurai et al. 2018)
	Collision of jets		Effect of different impinging velocity in impinging jet reactor	(Gao et al. 2015)
	Special effect		Micromixers design utilizing Coanda effect characterized by different feedback and splitter configuration	(Xu and Chu 2015)

## 1.2 *Passive Micromixer Designs*

This section reviews some designs of passive micromixers based on the geometrical modification.

### 1.2.1 **T- and Y-Shaped Micromixers**

Sarkar et al. (2014) evaluated the mixing efficiency of different microfluidic junctions, namely 1-1 and 1-2 junctions. The junction types are characterized by the concept of skewness at the inlet junction, or in other words, the average value of the angles between inlet channels and main channel. Validation of preliminary numerical simulation of (Sarkar et al. 2014) was conducted by comparing Y-micromixer simulation results with experimental data and theoretical results. The experiment was conducted with a similar preliminary simulation model with 750  $\mu\text{m}$  microchannel diameter. One of the inlets was applied with colourless water, and the other inlet was applied with dyed water. Image acquisition and analysis of the device were performed using high-speed camera on different flow rate conditions for both inlets (Sarkar et al. 2014). This study shows that asymmetric junctions give a better mixing performance for both type of mixing junctions. Furthermore, mixing performance in 1-2 microfluidic junctions was found better as compared to 1-1 microfluidic junction.

### 1.2.2 **Split and Recombination**

Ansari et al. (2010) designed a passive O-shaped micromixer incorporating unbalanced splits and recombination mixing mechanism (see Fig. 2). The main channel width was 300  $\mu\text{m}$  which equals to the width of two sub-channels. The difference in microchannel width was the primary cause of the unbalanced collisions due to unequal fluid flow in both microchannels. Analysis of mixing efficiency for different width ratio,  $W_1/W_2$  of 1.0, 1.4, 1.72 and 2.0 at different Reynolds number, shows that unbalanced collisions cause significant distortion. It was also found that higher mixing efficiency was attainable at  $W_1/W_2 = 2$ . The maximum mixing efficiency, except at  $Re = 10$ , showed that unbalanced collision was not very effective at low Reynolds number because of low inertial forces formed. On the other hand, rapid mixing was observed at  $Re > 40$ .

Nimafar et al. (2012) compared H-shaped micromixer with the T-shaped and O-shaped micromixers. The width, height and total length of the microchannels are 400  $\mu\text{m}$ , 400  $\mu\text{m}$  and 21 mm, respectively. The change in the dye colour intensity was used to determine the mixing efficiency calculated using greyscale images. The experiment was conducted at very low Reynolds number,  $0.08 < Re < 4.16$ . Results of the experiment showed that mixing index at the end region after 20 mm ( $Re = 0.083$ ) for T-micromixer, O-micromixer and H-micromixer are 38%, 55% and 92%, respectively.

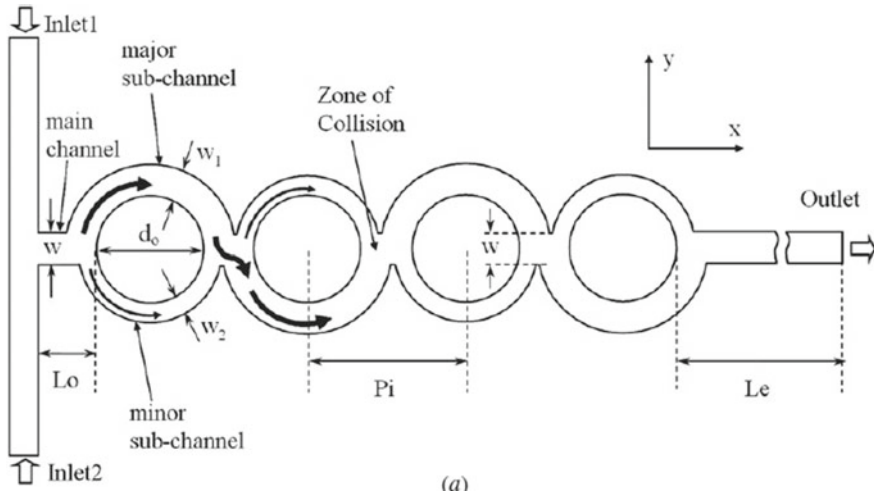


**Fig. 2** Geometrical configuration of unbalanced splits and collisions microfluidic device (Ansari et al. 2010)

Le The et al. (2015) proposed microfluidic device based on shifted trapezoidal blades (STB) design with the aim to achieve complete mixing within a short period of time. The STB design essentially incorporated several mixing mechanisms, namely unequal splitting and recombining, converging and diverging, recirculation and twisting (Le The et al. 2015). A significantly improved mixing was obtained attributed to asymmetrical splitting and recombining nature which eventually lead to chaotic advection. It was found that mixing of these fluids is highly dependent on diffusion effect for low regime  $Re \leq 1$ . In medium regime of  $1 \leq Re \leq 5$ , the flow rate is not high enough to produce vortices. At the same time, the molecular diffusion was reduced causing the mixing efficiency to decrease with increasing in Reynolds number. When the flow reaches the regime of  $5 \leq Re \leq 40$ , the mixing efficiency increases together with Reynolds number due to the presence of chaotic advection. In the regime of  $Re \geq 40$ , the efficiency slightly decreased with an increase in Reynolds number because of short residence time and reduced molecular diffusion. The highest mixing efficiency, which is around 95%, was obtained at  $Re = 40$ .

Sivashankar et al. (2016) laser-fabricated a 3D twisted passive micromixer that utilizes both splitting and recombining and chaotic advection as means of mixing enhancement mechanism. It was observed that the surface roughness due to the fabrication method by laser can induce vortices and eddies. The result interestingly shows that the three mixing units were enough to achieve full mixing where after three mixing units the concentration of the flow is almost constant.

Chen et al. (2018) compared two multi-layer micromixers: F-micromixer and E-micromixer. From  $Re = 0.5$  to 15, mixing efficiency was found to be decreasing with increasing in Reynolds number since mixing depends on molecular diffusion only. The mixing efficiency was found to be the lowest at  $Re = 15$ . When  $Re > 15$ ,

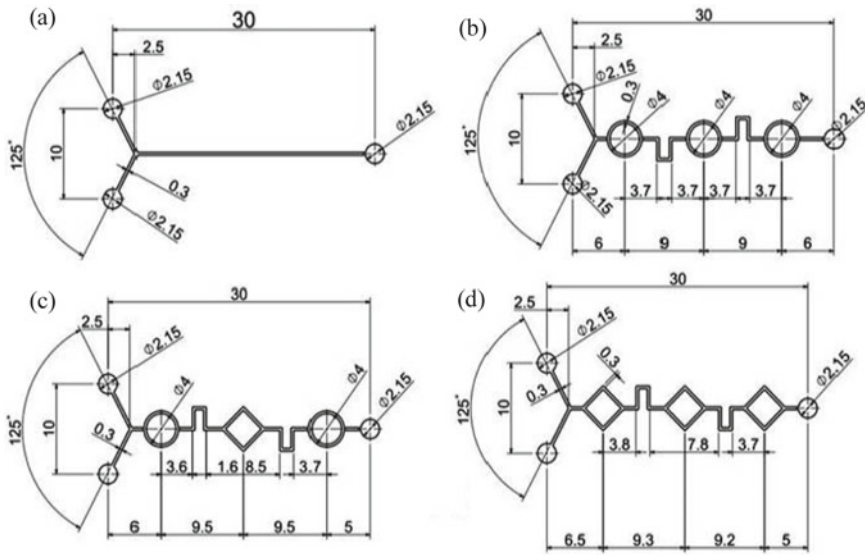


**Fig. 3** Different geometrical configuration used in this study (units in mm) **a** standard Y-micromixer with straight mixing channel, **b** YCSAR, **c** YRCSAR and **d** YRCSAR (Shah et al. 2019)

mixing efficiency increased with increasing in Reynolds number since convection effects start to become dominant (Chen et al. 2018). For  $Re > 25$ , all the considered micromixers' mixing efficiencies were significantly increased. Mixing efficiency of F-micromixer and E-micromixer for  $Re = 80$  were 92% and 94%, respectively.

Shah et al. (2019) evaluated the mixing index due to the chaotic advection of standard Y-micromixer, Y-shaped circle split and recombination (YCSAR), Y-shaped rhombus-circle split and recombination (YRCSAR) and Y-shaped rhombus split and recombination (YRSAR) (see Fig. 3). These micromixers were designed with the same dimension such that their channel width, channel depth and total length were  $300 \mu\text{m}$ ,  $200 \mu\text{m}$  and  $30 \text{ mm}$ , respectively. YCSAR, YRCSAR and YRSAR were used to induce chaotic advection mixing through the formation of Dean effect and transverse flow that eventually amplify the mixing effect (Shah et al. 2019). YRCSAR demonstrated the highest mixing efficiency followed by YCSAR, YRSAR and standard Y-micromixer.

### 1.2.3 Shape of Microchannels

Scherr et al. (2012) performed numerical simulation and experiment on the mixing index of a micromixer designed based on logarithmic spirals (see Fig. 4). Mixing index and pressure drop at different Reynolds numbers were compared with scaled models of Archimedes (Sudarsan and Ugaz 2006), Meandering-S (Jiang et al. 2004) and standard T-channel. Formation of Dean vortices at the curved channels was found

to enhance the mixing process. Moreover, the mixing efficiency was found to increase once  $Re > 15$  because of transition between diffusive mixing to convective mixing (Scherr et al. 2012). The results showed that mixing efficiency in logarithmic spirals are 10–15% higher compared to Archimedes and Meandering-S micromixers.

Li et al. (2012) performed study on mixing efficiency for zigzag micromixer. A standard Y-junction mixer with identical mixing length and channel dimension was designed to perform mixing performance comparison with the developed zigzag micromixer (turning angle  $35^\circ$  and  $20 \mu\text{m}$  outlet channel). It was found that the mixing in zigzag micromixer is significantly better compared to the standard Y-junction mixer.

Parsa et al. (2014) performed both experiment and numerical simulation to study relationship between ratio of amplitude to wavelength of convergent–divergent sinusoidal-shaped micromixer. The sinusoidal-shaped micromixers were varied by their ratio of amplitude to wavelength and their aspect ratio of microchannel cross section as shown in Fig. 5. It was reported that the mixing indices increase in shorter mixing length as the ratio of amplitude to wavelength increases. Furthermore, it was also found that the mixing index improved, while pressure drop reduced with the increasing aspect ratio of microchannel cross section.

A study on mixing performance of micromixer with serpentine microchannel was carried out by Chen et al. (2016b). Results of six different geometries indicate that the mixing efficiency decreases with the increase in  $Re$  from 0 to 0.1, predominantly governed by molecular diffusion. Furthermore, mixing efficiency is determined by residence time at low Reynolds number. When  $Re$  increases from 1 to 100, mixing performance increases due to convection. In addition, result showed a higher mixing efficiency and higher-pressure drop-in square-wave micromixer compared to multi-wave micromixer and zigzag micromixer (Chen et al. 2016b).

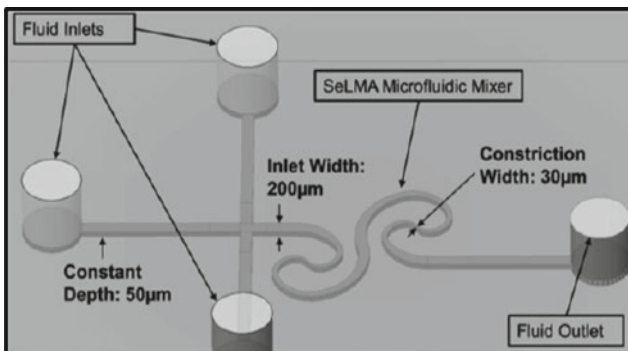


**Fig. 4** Configuration of micromixer based on logarithmic spirals (Scherr et al. 2012)

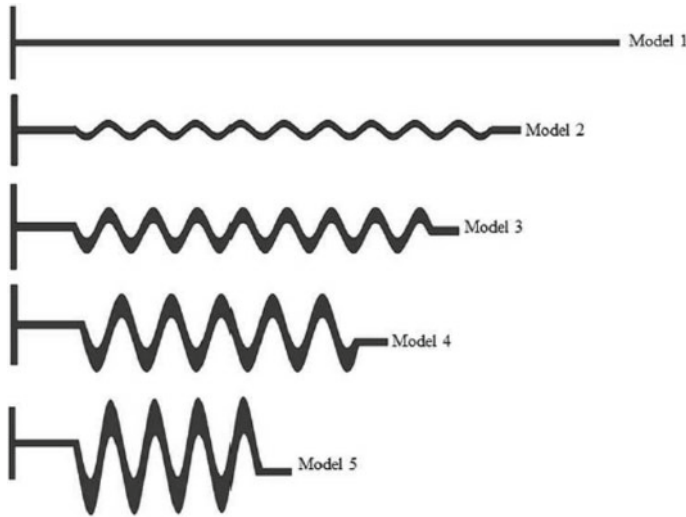


**Fig. 5** Top view of different designs of microfluidic devices (Parsa et al. 2014)

#### 1.2.4 Patterned Walls

The effect of additional grooves in passive micromixer using three different geometrical configurations was studied by Wang et al. (2012). The objective of the grooves with different dimensions (100, 200 and 300  $\mu\text{m}$  groove depth) was to ensure convection flows which occur once the laminar flow passes through the grooves, which in turn enhances the mixing process. Experimental and simulation results proved that the mixing performance increases significantly using these designs for  $1.0 < \text{Re} < 100$ . The groove depth of 100  $\mu\text{m}$  shows the highest mixing efficiency.

Kwak et al. (2016) studied the effects of positive staggered herringbone mixer (SHM) towards mixing performance. Mixing efficiency of this positive SHM was compared with negative SHM. SHM with forward flow direction has higher mixing efficiency compared to that of reverse flow direction. Positive SHM with both forward and reverse flow direction mixed the fluids completely after two cycles, while negative SHM with forward and reverse flow direction mixed the fluids completely after four and five cycles, respectively. Table 2 summarizes enhancement methods of the discussed passive micromixers.

### 1.3 Flow Driving Mechanism in Passive Mixing

Increasing demand for microfluidic devices has led to the development of active and passive flow driving mechanisms. An active flow driving mechanism usually requires expensive equipment (syringe pump) and power/energy. On the other hand,



**Table 2** Summary of key findings for mixing enhancement in passive micromixers

Passive micromixer design	Material	Analysis method	Finding/remark
T- and Y-shape with various angles (Sarkar et al. 2014)	Not specified	<ul style="list-style-type: none"> <li>Numerical simulation</li> <li>Experiment—dye visualization test</li> </ul>	<ul style="list-style-type: none"> <li>Asymmetric junctions give a better mixing performance</li> <li>1-2 microfluidic junction is found to be better compared to 1-1 microfluidic junction</li> </ul>
Unbalanced split and recombination of O-micromixer (Ansari et al. 2010)	PDMS by photolithography	<ul style="list-style-type: none"> <li>Numerical simulation</li> <li>Experiment—fluorescent visualization test</li> </ul>	<ul style="list-style-type: none"> <li>Unbalanced collisions between mixing fluids cause significant distortion</li> <li>Re = 10 shows that unbalanced collision is not very effective due to low inertial forces</li> <li><math>10 \leq Re \leq 80</math></li> </ul>
Split and recombination of H-micromixer (Nimafar et al. 2012)	PMMA by CNC engraving and milling	<ul style="list-style-type: none"> <li>Experiment—blue and yellow dye visualization test</li> </ul>	<ul style="list-style-type: none"> <li>Re = 0.083, mixing efficiency at region after 20 mm for T-micromixer, O-micromixer and H-micromixer are 38%, 55% and 92%, respectively</li> <li><math>0.08 &lt; Re &lt; 4.16</math></li> </ul>
Split and recombination of shifted trapezoidal blades mixer (Le The et al. 2015)	PDMS by photolithography	<ul style="list-style-type: none"> <li>Numerical simulation</li> <li>Experiment—pH test using phenolphthalein</li> </ul>	<ul style="list-style-type: none"> <li>Unequal cross-sectional area causes variation in fluid velocity which causes unequal collision</li> <li>More efficient mixing due to asymmetrical splitting and recombining</li> <li><math>1 \leq Re \leq 5</math>, mixing efficiency significantly decreased when Re increase</li> <li>The highest mixing efficiency of 95% was obtained at Re = 40</li> <li><math>0.5 \leq Re \leq 100</math></li> </ul>
Split and recombination of 3D twisted passive micromixer (Sivashankar et al. 2016)	PMMA by CO <sub>2</sub> laser machining	<ul style="list-style-type: none"> <li>Numerical simulation</li> <li>Experiment—dye visualization test and pH test using phenolphthalein</li> </ul>	<ul style="list-style-type: none"> <li>Mixing efficiency improved due to presence of chaotic advection and vortices at arc shape channel</li> <li>Surface roughness from fabrication improve mixing</li> <li>Three mixing units were enough to achieve full mixing</li> <li><math>1 \mu\text{L}/\text{min} \leq \text{flow rates} \leq 1000 \mu\text{L}/\text{min}</math></li> </ul>

(continued)

**Table 2** (continued)

Passive micromixer design	Material	Analysis method	Finding/remark
Split and recombination of F- and E-micromixer (Chen et al. 2018)	PMMA by CNC engraving and milling	<ul style="list-style-type: none"> <li>Experiment—pH test using phenolphthalein</li> </ul>	<ul style="list-style-type: none"> <li><math>0.5 \leq Re \leq 25</math>, presence of molecular diffusion only, mixing efficiency decrease with increasing in Reynolds number</li> <li><math>Re &gt; 15</math>, mixing efficiency was increased with increasing in Reynolds number due to convection effects</li> <li><math>Re = 80</math>, mixing efficiency of SESM and FESM close to 100%</li> <li><math>Re = 0.5, 1, 5, 15, 25, 40, 50, 80</math> and 100</li> </ul>
Split and recombination of YCSAR, YRCSAR and YRCSAR (Shah et al. 2019)	Borosilicate glass and silicone elastomer by 3D printing system	<ul style="list-style-type: none"> <li>Numerical simulation</li> <li>Experiment—mixing between red and blue ink fluid</li> </ul>	<ul style="list-style-type: none"> <li>Mixing efficiency increased due to chaotic advection</li> <li>YRCSAR demonstrated the highest mixing efficiency followed by YCSAR and YRSAR</li> <li><math>0.5 \leq Re \leq 100</math></li> </ul>
Micromixer based on logarithmic spirals, SeLMA (Scherr et al. 2012)	PDMS by photolithography	<ul style="list-style-type: none"> <li>Numerical simulation</li> <li>Experiment—fluorescent visualization test</li> </ul>	<ul style="list-style-type: none"> <li>Mixing efficiency increase with <math>Re</math> once <math>Re &gt; 15</math> due to transition between diffusive mixing to convective mixing</li> <li>Mixing efficiency of SeLMA are 10–15% higher compared to Archimedes and Meandering-S design</li> <li>Dean vortices at the curved channels enhance the mixing process</li> </ul>
Zigzag micromixer (Li et al. 2012)	PDMS by soft lithography	<ul style="list-style-type: none"> <li>Numerical simulation</li> <li>Experiment—mixing of sulphorhodamine B and fluorescein</li> </ul>	<ul style="list-style-type: none"> <li>Mixing of the developed zigzag micromixer was improved significantly compared to the standard Y-junction</li> <li>Smaller turning angles and smaller outlet channel width will provide better mixing</li> <li>Experimental flow rate = 0.67, 1.67, 5 and 10 <math>\mu\text{L/s}</math></li> </ul>

(continued)

**Table 2** (continued)

Passive micromixer design	Material	Analysis method	Finding/remark
Convergent-divergent sinusoidal shaped micromixer (Parsa et al. 2014)	PMMA by CO <sub>2</sub> laser machining	<ul style="list-style-type: none"> <li>Numerical simulation</li> <li>Experiment—mixing of methylene blue solution and pure water</li> </ul>	<ul style="list-style-type: none"> <li>Mixing index improved and pressure drop reduced with the increasing aspect ratio of microchannel cross section.</li> <li>Ratio of amplitude to wavelength increases, the mixing index increases</li> <li>Slight differences in results because simulation focus on horizontal mid plane while experiment cover the whole depth of microchannel</li> </ul>
Serpentine micromixer (Chen et al. 2016b)	PMMA by CNC engraving and milling	<ul style="list-style-type: none"> <li>Numerical simulation</li> <li>Experiment—blue and yellow dye visualization test</li> </ul>	<ul style="list-style-type: none"> <li>Mixing efficiency is decreasing when Re increase from 0 to 0.1</li> <li>Mixing efficiency is increasing when Re increase from 1 to 100</li> <li>Higher mixing efficiency and higher-pressure drop-in square-wave micromixer compared to multi-wave micromixer and zigzag micromixer</li> <li>Re = 0.1, 1, 10 and 100</li> </ul>
Patterned wall (grooves on the microchannel) (Wang et al. 2012)	PDMS by photolithography	<ul style="list-style-type: none"> <li>Numerical simulation</li> <li>Experiment—pH test using phenolphthalein</li> </ul>	<ul style="list-style-type: none"> <li>Design with 100 μm cylindrical grooves depth has highest mixing efficiency compared to 200 and 300 μm</li> <li>Re = 0.1, 1.0, 10 and 100</li> </ul>
Patterned wall (positive staggered herringbone mixer) (Kwak et al. 2016)	PDMS by photolithography	<ul style="list-style-type: none"> <li>Numerical simulation</li> <li>Experiment—fluorescent visualization test</li> </ul>	<ul style="list-style-type: none"> <li>Positive SHM have better mixing than negative SHM</li> <li>Forward flow direction provides better mixing than reverse flow direction</li> </ul>

the passive flow driving mechanism does not require energy as it mostly depends on the natural effects of surface tension, capillary action and gravity rather than using powered syringe pumps. The following section discusses some of the passively driven flow mechanism.

### 1.3.1 Surface Tension

Walker and Beebe (2002) proposed a simple passive fluid driving system that theoretically depends on surface energy to pump liquid from inlet to outlet. This passive

technique is governed by Young-Laplace equation (refer Eq. 1) where smaller drops of liquid possess higher internal pressure compared to larger drops.

$$\Delta P = \frac{2\gamma}{R} \quad (1)$$

where  $\Delta P$  is pressure difference across fluid interface,  $\gamma$  is surface tension and  $R$  is radius of liquid drop. Therefore, the difference in pressure gradient will force the water from pumping port (inlet) to reservoir port (outlet). In this case, 100  $\mu\text{L}$  drop of liquid was placed on the reservoir port while 0.5–5  $\mu\text{L}$  on pumping port. PDMS was used as the main material to fabricate the microfluidic device due to its hydrophobicity which kept the liquid droplet from spreading out. If somehow the liquid spread out, the Young–Laplace pressure is reduced and inhibit the system to drive the fluid flow. Additionally, the same pumping method was used to drive the fluid from the position with low to higher gravitational potential energy.

### 1.3.2 Capillary Action

Mukhopadhyay (2017) studied the effect of surface-area-to-volume ratio in surface-driven capillary flow. Effectiveness of several proposed designs was measured by the time required by the different fluids to travel from inlet port to outlet reservoir. The microfluidic devices were fabricated using PMMA by mask less lithography in cleanroom, with varying dimensions and number of micropillars to achieve different surface-area-to-volume ratio. There is basically one design without any pillars and other 3 designs of 150  $\mu\text{m}$ , 250  $\mu\text{m}$  and 350  $\mu\text{m}$  side lengths with 342, 214 and 132 individual pillars, respectively. It was demonstrated that the microchannel with larger surface area will increase the time required by the fluid meniscus to travel from inlet port to outlet port (Mukhopadhyay 2017). Furthermore, ethylene glycol flow based on surface-driven capillary flow inside the microchannel is slower due to its higher viscosity.

### 1.3.3 Gravity Driven

Analytical model to estimate generated flow rate gravity-driven pumping system was proposed by Mäki et al. (2015), focusing on utilization of hydrostatic pressure generated by gravitational potential energy to move liquid. At the same time, the fluid flow is reduced as the height difference decreases, lowering the hydrostatic pressure. Considering capillary forces inside the channel are opposite to the movement of fluid by hydrostatic pressure, the flow  $Q(t)$  can be calculated using Eq. 2 (inlet and outlet reservoir have same cross-sectional area).

$$Q(t) = \frac{\Delta p(t)}{R_{\text{hyd}}} = \frac{p_{\text{hyd}}(t) - \Delta p_{\text{cap}}}{R_{\text{hyd}}} \quad (2)$$

where  $\Delta p(t)$  is the total pressure drop,  $p_{\text{hyd}}(t)$  hydrostatic pressure of incompressible fluid,  $\Delta p_{\text{cap}}$  is capillary pressure drop and  $R_{\text{hyd}}$  hydraulic resistance of the channel. In order to verify this mathematical model, PDMS-based microfluidic device was fabricated using standard photolithography process with different vertical channel widths of 50, 100, 250 and 500  $\mu\text{m}$ . Comparison between the model and experimental result shows that the proposed model can estimate the height difference at improved accuracy due to the fact that it considers capillary pressure drop in the equation (Mäki et al. 2015). Model that does not consider the capillary pressure drop will overestimate the effectiveness of pumping and will reduce the accuracy of results.

## 2 Conclusions

Several micromixer technologies have been reviewed as they are foreseen handy in providing reliable insight for analysis of wastewater mixtures and their toxicities so that minimization of harmful effects can be addressed. Useful information can be extracted from the analysis on wastewater treatment as micromixer increases reacting fluid interfacial-area-to-volume ratio through the interaction of thin liquid films or tiny liquid droplets inside the microchannel. Micromixer is also useful for applications of wastewater analysis in the detection and removal of heavy metal and for determining drug, tobacco, alcohol and cocaine consumption within a community. However, due to unfavourable laminar flow inside the microchannels, micromixer suffers difficulties in achieving adequate mixing performance. Several designs have been presented in previous studies to address this issue by means of active and passive mixing. Active micromixers have substantially higher mixing performance at the expense of complex and sophisticated design as it is integrated with relevant actuators that exploit external energy input to initiate extra fluidic motion. Passive micromixer is preferable for some applications due to its simple configurations as mixing is enhanced by the manipulation of the microfluidic channels' geometry.

## References

- Ansari, M. A., Kim, K.-Y., Anwar, K., & Kim, S. M. (2010). A novel passive micromixer based on unbalanced splits and collisions of fluid streams. *Journal of Micromechanics and Microengineering*, 20(5), 55007–55018.
- Bijlsma, L., Botero-Coy, A. M., Rincón, R. J., Peñuela, G. A., & Hernández, F. (2016). Estimation of illicit drug use in the main cities of Colombia by means of urban wastewater analysis. *Science of the Total Environment*, 565, 984–993.
- Boczkaj, G., & Fernandes, A. (2017). Wastewater treatment by means of advanced oxidation processes at basic pH conditions: A review. *Chemical Engineering Journal*, 320, 608–633.
- Capretto, L., Cheng, W., Hill, M., & Zhang, X. (2011). Micromixing within microfluidic devices. In *Microfluidics* (pp. 27–68). Berlin, Heidelberg: Springer.

- Castiglioni, S., Senta, I., Borsotti, A., Davoli, E., & Zuccato, E. (2015). A novel approach for monitoring tobacco use in local communities by wastewater analysis. *Tobacco Control*, 24(1), 38–42.
- Chen, X., & Wang, X. (2015). Optimized modular design and experiment for staggered herringbone chaotic micromixer. *International Journal of Chemical Reactor Engineering*, 13(3), 305–309.
- Chen, C.-Y., Hsu, C.-C., Mani, K., & Panigrahi, B. (2016a). Hydrodynamic influences of artificial cilia beating behaviors on micromixing. *Chemical Engineering Processing: Process Intensification*, 99, 33–40.
- Chen, X., Li, T., Zeng, H., Hu, Z., & Fu, B. (2016b). Numerical and experimental investigation on micromixers with serpentine microchannels. *International Journal of Heat and Mass Transfer*, 98, 131–140.
- Chen, X., & Zhao, Z. (2017). Numerical investigation on layout optimization of obstacles in a three-dimensional passive micromixer. *Analytica Chimica Acta*, 964, 142–149.
- Chen, X., Shen, J., & Hu, Z. (2018). Fabrication and performance evaluation of two multi-layer passive micromixers. *Sensor Review*, 38(3), 321–325.
- Cortelezzi, L., Ferrari, S., & Dubini, G. (2017). A scalable active micro-mixer for biomedical applications. *Microfluidics and Nanofluidics*, 21(3), 31–47.
- Fu, H., Liu, X., & Li, S. (2017). Mixing indexes considering the combination of mean and dispersion information from intensity images for the performance estimation of micromixing. *RSC Advances*, 7(18), 10906–10914.
- Gao, Z., Han, J., Bao, Y., & Li, Z. (2015). Micromixing efficiency in a T-shaped confined impinging jet reactor. *Chinese Journal of Chemical Engineering*, 23(2), 350–355.
- Gartner, C. (2015). Flushing out smoking: Measuring population tobacco use via wastewater analysis. *Tobacco Control*, 24(1), 1–2.
- Guha, R., Xiong, B., Geitner, M., Moore, T., Wood, T. K., Velegol, D., et al. (2017). Reactive micromixing eliminates fouling and concentration polarization in reverse osmosis membranes. *Journal of Membrane Science*, 542, 8–17.
- Gupta, V., Carrott, P., Ribeiro Carrott, M., & Suhas, (2009). Low-cost adsorbents: growing approach to wastewater treatment—A review. *Critical Reviews in Environmental Science Technology*, 39(10), 783–842.
- Heshmatnezhad, F., Aghaei, H., & Nazar, A. R. S. (2017). Parametric study of obstacle geometry effect on mixing performance in a convergent-divergent micromixer with sinusoidal walls. *Chemical Product Process Modeling*, 12(1), 1–12.
- Izadi, M., Rahimi, M., & Beigzadeh, R. (2019). Evaluation of micromixing in helically coiled microreactors using artificial intelligence approaches. *Chemical Engineering Journal*, 356, 570–579.
- Jafarian, A., Pischevar, A., & Saidi, M. (2014). Modeling active micromixers with multiple micro-stirrers using smoothed particle hydrodynamics. *Scientia Iranica. Transaction B, Mechanical Engineering*, 21(4), 1390–1402.
- Jeon, N. L., Dertinger, S. K., Chiu, D. T., Choi, I. S., Stroock, A. D., & Whitesides, G. M. (2000). Generation of solution and surface gradients using microfluidic systems. *Langmuir*, 16(22), 8311–8316.
- Jiang, F., Drese, K. S., Hardt, S., Küpper, M., & Schönfeld, F. (2004). Helical flows and chaotic mixing in curved micro channels. *AIChE Journal*, 50(9), 2297–2305.
- Jiang, L., Wang, W., Chau, Y., & Yao, S. (2013). Controllable formation of aromatic nanoparticles in a three-dimensional hydrodynamic flow focusing microfluidic device. *RSC Advances*, 3(39), 17762–17769.
- Karvelas, E., Liosis, C., Benos, L., Karakasidis, T., & Sarris, I. (2019). Micromixing efficiency of particles in heavy metal removal processes under various inlet conditions. *Water*, 11(6), 1135.
- Khozeymeh-Nezhad, H., & Niazmand, H. (2018). A double MRT-LBM for simulation of mixing in an active micromixer with rotationally oscillating stirrer in high Peclet number flows. *International Journal of Heat and Mass Transfer*, 122, 913–921.

- Kim, H.-S., Kim, H.-O., & Kim, Y.-J. (2018). Effect of electrode configurations on the performance of electro-hydrodynamic micromixer. In *ASME 2018 16th International Conference on Nanochannels, Microchannels, and Minichannels*. American Society of Mechanical Engineers.
- Kim, N., Chan, W. X., Ng, S. H., & Yoon, Y.-J. (2018b). An acoustic micromixer using low-powered voice coil actuation. *Journal of Microelectromechanical Systems*, 27(2), 171–178.
- Kou, S., Nam, S.-W., Shumi, W., Lee, M.-H., Bae, S.-W., Du, J., et al. (2009). Microfluidic detection of multiple heavy metal ions using fluorescent chemosensors. *Bulletin of the Korean Chemical Society*, 30(5), 1173–1176.
- Kumar, V., Paraschivoiu, M., & Nigam, K. (2011). Single-phase fluid flow and mixing in microchannels. *Chemical Engineering Science*, 66(7), 1329–1373.
- Kwak, T. J., Nam, Y. G., Najera, M. A., Lee, S. W., Strickler, J. R., & Chang, W.-J. (2016). Convex grooves in staggered herringbone mixer improve mixing efficiency of laminar flow in microchannel. *PLoS ONE*, 11(11), 1–15.
- Le The, H., Le Thanh, H., Dong, T., Ta, B. Q., Tran-Minh, N., & Karlsen, F. (2015). An effective passive micromixer with shifted trapezoidal blades using wide Reynolds number range. *Chemical Engineering and Research Design*, 93, 1–11.
- Lee, C.-Y., Wang, W.-T., Liu, C.-C., & Fu, L.-M. (2016). Passive mixers in microfluidic systems: A review. *Chemical Engineering Journal*, 288, 146–160.
- Li, Y., Zhang, D., Feng, X., Xu, Y., & Liu, B.-F. (2012). A microsecond microfluidic mixer for characterizing fast biochemical reactions. *Talanta*, 88, 175–180.
- Liu, G., Ma, X., Wang, C., Sun, X., & Tang, C. (2018). Piezoelectric driven self-circulation micromixer with high frequency vibration. *Journal of Micromechanics and Microengineering*, 28(8), 1–12.
- Lu, M., Ozelik, A., Grigsby, C. L., Zhao, Y., Guo, F., Leong, K. W., et al. (2016). Microfluidic hydrodynamic focusing for synthesis of nanomaterials. *Nano Today*, 11(6), 778–792.
- Mäki, A.-J., Hemmilä, S., Hirvonen, J., Girish, N. N., Kreutzer, J., Hyttinen, J., et al. (2015). Modeling and experimental characterization of pressure drop in gravity-driven microfluidic systems. *Journal of Fluids Engineering*, 137(2), 1–8.
- Martínez-Huitle, C. A., & Panizza, M. (2018). Electrochemical oxidation of organic pollutants for wastewater treatment. *Current Opinion in Electrochemistry*, 11, 62–71.
- Michael, I., Rizzo, L., McArdell, C., Manaiia, C., Merlin, C., Schwartz, T., et al. (2013). Urban wastewater treatment plants as hotspots for the release of antibiotics in the environment: A review. *Water Research*, 47(3), 957–995.
- Mukhopadhyay, S. (2017). Experimental investigations on the interactions between liquids and structures to passively control the surface-driven capillary flow in microfluidic lab-on-a-chip systems to separate the microparticles for bioengineering applications. *Surface Review and Letters*, 24(06), 1–10.
- Nimafar, M., Viktorov, V., & Martinelli, M. (2012). Experimental comparative mixing performance of passive micromixers with H-shaped sub-channels. *Chemical Engineering Science*, 76, 37–44.
- Nouri, D., Zabihi-Hesari, A., & Passandideh-Fard, M. (2017). Rapid mixing in micromixers using magnetic field. *Sensors and Actuators, A: Physical*, 255, 79–86.
- Oller, I., Malato, S., & Sánchez-Pérez, J. (2011). Combination of advanced oxidation processes and biological treatments for wastewater decontamination—A review. *Science of the Total Environment*, 409(20), 4141–4166.
- Park, J.-Y., Kim, Y.-D., Kim, S.-R., Han, S.-Y., & Maeng, J.-S. (2008). Robust design of an active micro-mixer based on the Taguchi method. *Sensors and Actuators B: Chemical*, 129(2), 790–798.
- Parsa, M. K., Hormozi, F., & Jafari, D. (2014). Mixing enhancement in a passive micromixer with convergent–divergent sinusoidal microchannels and different ratio of amplitude to wave length. *Computers & Fluids*, 105, 82–90.
- Parvizian, F., Rahimi, M., & Azimi, N. (2012). Macro- and micromixing studies on a high frequency continuous tubular sonoreactor. *Chemical Engineering and Processing: Process Intensification*, 57, 8–15.

- Pérez, J., Llanos, J., Sáez, C., López, C., Cañizares, P., & Rodrigo, M. (2018). Development of an innovative approach for low-impact wastewater treatment: A microfluidic flow-through electrochemical reactor. *Chemical Engineering Journal*, 351, 766–772.
- Rodríguez-Álvarez, T., Racamonde, I., González-Mariño, I., Borsotti, A., Rodil, R., Rodríguez, I., et al. (2015). Alcohol and cocaine co-consumption in two European cities assessed by wastewater analysis. *Science of the Total Environment*, 536, 91–98.
- Ryu, S.-P., Park, J.-Y., & Han, S.-Y. (2011). Optimum design of an active micro-mixer using successive Kriging method. *International Journal of Precision Engineering and Manufacturing*, 12(5), 849–855.
- Sakurai, R., Yamamoto, K., & Motosuke, M. (2018). Concentration-adjustable micromixer using droplet injection into a microchannel. *Analyst*, 144, 2780–2787.
- Sarkar, S., Singh, K., Shankar, V., & Shenoy, K. (2014). Numerical simulation of mixing at 1–1 and 1–2 microfluidic junctions. *Chemical Engineering and Processing: Process Intensification*, 85, 227–240.
- Sasaki, N., Kitamori, T., & Kim, H.-B. (2006). AC electroosmotic micromixer for chemical processing in a microchannel. *Lab on a Chip*, 6(4), 550–554.
- Scherr, T., Quitadamo, C., Tesvich, P., Park, D. S.-W., Tiersch, T., Hayes, D., et al. (2012). A planar microfluidic mixer based on logarithmic spirals. *Journal of Micromechanics and Microengineering*, 22(5), 1–10.
- Schirmer, C., Posseckardt, J., Kick, A., Rebatschek, K., Fichtner, W., Ostermann, K., et al. (2018). Encapsulating genetically modified *Saccharomyces cerevisiae* cells in a flow-through device towards the detection of diclofenac in wastewater. *Journal of Biotechnology*, 284, 75–83.
- Shah, I., Kim, S. W., Kim, K., Doh, Y. H., & Choi, K. H. (2019). Experimental and numerical analysis of Y-shaped split and recombination micro-mixer with different mixing units. *Chemical Engineering Journal*, 358, 691–706.
- Shamloo, A., Vatankhah, P., & Akbari, A. (2017). Analyzing mixing quality in a curved centrifugal micromixer through numerical simulation. *Chemical Engineering and Processing: Process Intensification*, 116, 9–16.
- Shamsoddini, R. (2018). SPH investigation of the thermal effects on the fluid mixing in a microchannel with rotating stirrers. *Fluid Dynamics Research*, 50(2), 1–17.
- Shamsoddini, R., Sefid, M., & Fatehi, R. (2016). Incompressible SPH modeling and analysis of non-Newtonian power-law fluids, mixing in a microchannel with an oscillating stirrer. *Journal of Mechanical Science and Technology*, 30(1), 307–316.
- Sivashankar, S., Agambayev, S., Mashraei, Y., Li, E. Q., Thoroddsen, S. T., & Salama, K. N. (2016). A “twisted” microfluidic mixer suitable for a wide range of flow rate applications. *Biomicrofluidics*, 10(3), 1–13.
- Sudarsan, A. P., & Uguz, V. M. (2006). Fluid mixing in planar spiral microchannels. *Lab on a Chip*, 6(1), 74–82.
- Ta, B. Q., Lê Thanh, H., Dong, T., Thoi, T. N., & Karlsen, F. (2015). Geometric effects on mixing performance in a novel passive micromixer with trapezoidal-zigzag channels. *Journal of Micromechanics and Microengineering*, 25(9), 1–11.
- Tamrin, K., & Zahrim, A. (2017). Determination of optimum polymeric coagulant in palm oil mill effluent coagulation using multiple-objective optimisation on the basis of ratio analysis (MOORA). *Environmental Science Pollution Research*, 24(19), 15863–15869.
- Tang, X., Zheng, H., Teng, H., Sun, Y., Guo, J., Xie, W., et al. (2016). Chemical coagulation process for the removal of heavy metals from water: A review. *Desalination Water Treatment*, 57(4), 1733–1748.
- Tscharke, B. J., Chen, C., Gerber, J. P., & White, J. M. (2016). Temporal trends in drug use in Adelaide, South Australia by wastewater analysis. *Science of the Total Environment*, 565, 384–391.
- Walker, G. M., & Beebe, D. J. (2002). A passive pumping method for microfluidic devices. *Lab on a Chip*, 2(3), 131–134.



- Wang, L., Liu, D., Wang, X., & Han, X. (2012). Mixing enhancement of novel passive microfluidic mixers with cylindrical grooves. *Chemical Engineering Science*, *81*, 157–163.
- Wang, N., Zhang, X., Wang, Y., Yu, W., & Chan, H. L. (2014). Microfluidic reactors for photocatalytic water purification. *Lab on a Chip*, *14*(6), 1074–1082.
- Ward, K., & Fan, Z. H. (2015). Mixing in microfluidic devices and enhancement methods. *Journal of Micromechanics Microengineering*, *25*(9), 1–17.
- Xu, C., & Chu, Y. (2015). Experimental study on oscillating feedback micromixer for miscible liquids using the Coanda effect. *AIChE Journal*, *61*(3), 1054–1063.
- Xu, P., Zeng, G. M., Huang, D. L., Feng, C. L., Hu, S., Zhao, M. H., et al. (2012). Use of iron oxide nanomaterials in wastewater treatment: A review. *Science of the Total Environment*, *424*, 1–10.
- You, J. B., Kang, K., Tran, T. T., Park, H., Hwang, W. R., Kim, J. M., et al. (2015). PDMS-based turbulent microfluidic mixer. *Lab on a Chip*, *15*(7), 1727–1735.
- Zahrim, A., Nasimah, A., & Hilal, N. (2014). Pollutants analysis during conventional palm oil mill effluent (POME) ponding system and decolourisation of anaerobically treated POME via calcium lactate-polyacrylamide. *Journal of Water Process Engineering*, *4*, 159–165.
- Zuccato, E., Castiglioni, S., Senta, I., Borsotti, A., Genetti, B., Andreotti, A., et al. (2016). Population surveys compared with wastewater analysis for monitoring illicit drug consumption in Italy in 2010–2014. *Drug Alcohol Dependence*, *161*, 178–188.

# Conversion of Waste Transformer Oil into Grease



N. Suhaila A. Japar, Mohd Aizudin Abd Aziz, and N. W. Abdu Rahman

**Abstract** This work is aimed to study the viability of waste transformer oil (WTO) as grease's base oil. The shift of lubricant formulation towards high-performance materials and green formulation has led to the development of various lubricant formulations, including grease. Waste reduction is one of the formulation research trends where waste-based material, i.e. waste oil generated from automotive industries, is used as one of the grease constituents, and the grease's characteristics and performances are evaluated and compared to the conventional grease. Variability of waste oil composition, a mixture of conventional and synthetic oil, has led to inconsistent grease properties and performances. This issue, however, is uncommon in power industry-generated waste oil and becomes a potential alternative to replace the waste oil from automotive industries, thus creating this opportunity. It was found that, after conducting WTO analysis, incorporating WTO in grease formulation and evaluating the WTO-based grease characteristic, the WTO is viable to be used as grease base oil.

**Keywords** Waste transformer oil · Grease formulation · Sodium grease · Fumed silica grease · Oil and grease analysis

## 1 Introduction

Grease is a semisolid lubricant where a thickening agent is dispersed in a liquid lubricant. It is made up of three elements of base oil, thickener and additives. Mineral oil is the most commonly used base oil, but a wide range of other base oils types, such as synthetic oil, silicone and vegetable oil, also available to be used. Grease thickener, either soap or non-soap thickener, is used to trap the oil in its structure until it is ready to be utilized in lubrication.

Grease has been used for plenty of applications, involving machinery and moving parts, acts as a seal and provides protection against corrosion and at the same

---

N. S. A. Japar · M. A. Abd Aziz (✉) · N. W. Abdu Rahman  
Faculty of Chemical and Process Engineering Technology, Universiti Malaysia Pahang,  
Lebuhraya Tun Razak, 26300 Kuantan, Pahang, Malaysia  
e-mail: [maizudin@ump.edu.my](mailto:maizudin@ump.edu.my)

time being able to reduce noise and shock. Grease, similar to lubricating oil, serves primarily to keep moving part apart, reduces friction, transfers heat, carries away contaminants, transmits power, and wear and corrosion protection (Donley 2012). Historically, lubricant was used since Ancient Egypt, where back then—water is used to help in reducing friction between the sled and the sand to ease the movement of a statue. The grease-like substance was first identified back in 1400 BC, where animal fats were used to lubricate the axle of chariots.

### ***1.1 Current Trends in Grease***

The industrial development has come a long way, and the lubricant has gained its importance in the industry. The development and advancement of grease were based on the grease thickener since the mid-1880s. Up to this date, there is no significant development in terms of grease manufacturing, but the trends are changing based on rapid industrialization and urbanization. According to Gresham (2018), future trends in lubricant formulation including grease will keep emphasizing on protecting the environment, reducing waste, utilization of highly refined and synthetic base oil, and creating additives that deliver various performances (Gresham 2018).

Numerous researches have been conducted in developing new and improved grease formulation parallel with the current formulation direction. The grease formulations were primarily conducted to evaluate the potential and performance of selected material as one of the grease components either base oil, thickener or additive to see whether it is comparable or better than the conventional grease in delivering the proposed aim. Some studies that were conducted for the purpose of protecting the environment and waste reduction; however, investigating various environmentally friendly and waste-based materials to help in providing alternative material to produce eco-friendly grease and to reduce the abundant waste that threatens the environment, respectively.

### ***1.2 Waste Oil as Base Oil***

The generation of waste oil continues to increase annually in response to urbanization and industrialization. Although waste oil holds less than 10% breakdown of the total hazardous waste generated in Malaysia (Aja et al. 2016), some waste oil-related water pollution crises have been reported. However, legal waste oil disposal is rather costly, thus leading to illegal oil disposal and pollution. On the bright side, waste oil still has its economic value and it can be recovered, reclaimed, recycled, reused and converted into a new product such as fuel oils and lubricants, and this will promote environmental protection and reduce the number of wastes oil being disposed of.

Some researches had started in utilizing and employing waste oil in lubricant formulation, including grease to overcome the increasing waste oil generation and

environmental concern. Although several studies had focused on this topic, the problem of this approach is the variability of the waste oil composition due to the mixture of various types of waste oil, both mineral and synthetic oil, which will definitely exhibit inconsistent lubricant properties. This is common for waste oil generated by the automotive and machinery industries since there are numerous moving parts which lubricated with different lubricants, either mineral- or synthetic-based. This problem, however, is not apparent to waste oil generated from the power industry, for example, waste transformer oil (WTO). In a power station, the transformer oil type or brand that is used usually the same for every transformer. Hence, the chances of waste oil mixture are minimal.

WTO is a discarded transformer oil due to its quality that is no longer up to the standard. Presently, researches are carried out by reclaiming WTO as an alternative fuel oil either diesel or gasoline, due to its properties that are closed to the fuel oils (Nabi et al. 2013; Mohta and Chaware 2015). The initiative in using WTO to produce lubricant had not gained its emphasis yet. Up to this date, there is no research conducted in producing lubricant from WTO and there is also no prove saying that WTO is unsuitable as lubricant’s base oil. Several studies, however, were found to succeed in producing grease by utilizing virgin transformer oil as a base oil to provide unique properties to the grease (Hassan et al. 2013). This, in turn, indicates the viability of WTO as grease base oil and hence creating the opportunity in developing new lubricant formulation including grease, with WTO as base oil. The use of waste oil generated by the power industry will help in solving the variability of oil composition faced with waste oil from the automotive and machinery industries.

## 2 Experimental Work

Grease formulation involving WTO required four major phases (Fig. 1). The first phase involves only WTO, where WTO is collected, treated and analysed. Grease formulation took place in the second phase, where two types of NLGI grade 2 greases—sodium and fumed silica (FS) grease—are formulated using 67.5–82.5 and 92–94% of WTO, respectively. The greases then produced and analysed for their physical and chemical characteristics.

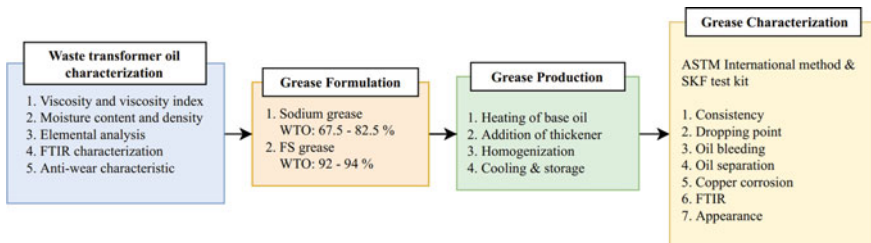


Fig. 1 Major phases of the overall research workflow

### 3 WTO Analysis

The WTO is first treated through settling, filtration and evaporation processes to remove any impurities presented in the WTO. The WTO condition is evaluated by identifying the WTO fluid properties—i.e. viscosity, density, and moisture content, contaminations and wear debris concentration—through FTIR and elemental analysis.

*Viscosity.* It is conducted using a glass capillary viscometer (Cannon-Fenske) with Cannon-Fenske tube size 150 and measured according to ASTM D445. The oil viscosity was measured at two temperatures of 40 and 100 °C, and these values are used to calculate the viscosity index.

*Moisture content.* It is evaluated using 807 KF tritino, a Karl Fischer titrator, to determine the water content presented in the oil.

*Density.* Density is analysed using a gas pycnometer. The supply of high purity helium gas is used as a medium in the process of density measurement. The result of the test is measured in g/ml.

*FTIR characterization.* It is conducted using the FTIR instrument, Thermo Scientific Nicolet iS5 FTIR Spectrometer and used to identify the compound existed and provide information on any contamination, additive and any chemical changes presented in the WTO.

*ICP-MS.* It is used to detect the concentration of wear metals, contaminants, or additive elements within the WTO. The results of the test are reported in terms of the element concentration (ppm or ppb) and compared to the standard provided by the Department of Environment (DOE), Malaysia.

### 4 Grease Production

The production of grease involves only four steps, which started by raising the base oil temperature, addition of thickener, homogenization of mixture, and lastly, cooling of product and storage. The composition for all grease's formulations are shown in Table 1.

**Table 1** Composition of sodium and FS grease

Samples		Grease composition (wt%)	
		WTO	Thickener
Sodium grease	SG <sub>1</sub>	82.5	17.5
	SG <sub>2</sub>	75	25
	SG <sub>3</sub>	67.5	32.5
FS grease	FG <sub>1</sub>	94	6
	FG <sub>2</sub>	93	7
	FG <sub>3</sub>	92	8

*Sodium grease.* The preparation of sodium grease is initiated by heating the WTO at 120 °C for at least 1 h with continuous stirring to remove traces of moisture. The WTO temperature is then increased to 180 °C. Sodium thickener is added gradually into the WTO, and the mixture is homogenized for at least 3 h until the smooth paste was obtained. The homogenization of the grease sample was conducted at an increased speed for at least 30 min without the presence of heat to allow uniform dispersion of mixture. After homogenization, grease is cooled to room temperature and stored in an enclosed container.

*FS grease.* The procedure in preparing FS grease was referred to Abdulbari et al. (2008). The preparation steps of FS grease are similar to sodium grease, but the operating temperature is different. After raising WTO's temperature for moisture removal, the temperature is then lowered to 80–90 °C. Fumed silica is added portion-wise into the oil and continuously homogenized at a constant temperature of within 80–90 °C (Abdulbari et al. 2008). The mixture then homogenized for at least 3 h until a gel-like paste is formed. The mixture is also homogenized at an increased speed for at least 30 min without the presence of heat to uniformly disperse the mixture. After homogenization, grease was cooled and stored.

## 5 Grease Characterization

Greases are characterized both physically and chemically to identify the properties of the grease. Grease consistency, dropping point, copper corrosion and anti-wear properties are the most commonly evaluated grease properties.

*Consistency.* It is evaluated using the SKF grease testing kit and penetrometer (ASTM D217). When using the SKF grease kit, an amount of grease sample was placed in between two glass plates and placed on top of an NLGI grade scale. Penetrometer (HK-2020) and mechanical grease worker (HK-269G) were used to determine the grease penetration number. Worked grease then was placed below the tip of the penetrometer cone, and the cone is allowed to drop into the grease. The depth of penetration is measured in tenths of a millimetre (mm/10).

*Dropping point.* It is conducted as described in standard ASTM D2265. Dropping point instrument, HK-2019 High-Temperature Dropping Point Apparatus, is used in this test with maximum operating temperature up to 400 °C. The dropping point then calculated using Eq. 1, where DP stands for dropping point, ODP is a thermometer reading when the first drop reaches the bottom of the test tube, and BT is the block oven temperature when the drop falls.

$$DP (^\circ\text{C}) = ODP + [(BT - ODP)/3] \quad (1)$$

*Oil bleeding.* It is conducted using the SKF's grease test kit with a small volume of grease samples. In this analysis, the grease sample was placed on a blotter paper and heated on a hotplate at 60 °C for 2 hours. The grease's bleed area percentage differences were measured and calculated by using Eqs. 2 and 3 between fresh and

aged grease, where  $S_{\text{Fresh}}$  and  $S_{\text{Used}}$ , respectively, stand for the bled area from the fresh and aged sample,  $D_{\text{AVi}}$  is the average diameter of the bled area and % Diff represents the bled area difference between fresh and used samples. Aged greases in this study refer to the grease that has been aged for 10 days at 70 °C.

$$S_i = 0.785 \times (D_{\text{AVi}}^2 - 100) \quad (2)$$

$$\% \text{ Diff} = 100 \times \frac{(S_{\text{Used}} - S_{\text{Fresh}})}{S_{\text{Fresh}}} \quad (3)$$

*Oil separation.* 150 g of grease sample was left untouched in an enclosed container for a month, and the oil separated on top of the grease surface was observed, collected and measured in weight percentage. It is desirable for the grease to released oil for less than 4%, according to Lugt (2013a) during storage.

*Copper corrosion.* Corrosion test was carried qualitatively through an observational technique to study the WTO and grease corrosiveness towards copper strips. This method was conducted in accordance with ASTM D130 for WTO and ASTM D4048 for greases (ASTMD130-18 2018; ASTMD4048-16e1 2016; Nye Lubricants 2016).

*FTIR characterization.* It is conducted using the FTIR instrument, Thermo Scientific Nicolet iS5 FTIR Spectrometer and used to identify the compound existed and provide information on any contamination, additive and any chemical changes presented in the prepared grease.

*Wear preventive test.* It is conducted for both treated WTO and selected greases by using four-ball tester in accordance with ASTM D4172b for the WTO and ASTM D2266 for grease sample (ASTM D4172-18 2018; ASTM D2266-01 2015) to study the friction and wear properties of base oil and grease as a result of a motion between the steel balls and to observe the formation of lubricant film on the worn surface using micrograph and energy dispersive X-ray (EDX) analysis.

## 6 Result and Discussion

### 6.1 WTO Analysis

WTO analysis was carried out to investigate the WTO condition. Based on the WTO analysis on its physical (Table 2), contamination and wear debris (Table 3), all were found favourable and comparable to most base oil used in grease formulations (Donley 2012).

WTO treatment is crucial since WTO was contaminated with water and unknown suspended materials that may be possible in causing undesirable issues. The treatment process was proved adequate to reduce the WTO water content from 0.14 to 0.05%. This reduction was also observed through the FTIR spectrum of the WTO

**Table 2** WTO's physicochemical properties

Base oil	Test method	Transformer oil	Treated WTO	Untreated WTO
Appearances	Visual	Clear and bright	Bright yellow	Amber
<i>Kinematic viscosity</i>				
@ 40 °C (cSt)	ASTM D445	9.55	10.06	9.95
@ 100 °C (cSt)		2.55	2.57	2.59
Viscosity index (VI)	ASTM D2270	92	97	85
Density (g/mL)	Gas pycnometer	0.895	0.875	0.926
Moisture content (%)	Karl Fischer	0.002	0.05	0.14
Copper corrosion	ASTM D130	1a	1a	–

**Table 3** Elemental analysis of WTO

Element	Formula	DOE specs (Hazardous Substance Division 2010)	Treated WTO
Beryllium	Be		<0.5 ppb
Sodium	Na		120.7 ppm
Magnesium	Mg		<0.1 ppm
Aluminium	Al		5.1 ppm
Potassium	K		<0.1 ppm
Calcium	Ca		<0.1 ppm
Vanadium	V		<0.5 ppb
Chromium	Cr	Max. 10 ppm	<0.5 ppb
Manganese	Mn		<0.5 ppb
Iron	Fe		<0.5 ppb
Cobalt	Co		<0.5 ppb
Nickle	Ni		<0.5 ppb
Copper	Cu		<0.5 ppb
Zinc	Zn		281.2 ppb
Arsenic	As	Max. 5 ppm	<0.5 ppb
Selenium	Se		<0.5 ppb
Molybdenum	Mo		<0.5 ppb
Silver	Ag		<0.5 ppb
Cadmium	Cd	Max. 2 ppm	<0.5 ppb
Antimony	Sb		<0.5 ppb
Barium	Ba		<0.5 ppb
Lead	Pb	Max. 100 ppm	384.9 ppb
Sulphur	S		22.8 ppb



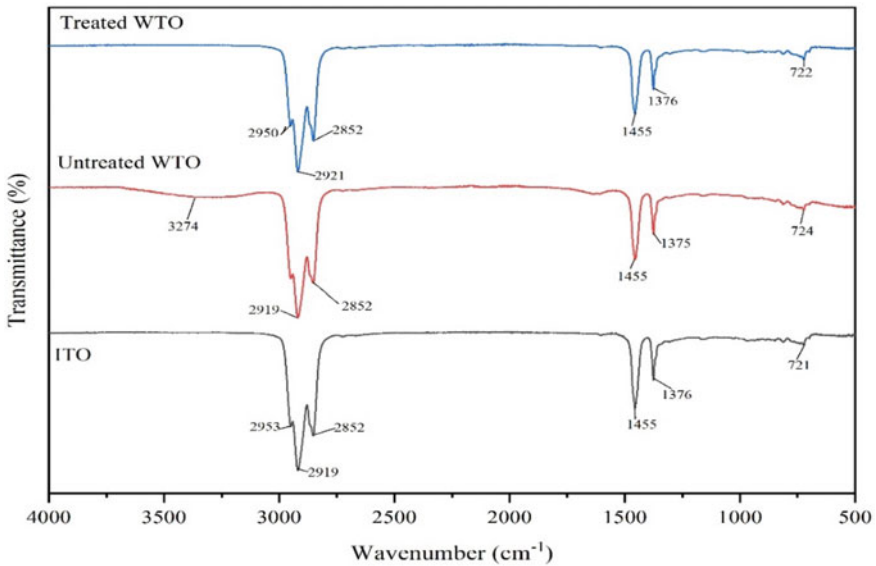


**Fig. 2** FTIR spectrum of virgin transformer oil (ITO), treated WTO and untreated WTO

(Fig. 2) before and after the treatment process, which transmittance band indicating the presence of O–H bond that represented water molecule in untreated WTO was undetected after WTO treatment. The contaminants such as wear debris also found in favourable concentration through elemental analysis (Table 3), complying with the standard set by the DOE, Malaysia, for recovered waste oil. The WTO's viscosity, however, unmanaged to be restored to its original value, though its resistance to viscosity change was slightly improved (Table 1).

The tribological study on WTO shows that the WTO's friction coefficient and wear scar diameter were 0.1158 and 743  $\mu\text{m}$ , respectively. This finding is comparable to some of the previous studies (Zuan et al. 2017; Hassan et al. 2016), but the addition of additive is recommended as the WTO film was too thin—due to WTO's low viscosity, to separate the contacting surfaces, thus causing wear to the contacting surfaces.

## 6.2 Grease Characteristic

Table 4 shows all evaluated grease's properties for both sodium and FS grease.

*Consistency.* Grease consistency depends on the type and amount of thickener, as well as the base oil's viscosity. According to Rizvi (2008), NLGI grades 2–3 greases exhibit the most grease-like behaviours and function (Rizvi 2008). This study aimed to produce NLGI grade 2 grease, both sodium and FS greases. Such greases were obtained when the WTO percentage is 67.5% in sodium grease and 92% in FS grease.

**Table 4** Sodium and FS grease characteristics

Grease	Composition, %		NLGI	Penetration number (mm/10)	Drop point (°C)	Oil bleed (%)	Oil separation (%)	Copper corrosion
	WTO	Thickener						
SG <sub>1</sub>	82.5	17.5	0	378	158	-9.54	0.27	1b
SG <sub>2</sub>	75	25	1	311	175	-11.67	0.07	1b
SG <sub>3</sub>	67.5	32.5	2	275	193	-18.04	0	1b
FG <sub>1</sub>	94	6	00	408	264	N/A	0.07	1b
FG <sub>2</sub>	93	7	1-0	344	312.3	-28.7	0	1b
FG <sub>3</sub>	92	8	2	287	>350	-15.4	0	1a

It was noticed that as the amount of WTO decreased, the grease becomes stiff due to the high amount of thickener in the formulation.

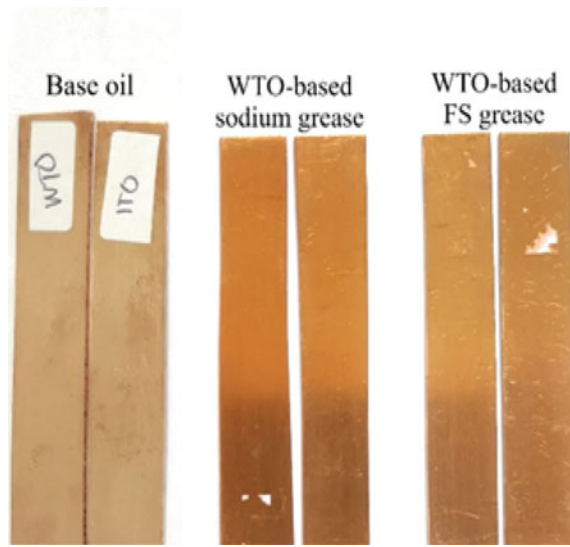
*Dropping point.* Typically, sodium grease has a dropping point of around 175 °C. WTO-based sodium grease has a dropping point as high as 200 °C. Previous studies in developing grease by utilizing waste oils also exhibited similar dropping points ranging from 165 to 190 °C (Iheme et al. 2014; Ebisike et al. 2016). This, in turn, concluded that at this temperature range, the sodium grease had reached the temperature limit where the grease structure started to break and release of WTO from the thickener matrix.

The highest dropping point observed for FS grease is above 300 °C at 93% WTO content, but when WTO percentage is dropped to below 93%, FS grease dropping point was not existing. This was due to the fumed silica's non-melt characteristic and high melting point (>1600 °C). Abdulbari et al. (2008) and Razali et al. (2017) also presented similar findings with FS-containing grease. On the other hand, FS greases were found decomposed after the test is carried out. Non-melt thickener often burns off over high temperatures even before it reached the grease dropping point because, at a point, the oil evaporated or burns off during the test and leaving the thickener residue to hardened and decayed (Corporation 2002; Abdulbari and Zuhan 2018).

*Oil bleeding.* Bots (2014) stated that the oil bleeding differences within -15 to +15% between used and fresh are desirable as they indicated that the grease still can be utilized without changing the re-lubrication intervals (Bots 2014). The positive value is indicating that aged grease bleeds more oil than fresh grease and vice versa. Sodium grease exhibited desirable oil bleeding at both ageing temperatures at the WTO percentage of 75 < WTO% < 82.5. As for FS grease, oil bleeding was observed the best at WTO percentage less than 93%.

Overall, it was observed that the decrease in WTO percentage and an increase in temperature led to a decrement of oil bleeding. This is because, when WTO content is reduced, the thickener content is increased, and the microstructure becomes denser and grease permeability is reduced along with the grease's oil bleed (Gonçalves et al. 2015). Not only that, but thermally ageing of grease also affecting the grease oil bleed where thermally aged grease will display much lower oil bleed measurement.

**Fig. 3** Graphical result of corrosion test on oil and grease



*Oil separation.* Excessive oil content and insufficient thickener in grease formulation result in oil separation from grease. It was shown that, from Table 4, only soft consistency greases ( $\leq$  NLGI 1) show oil separation on the grease surface. The amount of oil separated complied with an acceptable value of less than 4% (Lugt 2013b). As the WTO percentage is reduced and thickener content increases, the thickener was observed adequate to adsorb/hold the WTO in its matrix, which led to no oil separation occurred.

*Copper corrosion.* Figure 3 demonstrates the graphical results of the copper corrosion test conducted on base oil and selected greases. The stain on the copper strip indicates that the likelihood of the grease to cause corrosion on copper. In this study, sodium and FS grease corrosiveness are classified in class 1 (slightly tarnish). According to Kholijah et al. (2012), grease corrosion classified in Class 1 considered passed the ASTM corrosion test (Kholijah et al. 2012). From this, the results on grease corrosiveness test demonstrated that all grease constituents, base oil and thickener, were unlikely to cause corrosion to copper-containing metal.

### 6.2.1 Wear Preventive Characteristic

Oil is responsible for providing lubrication to the metal surface and grease is a sponge-like vessel to hold the oil in it until it is ready to be released for lubrication. The average COF of sodium and FS greases was found to be 0.119 and 0.133, respectively. The COF analysis shows that the thickener does not help in improving the grease resistance to friction since the COF of grease is closed to WTO's COF.

The COF of the present study is high when compared to some commercial greases and the previous grease tribological studies. This is again due to the absence of

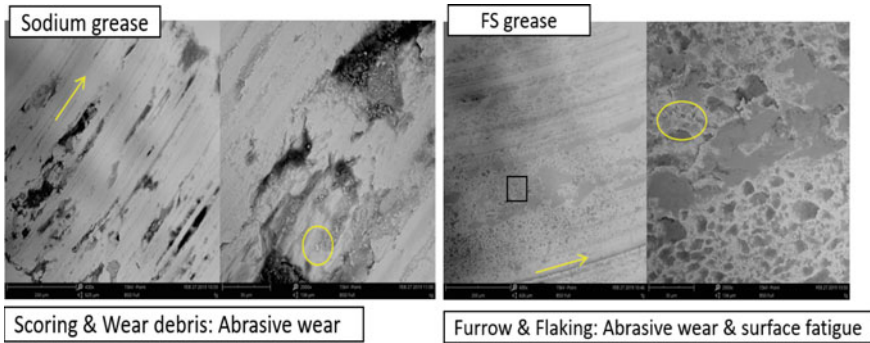


**Fig. 4** Wear micrograph of steel balls lubricated with sodium and FS grease

additive in grease. This test was conducted to study the anti-wear properties of the base grease itself without the additive—resulting in high COF due to no sacrificial layer to be worn during operation.

The wear micrograph (Fig. 4) does not show severe wear on the steel ball for both greases. Wear debris was visible which indicated removal of material through abrasion or adhesion mechanism. The wear scar diameter (WSD) measured under the microscope for both sodium and FS grease was 722 and 866  $\mu\text{m}$ , respectively. The EDX analysis of the worn surface shows the presence of iron (Fe), carbon (C) and oxygen (O), contributed by the steel ball, WTO and oxide layer. Both steel ball and WTO contain carbon elements in their composition; thus, there is a chance that the WTO layer was present. Element silicon (Si) was detected indicating the adherence of FS grease on the worn surface (Rawat et al. 2018).

## 7 Summary

Depending on the application and the operating and surrounding environmental conditions, grease with appropriate properties to serve the application can be chosen. Based on the WTO analysis, the treated WTO was concluded can be used as a base oil in grease formulation. The greases prepared using WTO were proved to have desirable properties of good structure and consistency, high dropping point with stable oil bleeding and no separated oil during the storage period, depending on the percentage of WTO. The oil's viscosity and VI, however, do not define whether or not the oil can be incorporated in the grease formulation since it is depended on the application of the grease. Oil of high viscosity often used in low-speed and high-load application and vice versa. Studies also proved that grease could be produced using low viscosity oil and hence concluded that WTO is viable to use as grease's base oil.

## References

- Abdulbari, H. A., & Zuhan, N. (2018). Grease formulation from palm oil industry wastes. *Waste and Biomass Valorization*, 9, 2447–2457.
- Abdulbari, H. A., Abid, R. T., & Mohammad, A. H. A. (2008). Fume Silica Base Grease. *Journal of Applied Chemistry*, 8, 687–691.
- Aja, O. C., Al-Kayiem, H. H., Zewge, M. G., & Joo, M. S. (2016). Overview of hazardous waste management status in Malaysia. In H. E.-D. M. Saleh, & R. O. A. Rahman (Eds.), *Management of hazardous wastes*. Rijeka: InTech.
- ASTM D2266-01. (2015). Standard test method for wear preventive characteristics of lubricating grease (four-ball method).
- ASTM D4048-16e1. (2016). Standard test method for detection of copper corrosion from lubricating grease.
- ASTM D130-18. (2018). Standard test method for corrosiveness to copper from petroleum products by copper strip test.
- ASTM D4172-18. (2018). Standard test method for wear preventive characteristics of lubricating fluid (four-ball method).
- Bots, S. (2014). Best methods for analyzing grease. *Machinery Lubrication*.
- Donley, E. (2012). *Handbook of advances in additive lubricants and grease technology* (Auris Reference).
- Ebisiike, K., Daniel, B., Anakaa, M., Kefas, H., & Olusunle, S. (2016). Effect of sodium hydroxide thickener on grease production. *Journal of the American Chemical Society*, 13, 1–8.
- Gonçalves, D., Graça, B., Campos, A. V., Seabra, J., Leckner, J., & Westbroek, R. (2015). Formulation, rheology and thermal ageing of polymer greases—Part I: Influence of the thickener content. *Tribology International*, 87, 160–170.
- Gresham, R. M. (2018). Short-term formulation trends. *Tribology & Lubrication Technology*, 74, 24–25.
- Hassan, A. M., Youssif, M. A., Mazrouaa, A. M., Shahba, R. M. A., & Youssif, M. A. E. (2013). Preparation of dielectric greases from some inorganic thickeners. *American Journal of Applied Chemistry*, 1, 9–16.
- Hassan, M., Syahrullail, S., & Ani, F. N. (2016). The tribological characteristics of the cactus and mineral oil. *Jurnal Teknologi (Sciences and Engineering)*, 78, 33–83.
- Hazardous Substance Division. (2010). *Guidelines on standard and specification of recovered waste oil in Malaysia*. Putrajaya, Malaysia: Department of Environment Malaysia.
- Iheme, C., Offurum, J. C., & Chukwuma, F. O. (2014). Production and blending of sodium based water-resistant lubricating greases from petroleum and petrochemical by-products. *American Journal of Computer Science and Engineering Survey*, 2, 70–78.
- Kholijah, A. M. S., Yeung, S. L. C., Sazwani, S., & Yunus, R. M. (2012). Production of high temperature grease from waste lubricant sludge and silicone oil. *Journal of Applied Chemistry*, 12, 1171–1175.
- Lugt, P. M. (2013a). Grease qualification testing. *Grease lubrication in rolling bearings* (pp. 346–347). West Sussex, UK: Wiley.
- Lugt, P. M. (2013b). Condition monitoring and maintenance. *Grease lubrication in rolling bearings* (pp. 283–337). West Sussex, UK: Wiley.
- Mohta, V., & Chaware, K. D. (2015). Preparation of alternative fuel from waste transformer oil and studying performance characteristics on diesel engine for different blends. *International Journal of Science and Research*, 4, 103–107.
- Nabi, M. N., Akhter, M. S., & Rahman, M. A. (2013). Waste transformer oil as an alternative fuel for diesel engine. *Procedia Engineering*, 56, 401–406.
- Noria Corporation. (2002). High-temperature grease guide. *Machinery Lubrication*.
- Nye Lubricants. (2016). *Learn more about copper corrosion testing*. Nye Lubricants.
- Rawat, S. S., Harsha, A. P., & Deepak, A. P. (2018). Tribological performance of paraffin grease with silica nanoparticles as an additive. *Applied Nanoscience*, 9, 305–315.

- Razali, M. N., Aziz, M. A. A., Hamdan, W. N. A. W. M., Salehan, N. A. M., & Rosli, M. Y. (2017). Synthesis of grease from waste oils and red gypsum. *Australian Journal of Basic and Applied Sciences*, *11*, 154–159.
- Rizvi, S. Q. A. (2008). *A comprehensive review of lubricant chemistry, technology, selection, and design*. West Conshohocken, PA: ASTM International.
- Zuan, A. M. S., Syahrullail, S., Yahya, W. J., Shafiq, M. N., & Fawwaz, Y. M. (2017). Tribological properties of potential bio-based lubricants from RBD palm stearin and palm fatty acid distillate. *Jurnal Teknologi (Sciences and Engineering)*, *79*, 21–26.

# Nanofiber-Immobilized $\beta$ -Galactosidase for Dairy Waste Conversion into Galacto-Oligosaccharides



Mailin Misson, Suryani Saallah, and Hu Zhang

**Abstract** Dairy industry waste effluents cause adverse environmental impact due to their high biological and chemical oxygen demand. Bioconversion into value-added products such as galacto-oligosaccharides (GOS) through  $\beta$ -galactosidase enzyme-mediated process would serve as a promising alternative for valorization of lactose-rich whey. This study aims to evaluate the functional ability of immobilized  $\beta$ -galactosidase enzyme for conversion of dairy waste into GOS. In the present study,  $\beta$ -galactosidase was immobilized on polystyrene nanofiber (PSNF) for enhanced enzyme stability and activity as well as reusability. PSNF surface was chemically modified using nitric acid ( $\text{HNO}_3$ ) to introduce functional groups for enzyme attachment. The stability of immobilized enzyme was evaluated at a range of pHs (4–11) and temperatures (10–70 °C) while the reusability was determined by measuring the enzyme activity after repeated uses. The immobilized enzyme was then applied for lactose conversion into GOS in batch and repeated batch systems. The findings showed that superior activity of the immobilized enzyme over free counterpart was observed at highly acidic (pH 4) or basic (pH 11) conditions and at elevated temperature up to 70 °C and exhibited activity up to 10 continuous cycles.  $\beta$ -galactosidase-PSNF had distinguished catalytic reaction profiles in repeated batch system by enhancing lactose conversion from 41 to 86% and GOS yield from 28 to 40% in comparison with conventional batch, suggesting an efficient valorization of lactose was achieved. Considering the numerous application and health benefits of GOS, conversion of lactose from dairy waste to GOS through an enzymatic approach presented in this study will not only decrease the environmental impact of dairy waste disposal but also contribute to economic development.

---

M. Misson (✉) · S. Saallah  
Biotechnology Research Institute, Universiti Malaysia Sabah, Jalan UMS,  
88400 Kota Kinabalu, Sabah, Malaysia  
e-mail: [mailin@ums.edu.my](mailto:mailin@ums.edu.my)

H. Zhang  
Henry E. Riggs School of Applied Life Sciences, Keck Graduate Institute,  
535 Watson Drive, Claremont, CA 91711, USA

# 1 Introduction

Dairy industry generates massive amounts of wastes rich in proteins, lipids, and carbohydrates that are susceptible to be transformed into valuable products with significant economic potential. Whey is a by-product of cheese and case in manufacturing with an annual production of approximately 200 million tons, corresponding to 6 million tons of lactose. The abundant amount of lactose in whey is associated with environmental problems due to their high biological and chemical oxygen demand (Mollea et al. 2013; Vasileva et al. 2016). Thus, bioconversion of lactose to value-added products such as galacto-oligosaccharides (GOS) has been seen as a promising approach for whey valorization, and currently, a subject of immense interest by researchers worldwide.

Galacto-oligosaccharides, a potent non-digestible oligosaccharide, are an essential class of dietary prebiotics regarded as ‘generally recognized as safe’ (GRAS) by the US Food and Drug Administration (FDA) and foods for specific health use in Japan (Jovanovic-Malinovska et al. 2012). GOS exerts beneficial effects on the intestinal microbiota and guts barrier function. The high stability of GOS under high temperatures and low pH environments, in addition to its low cariogenicity, caloric values, and sweetness have made GOS as commercially important functional ingredients in food products such as fermented milk, bread, confectionaries, and beverages (Ganzle 2012). GOS is present naturally in human and cow milk, honey and various types of fruits and vegetables. However, the amount of GOS present in these foods is too low to exert any significant health effect. Thus, the development of method for GOS production is necessary.

Synthesis of GOS can be performed via enzymatic transgalactosylation of lactose by  $\beta$ -galactosidases. Enzymes offer numerous advantages including environmentally friendly, higher specificity and selectivity, and lower energy requirement, yet their high price and poor operational stability limit their performance in their native state (Haghju et al. 2018; Wong et al. 2014). Immobilization of  $\beta$ -galactosidase onto a suitable matrix, particularly nanofibers, leads to promising solution to overcome these drawbacks.

Nanofibers produced through the cutting-edge technology of electrospinning offer several attractive features for enzyme immobilization. Besides their high surface area-to-volume ratio for significant improvement of the loading density and biocatalytic function, nanofibers also provide high flexibility and porosity, which endow them with low hindrance for mass transfer (Yunrong et al. 2010). More importantly, the collection of randomly arrayed nanofibers could form a membrane that enabled convenient separation of enzymes and products, ease of recovery, and allow the application of enzyme in large scale and continuous operations (De Jesús et al. 2016).

A considerable number of nanofibers made up of synthetic and natural polymers has been used for immobilization of  $\beta$ -galactosidase such as chitosan/polyvinyl alcohol (PVA) (Haghju et al. 2018) and poly (acrylonitrile-co-methyl methacrylate) poly (AN-co-MMA) (El-Aassar et al. 2013) using various immobilization approaches.



However, most of these methods favor the hydrolysis of lactose to glucose and galactose instead of GOS formation through transgalactosylation. To ensure efficient transgalactosylation of lactose to GOS, modulation of properties and local environment of the nanobiocatalyst is of fundamental importance.

It has been reported that the hydrophobic nature of polystyrene may beneficially promote transgalactosylation (Misson et al. 2016). Furthermore, the local environment of the nanobiocatalyst could reduce the diffusion path of nucleophilic molecules thus easily bind to the galactosyl–enzyme complex, hence favoring transgalactosylation than hydrolysis. Therefore, in this study, immobilization of  $\beta$ -galactosidase on acid-modified polystyrene nanofibers (PSNF) was conducted aiming to improve the enzyme stability and activity for lactose conversion into GOS. The biocatalytic performance of the immobilized enzyme at a range of temperature and pH was compared with the free enzyme. The reusability potential of the immobilized enzyme was tested up to 10 cycles of operation. Finally, the bioengineering performance of PSNF- $\beta$ -galactosidase in bioconversion of lactose into GOS was evaluated in batch and repeated batch systems.

## 2 Materials and Methods

### 2.1 Preparation of Nanofibrous Polystyrene by Electrospinning

Polystyrene solution was prepared by dissolving polystyrene (20% w/v) in DMF under mild stirring to form a homogenous solution. The solution was then allowed to cool at room temperature before fed into a 5 ml plastic syringe bearing a metal capillary (ID = 1.5 mm). The polystyrene nanofibers (PSNF) were produced by using the electrospinning system (Fig. 1) with voltage, flowrate, and duration were fixed at 25 kV, 2.5 ml/h and 3 h, respectively. The resultant PSNF was cast onto a metal-surface collector placed at 10 cm away from the needle tip. The PSNF was then detached from the collector surface and stored at room temperature for further use.

### 2.2 Enzyme Immobilization on Nanofibers

To introduce functional groups on the PSNF for enzyme attachment, the PSNF was immersed with nitric acid ( $\text{HNO}_3$ ) (69%) for 2 h at room temperature (An et al. 2015). The modified support was then rinsed with water and phosphate buffer saline (PBS pH 7.2) for three times to remove excess acids.  $\beta$ -galactosidase immobilization was carried out by submerging the nanofiber into  $\beta$ -galactosidase (2 mg/ml) solution in PBS and gently mixed overnight at 4 °C by agitation. The enzyme-bound nanofibers

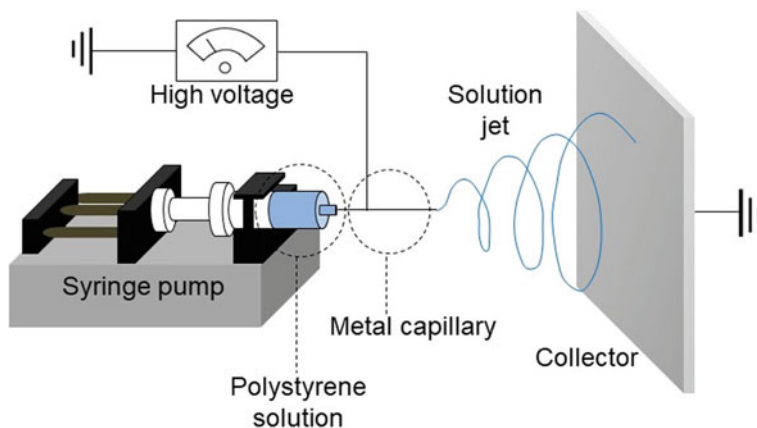


**Fig. 1** Setup of the electrospinning system

were separated from the reaction medium using forceps. Finally, the nanofibers were rinsed thoroughly with water to remove the free  $\beta$ -galactosidase.

### 2.3 Synthesis of Galacto-Oligosaccharides

Lactose solution (400 g/L) was prepared by dissolving lactose into PBS (pH 7.2) at 60 °C. The solution was allowed to cool down to 37 °C before addition of enzyme (free or immobilized). The enzymatic reaction was performed for 2 h in an orbital shaker with temperature of 37 °C and stirring speed of 200 rpm. After that, the sample was drawn and immediately heated in boiling water for 5 min to stop the reaction (Rodríguez-Colinas et al. 2014). Prior to high performance liquid chromatography (HPLC) analysis, the sample was filtered and diluted 40 times. Lactose conversion in repeated batch system was carried out in a recirculating spiral  $\beta$ -galactosidase-nanofiber reactor as described by Misson et al. (2017).

### 2.4 Chemical Analysis

Determination of sugar (lactose, glucose, and galactose) in the sample was performed by HPLC (Agilent, Germany) using an Aminex HPX-87H column (300 × 7.8 mm). The flow rate of a pre-degassed 8 mmol/L- $\text{H}_2\text{SO}_4$  mobile phase was set at 0.5 ml min<sup>-1</sup>. A total of 5  $\mu\text{l}$  samples was injected and the saccharides were detected with a refractive index detector. The column and the detector cell were maintained at 60 °C and 40 °C, respectively (Zheng et al. 2006). The lactose conversion (%) and GOS yield (%) were calculated using Eq. (1–2) (Gosling et al. 2009).

$$\text{Lactose conversion(\%)} = \frac{[\text{initial lactose}] - [\text{final lactose}]}{[\text{initial lactose}]} \times 100 \quad (1)$$

$$\text{GOS(\%)} = \% \text{conversion} - \% \text{glucose} - \% \text{galactose} \quad (2)$$

## 2.5 *Enzymatic Activity Assays*

The free and immobilized enzyme activity with a concentration of 2 mg/ml was measured according to the procedure described by Ansari and Husain (2012). The liberated product was measured by spectrophotometer at 405 nm and the concentration was calculated from the O-nitrophenol standard curve. One unit (1 U) of  $\beta$ -galactosidase is defined as the amount of enzyme which liberates 1  $\mu$ mole of O-nitrophenol per min under standard assay condition.

## 2.6 *Effect of PH and Temperature of Immobilized Enzyme*

pH and thermal stability of the free and immobilized enzyme (2 mg/ml) were examined by measuring the enzyme activity in PBS buffers with pH and temperature ranging from 4 to 11 and temperature 10–70 °C, respectively. The enzyme activity at pH 7 was used as a control (100%) for the calculation of other assay conditions.

## 2.7 *Reusability*

The recycling stability of the immobilized  $\beta$ -galactosidase was assessed by measuring the activity repeatedly after hydrolysis of ONPG substrate using PBS buffer (pH 7) at 37 °C. After each cycle, the immobilized enzyme was separated from the reaction medium and washed thoroughly with water. The activity was measured in the supernatant using the method described in Sect. 2.5. The immobilized enzyme was then re-suspended in freshly prepared substrate solution and enzymatic reaction was performed under the same conditions. The process was repeated up to 10 cycles of operation. The activity determined in the first cycle was considered as control and attributed to a relative activity of 100% for the determination of remaining activity after repeated uses.

## 2.8 Statistical Analysis

Data was collected in triplicates and analyzed using the statistical tool in MS Excel 2010. Each value corresponds to the mean of experimental data with an average standard deviation of <5%.

## 3 Results and Discussion

### 3.1 Morphological Observation of $\beta$ -Galactosidase-Nanofiber

Large surface area and good quality with minimal defects are two important criteria in nanofiber synthesis as enzyme carrier. Nanofibers with a large surface area are essential to accommodate high enzyme loading while presence of defects on nanofiber surface could possibly reduce enzyme adsorption capacity. The quality of the nanofiber is majorly affected by electrospinning operating variables such as polymer concentration, electric voltage, and the distance between needle tips and collector. The polymer concentration has been reported to strongly influence the quality of polystyrene nanofiber (PSNF) (Misson et al. 2016). Smooth surface, uniform size, and bead-free electrospun mat could be obtained when using 20% (w/v) polymer regardless of electric voltage or distance. The morphological observation of  $\beta$ -galactosidase-free and  $\beta$ -galactosidase-loaded PSNF under SEM visualization is shown in Fig. 2.

The distribution of  $\beta$ -galactosidase on the nanofiber surface was further visualized using fluorescence-assisted images under a fluorescence microscope. The enzyme was initially tagged with fluorescence molecules prior to immobilization. As Fig. 3a indicates, green fluorescence emitted from the FITC-tagged enzyme is observed equally distributed along the nanofibers surface indicating the presence of enzyme molecules. Negative control of non-fluorescence excitation of  $\beta$ -galactosidase-loaded nanofiber was used as a comparison (Fig. 3b) while nanofibers without enzyme under the same fluorescence conditions were used to account for the fluorescence background (Fig. 3c).

### 3.2 Stability of Immobilized $\beta$ -Galactosidase

The stability of the  $\beta$ -galactosidase-nanofiber assembly was evaluated at different pH and temperature and benchmarked with the activity of free enzyme (Fig. 4). Maximal enzyme activity for both free and immobilized  $\beta$ -galactosidase was found at pH 7. Interestingly, the immobilized enzyme showed greater activity at almost all tested pH conditions and extended the enzyme stability at extreme pH conditions.

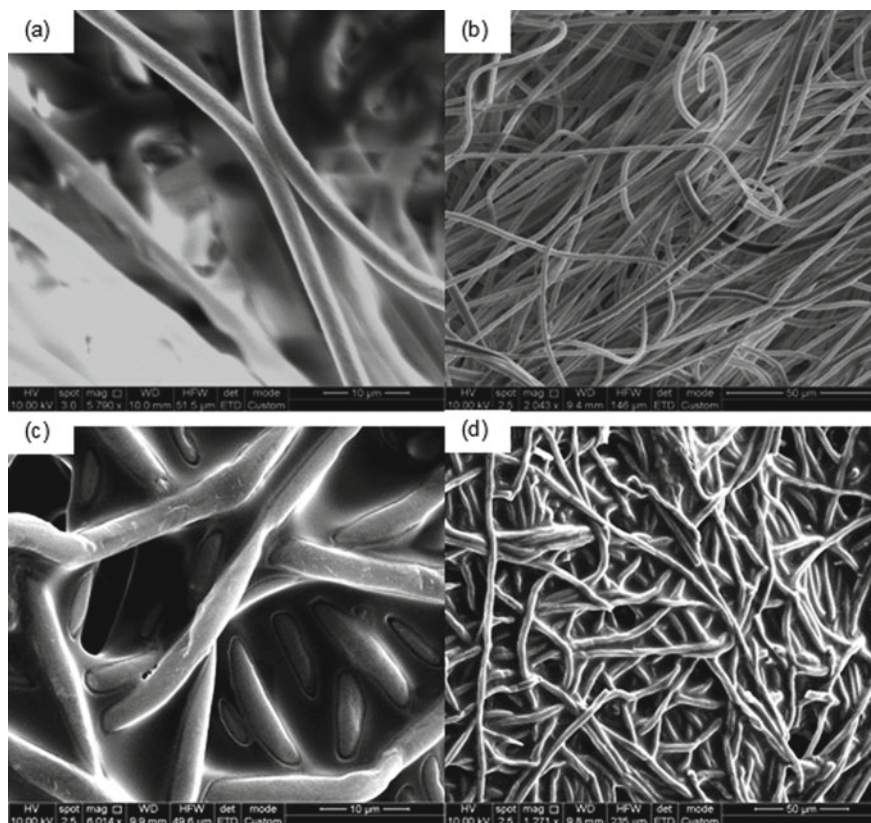


**Fig. 2** SEM images of **a–b**  $\beta$ -galactosidase-free nanofiber and **c–d**  $\beta$ -galactosidase-loaded nanofiber at 10  $\mu$ m and 50  $\mu$ m, respectively

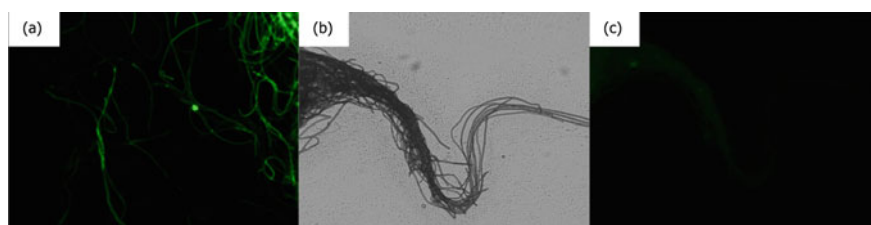


**Fig. 3** Visualization of **a** fluorescence image excitation of FITC-tagged  $\beta$ -galactosidase immobilized on nanofiber, **b** nanofiber- $\beta$ -galactosidase without fluorescence excitation as negative control and **c** nanofiber fluorescence background

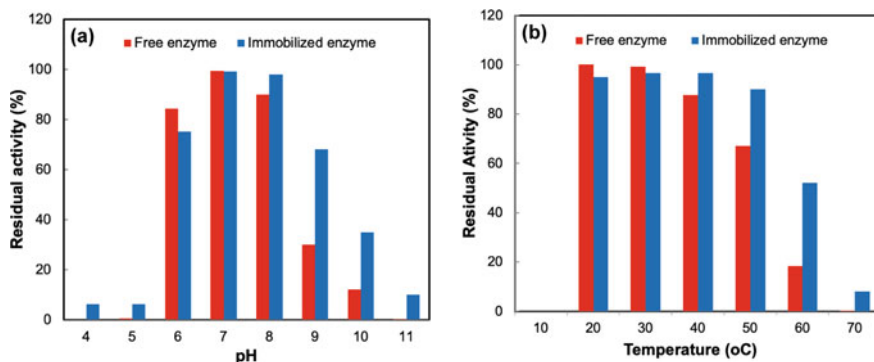


**Fig. 4** Stability of nanofiber-loaded  $\beta$ -galactosidase in comparison with free enzyme at different **a** pH and **b** temperature conditions. Each value corresponds to the mean of triplicate experimental data with an average standard deviation of  $<5\%$ . The activity of free enzyme (2.08 U/mg) at pH 7 was selected as a control (100%)

At highly acidic (below pH of 6) or highly basic pH (above pH of 10) (Fig. 3a), a noticeable enzyme activity was exhibited by the immobilized enzyme while the free counterpart indicated a complete loss of activity probably due to alteration of enzyme native structure (Neri et al. 2008). These findings signified the enzyme support environment could shelter or stabilize enzyme in extreme pH conditions.

Figure 4b presents the effect of temperature on the activity of free and immobilized  $\beta$ -galactosidase. As can be seen, there was no activity detected at the lowest temperature. The temperatures ranging from 20 to 40 °C was found optimal with comparable activity (nearly 100%) for both tested enzyme conditions. Beyond the optimal temperature, a significant drop of activity by free enzyme while the immobilized  $\beta$ -galactosidase continued to retain about 60 and 10% of its residual activity at 60 °C and 70 °C, respectively. The loss of enzyme activity may be due to the rupture of enzyme polypeptide chains that led to enzyme molecules denaturation at higher temperatures (Ansari et al. 2012). Meanwhile, the nanofiber matrix might be able to interact and protect the polypeptide chains in a harsh environment. This finding was in agreement with the reported study of immobilized  $\beta$ -galactosidase on zinc oxide nanoparticles. The optimal temperatures were extended from 50 to 60 °C (Husain et al. 2011).

### 3.3 Reusability of Immobilized $\beta$ -Galactosidase

The overall process for enzyme immobilization on nanofiber appears economically viable if the enzyme catalytic reaction is relatively high and reusable (Misson et al. 2015). A bench trial was conducted to evaluate the  $\beta$ -galactosidase activity up to 10 cycles of operation. The remaining activity of the enzyme in subsequent cycles

**Table 1** Recyclability study of the nanofiber-loaded  $\beta$ -galactosidase conducted up to 10 cycles of operation

Number of cycle	Residual enzyme activity (%)
1	100
2	95
3	72
4	66
5	55
6	38
7	32
8	28
9	22
10	20

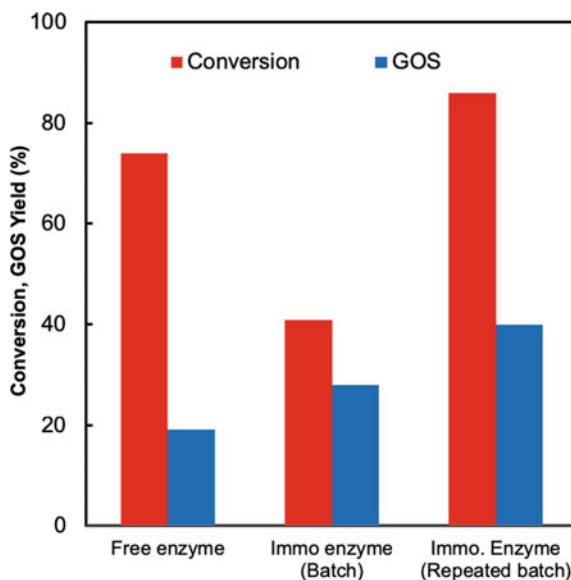
The activity determined at the first cycle was considered as a control (100%). (Operation conditions: at 37 °C with 2 mg/ml enzyme concentration in pH 7)

was measured by using the first cycle of reaction as a controlled study (100% activity). Table 1 tabulates the recyclability of the  $\beta$ -galactosidase-nanofiber assembly. The activity of the immobilized  $\beta$ -galactosidase was found to decrease gradually after several repeated uses. The first five cycles indicated a residual activity above 50%, while the remaining five cycles showed some remarkable activities within 20–38%. Its reusability up to 10 cycles provides promising benefits of immobilized  $\beta$ -galactosidase over free enzyme. As for comparison, some reported enzyme-matrix assembly only lasted for about seven (Xu et al. 2013) and six (Wu et al. 2005) cycles with the remaining activity of 20% and 35%, respectively. Hence, the findings of this study indicate the potential of  $\beta$ -galactosidase-nanofiber for GOS production on a larger scale.

### 3.4 Biocatalytic Performance of Free and Immobilized Enzyme

The biocatalytic performance of the  $\beta$ -galactosidase-nanofiber in converting lactose into galacto-oligosaccharide (GOS) was further investigated in batch and repeated batch system and further compared with the free enzyme (Fig. 5). The in-house fabricated recirculating spiral reactor has been reported in the previous study (Misson et al. 2017). Enzyme-containing nanofibers were spread onto a mesh as support. The mesh was rolled in a spiral form and located inside the reactor to enhance the surface area for catalytic reaction besides increasing mass transfer efficiency. Lactose inside the feed reservoir was also recirculated back into the reactor controlled by a pump to enhance the biocatalyst-substrate reaction time inside the reactor. As shown

**Fig. 5** Yield of lactose conversion and galacto-oligosaccharides (GOS) by free enzyme and immobilized enzyme in batch and repeated batch system using 400 g/L initial lactose concentration. (Operation conditions: at 37 °C with 2 mg/ml enzyme concentration in pH 7)



in Fig. 5, the lactose conversion by the free enzyme (75%) was higher than the immobilized enzyme in batch system (41%). The low conversion could be associated with low mass transfer and molecule diffusion within the enzyme-nanofiber network. Nevertheless, the immobilized enzyme appears to have a better catalytic capability for synthesizing GOS (28%) than the free counterpart (19%). In repeated batch system, the immobilized enzyme was observed more superior and that could be due to the higher surface area of biocatalytic reaction. The conversion (86%) and GOS (40%) yield were 1.2 times and 2.1 times higher than that of free enzyme. The hydrophobic nature of nanofibers reduced the water-driven hydrolysis activity and enhanced the selectivity toward transgalactosylation for GOS production (Misson et al. 2016).

## 4 Conclusion

A successful immobilization of  $\beta$ -galactosidase on the nanofiber surface was demonstrated as confirmed through observation using SEM and fluorescence microscopy. Enzyme stabilization in immobilization system was indicated by its superior activity at highly acidic (pH 4) or basic (pH 11) conditions and elevated temperature (70 °C). The  $\beta$ -galactosidase-nanofiber assembly exhibited promising benefits over free counterpart by retaining significant amount of enzyme activities up to 10 cycles of repeated uses. Overall,  $\beta$ -galactosidase-nanofiber shows an excellent catalytic performance in bioconversion of lactose-rich dairy waste into valuable product in recirculating column reactor and enhances the conversion from 41 to 86% and the GOS yield



from 28 to 40%. With remarkable enhancement of enzyme stability and noteworthy bioengineering performances, the nanofiber-immobilized  $\beta$ -galactosidase can be potentially applied in a large-scale application for waste conversion into value-added products.

## References

- An, H., Jin, B., & Dai, S. (2015). Fabricating polystyrene fiber-dehydrogenase assemble as a functional biocatalyst. *Enzyme and Microbial Technology*, 68, 15–22.
- Ansari, S. A., & Husain, Q. (2012). Lactose hydrolysis from milk/whey in batch and continuous processes by concanavalin A–Celite 545 immobilized *Aspergillus oryzae*  $\beta$  galactosidase. *Food and Bioprocess Technology*, 90(2), 351–359.
- Ansari, S. A., Satar, R., Alam, F., Alqahtani, M. H., Chaudhary, A. G., Naseer, M. I., et al. (2012). Cost effective surface functionalization of silver nanoparticles for high yield immobilization of *Aspergillus oryzae*  $\beta$ -galactosidase and its application in lactose hydrolysis. *Process Biochemistry*, 47, 2427–2433.
- De Jesús, M., Mancera-Andrade, E. A., Patiño, M. B. G., Arrieta-Baez, D., Cardenas, B., Martinez-Chapa, S. O., et al. (2016). Nanobiocatalysis: nanostructured materials—a minireview. *Biocatalysis*, 2, 1–24.
- El-Aassar, M. R., Al-Deyab, S. S., & Kenawy, E. R. (2013). Covalent immobilization of  $\beta$ -galactosidase onto electrospun nanofibers of poly (AN-co-MMA) copolymer. *Journal of Applied Polymer Science*, 127, 1873–1884.
- Ganzle, M. G. (2012). Enzymatic synthesis of galacto-oligosaccharides and other lactose derivatives (hetero-oligosaccharides) from lactose. *International Dairy Journal*, 22(22), 116–122.
- Gosling, A. A., Stevens, G. W., Barber, A. R., Kentish, S. E., Gras, S. L. (2009). Facile pretreatment of bacillus circulans  $\beta$ -galactosidase increases the yield of galactosyl oligosaccharides in milk and lactose reaction systems. *Journal of Agricultural and Food Chemistry*, 57, 11570–11574.
- Haghju, S., Bari, M. R., & Khaled-Abad, M. A. (2018). Affecting parameters on fabrication of  $\beta$ -D-galactosidase immobilized chitosan/poly (vinyl alcohol) electrospun nanofibers. *Carbohydrate Polymers*, 200, 137–143.
- Husain, Q., Ansari, S. A., Alam, F., & Azam, A. (2011). Immobilization of *Aspergillus oryzae* beta galactosidase on zinc oxide nanoparticles via simple adsorption mechanism. *International Journal of Biological Macromolecules*, 49, 37–43.
- Jovanovic-Malinovska, R., Fernandes, P., Winkelhausen, E., & Fonseca, L. (2012). Galacto-oligosaccharides synthesis from lactose and whey by beta-galactosidase immobilized in PVA. *Applied Biochemistry and Biotechnology*, 168, 1197–1211.
- Misson, M., Dai, S., Jin, B., Chen, B. H., & Zhang, H. (2016). Manipulation of nanofiber-based  $\beta$ -galactosidase nanoenvironment for enhancement of galacto-oligosaccharide production. *Journal of Biotechnology*, 222, 56–64.
- Misson, M., Jin, B., & Zhang, H. (2017). Recirculating spiral bioreactor for galactooligosaccharide production using polymer nanofiber- $\beta$ -galactosidase assembly. *Industrial and Engineering Chemistry Research*, 56, 12479–12487.
- Misson, M., Zhang, H., & Jin, B. (2015). Nanobiocatalyst advancements and bioprocessing applications. *Journal of Royal Society Interface*, 12, 1–8.
- Mollea, C., Marmo, L., & Bosco, F. (2013). Valorisation of cheese whey, a by-product from the dairy industry. In *TECH*.
- Neri, D. F. M., Balcao, V. M., Carneiro-Da-Cunha, M. G., Carvalho Jr, L. B., & Teixeira, J. A. (2008). Immobilization of  $\beta$ -galactosidase from *kluyveromyces lactis* onto a polysiloxane–polyvinyl alcohol magnetic (mPOS–PVA) composite for lactose hydrolysis. *Catalysis Communications*, 9, 2334–2339.

- Rodriguez-Colinas, B., Fernandez-Arrojo, L., Ballesteros, A. O., & Plou, F. J. (2014). Galactooligosaccharides formation during enzymatic hydrolysis of lactose: towards a prebiotic-enriched milk. *Food Chemistry*, 145, 388–394.
- Vasileva, N., Ivanov, Y., Damyanova, S., Kostova, I., & Godjevargova, T. (2016). Hydrolysis of whey lactose by immobilized  $\beta$ -galactosidase in a bioreactor with a spirally wound membrane. *International Journal of Biological Macromolecules*, 82, 339–346.
- Wong, D. E., Dai, M., Talbert, J. N., Nugen, S. R., & Goddard, J. M. (2014). Biocatalytic polymer nanofibers for stabilization and delivery of enzymes. *Journal of Molecular Catalysis. B, Enzymatic*, 110, 16–22.
- Wu, L., Yuan, X., & Sheng, J. (2005). Immobilization of cellulase in nanofibrous PVA membranes by electrospinning. *Journal of Membrane Science*, 250, 167–173.
- Xu, R., Zhou, Q., Li, F., & Zhang, B. (2013). Laccase immobilization on chitosan/poly(vinyl alcohol) composite nanofibrous membranes for 2,4-dichlorophenol removal. *Chemical Engineering Journal*, 222, 321–329.
- Yunrong, D., Junfeng, N., & Lifeng, Y. (2010). Electrospun nanofiber membranes as supports for enzyme immobilization and its application. *Progress in Chemistry*, 22, 1808–1818.
- Zheng, P., Yu, H., Sun, Z., Ni, Y., Zhang, W., Fan, Y., et al. (2006). Production of galactooligosaccharides by immobilized recombinant beta-galactosidase from *Aspergillus candidus*. *Biotechnology Journal*, 1, 1464–1470.

# Treatment of Petroleum-Based Industrial Wastewater Using Electrocoagulation Technology



Faten Ahada Mohd Azli, Abdul Aziz Mohd Azoddein, Mazrul Nizam Abu Seman, Agus Sahar Abdul Hamid, Tahfiz Tajuddin, and Said Nurdin

**Abstract** In the present study, electrocoagulation (EC) was used for the treatment of petroleum-based wastewater. The experiments were carried out using a continuous flow EC apparatus. Wastewater samples were taken from two different petroleum-based companies in East Coast and Melaka with an initial chemical oxygen demand (COD) of 16,000 ppm and 330 ppm, respectively. In this work, the current was varied from 1.0 to 4.0 A, the contact time was 5–20 min, and different electrode types (aluminium and stainless steel) were employed to achieve maximum COD removal. For medium COD wastewater (16,000 ppm), a maximum COD removal of 88% was achieved when the current, contact time and type of electrode were 2.0 A, 5 min, and aluminium, respectively. For the treatment of low COD wastewater sample (330 ppm), the performance of EC using aluminium as the electrode exhibited better COD removal than stainless steel.

**Keywords** Electrocoagulation · Petroleum industry · Wastewater · COD removal

## 1 Introduction

By 2035, the energy demand is expected to increase by 37% compared to 2013 (BP Energy Outlook 2035, 2015), with the major energy source coming from petroleum-based products (Jafarinejad & Jiang 2019). The increasing demand for petroleum-based products and growth of petroleum-based industry directly lead to increased wastewater from petroleum-based industries. According to Jafarinejad (2017), this industry uses the largest amount of water and at the same time generates a large amount of wastewater. Generally, a series of physical, chemical, and biological treatments are employed in a plant to treat the wastewater produced. However, the treatment requires a high cost. So, an alternative technology needs to be developed

---

F. A. Mohd Azli · A. A. Mohd Azoddein · M. N. Abu Seman (✉) · T. Tajuddin · S. Nurdin  
Faculty of Chemical and Process Engineering Technology, Universiti Malaysia Pahang,  
26300 Gambang, Pahang, Malaysia  
e-mail: [mazrul@ump.edu.my](mailto:mazrul@ump.edu.my)

A. S. Abdul Hamid  
MY Synergy Factors (M) Sdn. Bhd., Indera Mahkota, 25150 Kuantan, Pahang, Malaysia

© Springer Nature Singapore Pte Ltd. 2020  
A. Z. Yaser (ed.), *Advances in Waste Processing Technology*,  
[https://doi.org/10.1007/978-981-15-4821-5\\_4](https://doi.org/10.1007/978-981-15-4821-5_4)

for the mutual benefit of people and the environment. Other than that, Malaysia's DOE strictly regulates wastewater treatment, thus requiring it to be efficient and cost-effective.

Environmental quality and safety are issues of concern for the Malaysian government. Environmental pollution causes many serious problems, especially to aquatic life and human being. Several large refining and petrochemical plants exist in Malaysia, especially in the East Coast region. These industrial plants, especially petroleum refineries, generate a large amount of wastewater that contains many chemicals and suspended solids (Khan et al. 2015). According to Ashrafi et al. (2013), the concentration of organic and inorganic contaminants is commonly high in industrial wastewater and various types of treatment are used based on the concentration and types of contaminants. The wastewater needs to be treated before it can be discharged and must follow the regulation criteria (Altaher et al. 2011). As a consequence, the government has set legislations and guidelines for the industry. Each industrial sector must obey the guidelines set by the DOE.

Even though various methods are available for water and wastewater treatment, conventional methods require a high cost. The reuse of treated wastewater has gained preferable attention where it has several advantages over other sources of water including minimises pollution, expands groundwater resources by artificial recharge, and is a good nutrient source for landscape and farm irrigation (Saleem 2009; Saleem et al. 2000). Implementation of new environmentally friendly and cost-effective treatment method should be done. One of the technologies that are gaining attention is electrocoagulation.

Electrocoagulation is considered as an emerging technology combines the functions and advantages of conventional methods such as electrochemistry, coagulation and flotation (Kuokkanen et al. 2013). It applies the same concept as coagulation, in which the coagulant is generated from its own electrode without any need for additional chemical coagulant. Electrocoagulation is based on the electrolysis principle that consists of metal electrodes and electric current. The oxidation and reduction reactions occur at the anode and cathode, respectively. For example, using aluminium as electrode for both cathode and anode, the mechanism of ions generated by electrocoagulation can be explained by the following reactions (Jotin et al. 2012; El-Naas et al. 2009).

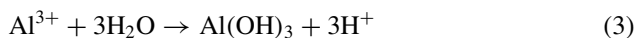
The oxidation reaction occurs at the anode,



The reduction reaction occurs at the cathode,



In the solution,



The electrodes generate coagulated species and metal hydroxides (i.e.  $\text{Al}(\text{OH})_3$ ) destabilise and aggregate the suspended solids. During the process, hydrogen ( $\text{H}_2$ ) gas is released and this helps the flocculated particles to float (Nasrullah et al. 2012). Electrocoagulation is an economical and environmentally friendly process because it is portable and only needs an optimum space to place the system. This process only uses a simple and compact reactor without generating secondary pollutants (Morenno-Casillas et al. 2007). Reviews of previous studies have stated that this is an appealing method for treating wastewater. It is also suitable for different types of industries. Other than that, the flocs produced by this process are large (Larue & Vorobiev 2003) and no extensive chemical is required (Ni'am et al. 2007). Electrocoagulation has been widely used in wastewater treatment from leachate (Zailani et al. 2018; Jotin et al. 2012; Orkun & Kuleyin 2012; Bouhezila et al. 2011; Top et al. 2011; Chiang et al. 1995), paper mill and pulp (Katal & Phlavanzadeh 2011; Ugurlu et al. 2008; Sridhar et al. 2011), and distillery spent wash (Khandegar & Saroha 2012; Krishna et al. 2010; Prasad & Srivastava 2009; Thakur et al. 2009) to reduce chemical oxygen demand (COD). However, the treatment of petroleum-based wastewater using electrocoagulation has not been reported much. Based on the review paper published by Khandegar and Saroha (2013) on wastewater treatment using EC for COD removal, out of 57 papers published within 1994–2013, only one paper related to petroleum refinery was published. Hence, this work focuses on the performance of the EC process for the treatment of petroleum wastewater samples, especially on COD reduction.

## 2 Experimental Work

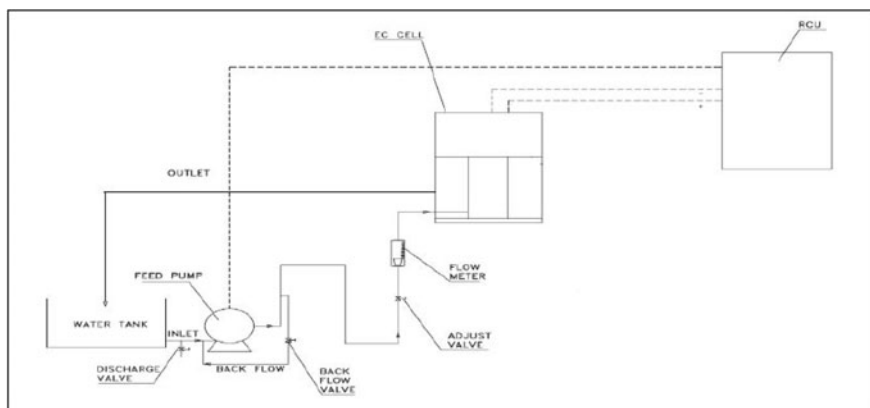
### 2.1 Enhancement of Electrocoagulation System

Figure 1a shows an electrocoagulation reactor. It consists of a feed tank, pump, backflow valve, bag filter, adjust valve, flow metre, discharge valve, EC cell, remote control unit (RCU) and discharge tank. All components are interconnected to make a complete electrocoagulation process as shown in Fig. 1b. The cross section and view of electrocoagulation reactor are shown in Fig. 1b. The electrocoagulation reactor was designed with the maximum flow rate of 60 L/h and equipped with a voltage regulator to control the current. The reactor has a DC output of 110 and 10 A (max) and an AC input of 220 V and 5 A. The complete process flow of electrocoagulation treatment is illustrated in Fig. 1c. In this work, two operating parameters (current [A] and contact time) and type of electrode (aluminium and stainless steel) were investigated to maximise the quality of wastewater after the treatment using electrocoagulation.



(a)

(b)



(c)

**Fig. 1** a Control panel, b side view of electrocoagulation reactor, and c complete process flow of electrocoagulation treatment

## 2.2 Sample

The enhanced EC system was tested with two samples taken from petroleum-based companies in the East Coast and Melaka.

## 2.3 Sample Testing

The quality of water in terms of COD value was analysed prior to and after the run using COD Digestion Reagent Vials High Range (435 COD HR). The removal efficiency of COD during the treatment was evaluated by using the following equation:

$$\%R = \frac{C_0 - C}{C_0} \times 100$$

where  $C_0$  and  $C$  are the concentrations of COD before and after the treatment, respectively.

# 3 Results and Discussion

## 3.1 Petroleum-Based Company in East Coast (PCEC)

The sample from PCEC was tested by setting different values of the current and contact time. Aluminium electrode was used as the sacrificial anode, and the initial value of COD was 16,000 ppm. The initial current was 1.0 A, and it was increased until 4.0 A within 5–20 min of contact time. The data are presented in Table 1. The value of COD (ppm) after electrocoagulation process showed a sharp decrease in a short contact time (5 min) and slowed down gradually. The final values of COD (ppm) were different between different current settings. For 1.0 A, the value gradually decreased as the time increased but the reading was considered higher compared to other currents used. When the current was set to 2.0 A, the COD value sharply decreased in short contact time within 5 min, and after that, the value varied as the time increased until it decreased to 1900 ppm after 20 min. As for the current setting of 3.0 A, the value of COD gradually decreased in 10 min, and after that, it varied as the time increased until the value reached 1980 ppm after 20 min. For the current setting of 4.0 A, the COD value sharply decreased after 5 min, but the value was higher compared to the current setting of 2.0 A and after 20 min, the value was 5500 ppm.

The clear trend of COD percentage removal for different currents and contact times is shown in Fig. 2. Higher COD removal was achieved when the current was

**Table 1** Removal efficiency of COD from PCEC sample with different current settings using aluminium electrode

Time (min)	Current (A)	pH	COD (ppm)	Removal efficiency of COD (%)
0	1.0	7.00	16,000	0
5		7.95	9200	42.5
10		8.83	8100	49.4
15		9.11	7900	50.6
20		9.32	7600	52.5
5	2.0	9.08	1910	88.0
10		9.62	1980	87.6
15		9.92	2040	87.3
20		10.37	1900	88.1
5	3.0	8.67	7400	53.8
10		9.84	2020	87.4
15		10.15	1990	87.6
20		10.67	1980	87.6
5	4.0	8.67	5100	68.1
10		9.84	5200	67.5
15		10.15	5500	65.6
20		10.67	5500	65.6

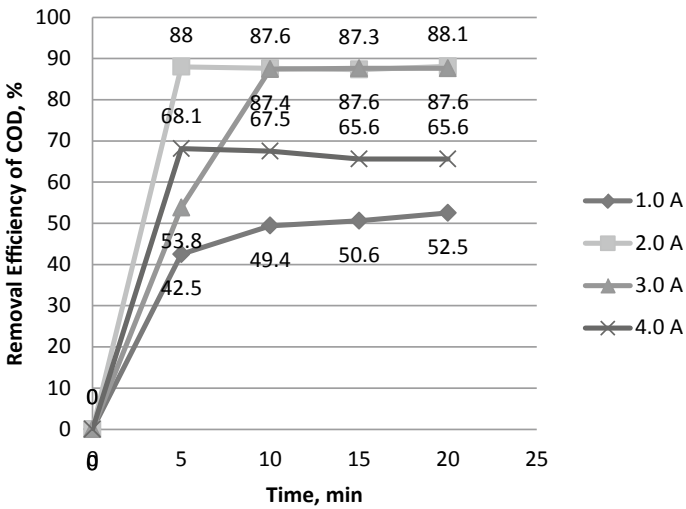


**Fig. 2** COD removal efficiency at different contact times for PCEC samples



increased from 1.0 to 3.0 A. However, the COD percentage removal sharply decreased when the current was increased to 4.0 A. The similar trend was observed by Zailani et al. (2018) and Jotin et al. (2012) when treating leachate wastewater using EC. Bayar et al. (2011) investigated the effect of current density on the COD removal efficiency of poultry slaughterhouse wastewater and found that in certain cases, the COD removal efficiency decreased as the current density was increased. An increment in the current density leads to an increase in the number of metal hydroxide ( $\text{Al}(\text{OH})_3$ ) flocs and indirectly improves the efficiency of pollutant removal. However, current density higher than the optimum value has no significant effect on pollutant removal efficiency due to sufficient metal hydroxide flocs available for sedimentation to occur (Khandegar & Saroha 2013). In the worst-case scenario, if the current density is higher than the optimum point, the produced ions will restabilise the flocs and reduce the removal efficiency (Zailani et al. 2018). At low current density (1.0 A), it was observed that the COD removal was increased from 42.5 to 52.5% as the contact time increased. For a longer contact time, there is an increase in the generation of flocs resulting in an increase in the COD removal efficiency (Khandegar & Saroha 2013). However, there is no significant effect of contact time on COD removal when the higher current setting was applied (2.0–4.0 A). In this case, when the contact time beyond the optimum point, the COD removal efficiency almost constant as sufficient numbers of flocs are available for the removal of the pollutant (Khandegar & Saroha 2013). From Fig. 2, the best contact time with the highest COD removal efficiency was observed for sample treated at 5 min using 2.0 A as current setting.

Overall, the best parameters for COD removal using electrocoagulation are 2.0 A current setting, 5 min contact time, and aluminium electrode as the sacrificial electrode, which reduced COD value from 16,000 to 1900 ppm with more than 88% removal. Figure 3 shows the water quality for PCEC sample before and after electrocoagulation process using 2.0 A current. The sample's colour changed from dark

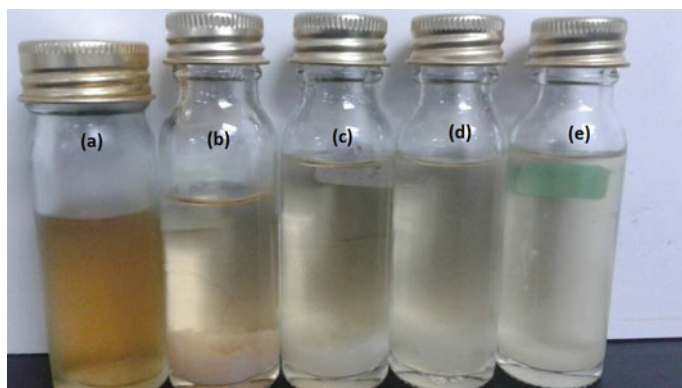


**Fig. 3** Water quality after EC using 2.0 A at different contact times of **a** 0 min, **b** 5 min, **c** 10 min, **d** 15 min, and **e** 20 min for PCEC sample

**Table 2** COD removal efficiencies from PCM sample with different electrodes

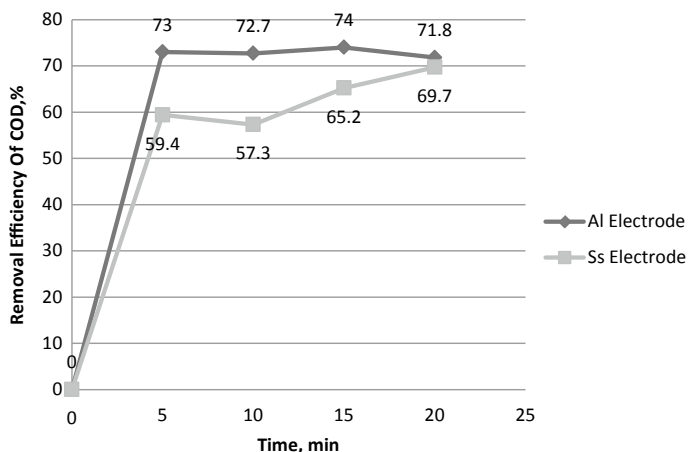
Time (min)	pH	Electrode	COD (ppm)	COD removal efficiency (%)
0	7.12	Aluminium	330	0
5	10.55	Aluminium	89	73.0
10	10.39	Aluminium	90	72.7
15	10.69	Aluminium	86	74.0
20	11.10	Aluminium	93	71.8
5	10.27	Stainless steel	134	59.4
10	11.66	Stainless steel	141	57.3
15	11.80	Stainless steel	115	65.2
20	11.79	Stainless steel	100	69.7

brown to colourless, which indicates successful electrocoagulation for the treatment of petroleum-based wastewater.

### 3.2 *Petroleum-Based Company in Melaka (PCM)*

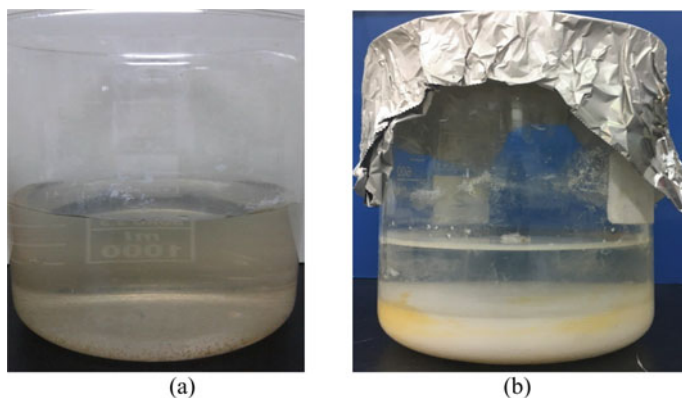
The initial COD value for PCM sample was 300 ppm. In this testing, the current was set to 2.0 A (based on PCEC results), and a different electrode was used to determine the best performance of electrocoagulation. The PCM sample was tested by using different types of electrode, aluminium and stainless steel. The results are given in Table 2. The COD (ppm) value sharply decreased in short contact time and slowly varied as the contact time increased as shown in Table 2. The aluminium electrode reduces the COD value from 330 to 89 ppm in short contact time. This value is higher compared to the one obtained by the stainless steel electrode, which decreased the value to 134 ppm in short contact time. As the contact time increased, the value of the COD also decreased for both types of electrode used, but for the aluminium electrode, the value slightly increased to 93 ppm after 15 min.

Figure 4 shows the relationship between the contact time of the electrode and the sample with the removal efficiency of COD. The percentage of COD removal efficiency sharply increased in short contact time. After that, the percentage varied as the contact time increased for both electrodes. Using the aluminium electrode resulted in a removal efficiency percentage of 73%, which was higher compared to the value obtained by the stainless steel electrode (59.4%). As the contact time increased, the stainless steel electrode showed gradually increasing removal percentage until 20 min of contact time, where the final value was 69.7%. Meanwhile, the removal percentage obtained for the aluminium electrode fluctuated, and the final percentage after 20 min of contact time was 71.8%. Furthermore, the aluminium electrode showed the highest percentage of COD removal (74%) at a contact time of 15 min. In contrast, the stainless steel electrode had the highest percentage of COD removal at 20 min contact time, which was 69.7%. This value is still lower



**Fig. 4** COD removal efficiency at different contact times for PCM sample using different electrodes (Al—Aluminium; Ss—Stainless Steel)

compared to that obtained when the aluminium electrode was used. The optimum reduction of COD was obtained at 5 min of contact time using the aluminium electrode with 2.0 A current. This shows that the aluminium electrode as the sacrificial electrode is better compared to the stainless steel electrode. Xu et al. (2002) investigated egg-processing wastewater treatment by EC using three different electrodes (iron, aluminium and stainless steel) and showed that aluminium performed better than stainless steel. Aluminium electrode has higher dissolution rate which produces more metal hydroxide ( $\text{Al}(\text{OH})_3$ ) compared to stainless steel where it resists towards corrosion contribute to a slower formation of ferrous hydroxide (Xu et al. 2002; El-Nass et al. 2009). Figure 5 shows the water quality for the PCM sample before and after electrocoagulation process using 2.0 A current and aluminium as the electrode.



**Fig. 5** Water quality of PCM **a** before and **b** after electrocoagulation

## 4 Conclusion

Electrocoagulation was successfully applied for the treatment of petroleum-based wastewater. The EC parameters, which are current, contact time and type of electrode, influenced the COD removal. In this work, the maximum COD removal efficiency was achieved at 88% and 74% for PCEC and PCM samples, respectively. This maximum COD removal was obtained when the current, contact time and type of electrode were 2.0 A, 5 min and aluminium, respectively. Petroleum-based industries will benefit from this eco-friendly and cost-effective technology in improving the wastewater treatment process. Thus, EC could be commercialised in the petroleum industry as the method of the wastewater treatment system.

**Acknowledgements** The authors would like to acknowledge the financial support from the Grant Knowledge Transfer Programme (I-WS/2 (UMP-15), RDU151005) and Universiti Malaysia Pahang (UMP).

## References

- Altaher, H., ElQada, E., & Omar, W. (2011). Pretreatment of wastewater streams from petroleum/petrochemical industries using coagulation. *Advances in Chemical Engineering and Science*, 1, 245–251.
- Ashrafi, O., Yerushalmi, L., & Haghithat, F. (2013). Greenhouse gas emission by wastewater treatment plants of the pulp and paper industry—modeling and simulation. *International Journal of Greenhouse Gas Control*, 17, 462–472.
- Bayar, S., Yildiz, Y. S., Yilmaz, A. E., & Irdemez, S. (2011). The effect of stirring speed and current density on removal efficiency of poultry slaughterhouse wastewater by electrocoagulation method. *Desalination*, 280(1–3), 103–107.
- Bouhezila, F., Hariti, M., Lounici, H., & Mameri, N. (2011). Treatment of the OUED SMAR town landfill leachate by an electrochemical reactor. *Desalination*, 280(1–3), 347–353.
- BP Energy Outlook 2035. (2015). London, United Kingdom.
- Chiang, L. C., Chang, J. E., & Wen, T. C. (1995). Indirect oxidation effect in electrochemical oxidation treatment of landfill leachate. *Water Research*, 29(2), 671–678.
- El-Naas, M. H., Al-Zuhair, S., Al-Lobaney, A., Makhlof, S. (2009). Assessment of electrocoagulation for the treatment of petroleum refinery wastewater. *Journal of Environmental Management*, 91(1), 180–185.
- Jafarnejad, S. (2017). *Petroleum waste treatment and pollution control* (1st ed.). Oxford, USA: Elsevier, Butterworth-Heinemann.
- Jafarnejad, S., & Jiang, S. C. (2019). Current technologies and future directions for treating petroleum refineries and petrochemical plants (PRPP) wastewaters. *Journal of Environmental Chemical Engineering*, 7, 103326.
- Jotin, R., Ibrahim, S., & Halimoon, N. (2012). Electrocoagulation for removal of chemical oxygen demand in sanitary landfill leachate. *International Journal of Environmental Sciences*, 3(2), 921–930.
- Katal, R., & Pahlavanzadeh, H. (2011). Influence of different combinations of aluminum and iron electrode on electrocoagulation efficiency: application to the treatment of paper mill wastewater. *Desalination*, 265(1), 199–205.

- Khan, W. Z., Najeeb, I., Tuiyebayeva, M., & Makhtayeva, Z. (2015). Refinery wastewater degradation with titanium dioxide, zinc oxide, and hydrogen peroxide in a photocatalytic reactor. *Process Safety and Environmental Protection*, 94, 479–486.
- Khandegar, V., & Saroha, A. K. (2013). Electrocoagulation for the treatment of textile industry effluent—a review. *Journal of Environmental Management*, 128, 949–963.
- Khandegar, V., & Saroha, A. K. (2012). Electrochemical treatment of distillery spent wash using aluminum and iron electrodes. *Chinese Journal of Chemical Engineering*, 20(3), 439–443.
- Kuokkanen, V., Kuokkanen, T., Rämö, J., & Lassi, U. (2013). Recent applications of electrocoagulation in treatment of water and wastewater—a review. *Green and Sustainable Chemistry*, 3, 89–121.
- Krishna, B. M., Murthy, U. N., Kumar, B. M., & Lokesh, K. S. (2010). Electrochemical pretreatment of distillery wastewater using aluminum electrode. *Journal of Applied Electrochemistry*, 40, 663–673.
- Larue, O., & Vorobiev, E. (2003). Floc Size estimation in iron induced electrocoagulation and coagulation using sedimentation data. *International Journal of Mineral Processing*, 71, 115.
- Moreno-Casillas, H. A., Cocke, D. L., Gomes, J. A. G., Moerkovsky, P., Parga, J. R., & Peterson, E. (2007). Electrocoagulation mechanism for COD removal. *Separation and Purification Technology*, 56(2), 204–211.
- Nasrullah, M., Singh, L., & Wahid, Z. A. (2012). Treatment of sewage by electrocoagulation and the effect of high current density. *Energy and Environmental Engineering Journal*, 1(1), 27–31.
- Ni'am, M. F., Othman, M. F., Sohaili, J., & Fauzia, Z. (2007). Electrocoagulation technique in enhancing cod and suspended solids removal to improve wastewater quality. *Water Science & Technology*, 56(7), 47–53.
- Orkun, M. O., & Kuleyin, A. (2012). Treatment performance evaluation of chemical oxygen demand from landfill leachate by electro-coagulation and electro fenton technique. *Environmental Progress & Sustainable Energy*, 31(1), 59–67.
- Prasad, R. K., & Srivastava, S. N. (2009). Electrochemical degradation of distillery spent wash using catalytic anode: factorial design of experiments. *Chemical Engineering Journal*, 146(1), 22–29.
- Saleem, M. (2009). Wastewater reuse potential in Pakistan: guidelines for environmental and public health protection. *International Journal of Environmental Engineering*, 1(3), 1–13.
- Saleem, M., Bukhari, A. A., & Al-Malack, M. H. (2000). Removal efficiency of indicator microorganisms in the Al-Khobar wastewater treatment plant. *Environmental Engineering Science*, 17(4), 227–232.
- Sridhar, R., Sivakumar, V., Immanuel, V. P., & Maran, J. P. (2011). Treatment of pulp and paper industry bleaching effluent by electrocoagulant process. *Journal of Hazardous Materials*, 186(2–3), 1495–1502.
- Thakur, C., Srivastava, V. C., & Mall, I. D. (2009). Electrochemical treatment of a distillery wastewater: parametric and residue disposal study. *Chemical Engineering Journal*, 148(2–3), 496–505.
- Top, S., Sekman, E., Hosver, S., & Bilgili, M. S. (2011). Characterisation and electrocoagulative treatment of nanofiltration concentrate of a full-scale landfill leachate treatment plant. *Desalination*, 268(1–3), 158–162.
- Ugurly, M., Gurses, A., Dogar, C., & Yalcin, M. (2008). The removal of lignin and phenol from paper mill effluents by electrocoagulation. *Journal of Environmental Management*, 87(3), 420–428.
- Xu, L. J., Sheldon, B. W., Larick, D. K., & Carawan, R. E. (2002). Recovery and utilization of useful by-products from egg processing wastewater by electrocoagulation. *Poultry Science*, 81(6), 785–792.
- Zailani, L. W. M., Hamdan, N. S. M., & Zin, N. S. M. (2018). Removal efficiency of electrocoagulation treatment using aluminium electrode for stabilized leachate. In IOP Conference Series: Earth and Environmental Science (vol. 140, pp. 012049).

# Activated Carbon from Meranti Wood Sawdust Waste Prepared by Microwave Heating for Dye Removal



Mohd Azmier Ahmad, Mohamad Firdaus Mohamad Yusop,  
and Soon Huat Tan

**Abstract** Ionic dyes pose a great difficulty to be eliminated in wastewater by conventional methods due to their highly soluble properties. This study aims to synthesis meranti wood-based activated carbon (MWAC) for methylene blue (MB) dye removal from aqueous solution. The MWAC was produced via physiochemical activation method which involves potassium hydroxide (KOH) treatment, carbon dioxide (CO<sub>2</sub>) gasification and microwave heating. Optimum preparation conditions of MWAC were found at microwave radiation power, radiation time and impregnation ratio (IR) of 365 W, 4.63 min and 0.85, respectively, which resulted in 88.0% of MB removal and 31.17% of MWAC yield. This sample shows high Brunauer–Emmet–Teller (BET) surface area and total pore volume of 1257.22 m<sup>2</sup>/g and 0.587 cm<sup>3</sup>/g, respectively. The MB adsorption equilibrium followed Langmuir isotherm with monolayer adsorption capacity of 344.83 mg/g. MB adsorption onto MWAC followed pseudo-second-order kinetic model while thermodynamic studies confirmed the exothermic in nature. Mechanism studies revealed that the adsorption process was controlled by film diffusion mechanism.

**Keywords** Activated carbon · Adsorption · Meranti wood · Microwave heating · Methylene blue

## 1 Introduction

### 1.1 Dyes and Their Dark Sides

With the increasing of world's population, the demand for colour around the globe is increasing as well. Therefore, the usage of dyes skyrocketed in industries of textiles, papers, cosmetics, toys and foods (Yagub et al. 2014). The annual worldwide production of synthetic dyes is within 700,000–1,000,000 t. Out of these amount, 280,000

---

M. A. Ahmad (✉) · M. F. M. Yusop · S. H. Tan  
School of Chemical Engineering, Universiti Sains Malaysia, Engineering Campus,  
14300 Nibong Tebal, Penang, Malaysia  
e-mail: [chazmier@usm.my](mailto:chazmier@usm.my)

© Springer Nature Singapore Pte Ltd. 2020  
A. Z. Yaser (ed.), *Advances in Waste Processing Technology*,  
[https://doi.org/10.1007/978-981-15-4821-5\\_5](https://doi.org/10.1007/978-981-15-4821-5_5)

tons are dumped as industrial wastewater and causing severe water pollution. Dyes wastewater can exist in the system for a long time since dyes molecules are stable and reluctant to decompose upon the exposure of light, heat and oxidizing chemicals (Kono 2015). Small amount of dyes molecules is enough to cause harm to the aquatic organisms and hindered the sunlight penetration, thus affecting the photosynthesis of aquatic plants (Balarak et al. 2015).

Methylene blue (MB) is among the toxic type of dyes that can cause various health issues if expose to human for an adequate time such as vomiting, shock, eye burn, cyanosis, jaundice, tissue necrosis, quadriplegia and mental confusion (Kushwaha et al. 2014). The degradation process of MB dye is slow, complex and yielding potential carcinogenic and mutagenic products (Porhemmat et al. 2017). Considering the harmful effects caused by MB dye on human, aquatic creatures, plants and environment, it is vital to treat them before being discharged into receiving streams. Their highly soluble in water and recalcitrant to biodegrade properties makes them very challenging to be treated by most of the conventional treatment methods. In this study, an attempt was made to treat MB dye via adsorption process using activated carbon (AC) as an adsorbent.

## 1.2 Furniture Industry in Malaysia

The demand of wooden-based furniture is increasing worldwide and this industry accounts for considerable portion of global trade (Azizi et al. 2016). In 2014, the total amount of world furniture consumption was USD 455 billion and is expected to grow 2.8% in the following years (Govoni 2016). Malaysia is one of the top ten largest exporters of furniture in the world for several years now, with total export earnings of USD 2.25 billion in 2016. Furniture made in Malaysia has been exported to 160 countries, mainly to USA, Japan, Singapore and Australia (Tey 2017). Owing to its plentiful resources of timber, Malaysia is in the right track to reach net income of USD 12.53 billion from furniture industry by the year 2020 (MIFF 2018). Original design with high aesthetical value, good quality of raw materials and wide range of products variety are the main factors contributing to the success of furniture industry in Malaysia.

Meranti wood (MW) sawdust yielded from *red meranti* species or scientifically known as *shorea spp.* is common and famous hardwood species in Malaysia (Rafiqul & Mimi Sakinah 2012). *Red meranti* can grow up to 20–40 m in height and 1–2 m of trunk diameter. In terms of application, *red meranti* is widely used to make interior and outdoor furniture, plywood, general construction material, concrete forms, veneer and boatbuilding. Sawdust from meranti wood is prone to biodegradable, having relatively hard texture and enriched with carbons, which makes them a great choice to be converted into meranti wood-based activated carbon (MWAC).

### ***1.3 Preparation of Activated Carbon***

There are two important steps in producing AC, namely carbonization step and activation step. Carbonization step can be defined as a step to convert the precursor into a material containing high amount of carbon or also known as char. This step occurs in an oxygen-free atmosphere at temperature between 450 and 700 °C. At this point, the elimination process of moisture, volatile organic matter and non-carbon elements such as sulphur, nitrogen, oxygen and hydrogen are taking place.

In order to enhance the porosity and surface area of the sample, physiochemical activation step is done by impregnation of char with chemical activating agent, followed by gasification treatment using oxidizing gas while the char is heated. Char is traditionally activated using conventional furnace but recently, most researchers has been switching into microwave heating technique due to several advantages it offers. The production of AC using conventional furnace is time consuming and energy extensive process. Therefore, the microwave heating technique is employed in this study to activate the samples. This technique can save time, energy and activation gas significantly. Higher yield of AC is also obtained via microwave heating.

AC with optimum adsorption performance and yield are desirable for efficiency purpose. However, to find optimum preparation conditions are difficult due to the conflicted interest region between AC's performance and yield. Therefore, the response surface methodology (RSM) was used in this study to determine the optimum preparation conditions.

### ***1.4 Research Objectives***

The objectives of this study are as follows:

1. To optimize the MWAC preparation conditions (radiation power, radiation time and KOH: char impregnation ratio) in order to obtain MWAC with high yield and MB removal.
2. To investigate the effect of initial dyes concentration and contact time of optimized MWAC on MB removal.
3. To study the adsorption isotherm, kinetics and mechanism behaviour of MB adsorption on optimized MWAC.



**Table 1** List of chemicals

Chemical	Supplier	Purity (%)	Purpose
Potassium hydroxide (KOH)	Riedel-el Haen, Germany	>85	Activating agent
Hydrochloric acid (HCl)	Merck, Germany	37	AC wash and pH adjustment
Sodium hydroxide (NaOH)	Essex, UK	99	pH adjustment
Methylene blue (MB)	Sigma-Aldrich (M) Sdn. Bhd.	85	Adsorbate

## 2 Methodology

### 2.1 Materials and Chemicals

Sawdust of meranti wood (MW) was collected at a wood factory located in Sungai Petani, Kedah, Malaysia. In original form, the sawdust was relatively dried, free from any impurities and relatively uniform in size and shape in the range of 5–10 mm. Table 1 shows the chemicals used in this study.

Nitrogen gas ( $N_2$ ) and carbon dioxide gas ( $CO_2$ ), both with purity of 99.99%, were used in this study.  $N_2$  gas was used to purge through the furnace during carbonization process to create an inert atmosphere while  $CO_2$  gas was used as gasification agent in activation step to prepare MWAC.

### 2.2 Experimental Setup

The preparation of char was conducted using the experimental setup as shown in Fig. 1. The equipment used consists of vertical tubular furnace having dimension of 500 mm long with 82 mm diameter with programmable controller (Model Carbolite, USA). A stainless steel tubular cylinder with inner diameter of 25 and 150 mm long used for placing the sample was held in the centre of the furnace. A wire mesh made of stainless steel is place at the bottom of cylinder to prevent the sample from falling out. The flue gas emitted from the reactor was condensed using a condenser at the bottom of the vertical tubular furnace. All the connecting pipes were made of Teflon tubing joined by stainless steel fittings. In addition, the rig consists of flow meter to adjust and maintain the gas flow rate to the furnace.

Char activation by microwave heating was carried out using commercial microwave with some modifications as shown in Fig. 2. The microwave has a power controller to select different power levels and a timer for various exposure times. Gas flow meter was used to measure the flow rate of supplied  $CO_2$  to microwave. Connecting pipe in system was made from Teflon tubing. Microwave heating was carried

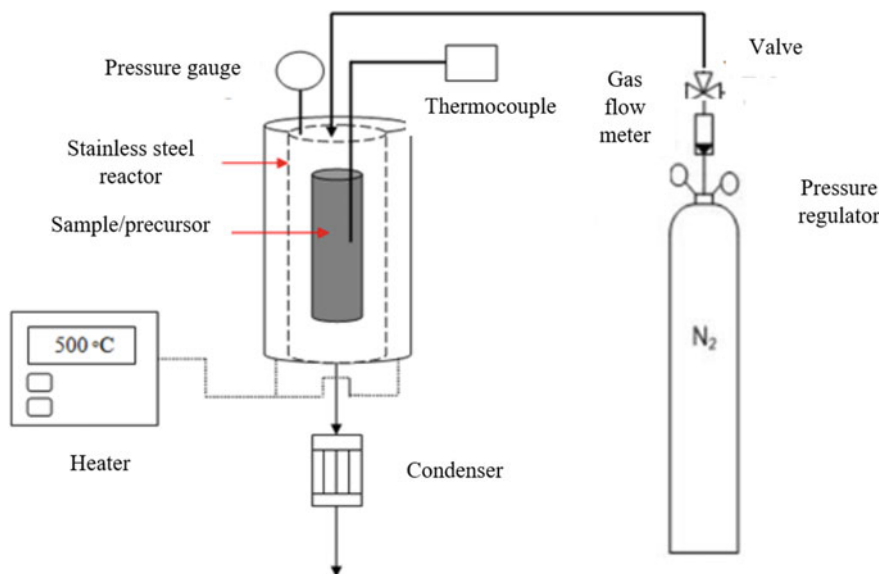


Fig. 1 Schematic diagram of char preparation unit

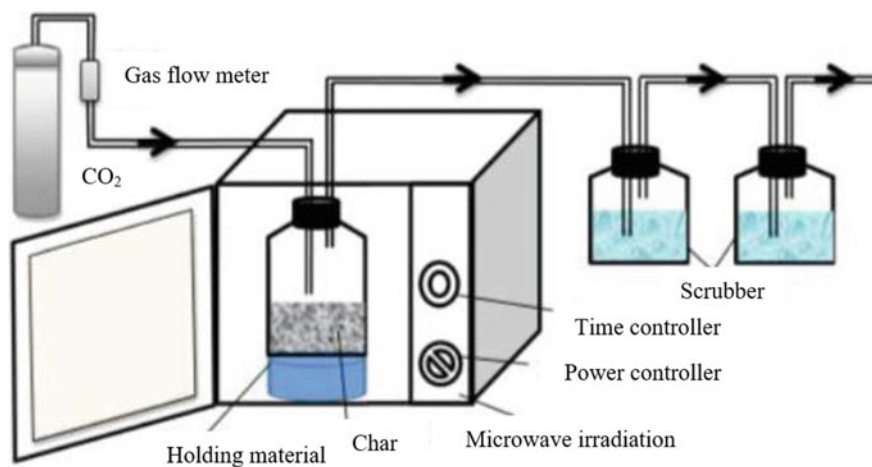


Fig. 2 Schematic diagram of microwave irradiation setup diagram

out in Pyrex glass reactor (diameter 7 cm and length 21 cm) fixed in the chamber of microwave oven. N<sub>2</sub> gas (150 ml/min) was used to purge air in the reactor before the activation start as well as during activation step.

## 2.3 Experimental Procedure

### 2.3.1 Preparation of MWAC

The carbonization process of meranti wood sawdust involves temperature of 500 °C under the purging of N<sub>2</sub> gas of 150 cm<sup>3</sup>/min for 1 h. The product of carbonization process which referred as char was unloaded from the tubular reactor. This char was impregnated with potassium hydroxide (KOH) which acts as chemical activating agent on specific amount of KOH: char ratio known as impregnation ratio (IR). IR was calculated based on the following equation:

$$IR = \frac{W_{KOH}}{W_{char}} \quad (1)$$

where  $W_{KOH}$  and  $W_{char}$  are dry weight of KOH pellets and dry weight of char, respectively. An adequate amount of deionized water was added into the mixture of char and KOH to dissolve the KOH pellets. The next step involves the physical activation using CO<sub>2</sub> gas as activating agent and the process is radiated using microwave. Firstly, KOH-impregnated char was placed in Pyrex glass reactor and loaded in the chamber of microwave. After that, the microwave irradiation was carried out based on the targeted radiation time and radiation power under a constant CO<sub>2</sub> flow of 150 cm<sup>3</sup>/min. After the physical activation process finished, the sample was unloaded and undergone washing process using deionized water until the pH of washing solution reach neutral. The pH was measured using pH meter (Delta 320, Mettler Toledo, China). The sample was then dried inside oven for 24 h at 110 °C. This MWAC sample was kept inside air-tight containers for characterization and adsorption studies.

### 2.3.2 Preparation of Stock and Adsorbate Solution

Stock solution of MB dye was prepared by dissolving 1.0 g of MB dye powder in a 1 L of volumetric flask. The test dye solutions having concentrations of 25–300 mg/L were prepared through fresh dilution of initial stock solution using deionized water prior to each adsorption study by using Eq. 2.

$$M_1 V_1 = M_2 V_2 \quad (2)$$

where  $M_1$ ,  $V_1$ ,  $M_2$  and  $V_2$  were concentration of stock solution, volume of stock solution, concentration of desired MB solution and volume of desired MB solution, respectively.

### 2.3.3 Batch Adsorption and Analysis System

200 mL of MB solution and 0.2 g of MWAC were added into the 250 mL flasks and then loaded inside isothermal water-bath shaker (Model Protech, Malaysia). A small sample of MB solution was withdrawn from the dye solution at definite time intervals by using 3 mL of disposable syringe. The dye concentration was determined using double beam UV-Visible spectrometer (Model Shimadzu UV-1800, Japan) at maximum wavelength of MB at 664 nm. The absorption spectrum determined the wavelength at which the maximum absorbance was attained.

### 2.3.4 Experimental Design for MWAC Preparation

Response surface methodology (RSM) was effectively in determining the optimal control variables that result in the maximum or minimum response over the field of interest. In this study, the optimum MWAC preparation conditions produced maximum MB removal and MWAC's yield. The preparation variables being studied were  $x_1$ , radiation power (144–736 W);  $x_2$ , radiation time (2.6–9.4 min) and  $x_3$ , KOH:char impregnation ratio (IR: 0.0–2.51) with MB initial concentrations of 100 mg/L.

A standard RSM design was employed using central composite design (CCD) in this study to evaluate the MWAC preparation variables. This method is widely used for fitting quadratic surface to experimental data to find the optimize parameters with minimum set of experiments conducted and evaluating the interaction between the variables. Table 2 summarizes the complete design matrix of the present experiments.

Since three variables were investigated in this study, a total of 20 runs of experiments comprised of 8 of factorial points, 6 of axial points and 6 replicates were used in this study. Two responses namely MB dye removal ( $Y_1$ ) and MWAC's yield ( $Y_2$ ) were investigated. The equation used to construct the empirical model that to correlate variables studied with the responses was given as follows:

$$y = (b_o + \varepsilon) + \sum_{i=1}^3 b_i x_i + \sum_{i=1}^3 b_{ii} x_i^2 + \sum_{i=1}^3 \sum_{j=i+1}^3 b_{ij} x_i x_j \tag{3}$$

where:

- $y$  predicted response
- $b_o$  and  $b_i$  constant coefficient and linear coefficient
- $b_{ij}$  quadratic coefficients
- $x_i$  and  $x_j$  coded value of variables

Design Expert software version 8.0.6 (STAT-EASE Inc. Minneapolis, USA) was used to fit the experimental data and regression analysis to the developed model.

**Table 2** Complete design matrix for MWAC preparation

Run	MWAC preparation parameters		
	Radiation power, $x_1$ (W)	Radiation time, $x_2$ (min)	IR, $x_3$
1	264 (-1)	4.0 (-1)	0.50 (-1)
2	440 (0)	2.6 (-1.628)	1.25 (0)
3	440 (0)	6.0 (0)	1.25 (0)
4	264 (-1)	4.0 (-1)	2.00 (+1)
5	440 (0)	6.0 (0)	1.25 (0)
6	440 (0)	6.0 (0)	1.25 (0)
7	736 (+1.628)	6.0 (0)	1.25 (0)
8	440 (0)	6.0 (0)	1.25 (0)
9	144 (-1.628)	6.0 (0)	1.25 (0)
10	264 (-1)	8.0 (+1)	2.00 (+1)
11	440 (0)	6.0 (0)	2.51 (1.628)
12	264 (-1)	8.0 (+1)	0.50 (-1)
13	440 (0)	6.0 (0)	1.25 (0)
14	440 (0)	9.4 (+1.628)	1.25 (0)
15	616 (+1)	4.0 (-1)	0.50 (-1)
16	616 (+1)	8.0 (+1)	2.00 (+1)
17	616 (+1)	8.0 (+1)	0.50 (-1)
18	616 (+1)	4.0 (-1)	2.00 (+1)
19	440 (0)	6.0 (0)	1.25 (0)
20	440 (0)	6.0 (0)	0.00 (-1.628)

### 2.3.5 Surface Area Characterization

Surface area was important in providing sites for adsorption process to take place. Surface area of samples were determined by using Micromeritics ASAP 2020 volumetric adsorption analyser, which is based on nitrogen gas adsorption at 77 K. System is operated by measuring quantity of gas absorbed onto a solid surface at equilibrium vapour pressure by static volumetric method. Surface area was measured from adsorption isotherm using Brunauer–Emmett–Teller (BET) equation. Total pore volume was estimated to be liquid volume of nitrogen at a relative pressure of 0.99.

### 2.3.6 Batch Adsorption Equilibrium Studies

Under batch equilibrium studies, the effect of initial dye concentration, contact time and solution temperature on the MB adsorption uptake was investigated. 0.2 g of MWAC was added into 200 mL of MB solution with six different initial concentrations of 25, 50, 100, 200, 250 and 300 mg/L. A small sample of MB solution was

withdrawn and the concentration of the sample was measured until an equilibrium state was achieved by the adsorption system. For equilibrium studies, the MB amount adsorbed by MWAC at equilibrium was determined by using the following equation:

$$q_e = \frac{(C_o - C_e)V}{M} \quad (4)$$

where  $q_e$ ,  $C_o$ ,  $C_e$ ,  $V$  and  $M$  were amount of MB adsorbed by MWAC at equilibrium, initial concentration of MB solution, concentration of MB solution at equilibrium, volume of solution and mass of MWAC, respectively. The MB dye removal (%) can be expressed as follows:

$$\text{MB removal (\%)} = \frac{(C_o - C_e)}{C_o} \times 100\% \quad (5)$$

The MWAC's yield was calculated by using the following formula:

$$\text{Yield (\%)} = \frac{W_c}{W_o} \times 100\% \quad (6)$$

where  $W_c$  and  $W_o$  were dry weight of MWAC and dry weight of precursor, respectively.

### 2.3.7 Effect of Initial Dye Concentration and Contact Time

For the purpose of studying the effect of initial dye concentrations and contact time towards dyes adsorption uptake and dyes percentage removal, 200 mL of MB solutions with six known initial concentration of 25, 50, 100, 200, 250 and 300 mg/g were prepared in a series of 250 mL Erlenmeyer flasks. Then, 0.2 g of MWAC was added into these flasks and the flasks was covered with aluminium foil to prevent any water loss through evaporation process throughout the experiment. These flasks were placed inside an isothermal water shaker bath at constant temperature of 30 °C and agitation speed of 150 rpm until equilibrium stage was attained.

### 2.3.8 Adsorption isotherm

The study of adsorption isotherm was carried out by fitting the experimental equilibrium data onto four isotherm models, namely Langmuir, Freundlich, Temkin and Dubinin–Radushkevich. The suitability of the isotherm equations in fitting the equilibrium data was evaluated by making comparison between the correlation coefficients,  $R^2$  value. The model which has a better agreement with the adsorption equilibrium data has  $R^2$  value that approaching unity, indicating that the model was fitted well. Langmuir isotherm is based on the theory that the adsorbate molecules

form a monolayer coverage on the surface of adsorbent, thus totally contribute to the maximum adsorption capacity. The linear form of Langmuir equation is as follows (Langmuir 1918):

$$\frac{C_e}{q_e} = \frac{C_e}{q_m} + \frac{1}{K_L q_m} \quad (7)$$

where  $q_e$  is the amount of MB adsorbed at equilibrium (mg/g),  $q_m$  is monolayer adsorption capacity of the AWAC (mg/g),  $C_e$  is equilibrium concentration of MB and  $K_L$  is Langmuir adsorption constant related to the free energy adsorption.

Freundlich isotherm assumes that the sorption of adsorbate occurs on the heterogeneous surface of the adsorbent. The linear form of equation for this isotherm is given as follows (Freundlich 1906):

$$\log q_e = \frac{1}{n_F} \log C_e + \log K_F \quad (8)$$

where  $q_e$  is the amount of MB adsorbed per unit mass of AWAC (mg/g),  $K_F$  is Freundlich isotherm constant (mg/g)(L/mg)<sup>1/n</sup>, which indicates the relative adsorption capacity of the MWAC related to the bonding energy,  $C_e$  is equilibrium concentration of the MB (mg/L) and  $n_F$  is the heterogeneity factor.

Temkin isotherm considers the effect of adsorbate interaction on the adsorbent based on uniformly distributed binding energies. Its linear form of equation is as follows (Temkin and Pyzhev 1940):

$$q_e = B_T \ln A_T + B_T \ln C_e \quad (9)$$

where  $B_T$  is  $R_T/b_T$  constant related to the heat of adsorption (L/mg),  $q_e$  is amount of MB adsorbed at equilibrium (mg/g),  $C_e$  is equilibrium concentration of MB (mg/L),  $T$  is absolute temperature,  $R$  is universal gas constant (8.314 J/mol K) and  $A_T$  is equilibrium binding constant (L/mg).

Dubinin and Radushkevich (1947) were first introduced to study the adsorption of subcritical vapours onto micropore solids that follow pore filling mechanism. This isotherm was utilized to differentiate the physical and chemical adsorption. Dubinin–Radushkevich can be mathematically written as follows:

$$q_e = q_s \exp(-B_{DR} \varepsilon^2) \quad (10)$$

where  $\varepsilon$  can be correlated:

$$\varepsilon = RT \ln \left[ 1 + \frac{1}{C_e} \right] \quad (11)$$

$$E_{DR} = \frac{1}{\sqrt{2B_{DR}}} \quad (12)$$

where  $q_e$ ,  $Q_{DR}$ ,  $C_e$ ,  $K_L$ ,  $E_{DR}$  and  $R$  were amount of adsorbate adsorbed on the surface at equilibrium (mg/g), monolayer adsorption capacity of the adsorbent (mg/g), adsorbate concentration at equilibrium (mg/L), Langmuir adsorption constant related to the free energy adsorption (L/mg), free energy (kJ/mol) and gas constant (8.314 J/mol K), respectively.

### 2.3.9 Batch Adsorption Kinetics and Diffusion Mechanism

The method of evaluation of batch kinetic studies was identical to the batch equilibrium experiments. The aqueous dye samples of each respective flask were withdrawn at predetermined time intervals. The adsorption uptake of MB by MWAC at any time  $t$ ,  $q_t$  (mg/g) was expressed:

$$q_t = \frac{(C_o - C_t)V}{W} \tag{13}$$

where  $q_t$ ,  $C_o$ ,  $C_t$ ,  $V$  and  $M$  were amount of adsorbate adsorbed on the surface at time  $t$  (mg/g), initial concentration of adsorbate solution (mg/L), concentration of adsorbate solution at time  $t$  (mg/L), volume of solution (ml) and mass of MWAC, respectively.

Three kinetic models were used to test the kinetic data which were pseudo-first order, pseudo-second order and Elovich. Besides comparing the correlation factor,  $R^2$  to find the best model that fit kinetics data, normalized standard deviation was used too. Normalized standard deviation measured the variance between experimental data and data obtained using the kinetics model equation. The model that fitted the kinetics data the best yielded low value of normalized standard deviation. The equation used to find normalized standard deviation is as follows:

$$\Delta q_t (\%) = 100 \sqrt{\frac{\sum [(q_{t,exp} - q_{t,cal}) / q_{t,cal}]^2}{(n - 1)}} \tag{14}$$

where  $q_{t,exp}$ ,  $q_{t,cal}$  and  $n$  were measured amount of adsorbate adsorbed at time  $t$ , calculated amount of adsorbate adsorbed at time  $t$  and number of data points, respectively.

The study on adsorption kinetics involves pseudo-first-order model (Lagergren and Svenska 1898) and pseudo-second-order model (Ho and Mckay 1999), given by Eqs. 15 and 16, respectively:

$$\ln(q_e - q_t) = \ln q_e - k_1 t \tag{15}$$

$$\frac{t}{q_t} = \frac{1}{q_e^2 k_2} + \frac{1}{q_e} t \tag{16}$$



where  $q_t$  is amount of MB adsorbed at time  $t$  (mg/g),  $q_e$  is amount of MB adsorbed at equilibrium (mg/g),  $k_1$  is pseudo-first-order rate constant of adsorption (1/min) and  $k_2$  is pseudo-second-order rate constant of adsorption (g/mg h).

The Elovich kinetic model is used to determine the kinetics of adsorbate chemisorption onto heterogeneous solids. It is quite restricted, as it only describes limiting property ultimately reached by kinetic curves. The Elovich equation is as follows:

$$q_t = \frac{1}{\beta_E} \ln(\alpha_E \beta_E) + \frac{1}{\beta_E} \ln t \quad (17)$$

where  $q_t$ ,  $\alpha_E$  and  $\beta_E$  were amount of adsorbate adsorbed at time  $t$  (mg/g), initial sorption rate (mg/g h) and constant related to the extent of surface coverage and activation energy for chemisorption (g/mg), respectively. The value of  $1/\beta_E$  reflects the number of sites available for adsorption, whereas the value of  $(1/\beta_E) \ln(\alpha_E \beta_E)$  indicates adsorption quantity when  $\ln t$  is equal to zero.

The kinetics data were used to fit the diffusion mechanism model of intraparticle diffusion. Weber's intraparticle diffusion model is an empirical function that gives an insight and explains the diffusion mechanism in adsorption process. As the name suggest, this model assumes that intraparticle diffusion is the rate limiting step of the adsorption process and is given as follows (Weber & Chakkravorti 1974):

$$q_t = K_p t^{1/2} + C \quad (18)$$

where  $q_t$ ,  $C$  and  $K_p$  were amount of adsorbate adsorbed at time  $t$  (mg/g), constant related to boundary layer thickness and intraparticle diffusion rate constant (mg/g h<sup>1/2</sup>), respectively. A plot of  $q_t$  against  $t^{1/2}$  forms a straight line which indicates the existence of intraparticle diffusion. If the straight line passing through the origin, then the rate limiting step was confirmed to be controlled by intraparticle diffusion.

### 3 Results and Discussion

There are four main sections under this chapter. The first section explores the optimization of MWACs' preparation conditions. Second section provides the characteristics of the optimized MWAC in terms of surface area and pore characteristics. Third section discusses the results for batch equilibrium studies where the effect of initial dye concentration and contact time towards MWAC's adsorption performance were evaluated. Then, the isotherm, kinetics and mechanism studies were discussed.

### 3.1 Experimental Design

An entire design matrix for MWAC’s preparation was given in Table 3. For MB removal and MWAC’s yield responses, quadratic type of models was choose as suggested by the software. The final empirical models of MWAC in the form of codec factors were as follows;

MB removal (%),  $Y_{MB}$

$$Y_{MB} = 95.47 + 4.58X_1 + 2.62X_2 + 3.27X_3 - 5.10X_1^2 - 3.35X_2^2 - 4.61X_3^2 - 1.20X_1X_2 + 0.47X_1X_3 - 0.072X_2X_3 \tag{3.1}$$

**Table 3** Experimental design matrix for preparation of MWAC

Run	Level			MWAC’s preparation variables			Responses	
				Radiation power, $X_1$ (W)	Radiation time, $X_2$ (min)	IR, $X_3$	MB removal, $Y_{MB1}$ (%)	MWAC’s yield, $Y_{MWAC}$ (%)
1	0	0	+1.628	440	6.0	2.51	89.11	14.92
2	0	0	0	440	6.0	1.25	95.60	31.07
3	0	0	0	440	6.0	1.25	95.24	31.17
4	+1	-1	-1	616	4.0	0.50	83.55	22.12
5	-1	-1	-1	264	4.0	0.50	72.57	26.87
6	0	-1.628	0	440	2.6	1.25	80.11	27.63
7	+1	-1	+1	616	4.0	2.00	90.44	21.15
8	+1.628	0	0	736	6.0	1.25	86.57	15.94
9	0	+1.628	0	440	9.4	1.25	90.45	17.85
10	+1	+1	-1	616	8.0	0.50	86.77	17.86
11	0	0	0	440	6.0	1.25	95.78	30.73
12	0	0	0	440	6.0	1.25	95.11	30.72
13	0	0	-1.628	440	6.0	0.00	74.33	19.90
14	+1	+1	+1	616	8.0	2.00	91.64	15.05
15	0	0	0	440	6.0	1.25	95.56	30.86
16	0	0	0	440	6.0	1.25	95.77	30.67
17	-1.628	0	0	144	6.0	1.25	74.11	27.52
18	-1	+1	+1	264	8.0	2.00	83.57	22.12
19	-1	+1	-1	264	8.0	0.50	78.85	22.87
20	-1	-1	+1	264	4.0	2.00	75.85	25.04

MWAC's yield (%),  $Y_{MWAC}$

$$Y_{MWAC} = 30.82 - 2.94X_1 - 2.47X_2 - 1.08X_3 - 2.89X_1^2 - 2.53X_2^2 - 4.41X_3^2 - 0.43X_1X_2 - 0.15X_1X_3 - 0.097X_2X_3 \tag{3.2}$$

The results of ANOVA for MB removal and MWAC's yield were given in Tables 4 and 5, respectively. The model  $F$ -value and Prob  $> F$  values obtained for the response of MB removal by MWAC were found to be 48.73 and less than 0.0001, respectively, hence, confirming the significance of the model. The significant terms were revealed to be radiation power ( $X_1$ ), radiation time ( $X_2$ ), IR ( $X_3$ ), quadratic of radiation power ( $X_1^2$ ), quadratic of radiation time ( $X_2^2$ ) and quadratic of IR ( $X_3^2$ ). The other terms were

**Table 4** ANOVA results for MB removal by MWAC

Source	Sum of squares	DF	Mean square	$F$ -value	Prob $> F$
Model	1249.10	9	138.79	48.73	<0.0001
$x_1$	286.17	1	286.17	100.48	<0.0001
$x_2$	93.90	1	93.90	32.97	0.0002
$x_3$	145.76	1	145.76	51.18	<0.0001
$x_1^2$	374.76	1	374.76	131.58	<0.0001
$x_2^2$	162.01	1	162.01	56.89	<0.0001
$x_3^2$	306.48	1	306.48	107.61	<0.0001
$x_1x_2$	11.47	1	11.47	4.03	0.0725
$x_1x_3$	1.77	1	1.77	0.62	0.4491
$x_2x_3$	0.042	1	0.042	0.015	0.9057
Residual	28.48	10	2.85		

**Table 5** ANOVA results for MWAC's yield

Source	Sum of squares	DF	Mean square	$F$ -value	Prob $> F$
Model	638.78	9	70.98	45.61	< 0.0001
$x_1$	118.31	1	118.31	76.03	< 0.0001
$x_2$	83.22	1	83.22	53.48	< 0.0001
$x_3$	15.91	1	15.91	10.22	0.0095
$x_1^2$	120.21	1	120.21	77.26	< 0.0001
$x_2^2$	92.31	1	92.31	59.33	< 0.0001
$x_3^2$	280.87	1	280.87	180.51	< 0.0001
$x_1x_2$	1.48	1	1.48	0.95	0.3522
$x_1x_3$	0.18	1	0.18	0.12	0.7410
$x_2x_3$	0.075	1	0.075	0.048	0.8309
Residual	15.56	10	1.56		

found to be insignificant due to the extremely low of impact they pose towards this response. According to *F*-value, MB removal was affected mostly by the variables in the sequence of radiation power, IR and radiation time.

The model for MWAC's yield was significant due to high model *F*-value of 45.61 and Prob > *F* value of less than 0.0001. Radiation power scores the highest *F*-value of 76.03. For this response, the significant terms were radiation power ( $X_1$ ), radiation time ( $X_2$ ) and IR ( $X_3$ ) together with the quadratic factor of radiation power ( $X_1^2$ ), radiation time ( $X_2^2$ ) and IR ( $X_3^2$ ). The effect of the variables towards the responses is shown in Fig. 3.

The adsorption performance of MWAC was low at low radiation power and IR. As these variables increased, the adsorption performance of MWAC was getting

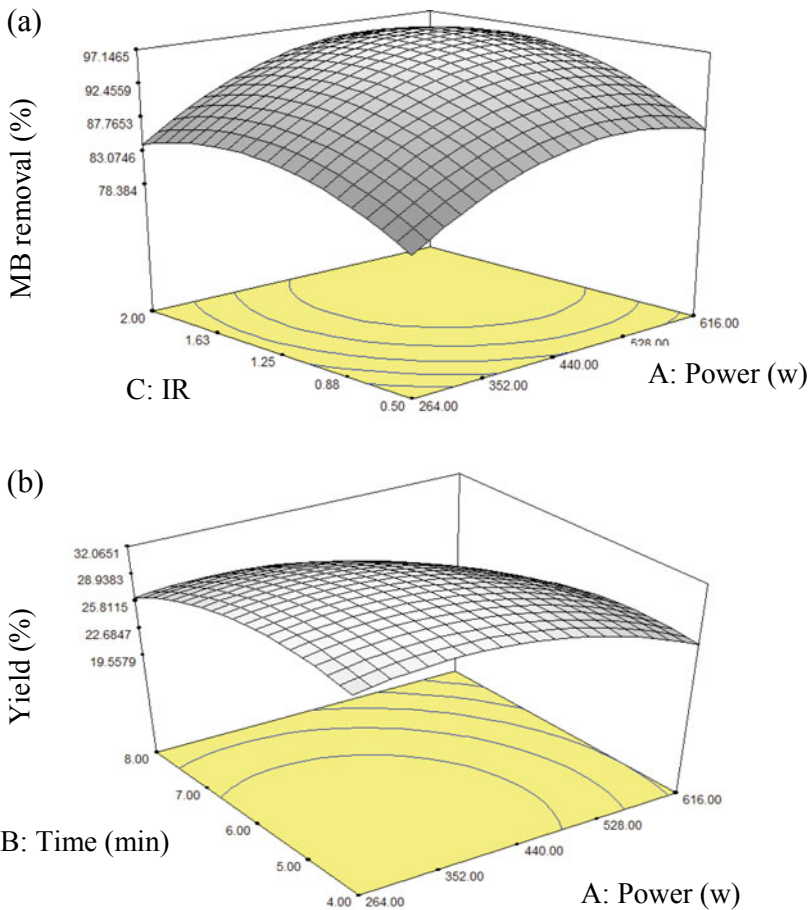


**Fig. 3** Three-dimensional response plot for **a** MB removal (effect of radiation power and IR, radiation time = 6 min) and **b** MWAC's yield (effect of radiation power and radiation time, IR = 1.25)

**Table 6** Model validation for MWAC prepared for MB removal

Radiation power, $X_1$ (W)	Radiation time, $X_2$ (min)	IR, $X_3$	MB removal, $Y_{MB}$ (%)			MWAC's yield, $Y_{AC}$ (%)		
			Predicted	Actual	Error	Predicted	Actual	Error
365	4.6	0.85	86.00	88.43	2.75	31.17	31.64	1.49

better, proven by the increasing percentage of MB removal. Preparation conditions that enhanced the deficiency of MWAC's performance in MB removal were high radiation power and very low or very high IR. Extremely high radiation power causes the  $CO_2$  molecules to pose higher kinetic energy, thus bombarding the char's surface to the extent where the pores network was ruptured. Exceptionally high of IR cause the pores to be blocked by the excess  $K_2CO_3$  ions, whereas too low of IR cause the chemical activation process to be less effective, thus low number of pores were developed. At the lowest value of radiation power and radiation time, MWAC's yield achieved the highest value due to an incomplete elimination process of the volatile matter and tar that take place. These volatile matter and tar compounds added more weight to the MWAC, thus higher yield was obtained. While both of variables increased, the MWAC's decreased consistently.

High MB removal and MWAC's yield make the process of MWAC production to be more time-saving and resources-efficient. However, their interest region was different with the variables. To solve this, the function of desirability was employed using Design Expert software. The responses of MB removal and MWAC's yield were set to be maximum, whereas the three variables of radiation power, radiation time and IR were set to be minimum. The optimum radiation power, radiation time and IR for the preparation of MB-MWAC (365 W, 4.63 min and 0.85, respectively) were obtained as shown in Table 6 with MB removal of 86.0% and yield of 31.17.

### 3.2 Surface Area and Pore Characteristics

The MW was found to pose small amount of BET surface area and mesopores surface area which were 1.27 and 0.0019  $m^2/g$ , respectively, as shown in Table 7. After undergo carbonization process, the surface area as well as total pore volume were

**Table 7** Surface area and pore characteristics of the samples

Sample	BET surface area ( $m^2/g$ )	Mesopores surface area ( $m^2/g$ )	Total pore volume ( $cm^3/g$ )	Average pore diameter (nm)
MW	1.27	0.0019	0.0001	2.48
MW char	453.25	278.11	0.3820	2.59
MWAC	1257.22	825.58	0.5870	2.82

found to rise due to the water and volatile matter removed from the precursors. When these components evaporate and leave the samples, vacant spaces which associated with pores network were developed. It was also noticed that carbonization process was successful to increase the average pore diameter within mesopores region.

During chemical activation process, KOH dissolved in water to produce metallic potassium ions,  $K_2CO_3$ . These metallic ions are mobile which enables them to access the vacant spaces on chars and penetrate into the skeleton of chars even deeper. As the result, the enhancement of pores network occurs effectively. Impregnated chars were further activated using  $CO_2$  gas and heated with microwave. Energy from microwave radiation was absorbed by the samples and causing them to vibrate due to the vigorous collision between atoms and molecules. This rapid process produces enormous heat that elevated the temperature of the samples. As the consequence, volatile matter, especially tar compound that survive during carbonization process was further removed during this activation stage, thus increase the porosity of the samples, which resulted in high total pore volume of  $0.5870 \text{ cm}^3/\text{g}$ .  $CO_2$  gasification, on the other hand, bombarded the samples and causing the widening effect of pores. Besides that, the trapped  $K_2CO_3$  ions inside the samples can be removed by the action of  $CO_2$  gasification.

### 3.3 Batch Adsorption Studies

The adsorption behaviour of MB onto optimized MWAC was evaluated by performing studies on adsorption equilibrium, kinetics and mechanism. Each one of these studies is crucial in providing different types of information regarding the nature of the adsorbate–adsorbent system. The plots of MB adsorption uptakes versus time and MB removal versus time are shown in Figs. 4 and 5, respectively.

Both MB uptakes and MB removal increased with time until to a point where a constant value reached, indicating that the adsorption capacity of the samples had reach their limit, thus no more MB molecules can be adsorbed. In the beginning, MWAC with plenty of vacant active sites was available to be occupied by the MB molecules. After sometimes, the number of the remaining active sites decreased and the repulsion between MB molecules in the aqueous solution and solid phase becomes greater (Islam et al. 2017). Eventually, an equilibrium state was attained where the number of MB molecules being adsorbed and desorbed by MWAC was equal in amount (Zhou et al. 2017).

As the initial concentration MB concentration increased from 25 to 300 mg/L, the adsorption uptakes of MB molecules increased from 23.56 to 240.78 mg/g. This occurrence can be explained by the development of larger mass transfer driving force at higher initial concentration to overcome the mass transfer resistance of the MB dye between aqueous solution and solid phase, thus promoting higher MB uptake as a result (Tharaneedhar et al. 2017). An equilibrium state was attained faster by the lower MB initial concentration (25, 50 and 100 mg/L) which was around 4–6 h, whereas for higher MB initial concentration, the equilibrium state was only reached

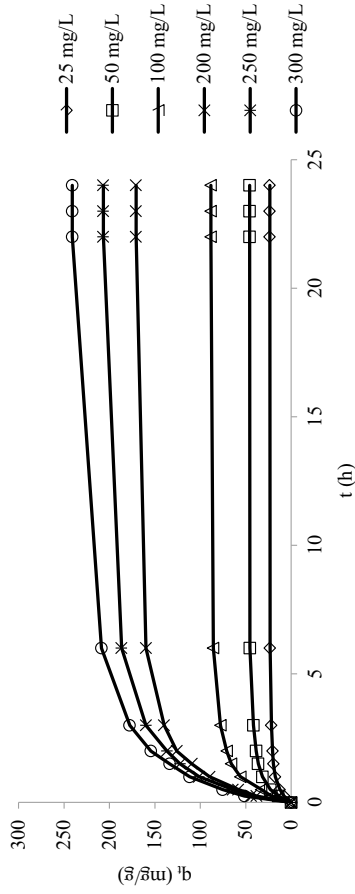


**Fig. 4** MB adsorption uptake versus adsorption time at various initial concentrations by MB-MWAC at 30 °C

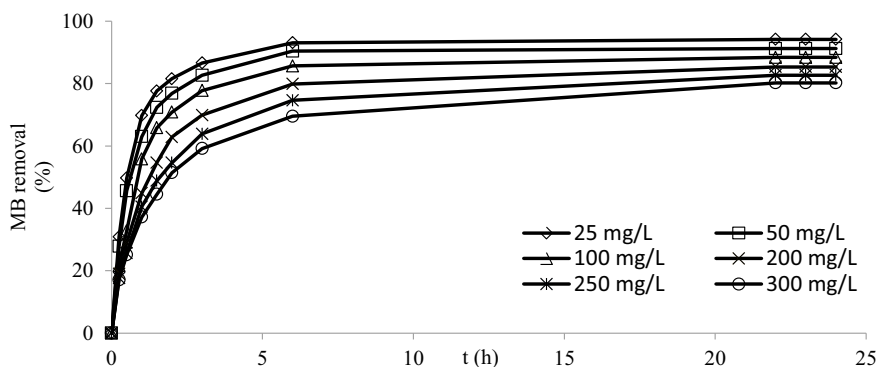


**Fig. 5** MB removal versus adsorption time at various initial concentrations on MB-MWAC at 30 °C

by the systems at 22–24 h. At lower initial concentration, less competition occurs between the solute molecules to be adsorbed by the MWAC; therefore, equilibrium state was achieved faster.

### 3.4 MB Adsorption Isotherms

The plots of linearized equations for isotherms for MB adsorption on optimized MWAC were given in Fig. 6. All the parameters and constants of these isotherms taking place at temperature of 30 °C are summarized in Table 8. The best adsorbate–adsorbent system was selected based on the value of correlation coefficient,  $R^2$ . Based on  $R^2$  values as shown in Table 8, all the isotherm models fitted the equilibrium data in the sequence of Langmuir > Freundlich > Temkin > Dubinin–Radushkevich.

The adsorption of MB dye molecules was taking place on the homogenous active sites available on the surface of MWAC. Each one of these active sites is only capable in accepting one adsorbate molecules per adsorption process due to the monolayer nature of adsorbent. The Langmuir maximum monolayer adsorption capacity,  $Q_m$  for MB-MWAC was 344.83 mg/g. Two important parameters harvested from Freundlich isotherm were heterogeneity factor,  $n_F$  and Freundlich constant,  $K_F$ . The  $n_F$  value was in the range of 1–10, indicated favourable adsorption process for the system.  $K_F$  value characterized the strength of adsorption's bonding energy (Tran et al. 2017). MB-TWAC obtained high  $K_F$  value of 50.32 which signified higher bonding energy between MB and MWAC, which leads to higher adsorption capacity.



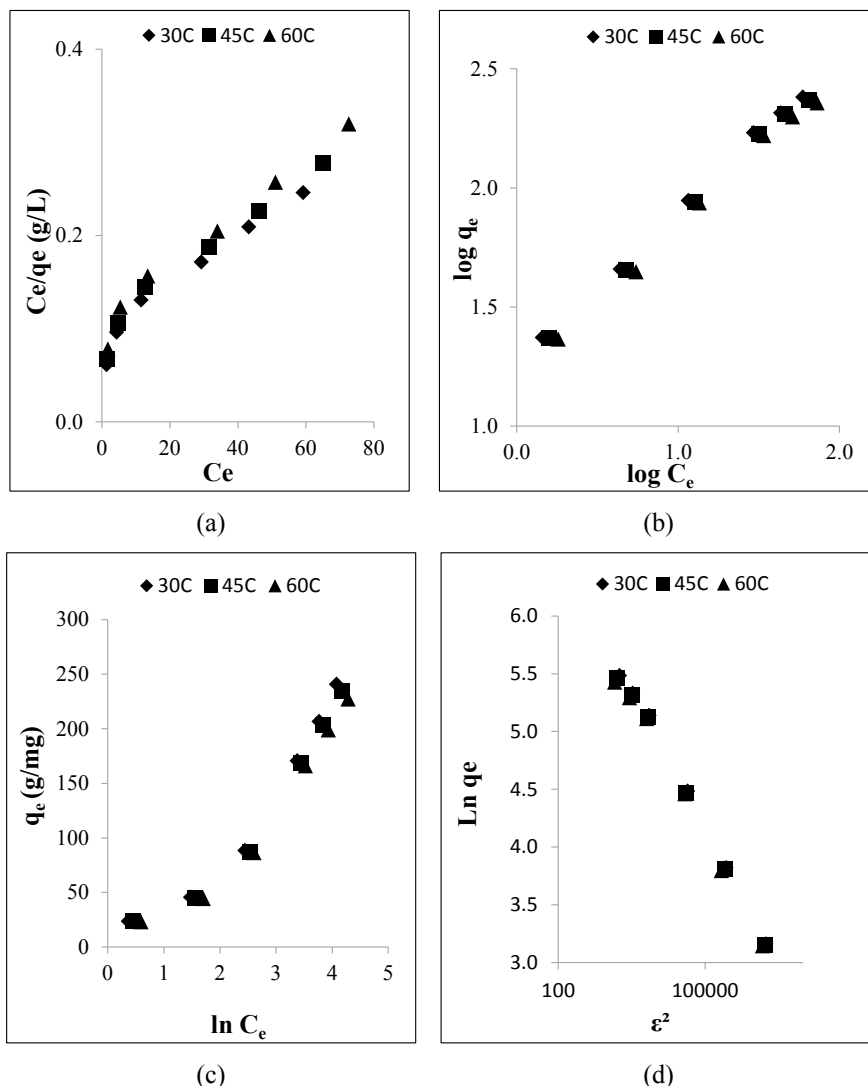


**Fig. 6** Plots of **a** Langmuir, **b** Freundlich, **c** Temkin and **d** Dubinin–Radushkevich for MB adsorption onto MWAC

### 3.5 MB Adsorption Kinetics

Three kinetics models namely pseudo-first order, pseudo-second order and Elovich were employed in this study to give better insight on kinetic behaviour of the adsorption systems studied. The linearized plots of pseudo-first order, pseudo-second order and Elovich kinetics models for MB adsorption by optimized MWAC at 30 °C were,

**Table 8** Isotherm parameters for adsorption of MB by MWAC at 30 °C

Isotherms	Parameters	Adsorption system
Langmuir	$Q_m$ (mg/g)	344.83
	$K_L$ (L/mg)	0.0366
	$R^2$	0.9982
Freundlich	$n_F$	2.54
	$K_F$ (mg/g) (L/mg) <sup>1/n</sup>	46.74
	$R^2$	0.9622
	$1/n_F$	0.3937
Temkin	$B_T$ (L/mg)	59.86
	$A_T$ (L/mg)	0.6527
	$R^2$	0.9334
Dubinin–Radushkevich	$E_{DR}$ (J/mol)	707.11
	$Q_{RD}$	141.12
	$R^2$	0.6816

respectively, given in Figs. 7, 8 and 9, whereas the parameters corresponding with these kinetics models were presented in Table 9.

Pseudo-second-order kinetic model yielded the highest  $R^2$  values for all MB adsorption systems involved with high  $R^2$  values of  $0.9924 < R^2 < 0.9993$  and low normalized standard deviation of  $2.92 < \Delta q_t < 14.47$ . The lower the normalized standard deviation, the more accurate calculated  $q_e$  in predicting experimental  $q_e$ .

The pseudo-first-order kinetic model produced satisfactory  $R^2$  value with high normalized standard deviation. Both  $k_1$  and  $k_2$  were found to decrease with increase in initial concentration for all MB systems studied. At higher initial concentration, the ratio of MB molecules to available surface of MWAC was high, resulting slower adsorption process and lower rate constant (Islam et al. 2015).

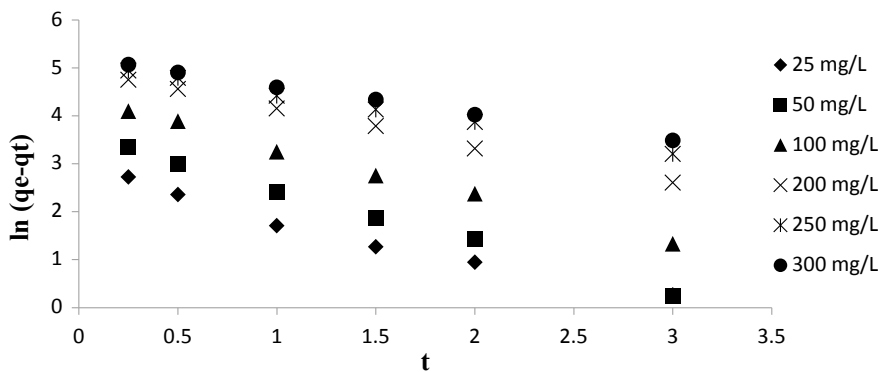


**Fig. 7** Linearized plots of pseudo-first-order kinetic model for MB-MWAC

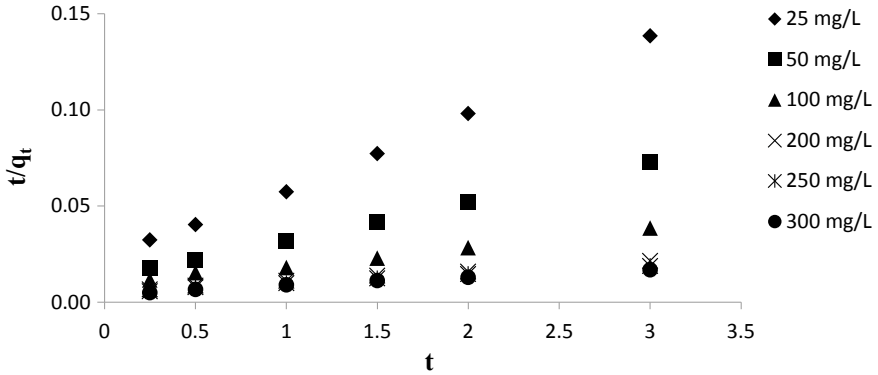


Fig. 8 Linearized plots of pseudo-second-order kinetic model for MB-MWAC

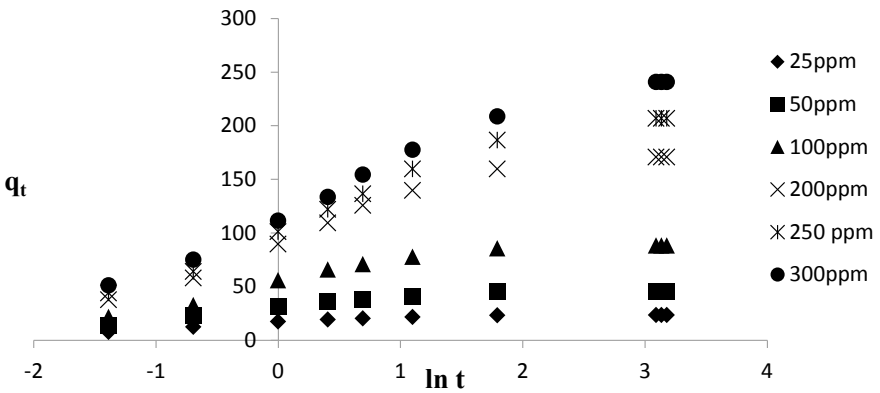


Fig. 9 Linearized plots of elovich kinetic model for MB-MWAC

### 3.6 MB Diffusion Mechanism

The adsorption mechanism comprises (i) film or external mass transfer diffusion, (ii) pore diffusion or intraparticle diffusion and (iii) adsorption of the adsorbate on the surface of the adsorbents. Intraparticle diffusion plot was employed to give a better highlight on the mechanisms of adsorption systems studied as shown in Fig. 10. It was noticed that the plot was multi-linear with three different portions, reflecting three mechanism pathways were involved. Each one of these portions represents different stages in adsorption process. Film layer diffusion was the key characteristic for the first portion where external mass transfer associated with strong electrostatic attraction took place between MB molecules and external surface of MWAC. Adsorption process in this region was fast and completed within 25 min.

**Table 9** Kinetic parameters for MB-MWAC at 30 °C

Initial dye concentration (mg/L)	$q_{e, \text{exp}}$ (mg/g)	Pseudo-first order			Pseudo-second order			Elovich				
		$q_{e, \text{cal}}$ (mg/g)	$k_1$	$R^2$	$\Delta q_t$ (%)	$q_{e, \text{cal}}$ (mg/g)	$k_2$	$R^2$	$\Delta q_t$ (%)	$\alpha_E$	$\beta_E$	$R^2$
25	23.56	15.69	1.103	0.9717	33.39	25.71	0.073	0.9983	9.11	45.22	2.66	0.884
50	45.61	35.35	1.004	0.9876	22.49	50.00	0.033	0.9993	9.63	26.63	5.69	0.826
100	88.43	75.72	0.879	0.9876	14.37	101.23	0.010	0.9929	14.47	9.14	11.26	0.824
200	170.72	140.16	0.788	0.9811	17.90	192.31	0.004	0.9971	12.65	4.98	19.32	0.925
250	206.73	161.76	0.626	0.9933	21.75	212.77	0.004	0.9941	2.92	2.30	24.60	0.914
300	240.78	179.61	0.573	0.9944	25.40	232.56	0.004	0.9924	3.41	1.74	28.78	0.923

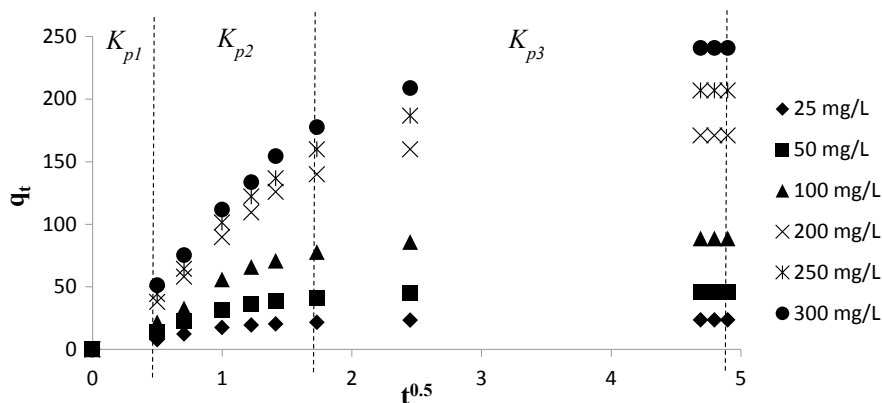


**Fig. 10** Plots of intraparticle diffusion model for MB adsorption by MWAC

The second portion was the gradual adsorption stage where the intraparticle diffusion was the rate limiting step (Wang et al. 2015). It involves diffusion of MB molecules from solution to the interior of MWAC. The third portion was the final equilibrium stage where intraparticle diffusion starts to slow down due to exceptionally low number of MB molecules left in the solution. The plot did not pass through the origin and the higher values of  $K_{p1}$  compared to  $K_{p2}$  at all initial concentration specified that boundary layer diffusion was the dominant mechanism until the exterior active sites are completely occupied. On the other hand, intraparticle diffusion mechanism was the rate limiting step only after a prolonged contact time (Jung et al. 2016).

The constants values obtained from the intraparticle diffusion plot of MB adsorption onto MWAC at 30 °C were tabulated in Table 10. It was observed that the value of  $K_{pi}$  for all three regions increased with initial MB concentration. At higher initial concentration, the driving force for mass transfer was higher, thus enhancing the MB diffusion rate. The values of  $C_i$  were also found to increase with initial concentrations for all three regions, signalling the increment in the boundary layer thickness (Marrakchi et al. 2017). The lines for all MB initial concentrations did not pass through the origin. This finding concluded that the adsorption of MB by MWAC was controlled by film diffusion mechanism.

## 4 Conclusion

Meranti wood sawdust was successfully converted to MWAC via physiochemical activation and heated with microwave radiation. Optimum preparation conditions for MWAC were determined at 365 W, 4.63 min and 0.85, which resulted in 88.0% of MB removal and 31.17% of yield. The optimized MWAC was found to pose high BET surface area of 1257.22 m<sup>2</sup>/g and mesopores surface area of 0.587 cm<sup>3</sup>/g. The

**Table 10** Intraparticle diffusion model constant and  $R^2$  values for adsorption of MB on MWAC

MB initial concentrations (mg/L)	$K_{p1}$ (mg/g h <sup>1/2</sup> )	$K_{p2}$ (mg/g h <sup>1/2</sup> )	$K_{p3}$ (mg/g h <sup>1/2</sup> )	$C_1$	$C_2$	$C_3$	$R_1^2$	$R_2^2$	$R_3^2$
25	15.43	8.73	0.12	0	7.66	22.90	1	0.8923	0.9948
50	27.86	17.84	0.17	0	9.37	44.82	1	0.9302	0.9948
100	43.26	42.75	1.18	0	13.67	82.79	1	0.9119	0.9948
200	85.84	80.68	4.65	0	16.43	148.42	1	0.9702	0.9948
250	98.30	91.93	8.52	0	19.05	165.82	1	0.9815	0.9948
300	102.66	100.11	13.63	0	24.79	175.40	1	0.9892	0.9948

MB uptake increased with the increased of the initial MB concentration and contact time. Isotherm studies found that MB removal followed Langmuir with maximum monolayer adsorption capacity of 344.83 mg/g. Kinetics studies revealed that all adsorption systems studies followed pseudo-second-order kinetic model, whereas mechanism studies divulged that the adsorption process for all systems was controlled by film diffusion mechanism.

**Acknowledgements** The work was supported by the Research University Grant (8014061) and Bridging Grant (6316195) from Universiti Sains Malaysia.

## References

- Azizi, M., Mohebbi, N., & De Felice, F. (2016). Evaluation of sustainable development of wooden furniture industry using multi criteria decision making method. *Agriculture and Agricultural Science Procedia*, 8, 387–394.
- Balarak, D., Jaafari, J., Hassani, G., Mahdavi, Y., Tyagi, I., & Agarwal, S. (2015). The use of low cost adsorbent (Canola residues) for the adsorption of methylene blue from aqueous solution: isotherm, kinetic and thermodynamic studies. *Colloid and Interface Science Communications*, 7, 16–19.
- Dubinin, M. M., & Radushkevich, L. V. (1947). The equation of the characteristic curve of activated charcoal. *Proceedings of the Academy of Sciences of the USSR*, 55, 331–337.
- Freundlich, H. M. F. (1906). Over the adsorption in solution. *The Journal of Physical Chemistry*, 57, 385–471.
- Govoni, P. (2016). World furniture outlook on global markets. Furniture & Furnishing Export International. Available: <http://www.furnitureandfurnishing.com/html/jan16/csil-world-report-world-furniture-outlook-on-global-markets.php>. Accessed February 11, 2017.
- Ho, Y. S., & McKay, G. (1999). Sorption of dye from aqueous solution by peat. *Chemical Engineering Journal*, 70, 115–124.
- Islam, M. A., Ahmed, M. J., Khanday, W. A., Asif, M., & Hameed, B. H. (2017). Mesoporous activated carbon prepared from NaOH activation of rattan (*Lacosperma secundiflorum*) hydrochar for methylene blue removal. *Ecotoxicology and Environmental Safety*, 138, 279–285.
- Islam, M. A., Benhouria, A., Asif, M., & Hameed, B. (2015). Methylene blue adsorption on factory-rejected tea activated carbon prepared by conjunction of hydrothermal carbonization and sodium hydroxide activation processes. *Journal of the Taiwan Institute of Chemical Engineers*, 52, 57–64.
- Jung, K. W., Choi, B. H., Hwang, M. J., Jeong, T. U., & Ahn, K. H. (2016). Fabrication of granular activated carbons derived from spent coffee grounds by entrapment in calcium alginate beads for adsorption of acid orange 7 and methylene blue. *Bioresource Technology*, 219, 185–195.
- Kono, H. (2015). Preparation and characterization of amphoteric cellulose hydrogels as adsorbents for the anionic dyes in aqueous solutions. *Gels*, 1, 94–116.
- Kushwaha, A. K., Gupta, N., & Chattopadhyaya, M. C. (2014). Removal of cationic methylene blue and malachite green dyes from aqueous solution by waste materials of daucus carota. *Journal of Saudi Chemical Society*, 18, 200–207.
- Lagergren, S., & Svenska, K. (1898). About the theory of so-called adsorption of soluble substances. *Sven Vetenskapsakad Handlingar*, 24, 1–39.
- Langmuir, I. (1918). The adsorption of gases on plane surfaces of glass, mica and platinum. *Journal of the American Chemical Society*, 40, 1361–1403.
- Marrakchi, F., Ahmed, M. J., Khanday, W. A., Asif, M., & Hameed, B. H. (2017). Mesoporous-activated carbon prepared from chitosan flakes via single-step hydroxide activation for the adsorption of methylene blue. *International Journal of Biological Macromolecules*, 98, 233–239.

- MIFF. (2018). Malaysian International Furniture Fair. Available: <http://2018.miff.com/about-miff/malaysian-furniture-industry/>. Accessed January 11, 2017.
- Porhemmat, S., Ghaedi, M., Rezvani, A. R., Azghandi, M. H. A., & Bazrafshan, A. A. (2017). Nanocomposites: synthesis, characterization and its application to removal azo dyes using ultrasonic assisted method: modeling and optimization. *Ultrasonics Sonochemistry*, 38, 530–543.
- Rafiqul, I. S. M., & Mimi Sakinah, A. M. (2012). Kinetic studies on acid hydrolysis of meranti wood sawdust for xylose production. *Chemical Engineering Science*, 71, 431–437.
- Temkin, M. I., & Pyzhev, V. (1940). Kinetics and ammonia synthesis on promoted iron catalyst. *Acta Physicochimica USSR*, 12, 327–356.
- Tey, K. (2017). Strengthening the furniture industry. Metro News. Available: <https://www.thestar.com.my/metro/community/2017/06/20/strengthening-the-furniture-industry-threeday-fair-serves-as-platform-to-promote-products-for-export/>. Accessed February 11, 2017.
- Tharaneedhar, V., Senthil Kumar, P., Saravanan, A., Ravikumar, C., & Jaikumar, V. (2017). Prediction and interpretation of adsorption parameters for the sequestration of methylene blue dye from aqueous solution using microwave assisted corncob activated carbon. *Sustainable Materials and Technologies*, 11, 1–11.
- Tran, H. N., Wang, Y.-F., You, S.-J., & Chao, H.-P. (2017). Insights into the mechanism of cationic dye adsorption on activated charcoal: the importance of  $\pi$ - $\pi$  interactions. *Process Safety and Environmental Protection*, 107, 168–180.
- Wang, P., Ma, Q., Hu, D., & Wang, L. (2015). Removal of reactive blue 21 onto magnetic chitosan microparticles functionalized with polyamidoamine dendrimers. *Reactive & Functional Polymers*, 91, 43–50.
- Weber, T. W., & Chakkravorti, R. K. (1974). Pore and solid diffusion models for fixed-bed adsorbers. *AIChE Journal*, 20, 228–238.
- Yagub, M. T., Sen, T. K., Afroze, S., & Ang, H. M. (2014). Dye and its removal from aqueous solution by adsorption: a review. *Advances in Colloid and Interface Science*, 209, 172–184.
- Zhou, L., Yu, Q., Cui, Y., Xie, F., Li, W., Li, Y., et al. (2017). Adsorption properties of activated carbon from reed with a high adsorption capacity. *Ecological Engineering*, 102, 443–450.



# A Study on the Adsorption of 2,4,6-Trichlorophenol by Palm Kernel Cake



Duduku Krishnaiah, Awang Bono, Collin G. Joseph, S. M. Anisuzzaman, and Lester Venantius

**Abstract** In this study, 2,4,6-trichlorophenol (TCP) adsorption on palm kernel cake (PKC) was examined. The effects of the initial concentration, agitation time, solution temperature and pH on TCP adsorption were examined in batch adsorption studies. The adsorption capacity was positively related to the initial concentration and agitation time and negatively related to the pH and solution temperature. Experimental data indicated that the Langmuir isotherm best fits the data (maximum monolayer adsorption capacity of 22.22 mg/g at 30 °C). The adsorption kinetics followed a pseudo-second-order kinetic model. Analysis of various thermodynamic parameters indicated that the adsorption was non-spontaneous and exothermic, whereas the Elovich equation and the pseudo-second-order kinetic model determined that chemisorption was the rate-controlling step.

**Keywords** Palm kernel cake · 2,4,6 trichlorophenol · Adsorption · Isotherm · Kinetics

## 1 Introduction

The removal of contaminants of emerging concern from contaminated industrial effluents, such as 2,4,6-trichlorophenol (TCP), is very important in developing countries. TCP has been reported in wastewater from pesticide, wood, pharmaceutical, and dye manufacturing plants, as well as in wastewater from paper and pulp industries and water disinfection processes (Fan et al. 2011; Hameed 2007; Hameed et al. 2008, 2009; Siva Kumar et al. 2012). TCP is a major concern due to its toxicity, mutagenic and carcinogenic properties. Its harmful effect on the human nervous system is well documented, and it causes secondary health disorders, such as respiratory,

---

D. Krishnaiah (✉) · A. Bono · S. M. Anisuzzaman · L. Venantius  
Chemical Engineering Program, Faculty of Engineering, Universiti Malaysia Sabah, 88400 Kota Kinabalu, Sabah, Malaysia  
e-mail: [krishna@ums.edu.my](mailto:krishna@ums.edu.my)

C. G. Joseph  
Water Research Unit, Faculty of Science and Natural Resources, Universiti Malaysia Sabah, 88400 Kota Kinabalu, Sabah, Malaysia

cardiovascular and gastrointestinal disorders. The stable C-Cl bond and position of the chlorine atoms relative to the hydroxyl group are responsible for TCP's toxicity and persistence in the biological environment (Chen et al. 2009; Hameed et al. 2008, 2009; Siva Kumar et al. 2012). As a result of its high toxicity, carcinogenic properties and structural stabilization in the environment, the removal of TCP from the environment is an imperative remediation target.

An Internet literature survey revealed that researchers attempted to use various treatment methods to remove TCP from wastewater streams. Methods employing biological treatments, catalytic wet oxidation, photochemical treatment and adsorption technologies have been widely explored and investigated (Fan et al. 2011; Hameed 2007; Hameed et al. 2008, 2009; Joseph et al. 2011; Li Puma et al. 2008; Siva Kumar et al. 2012). However, the adsorption remains the fastest removal method, especially if the wastewater stream is in constant motion. Adsorbent technologies using coconut-based activated carbon (Hameed et al. 2008), *loosestrife*-based activated carbon (Fan et al. 2011), activated clay (Hameed 2007) and biosorption using *Acacia leucocephala* bark (Siva Kumar et al. 2012) have successfully removed TCP from wastewater streams. Other types of non-organic and organic-based adsorbents have also been studied for this purpose, such as siliceous material, zeolite, chitin, chitosan, peat, biomass, sawdust, rice husk, bark, fly ash, sludge, a guava seed and red mud. All of these materials have been proven to be successful to a certain extent (Ahmaruzzaman 2008; Joseph et al. 2007).

Adsorption by activated carbon is one of the most effective and extensively used techniques to treat high-strength and low-volume chlorinated phenolic wastewater. This method is favored due to its fast adsorption kinetics and simple design (Hameed et al. 2009). The effectiveness of this adsorbent is attributed to its structural characteristics and porous texture. Its large surface area and ease with which its chemical nature can be modified using chemical treatment make it a suitable choice for the removal of pollutants in wastewater streams (Ahmaruzzaman 2008). However, activated carbon presents several weaknesses. The regeneration of saturated carbon is costly, complicated and usually results in significant material loss. The use of carbon based on relatively expensive precursors has economic drawbacks and is unjustifiable for most pollution control applications, including non-renewable drawbacks (Ahmaruzzaman 2008; Hameed et al. 2009, 2008; Anisuzzaman et al. 2015, 2016; Krishnaiah et al. 2017). Besides, the literature survey indicated that polymer-based adsorbents are widely used to remove chlorinated phenolic compounds, but this process is not cost effective (Siva Kumar et al. 2012).

Thus, the search for new materials with high adsorptive capacities is currently the focus of an adsorbent investigation. Biodegradable and disposable adsorbents would constitute another advantage due to their low cost. Over the last decade, researchers have published studies suggesting industrial solid waste as a suitable precursor for adsorbents. However, to the best of the author's knowledge, the adsorption of TCP to palm kernel cake PKC has not been reported in the literature. PKC, an industrial waste from palm oil mill effluent (POME), is readily available and abundant. This promising material could be an alternative to the more costly wastewater treatment

processes that are currently employed. Besides, PKCs are readily available, disposable, biodegradable and cheap due to their waste-to-wealth benefits. Spent PKC can be ashed and used as fertilizer. The adsorbed TCP will easily decompose during this process, rendering the ash innocuous (Joseph et al. 2011).

## ***1.1 Research Objectives***

In this work, the adsorption of TCP to PKC was studied and evaluated as a promising adsorbent for wastewater remediation. Parametric studies focusing on the pH, contact time, temperature and initial concentration of TCP are presented in this paper. The equilibrium and kinetic data of the adsorption were also analyzed to better understand the mechanism of TCP adsorption to the PKC.

## **2 Methodology**

### ***2.1 Materials and Methods***

The PKC used as an adsorbent in this study was obtained from a palm oil refinery mill in Kunak, Sabah. The 2,4,6-trichlorophenol (98%) obtained from Aldrich was used without further purification. The chemical formula of TCP is  $C_6H_3Cl_3O$ , and its molecular weight is 197.46 g/mol.

### ***2.2 Preparation of Palm Kernel Cake***

The PKC was solar dried for 30 days and then washed several times with distilled water before oven drying at 80 °C overnight. The dried PKC was ground and sieved to obtain particles between 50 and 80  $\mu\text{m}$  in size. These PKC particles were stored in a closed container until needed.

### ***2.3 Batch Equilibrium and Kinetic Studies***

Batch adsorption experiments using 250 ml Erlenmeyer flasks were performed in a mechanical shaker equipped with a thermostatic water bath at a fixed 30 °C. To elucidate the effect of pH, 100 ml of a 100 mg/l TCP solution and 1.0 g of PKC were added into a series of flasks at different pH values. The pH values of the TCP

solutions were adjusted in the range of 2–12 using 0.1 M HCl and/or 0.1 M NaOH solutions and then agitated for 90 min before sample extraction.

A similar setup was used to investigate the effect of contact time and equilibrium time, but the samples were agitated for different times, ranging from 0 to 150 min until a steady state was reached. The effects of temperature on the adsorption mechanism of TCP onto PKC were studied by performing adsorption experiments at 30, 40 and 50 °C. To study the effect of initial concentration on the adsorption of TCP onto PKC, the concentrations of the TCP solution were varied (100, 150 and 200 mg/l) at its natural pH of 6. All experiments were conducted in triplicate unless stated otherwise. The extracted samples were filtered through Whatman 0.45  $\mu\text{m}$  filter paper before analysis to minimize the interference of fine particles. The concentrations of extracted samples were determined by a UV spectrophotometer (Jasco V-650) at its maximum wavelength of 298.8 nm. The amount of TCP adsorbed per unit mass of the adsorbent was evaluated by using the following equation:

$$q_e = \frac{(C_0 - C_e) \times V}{W} \quad (1)$$

The percent removal of TCP was calculated as follows:

$$\text{Removal (\%)} = \frac{(C_0 - C_e)}{C_0} \times 100\% \quad (2)$$

where  $C_0$  and  $C_e$  (mg/L) are the liquid-phase concentrations of TCP at the initial and the equilibrium stages, respectively,  $V$  is the volume of the solution (L) and  $W$  is the mass of dry adsorbent used (g) (Hameed et al. 2008). The equilibrium data obtained were analyzed using the Langmuir, Freundlich, Temkin, and Redlich–Peterson (R–P) isotherms, and the characteristic parameters for each isotherm were determined.

## 2.4 Chemical Characteristics of Palm Kernel Cake

Fourier transform infra-red spectroscopy (FTIR) was performed to determine the presence of the surface functional groups on the PKC before and after TCP adsorption. The spectra were recorded between 4000 and 400  $\text{cm}^{-1}$ .

## 3 Results and Discussion

### 3.1 Chemical Characteristics of Palm Kernel Cake

The obtained FTIR spectra revealed various functional groups on the prepared palm kernel cake. Figure 1 shows the FTIR spectra of PKC before and after adsorption. The broadband at 3353.17  $\text{cm}^{-1}$  found in the spectrum of the PKC before and after

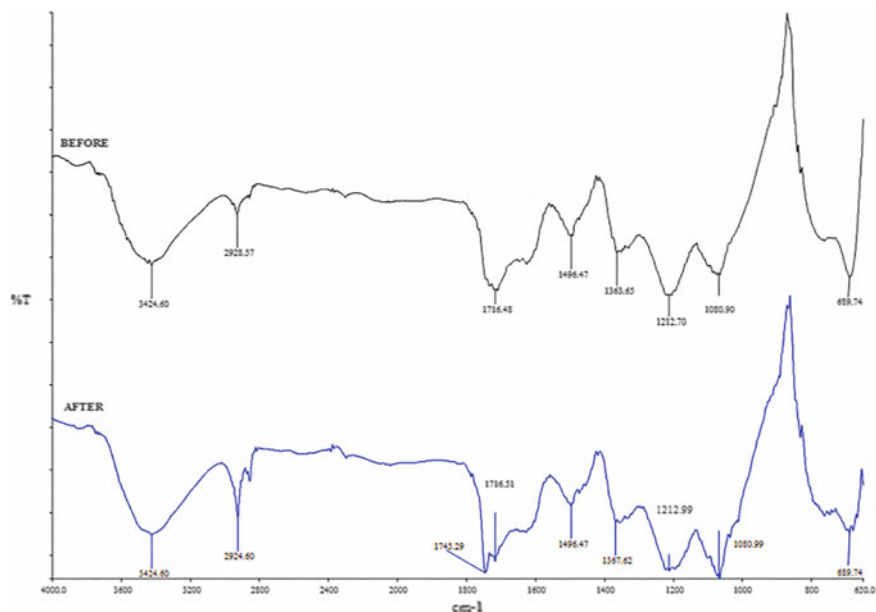


**Fig. 1** FTIR spectra of PKC before and after adsorption

TCP adsorption can be assigned to O–H stretching vibration of hydroxyl functional groups, including hydrogen bonding. The other peaks detected on the activated carbon before TCP adsorption were located at 2928.57, 1716.48, 1496.47, 1363.65, 1212.70 and 1080.90  $\text{cm}^{-1}$  and assigned to C–H stretching (alkanes), C=O stretching (carboxylic),  $\text{NO}_2$  aromatic, CH plane bending (alkenes) C–C stretching (ketone) and C–O stretching (alcohol), respectively. Comparing the two spectra indicated that the functional groups were not chemically altered by the adsorbed TCP, although some shifting to the left was observed. These data indicate that PKC is a suitable adsorbent for TCP, as the adsorption process did not deactivate or alter the active sites on the adsorbent. It is, therefore, possible to regenerate the PKC for continuous use. A new peak was detected at 1745.29  $\text{cm}^{-1}$  and assigned as C=O stretching (ester). The changes in the peaks might be due to the overlapping of the functional group itself.

### ***3.2 Effect of Agitation Time and TCP Initial Concentration on Adsorption Equilibrium***

The adsorption was carried out using 1.0 g of PKC with 100 ml of TCP solution at a fixed temperature of 30 °C in a constant isothermal water bath with an agitation speed of 8/10. The natural pH of the solution was 6.2, which was not adjusted. Figure 2a

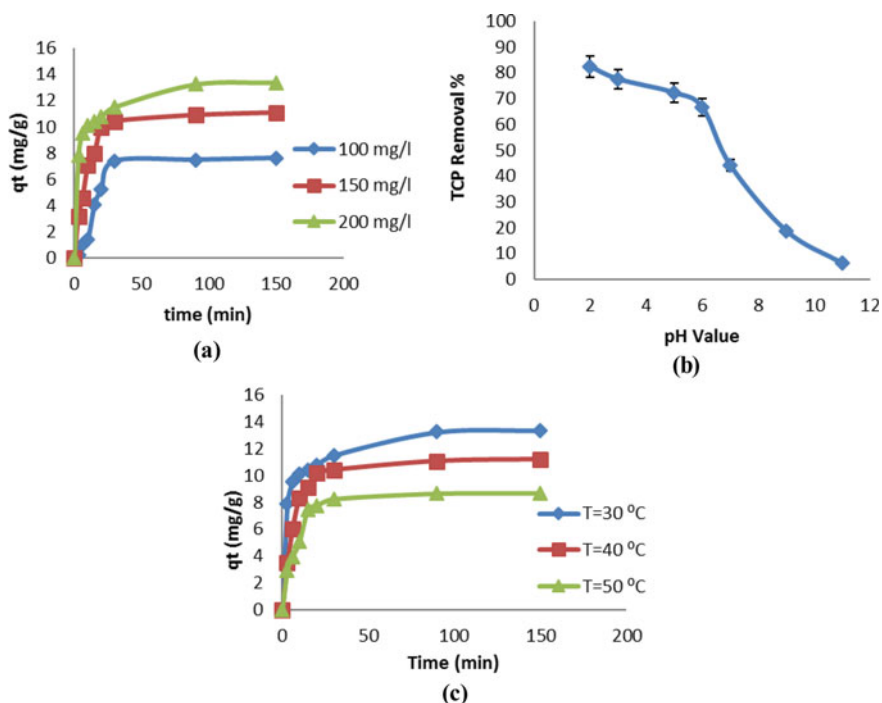


**Fig. 2** Effect of agitation time (a) on the adsorption of TCP for various initial concentrations at fixed temperature (30 °C), solution pH (b) at fixed concentration (200 mg/l) and temperature (30 °C) and temperature (c) at fixed concentration (200 mg/l)

shows the effect of agitation time and TCP initial concentration on the removal of TCP by the prepared PKC.

The plots show that the adsorption of TCP correlated positively with the agitation time and attains equilibrium earlier for solutions with lower initial concentrations. The adsorption curves were smooth and continuous leading to saturation. The results revealed that the TCP adsorption was fast at the initial stages of the contact period and slowed thereafter near the equilibrium. This phenomenon could be attributed to a large number of vacant surface sites available for adsorption during the initial stage. After some time had elapsed, the remaining vacant surface sites were difficult to occupy due to the repulsive forces between the solute molecules on the solid and bulk phases. A similar trend was observed for the adsorption of TCP on activated clay (Hameed 2007) and activated carbon derived from *loosestrife* (Fan et al. 2011). An equilibrium time of 30–90 min was needed for solutions with initial concentrations of 100–150 mg/l. However, longer times were required for higher initial concentrations (200 mg/l) to reach equilibrium. Specifically, solutions with higher initial concentrations reached equilibrium after 90 and 150 min. Hameed et al. found that the equilibrium time for the adsorption of TCP by coconut shell-based activated

carbon was 15–90 min for TCP initial concentrations of 25–150 mg/l. However, solutions with higher initial concentrations (200 and 250 mg/l) required up to 130 min to reach equilibrium (Hameed et al. 2008). Hameed found that TCP solutions with initial concentrations below 150 mg/l required almost 30 min to reach equilibrium when adsorbing to activated clay; this time exceeded 60 min for higher initial concentrations (Hameed 2007). Furthermore, Fan et al. reported that the equilibrium time for the adsorption of TCP by activated carbon derived from *loosestrife* was below 100 min for initial TCP concentration of 50–150 mg/l and more than 100 min for higher initial concentration of TCP (Fan et al. 2011). These data show that the adsorption performance of the PKC prepared in this study was comparable with the works of previous researchers.

TCP was adsorbed quickly due to the high affinity of the interacting groups on the surface of the PKC. The high adsorption rate at the beginning of adsorption could be attributed to the adsorption of TCP on the exterior surface of the adsorbent. When the exterior surface was saturated, the TCP entered into the pores of the adsorbent and was absorbed by the interior surface of the particles (Hameed 2007). The adsorption rate can vary because it depends on several parameters, such as the stirring rate, structural properties of the adsorbent, adsorbent dosage and adsorbate properties. The amount of TCP adsorbed by the PKC increases with time for all initial concentrations (100–200 mg/l) and eventually reaches a constant value beyond which no more TCP is removed from the solution. At this point, the amount of TCP desorbing from the PKC is in a state of dynamic equilibrium with the amount of the TCP being adsorbed to the PKC. The amount of TCP adsorbed at the equilibrium time reflects the maximum adsorption capacity of the adsorbent under these operating conditions. In this study, the adsorption capacity at equilibrium,  $q_e$ , increased from 7.38 to 13.24 mg/g when the initial concentration increased from 100 to 200 mg/l. When the initial concentration increased, the mass transfer driving force grew, which also increased the adsorption of TCP.

### 3.3 Effect of Solution pH on Adsorption of TCP

Figure 2b shows the effect of solution pH on the removal of TCP by the prepared PKC, together with the error bars representing the deviation errors for the replicate data. The fraction of removed TCP inversely correlated with the solution pH and the readings obtained from the replicates for each solution pH were quite consistent, yielding relatively small deviation errors. In this study, the highest TCP removal rate of 82.47% was achieved at pH 2 with an initial TCP concentration of 200 mg/l. This maximum value could be attributed to the acidic nature of the PKC; its unadjusted pH was approximately 6. At a solution pH lower than 6, the average total surface charge should be positive, whereas it would be negative at higher solution pH values. The TCP uptake was the highest at pH values that were below the  $pK_a$  of TCP because the TCP was undissociated and the dispersion interactions predominated at acidic pH values (Hamdaoui and Naffrechoux 2007). The concentration of unionized species

of halogenated organic compounds was high, which did not favor the repulsion between the PKC surface and the molecular species of TCP, and thereby increased the electrostatic attractions between the TCP molecules and the adsorption sites. However, the 2,4,6-TCP uptake was lower at basic pH values due to the electrostatic repulsions between the negative surface charge and the chlorophenolate anions and the electrostatic repulsion between the chlorophenol anions in solution (Hamdaoui and Naffrechoux 2007). Furthermore, the OH<sup>-</sup> ions and the ionic species of TCP may compete for adsorption sites. Similar trends were reported for the adsorption of TCP on coconut shell-based activated carbon (Radhika and Palanivelu 2006) and activated clay (Hameed 2007).

### 3.4 Effect of Temperature on Adsorption of TCP

The effect of temperature on the adsorption capacity of PKC was studied by carrying out a series of isotherms at 30, 40 and 50 °C using an initial TCP concentration of 200 mg/L without adjusting the pH. The equilibrium uptake of TCP by PKC was significantly affected by the temperature. Figure 2c shows the effect of temperature on the equilibrium adsorption capacity of PKC. The temperature inversely correlated with the removal of TCP. The decrease in the adsorption capacity at increased temperatures indicated that the adsorption of TCP onto PKC is exothermic. A similar trend was also observed by Bilgili for the 4-chlorophenol adsorption to XAD-4 resin (Bilgili 2006). Furthermore, Fan et al. found that the removal of TCP by activated carbon derived from *loosestrife* decreased as the temperature of the solution increased (Fan et al. 2011). This trend may be attributed to the weakening of adsorptive forces between the active sites of the adsorbent and adsorbate species as well as between the adjacent molecules of the adsorbed phase (Panday et al. 1986). The adsorption capacities of PKC were determined to be 13.37, 11.20 and 8.68 mg/g at 30, 40 and 50 °C, respectively. The optimum temperature for TCP adsorption to PKC was 30 °C.

### 3.5 Adsorption Isotherm on Equilibrium Data for the Adsorption of TCP on PKC

The analysis of the isotherm data is important to develop an equation that correctly represents the results and could be used for design purposes. Four isotherm models, the Langmuir, Freundlich, Temkin, and Redlich–Peterson (R–P) models, were used to describe the equilibrium characteristics of adsorption. The Langmuir model presents a clear concept of monomolecular adsorption on energetically homogeneous surfaces and can be expressed as follows (Mahmoud et al. 2012):

$$q_e = \frac{q_{\max} K_L C_e}{1 + K_L C_e} \quad (3)$$



where  $q_{max}$  (mg/g) (mg/ml) is the maximum amount of the adsorbate per unit weight of the adsorbent to form a complete monolayer on the surface.  $K_L$  (l/mg) is the Langmuir constant related to the affinity of the binding sites. Linearizing Eq. 3 yields Eq. 4:

$$\frac{C_e}{q_e} = \frac{1}{q_{max} K_L} + \frac{C_e}{q_{max}} \tag{4}$$

The values of the constants can be determined from the intercept and the slope of the linear plot of the experimental data of  $(\frac{C_e}{q_e})$  versus  $C_e$ . In addition, the essential feature of the Langmuir isotherm can be expressed  $R_L$  using, a dimensionless constant referred to as the separation factor or equilibrium parameter, which is calculated using the following equation:

$$R_L = \frac{1}{1 + K_L C_0} \tag{5}$$

where  $K_L$  is the Langmuir adsorption constant related to the free energy of adsorption (L/mg) and  $C_0$  is the highest initial adsorbate concentration (mg/L). The value of the separation factor classifies the adsorption process as follows:

- Unfavorable ( $R_L > 1$ )
- Linear ( $R_L = 1$ )
- Favorable ( $0 < R_L < 1$ )
- Irreversible ( $R_L = 0$ ).

Figure 3a shows the Langmuir isotherm for TCP adsorption onto PKC at 30 °C with initial concentrations varying from 100 to 200 mg/L. Thus, the  $q_{max}$  and  $K_L$  can be determined by comparing the linear equation of the Langmuir isotherm with

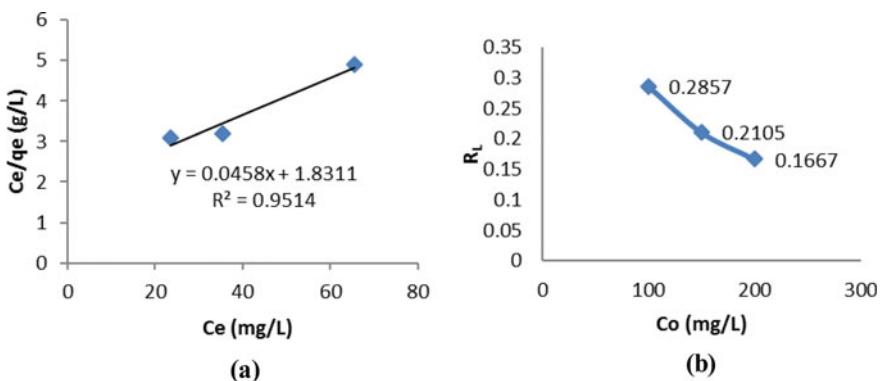


**Fig. 3** Langmuir isotherm (a) for TCP adsorption onto PKC at 30 °C with initial concentrations varying from 100 to 200 mg/l and the effect of the initial concentration of TCP on the separation factor,  $R_L$  (b)

Eq. (4). This method yielded  $q_{\max}$  and  $K_L$  values of 22.22 mg/g and 0.025 L/mg, respectively, at 30 °C with an  $R^2$  of 0.951.

Figure 3b represents the calculated  $R_L$  values versus the initial concentration of TCP at 30 °C. All  $R_L$  values fell between 0 and 1, indicating that the adsorption of TCP on PKC was favorable at the studied conditions. However, as the initial concentration increased from 100 to 200 mg/L, the  $R_L$  value decreased from 0.2857 to 0.1667. This change indicated that the adsorption was more favorable at higher concentrations.

The Freundlich model is an empirical equation based on sorption on heterogeneous surfaces or surfaces supporting sites of varied affinities. This model assumes that the stronger binding sites are occupied first and that the binding strength decreases as the number of occupied sites increases. The isotherm is expressed as follows:

$$q_e = K_F C_e^{\frac{1}{n}} \quad (6)$$

where  $K_F$  (mg/g (l/mg) $^{1/n}$ ) and  $n$  are the Freundlich constants related to sorption capacity and sorption intensity of the adsorbent, respectively.  $K_F$  can be defined as the adsorption or distribution coefficient and represents the quantity of adsorbate adsorbed onto an adsorbent for a unit equilibrium concentration (Hameed et al. 2008). The linear form of the Freundlich isotherm model can be defined by the following equation:

$$\ln q_e = \ln K_F + \frac{1}{n} \ln C_e \quad (7)$$

The applicability of the Freundlich sorption isotherm was analyzed by plotting  $q_e$  inverse  $\ln C_e$ . This plot yields a straight line with a slope equal to  $1/n$ . The value of this slope ranges between 0 and 1 is a measure of the adsorption intensity or surface heterogeneity. The surface becomes more heterogeneous as the value of the slope approaches zero, and the value of  $1/n$  below one indicates a normal Langmuir isotherm, while a value of  $1/n$  above one is indicative of cooperative adsorption (El-Sayed 2011; Hameed et al. 2008). The constants  $K_F$  and  $n$  can be determined by comparing Eq. 7 with the linear Freundlich sorption isotherm as shown in Fig. 4a. The values of  $K_F$  and  $n$  were determined to be 1.553 and 1.887, respectively, at 30 °C with an  $R^2$  of 0.911. The  $1/n$  value for the Freundlich model, which was 0.53 (below 1), indicated a normal Langmuir isotherm.

The Temkin isotherm contains a factor that explicitly takes the adsorbent–adsorbate interactions into account. According to the model, the heat of adsorption of all the molecules in the layer decreases linearly with coverage due to the adsorbent–adsorbate interactions. The adsorption is characterized by a uniform distribution of binding energies up to a specific maximum binding energy. The Temkin isotherm is expressed as follows:

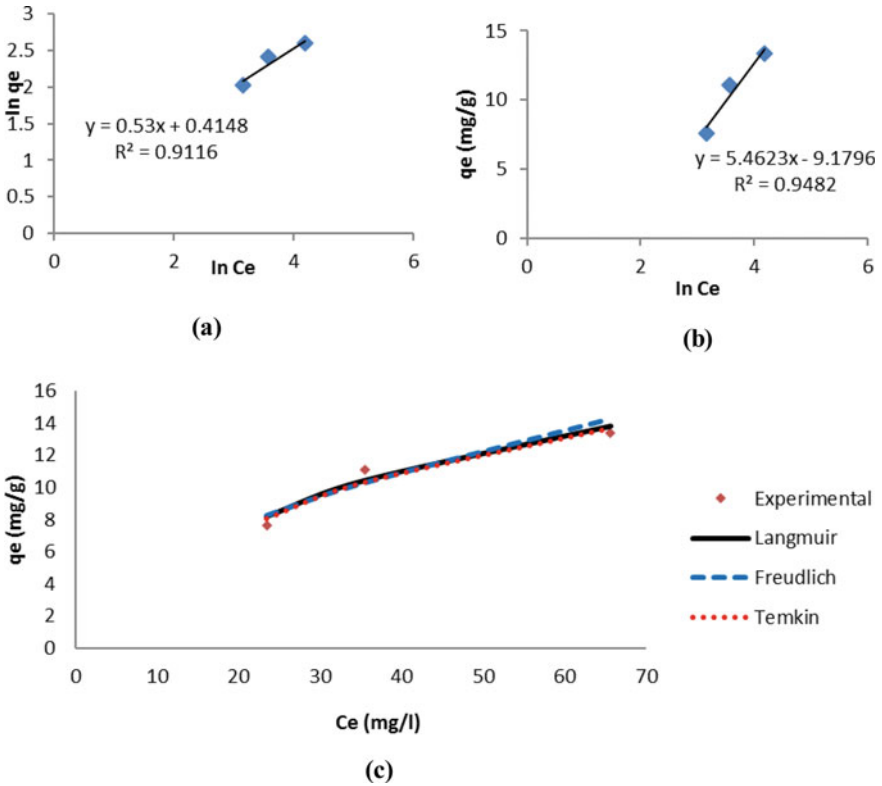


**Fig. 4** Freundlich isotherms (a) and Temkin isotherms (b) for TCP adsorption onto PKC at 30 °C with an initial TCP concentration of 200 mg/L and equilibrium adsorption isotherms (c) of TCP on PKC at 30 °C fitted to the Langmuir, Freundlich and Temkin models

$$q_e = \left( \frac{RT}{b_T} \right) \ln(AC_e) \tag{8}$$

where  $RT/b_T = B$  (J/mol), which is the Temkin constant related to the heat of sorption.  $An$  (l/g) is the equilibrium binding constant corresponding to the maximum binding energy.  $R$  (8.314 J/mol K) is the universal gas constant, and  $T$  (K) is the absolute solution temperature (Hameed et al. 2008). The Temkin isotherm can be linearized to form Eq. 9:

$$q_e = B \ln A + B \ln C_e \tag{9}$$

The constants  $A$  and  $B$  can be determined by plotting  $\ln C_e$  versus  $q_e$  (El-Sayed 2011). Hence, these constants can be determined by comparing Eq. 9 to the linear Temkin isotherm as shown in Fig. 4b. The values of  $A$  and  $B$  were determined to be 0.1863 and 5.462, respectively, at 30 °C with  $R^2$  of 0.948.

The Redlich–Peterson (R–P) equation is widely used as a compromise between the Langmuir and Freundlich systems. This model has three parameters and incorporates the advantages of the Langmuir and Freundlich models. R–P model can be represented as follows:

$$q_e = \frac{K_{RP}C_e}{1 + (\alpha C_e)^\beta} \tag{10}$$

where  $K_{RP}$  (l/g) and  $\alpha$  (l/mg)<sup>β</sup> are the Redlich–Peterson isotherm constants.  $\beta$  is the exponent, which lies between 0 and 1. The R–P model has two limiting cases: when  $\beta = 1$ , the R–P model is reduced to the Langmuir equation, whereas when  $\beta = 0$ , the R–P equation transforms into Henry’s law. The Redlich–Peterson isotherm contains three unknown parameters ( $K_{RP}$ ,  $\alpha$  and  $\beta$ ), which cannot be identified using the linearized Redlich–Peterson isotherm. Therefore, the Redlich–Peterson linearized isotherm model cannot explain the adsorption isotherm of TCP onto PKC (Subramanyam and Das 2009).

The three nonlinear equations were solved using the MS-EXCEL software. The isotherms of TCP adsorption onto PKC predicted from all three models are plotted in Fig. 4c. The values obtained for the correlation coefficient,  $R^2$ , and the constants for the models are summarized in Table 1. The Langmuir model yielded the best fit with the highest  $R^2$  value of 0.997. Thus, the Langmuir isotherm was the most suitable equation to describe the adsorption equilibrium of TCP on PKC. Figure 4c indicates that the  $q_e$  values predicted by the Langmuir model agreed well with the experimental values. The suitability of the Langmuir isotherm to fit the data was confirmed by the Freundlich model, as the  $1/n$  value from the Freundlich was below 1, which indicated a normal Langmuir isotherm.

Confirmation of the experimental data to the Langmuir isotherm equation indicated the homogeneous nature of the PKC surface; the adsorption activation energy of each TCP molecule/PKC was equal. The results also demonstrated the formation of a monolayer of TCP molecules at the outer surface of the PKC. The Langmuir isotherm also indicates a number of additional mechanisms: (1) adsorption take place at specific homogeneous sites within the adsorbent; (2) once a TCP molecule occupies a site, no further adsorption can take place at that site; (3) the strength of the

**Table 1** The Langmuir, Freundlich and Temkin isotherm model constants and correlation coefficients for the adsorption of TCP on PKC at 30 °C

Isotherm	Parameters
Langmuir	$Q = 22.22$ mg/g $K_L = 0.025$ l/mg $R^2 = 0.951$
Freundlich	$K_F = 1.553$ mg/g (l/mg) <sup>1/n</sup> $1/n = 0.530$ $R^2 = 0.911$
Temkin	$A = 0.1863$ l/g $B = 5.462$ J/mol $R^2 = 0.948$

**Table 2** Comparison of maximum monolayer adsorption capacity of various adsorbates on different adsorbents

Adsorbent	Adsorbate	Maximum monolayer adsorption capacity (mg/g)	Reference
Palm kernel cake (PKC)	2,4,6-Trichlorophenol	22.22	This work
Palm kernel fiber	Methylene blue (MB) Crystal violet (CV) Lead ions	95.4 78.9 49.9	El-Sayed (2011) El-Sayed (2011) Ho and Ofomaja (2005)
Rice straw-based carbon	3-Chlorophenol	14.20	Wang et al. (2007)
Anaerobic granular sludge	4-Chlorophenol	6.32	Gao and Wang (2007)
Activated clay	2,4,6-Trichlorophenol	123.46	Hameed (2007)
Coconut shell-based commercial grade activated carbon	2,4,6-Trichlorophenol	112.35	Radhika and Palanivelu (2006)

intermolecular attractive forces is believed to decrease rapidly with distance; (4) the adsorbent has a finite capacity for the adsorbate (at equilibrium, a saturation point is reached where no further adsorption can occur); (5) all sites are identical and energetically equivalent and (6) the adsorbent is structurally homogeneous (Mahmoud et al. 2012).

A similar trend was observed for the adsorption of 3-chlorophenol on rice straw-based carbon (Wang et al. 2007) and the adsorption of 4-chlorophenol on anaerobic granular sludge (Gao and Wang 2007). However, some studies have found that the Freundlich model yielded a better fit than the Langmuir model for the adsorption of chlorophenol using different adsorbents (Hameed 2007; Radhika and Palanivelu 2006). Table 2 shows the maximum monolayer adsorption capacity of various types of chlorophenols on different adsorbents. The PKC adsorbent prepared in this study had an adsorption capacity of 22.22 mg/g and was comparable to several previous works found in the literature.

### 3.6 Adsorption Kinetic Studies of TCP Adsorption by PKC

The kinetics of adsorption describes the rate of adsorbate uptake on the adsorbent, which determines the equilibrium time. The kinetic parameters are helpful to predict the adsorption rate, which yields important information for the design and modeling of processes. Three famous models are commonly used to describe the kinetics of processes: the pseudo-first order, pseudo-second order, and Elovich equations.

The pseudo-first-order kinetic model has been widely used to predict sorption kinetics. The model is defined as follows:

$$\frac{d_q}{d_t} = k_1(q_e - q) \quad (11)$$

Integrating Eq. (11) with respect to the boundary conditions  $q = 0$  at  $t = 0$  and  $q = q_e$  at  $t = t$ , Eq. (11) yields

$$\ln(q_e - q) = \ln q_e - k_1 t, \quad (12)$$

where  $q_e$  and  $q_t$  (mg/g) are the amounts of adsorbate adsorbed at equilibrium and at any time,  $t$  (h), respectively, and  $k_1$  ( $\text{h}^{-1}$ ) is the adsorption rate constant. The value of  $k_1$  can be determined by plotting  $\ln(q_e - q)$  versus  $t$  (Hameed et al. 2008; Qiu et al. 2009). Figure 5a shows the pseudo-first-order kinetic model for the adsorption of TCP on PKC at 30 °C. The  $R^2$  values were relatively small and varied from 0.769 to 0.947 for initial TCP concentrations of 100–200 mg/l. Besides, the experimental  $q_e$  values did not agree with the calculated values obtained from the linear plots. This discrepancy shows that the adsorption of TCP on the PKC is not a first-order reaction.

The pseudo-second-order equation based on equilibrium adsorption is expressed as follows:

$$\frac{d_q}{d_t} = k_2(q_e - q)^2 \quad (13)$$

Integrating Eq. (13) with respect to the boundary conditions  $q = 0$  at  $t = 0$  and  $q = q_e$  at  $t$

$$\frac{t}{q_t} = \frac{1}{k_2 q_e^2} + \frac{1}{q_e} t, \quad (14)$$

where  $k_2$  (g/mg h) is the rate constant of second-order adsorption. The slope of the linear plot of  $t/q_t$  versus  $t$  has a slope equal to  $1/q_e$  and an intercept equal to  $1/k_2 q_e^2$ . Thus, the constant  $k_2$  can be determined (Hameed et al. 2008; Qiu et al. 2009). Figure 5b shows the pseudo-second-order kinetic model for the adsorption of TCP on PKC at 30 °C. The values of  $k_2$  and  $R^2$  obtained from the plot are tabulated in Table 3. Figure 5c shows that the calculated  $q_e$  values closely approximate the experimental values. Besides, the  $R^2$  value approached 1 for TCP concentrations of 150–200 mg/l, indicating that a second-order kinetic model can be used to describe the adsorption of TCP on PKC.

The Elovich equation is one of the most useful models for describing activated chemisorptions. The Elovich equation can be expressed as follows:

$$q_t = \left(\frac{1}{b}\right) \ln(ab) + \left(\frac{1}{b}\right) \ln t \quad (15)$$

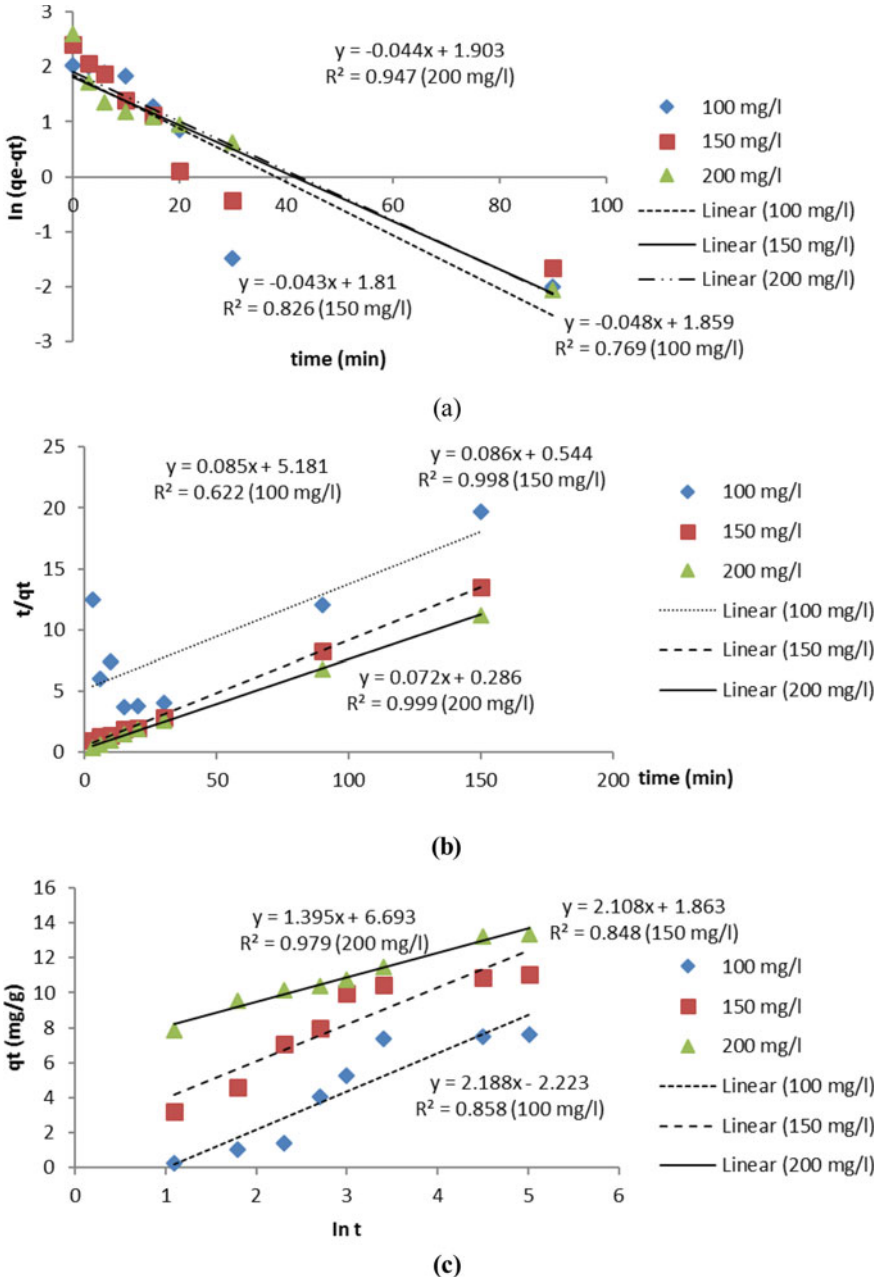


**Fig. 5** (a) Pseudo-first-order kinetic model, (b) pseudo-second-order kinetic model, (c) Elovich kinetic model, for the adsorption of TCP on PKC at 30 °C

**Table 3** Pseudo-first-order model, pseudo-second-order model and Elovich equation constants and correlation coefficients for the adsorption of TCP on prepared PKC at 30 °C

Initial TCP concentration (mg/l)	$q_{e,exp}$ (mg/g)	Pseudo-first-order kinetic model			Pseudo-second-order kinetic model			Elovich equation			
		$q_{e,cal}$ (mg/g)	$k_1$ ( $\text{min}^{-1}$ )	$R^2$	$q_{e,cal}$ (mg/g)	$k_2$ ( $\text{g}/\text{mg min}$ )	$R^2$	$q_{e,cal}$ (mg/g)	$a$	$b$	$R^2$
100	7.607	6.417	0.048	0.769	11.795	$1.4 \times 10^{-3}$	0.622	8.632	0.792	0.457	0.858
150	11.076	6.110	0.043	0.826	11.628	0.0136	0.998	11.601	5.102	0.474	0.848
200	13.368	6.706	0.044	0.947	13.889	0.0181	0.999	13.681	169.28	0.717	0.979



where  $a$  and  $b$  are the constants for this model obtained from the slope and intercept of the linear plot of  $q_t$  versus  $\ln t$  (Hameed et al. 2008; Qiu et al. 2009). Figure 5c shows the Elovich kinetic model for the adsorption of TCP on PKC at 30 °C. The values of  $a$ ,  $b$  and  $R^2$  obtained from the plot are tabulated in Table 3. The  $R^2$  values varied from 0.848 to 0.979 for initial TCP concentrations of 100–200 mg/l. Furthermore, the  $q_e$  calculated by the Elovich equation closely approximated the experimental values. The values of  $k_1$  and  $R^2$  obtained from the pseudo-first, second and Elovich equation plot are tabulated in Table 3 for comparison.

### 3.7 Validity of Kinetic Model

The applicability of the kinetic model to describe the adsorption process was further validated by the normalized standard deviation,  $\Delta q_e$  (%), which is defined as follows:

$$\Delta q_e(\%) = 100 \sqrt{\frac{\sum \left[ \frac{q_{e,\text{exp}} - q_{e,\text{cal}}}{q_{e,\text{exp}}} \right]^2}{N - 1}} \quad (16)$$

where  $N$  is the number of data points, and  $q_{e,\text{exp}}$  and  $q_{e,\text{cal}}$  (mg/g) are the experimental and calculated equilibrium adsorption capacity values, respectively (Tan et al. 2009).

The  $\Delta q_e$  value obtained for the pseudo-first-order kinetic model was 48.68%, which was relatively high compared to the  $\Delta q_e$  values of 39.19 and 10.23% obtained for the pseudo-second-order kinetic model and the Elovich equation, respectively. The pseudo-second-order model was the most suitable equation to describe the adsorption kinetics of TCP on the prepared PKC because it showed the highest  $R^2$  values (approaching 1) and the lowest  $\Delta q_e$  value. This finding suggested that the overall rate of the adsorption process was controlled by chemisorption, which involves valency forces through the sharing or exchange of electrons between the sorbent and sorbate (Ho and McKay 1999). Similar phenomena have been observed for the adsorption of TCP to activated clay (Hameed 2007) and coconut shell-based activated carbon (Radhika and Palanivelu 2006)

### 3.8 Adsorption Thermodynamics of TCP Adsorption by PKC

The original concepts of thermodynamics assumed that the entropy change is the driving force in an isolated system where energy cannot be gained or lost. The Gibbs free energy change,  $\Delta G^0$ , is the fundamental criterion of spontaneity. Reactions occur spontaneously at a given temperature if  $\Delta G^0$  is a negative quantity. Thus, thermodynamic parameters, such as free energy, enthalpy and entropy changes, can be estimated using the relationship between equilibrium constants and temperature. The

values of  $\Delta H^\circ$  and  $\Delta S^\circ$  were computed using the following equation and presented in (Fig. 6)

$$\ln K_d = \frac{\Delta S^\circ}{R} - \frac{\Delta H^\circ}{RT} \tag{17}$$

where  $K_d$  is the distribution coefficient, which can be calculated by the following equation:

$$K_d = \frac{C_{Ae}}{C_e} \tag{18}$$

where  $C_{Ae}$  ( $\text{mg L}^{-1}$ ) is the amount adsorbed on the solid at equilibrium, and  $C_e$  ( $\text{mg L}^{-1}$ ) is the equilibrium concentration. The values  $\Delta H^\circ$  and  $\Delta S^\circ$  were calculated from the slope and intercept of a plot  $\ln K_d$  versus  $1/T$ .  $\Delta G^\circ$  can be calculated using the following equation:

$$\Delta G^\circ = -RT \ln K_d \tag{19}$$

where  $\Delta G^\circ$  is the standard free energy change (J),  $R$  is the universal gas constant ( $8.314 \text{ J/mol K}$ ) and  $T$  is the absolute temperature (K) (Hameed et al. 2009).

The thermodynamic parameters of the adsorption process, such as  $\Delta H^\circ$ ,  $\Delta S^\circ$ , and  $\Delta G^\circ$ , are listed in Table 4. The negative value of  $\Delta S^\circ$  indicates that the entropy at the solid-solution interface decreased during the adsorption process. The negative  $\Delta H^\circ$  value indicates that the adsorption is exothermic, which is consistent with the results

**Fig. 6** Thermodynamic plot of the adsorption of TCP to PKC at 30, 40 and 50 °C with TCP for an initial concentration of 200 mg/l

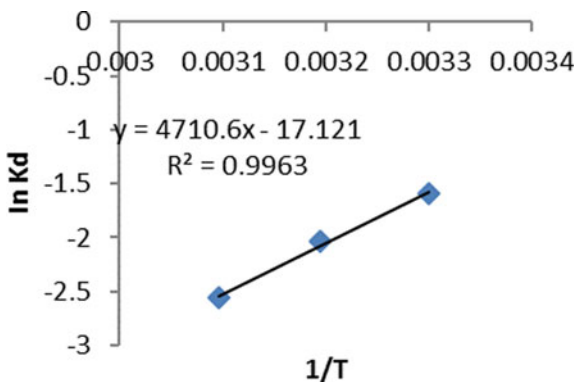


**Table 4** Thermodynamic parameters for the adsorption of TCP onto PKC

$\Delta H^\circ$ (kJ/mol)	$\Delta S^\circ$ (J/mol K)	$\Delta G^\circ$ (kJ/mol)		
		30 °C	40 °C	50 °C
-39.16	-142.33	+3.97	+5.39	+6.81

of the adsorption isotherms and the decreased TCP uptake observed with increased solution temperatures. The free energy changes ( $\Delta G^\circ$ ) were positive, reflecting the non-spontaneous nature of the adsorption process for the tested temperatures. Kara et al. suggested that the  $\Delta H^\circ$  of physisorption is smaller than 40 kJ/mol. Generally, the  $\Delta G^\circ$  for physisorption is less than that for chemisorption. The former is between  $-20$  and  $0$  kJ/mol and the latter is between  $-80$  and  $-400$  kJ/mol (Kara et al. 2003). Therefore, the values of  $\Delta H^\circ$  and  $\Delta G^\circ$  all suggested the same fact: the adsorption of TCP onto the PKC prepared in this study was mainly a chemisorption process.

## 4 Conclusions

The present investigation showed that PKC can remove TCP from aqueous solutions over a wide range of concentrations. The adsorption of TCP positively correlated with the agitation time and initial concentration. Moreover, acidic pH values favored the adsorption of TCP. The equilibrium data were fitted to the nonlinear Langmuir, Freundlich, Temkin, and Redlich–Peterson models and the equilibrium data were best described by the Langmuir isotherm model, with a maximum monolayer adsorption capacity of 22.22 mg/g at 30 °C. The  $R_L$  values negatively correlated with the initial TCP concentration, which indicates that the adsorption was favored by higher concentrations. The kinetic data were tested using a pseudo-first order, pseudo-second order and the Elovich model. The kinetics of the adsorption process were followed by a pseudo-second-order kinetic model, suggesting that the adsorption process was controlled by chemisorption. The positive value of  $\Delta G^\circ$  signifies that the adsorption reaction was non-spontaneous. The negative value of  $\Delta H^\circ$  indicates that the adsorption process was exothermic. FTIR analysis was conducted on the prepared PKC before and after TCP adsorption to study its surface chemistry. These data indicate that the adsorption potential of the PKC was comparable to other adsorbents reported in earlier studies.

**Acknowledgements** This research was supported by the Center of Research and Innovation, Universiti Malaysia Sabah (Grant No. FRG0203-SG-1/2010) and is gratefully acknowledged.

## References

- Anisuzzaman, S. M., Joseph, C. G., Krishnaiah, D., Bono, A., & Ooi, L. C. (2015). Parametric and adsorption kinetic studies of methylene blue removal from simulated textile water using durian (*Durio zibethinus* Murray) skin. *Water Science and Technology*, 72(6), 896–907.
- Anisuzzaman, S. M., Bono, A., Krishnaiah, D., & Tan, Y. Z. (2016). A study on dynamic simulation of phenol adsorption in activated carbon packed bed column. *Journal of King Saud University—Engineering Sciences*, 28(1), 47–55.
- Ahmaruzzaman, M. (2008). Adsorption of phenolic compounds on low-cost adsorbents: A review. *Advances in Colloid and Interface Science*, 143, 48–67.

- Bilgili, M. S. (2006). Adsorption of 4-chlorophenol from aqueous solutions by xad-4 resin: Isotherm, kinetic, and thermodynamic analysis. *Journal of Hazardous Materials*, 137, 157–164.
- Chen, G.-C., Shan, X.-Q., Wang, Y.-S., Wen, B., Pei, Z.-G., Xie, Y.-N., et al. (2009). Adsorption of 2,4,6-trichlorophenol by multi-walled carbon nanotubes as affected by Cu(II). *Water Research*, 43, 2409–2418.
- El-Sayed, G. O. (2011). Removal of methylene blue and crystal violet from aqueous solutions by palm kernel fiber. *Desalination*, 272, 225–232.
- Fan, J., Zhang, J., Zhang, C., Ren, L., & Shi, Q. (2011). Adsorption of 2,4,6-trichlorophenol from aqueous solution onto activated carbon derived from loosestrife. *Desalination*, 267, 139–146.
- Gao, R., & Wang, J. (2007). Effects of pH and temperature on isotherm parameters of chlorophenols biosorption to anaerobic granular sludge. *Journal of Hazardous Materials*, 145, 398–403.
- Hamdaoui, O., & Naffrechoux, E. (2007). Modeling of adsorption isotherms of phenol and chlorophenols onto granular activated carbon: Part II. Models with more than two parameters. *Journal of Hazardous Materials*, 147, 401–411.
- Hameed, B. H. (2007). Equilibrium and kinetics studies of 2,4,6-trichlorophenol adsorption onto activated clay. *Colloids and Surfaces A: Physicochemical and Engineering Aspects*, 307, 45–52.
- Hameed, B. H., Tan, I. A. W., & Ahmad, A. L. (2009). Preparation of oil palm empty fruit bunch-based activated carbon for removal of 2,4,6-trichlorophenol: Optimization using response surface methodology. *Journal of Hazardous Materials*, 164, 1316–1324.
- Hameed, B. H., Tan, I. A. W., & Ahmad, A. L. (2008). Adsorption isotherm, kinetic modeling and mechanism of 2,4,6-trichlorophenol on coconut husk-based activated carbon. *Chemical Engineering Journal*, 144, 235–244.
- Ho, Y.-S., & McKay, G. (1999). Pseudo-second order model for sorption processes. *Process Biochemistry*, 34, 451–465.
- Ho, Y. S., & Ofomaja, A. E. (2005). Kinetics and thermodynamics of lead ion biosorption on palm kernel fibre from aqueous solution. *Process Biochemistry*, 40, 3455–3461.
- Joseph, C. G., Bono, A., Krishnaiah, D., & Soon, K. O. (2007). Sorption studies of methylene blue dye in aqueous solution by optimised carbon prepared from guava seeds (*Psidium guajava* L.). *Journal Materials Science*, 13, 83–87.
- Joseph, C. G., Li Puma, G., Bono, A., Taufiq-Yap, Y. H., & Krishnaiah, D. (2011). Operating parameters and synergistic effects of combining ultrasound and ultraviolet irradiation in the degradation of 2,4,6-trichlorophenol. *Desalination*, 276, 303–309.
- Kara, M., Yuzer, H., Sabah, E., & Celik, M. S. (2003). Adsorption of cobalt from aqueous solutions onto sepiolite. *Water Research*, 37, 224–232.
- Krishnaiah, D., Joseph, C. G., Anisuzzaman, S. M., Daud, M., & Sundang, M. (2017). Removal of chlorinated phenol from aqueous solution utilizing activated carbon derived from papaya (*Carica Papaya*) seeds. *Korean Journal of Chemical Engineering*, 34(5), 1377–1384.
- Li Puma, G., Bono, A., Krishnaiah, D., & Collin, J. G. (2008). Preparation of titanium dioxide photocatalyst loaded onto activated carbon support using chemical vapor deposition: A review paper. *Journal of Hazardous Materials*, 157, 209–219.
- Mahmoud, D. K., Salleh, M. A. M., & Karim, W. A. (2012). Langmuir model application on solid-liquid adsorption using agricultural wastes: Environmental application review. *Journal of Purity, Utility Reaction and Environment*, 1, 200–229.
- Panday, K. K., Prasad, G., & Singh, V. N. (1986). Use of wollastonite for the treatment of Cu (II) rich effluents. *Water, Air, and Soil pollution*, 27, 287–296.
- Qiu, H., Lv, L., Pan, B., Zhang, Q., Zhang, W., & Zhang, Q. (2009). Critical review in adsorption kinetic models. *Journal of Zhejiang University Science A*, 10, 716–724.
- Radhika, M., & Palanivelu, K. (2006). Adsorptive removal of chlorophenols from aqueous solution by low cost adsorbent—Kinetics and isotherm analysis. *Journal of Hazardous Materials*, 138, 116–124.
- Siva Kumar, N., Woo, H.-S., & Min, K. (2012). Equilibrium and kinetic studies on biosorption of 2,4,6-trichlorophenol from aqueous solutions by *Acacia leucocephala* bark. *Colloids and Surfaces B: Biointerfaces*, 94, 125–132.

- Subramanyam, B., & Das, A. (2009). Linearized and non-linearized isotherm models comparative study on adsorption of aqueous phenol solution in soil. *International Journal of Environmental Science and Technology*, 6, 633–640.
- Tan, I. A., Ahmad, A. L., & Hameed, B. H. (2009). Fixed-bed adsorption performance of oil palm shell-based activated carbon for removal of 2,4,6-trichlorophenol. *Bioresource Technology*, 100, 1494–1496.
- Wang, S.-L., Tzou, Y.-M., Lu, Y.-H., & Sheng, G. (2007). Removal of 3-chlorophenol from water using rice-straw-based carbon. *Journal of Hazardous Materials*, 147(1–2), 313.

# Development of Low-Cost Aerobic Bioreactor for Decentralized Greywater Treatment



Asa Paramesti, Bimo Adiartha Damarjati, Adhika Widyaparaga, Deendarlianto, Aswati Mindaryani, Lisendra Marbelia, and Wiratni Budhijanto

**Abstract** Centralized greywater treatment with aerobic activated sludge process normally needs a very large footprint which could be challenging in some places, such as in hilly and densely populated areas with limited vacant land. For these areas, decentralized wastewater treatment technology might be an appropriate solution for preventing pollution by greywater. This study presents the design of low-cost and simple aerobic bioreactor for greywater treatment. The bioreactor was equipped with a microbubble generator (MBG) as a highly efficient aerator and pumice stones for bacterial attachment media. The pumice stones served as immobilization media for activated sludge bacteria so that additional sedimentation step was not required and better effluent quality was achieved. We ran the MBG intermittently and investigated the optimum on–off interval which maintained the required level of dissolved oxygen (DO) with minimum energy consumption. The test also included chemical oxygen demand (COD) removal for the bioreactor performance evaluation. The bioreactor showed the potential to be used as a low-cost portable unit with easy operation and maintenance to make it suitable for greywater treatment at the household scale.

**Keywords** Greywater · Aerobic · Microbubble generator · COD removal · Attached culture

## 1 Introduction

The need for clean water increases with the growing population. The escalation of clean water demand is consequently followed by the increase of wastewater emission, i.e. blackwater and greywater. Blackwater refers to the wastewater from flush

---

A. Paramesti · B. A. Damarjati · A. Mindaryani · L. Marbelia · W. Budhijanto (✉)  
Bioresource Engineering Group, Department of Chemical Engineering, Faculty of Engineering,  
Universitas Gadjah Mada, Yogyakarta 55281, Indonesia  
e-mail: [wiratni@ugm.ac.id](mailto:wiratni@ugm.ac.id)

A. Widyaparaga · Deendarlianto  
Department of Mechanical and Industrial Engineering, Faculty of Engineering, Universitas  
Gadjah Mada, Yogyakarta 55281, Indonesia

© Springer Nature Singapore Pte Ltd. 2020  
A. Z. Yaser (ed.), *Advances in Waste Processing Technology*,  
[https://doi.org/10.1007/978-981-15-4821-5\\_7](https://doi.org/10.1007/978-981-15-4821-5_7)

toilets, while the term of greywater is used for all household uses other than toilets. On average, people produce 225 L of greywater every day (Morel and Diener 2006). In several cities, greywater is directly emitted to the environment without special treatment and becomes an uncontrollable source of pollution. In 2016, 131,000 toddlers in the world died due to limited clean water availability (UN Inter-agency Group 2017).

This study is focused on small-scale greywater treatment technology. Greywater is classified as low strength wastewater which can be easily and effectively processed with aerobic activated sludge (Chan et al. 2009). However, it is generally perceived that the development of proper greywater treatment needs big investment for construction and operational costs. Also, it usually needs a large footprint.

A large portion of the operational cost is the cost of energy for aeration. Aeration is a key component that determines the success of greywater treatment technology. Therefore, to reduce the cost of greywater treatment, a highly efficient aerator is needed. This particular aerator is defined as that which consumes the least amount of energy to produce the highest level of dissolved oxygen (DO). This study introduces greywater treatment technology with a microbubble generator (MBG) as an aerator. MBG very well fits the aforementioned requirement of an aerator for more affordable technology.

The MBG has been proven as a better aeration technology than the conventional ones. Compared to most conventional aerators, aeration using an MBG does not need an air compressor so that energy consumption (kWh/mg DO) is lower (Budhijanto et al. 2015). A previous study (Pradana et al. 2016) conducted a comparison between MBG and conventional aerator for landfill leachate treatment in an Integrated Waste Disposal Site (TPST) in Yogyakarta and reported that although MBG still required a pump in its operation, it consumed less energy than the conventional aerator. Also, MBG was effective in maintaining a sufficient DO level and in removing COD from the wastewater.

Due to the characteristics of its micro-sized bubbles, MBG claims many advantages. Micro-sized bubbles develop high partial pressure of a dissolved gas component in the bubble, which is an excellent driving force for gas dissolution. Micro-sized bubbles also create large interfacial area per volume for oxygen transfer from the bubbles to the liquid bulk. Slow rising velocity, which is the effect of micro-sized bubbles too, also further increases the dissolution rate (Tsuke 2015). The superior claims of micro-sized bubbles were supported by experiments that compared MBG to conventional gas distributors (e.g. perforated plate and constant-flow nozzle), which confirmed that MBG was much more efficient for gas transfer into the liquid phase (Khuntia and Majumder 2012).

However, MBG also has some disadvantages that should be tackled. MBG produced a high flow rate of two-phase flow containing water and microbubbles. In turbulent flow, there is a tendency for coalescence and collision among bubbles. The design of MBG configuration is crucial in minimizing coalescence tendency (Deendarlianto et al. 2015; Budhijanto et al. 2015).

In addition to the aforementioned physical disadvantages of MBG, another possible drawback of MBG is the reduction in the microorganism population needed to

degrade organic materials (Budhijanto et al. 2015). The reduction occurs when viable cells are sucked by the pump and unintentionally broken by mechanical forces in the pumping system. It happens because the cells adhere strongly to the bubble surface and hence become an integral part of the two-phase fluid flow (Liu et al. 2012).

A previous research has shown that the use of MBG increased soluble chemical oxygen demand (sCOD) removal in both closed (Shalindry et al. 2015) and open wastewater treatment pond (Budhijanto et al. 2015). This study is focused on designing household-scale greywater treatment for areas where a decentralized wastewater system is preferable compared to a centralized one. Some of the cases in which a decentralized wastewater system is more applicable are hilly landscapes, highly populated areas with expensive land, and remote areas with scarce habitation. The purpose of the study is to design an affordable aerobic bioreactor for a decentralized greywater system. The energy cost for aeration is minimized by using MBG as a highly efficient and low-cost aerator (Pradana et al. 2016). Besides, the bioreactor is packed with pumice stones as bacterial immobilization media to increase the solids retention time (SRT) so that the hydraulic retention time (HRT) could be increased and bioreactor size could be minimized.

The immobilization media can be chosen from a vast array of materials, which include both organic or inorganic materials. The organic materials from natural lignocellulose such as coconut husk fibre and ridge gourd fibre are cheaper, have wider surface area per unit volume, higher porosity, low specific gravity, and a higher rate of biofilm formation compared to inorganic materials. Besides, natural fibre can also function as a substrate for the bacteria. However, organic materials have a shorter lifetime (Chanakya and Khuntia 2013).

Bio-balls as synthetic support material for bacteria have been studied in a sequencing batch reactor (Tomaszek and Masłon 2015). Wastewater treatment reached high efficiency because of the dense biofilm attached to the support material. Previous work (Budhijanto et al. 2015) also studied aerobic wastewater treatment with bio-balls as immobilization media. A microbubble generator was used as an aerator in this experiment. The use of bio-balls could prevent microorganisms from being sucked into the microbubble generator pump. However, when the bio-ball is no longer used, it becomes problematic plastic waste.

Pumice stone as inorganic support material for biofilm has been investigated (Ebrahimi and Borghei 2011). Pumice stone is easy to find and cheap. It also has higher specific area and porosity. Aerobic reactor with pumice stone as support material can reach 88% of COD removal (Ebrahimi and Borghei 2011).

This study was carried out in two stages of experiments, and both were conducted in a closed aerated tank. The tank was packed with pumice stones as the media for the attached culture. Attached growth media were used to prevent the suction of free-floating bacteria into the MBG pump and to avoid wash-out at a high inlet flow rate. The first stage of the experiment was the selection of tank configuration and conducted using tap water. The second stage was conducted using synthetic greywater and aimed to determine of optimum airflow rate into the MBG and optimum on-off interval of MBG operation to reduce energy consumption.



## 2 Materials and Methods

### 2.1 Materials

#### 2.1.1 Synthetic Greywater

Synthetic greywater was used as the substrate in this experiment. The composition of the substrate was similar to that of typical greywater. This substrate was composed of 1.5 g/L of tapioca starch and 0.1 g/L of cane sugar which were obtained from local market in Yogyakarta and 0.1 g/L of technical grade urea and 0.15 g/L of technical grade  $\text{KH}_2\text{PO}_4$  which were obtained from Tani Maju Trading Company in Yogyakarta (Budhijanto et al. 2015). The substrate was homogenized in the feed tank before periodically being fed into the aerobic tank.

#### 2.1.2 Inoculum

The inoculum used in this experiment was taken from the second aerated pond of Balai Instalasi Pengelolaan Air Limbah Sewon (communal wastewater facility managed by the local government), Bantul, Indonesia. This inoculum was taken from a depth of 2 m from the water surface. The inoculum was first acclimatized for 1 month. Acclimatization was carried out by growing the inoculum in the reactor with synthetic greywater as the substrate with dissolved oxygen maintained higher than 1 mg/L (Gerardi 2006). Acclimatization was assumed to be completed when biofilms had visibly covered the immobilization media (Sumiyati et al. 2018).

### 2.2 Methods

#### 2.2.1 Bioreactor Setup

The bioreactor was constructed of a 520 L commercial water tank, household centrifugal pump (125 W, maximum flow rate of 30 L/min), one head of MBG (orifice type with porous pipe and discharge diameter of 18 mm), and flow metres to adjust gas and liquid flow rates. Figure 1a shows the basic assembly of the aerated-tank system. The MBG was placed on the middle-top of the tank slightly below water surface and facing downward to maximize the coverage of the bubbles in the tank. The suction for the MBG was placed in the middle of the tank height. With this suction position, when the tank was inoculated by activated sludge, the microorganisms that would mostly grow on the bottom area of the tank would not be sucked into the MBG.

Immobilization media were used in our bioreactor design to improve microorganism activity and prevent wash-out at a high flow rate of greywater. The pumice

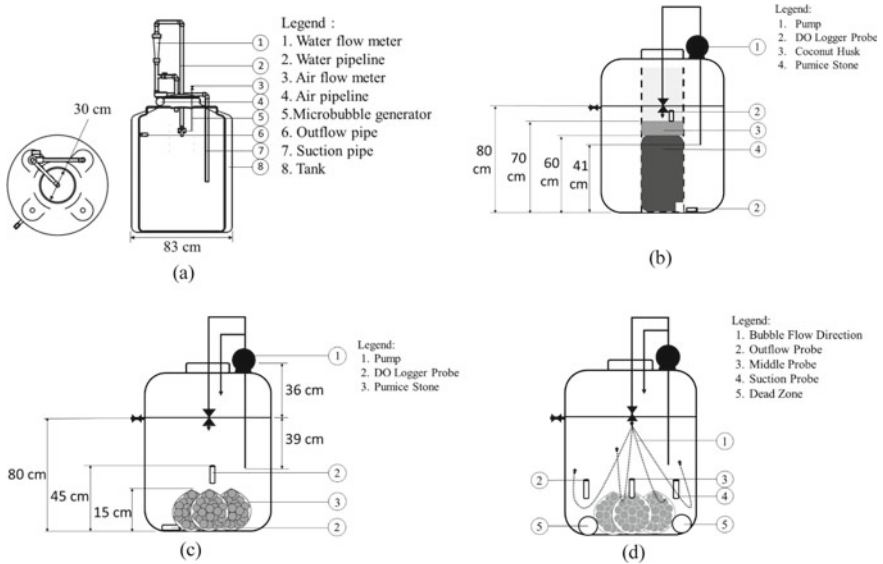


**Fig. 1** Configuration of aerated tank: **a** basic configuration without immobilization media, **b** configuration A (pumice stones in the middle of the tank), **c** configuration B (pumice stones in the bottom of the tank), **d** estimated bubble flow direction in the tank

stone was chosen as the immobilization media for bacteria attachment because of its large surface area (Donlan 2002). Pumice stone has 64–85% by volume of porosity (Lockwood and Hazzlet 2010) and 28–54 m<sup>2</sup>/g of specific area (Soleimani et al. 2019). Two configurations with a different arrangement of the pumice stones inside the bioreactor were compared (Fig. 1b and c), to choose the best configuration which reached the highest DO (at least 2 mg/L).

Figure 1b illustrates Tank A, which is a tank with pumice stones placed in a cylindrical mesh compartment in the middle of the tank. A bed of coconut husk was placed above the pumice stone packing. Tank B presented in Fig. 1c was a tank with pumice stones packed in several mesh bags placed at the middle-bottom of the tank. The amount of pumice stones is about ten percent of the liquid volume. The tanks were filled with tap water until the water surface was 80 cm from the bottom so that the total volume of the water and pumice stones in the tank was 430 L. The pump was operated with intermittent on–off, i.e. it was switched on for an hour and then switched off for the next hour, to evaluate the reactor performance in terms of DO changes during the on-period and during the off-period. The best configuration between Tank A and Tank B was chosen based on the highest and homogeneous DO. The value of DO is considered homogeneous if the DO value at two measurement points is not significantly different. The chosen configuration was then used for the aerobic digestion experiment with synthetic greywater.

The first step to be conducted to start the aerobic digestion experiment was acclimatization. Acclimatization was a treatment used to grow and prepare the inoculum to adapt to its new environment. In this experiment, acclimatization was conducted by excessive aeration and batch feeding with the synthetic greywater. Selected reactor configuration was filled up with acclimatized bacteria and was periodically evaluated in terms of DO value. The MBG was operated at  $Q_L$  25 L/min and  $Q_g$  1.65 L/min. The logged data of DO were compared to those in the same reactor configuration filled with tap water. The experiment with tap water exhibited the maximum DO that an MBG could provide in the tank when no bacterial activity was present. On the other hand, the experiment with sludge and synthetic greywater aims to determine the remaining DO concentration after the consumption by the bacteria in the tank. By comparing the DO profiles of both experiments, we evaluated the success of the MBG in supplying the oxygen for the aerobic digestion of the synthetic greywater.

### 2.2.2 Optimization of Aeration Mode for Energy Minimization

Effective intermittent aeration is characterized by a slow DO decrease rate when the pump is switched off. There is a positive correlation between DO decrease rate with the flow rate of air intake by MBG (Kawahara et al. 2009). Therefore, in this study, airflow rate optimization was conducted using Tank B which was the best bioreactor configuration.

Based on the results of the previous experiment, the substrate was pumped into the bioreactor by the Jebao DP-04 dosing pump, with 10 days of hydraulic retention time (HRT). Airflow rate ( $Q_g$ ) was varied at 1.65 and 0.8 L/min, while the water flow rate was maintained at 25 L/min.

Figure 1d shows the bioreactor design used in this experiment. DO logger probes were placed in three places, which are in the middle, at the suction side, and at the outflow side. The suction side was the same as the suction pipe of the pump, and the outflow side was the same as the bioreactor outlet side. The pump was turned on for half an hour to evaluate the maximum DO that could be reached and then was turned off until the DO reached 1 mg/L to measure the decreasing rate of DO at each airflow rate ( $Q_g$ ) value. The experiment for each  $Q_g$  value was replicated to validate the result. From this experiment, we chose the optimum  $Q_g$  value based on the stability of DO values during on- and off-periods and also the duration in maintaining the DO value above 1 mg/L after the pump was switched off.

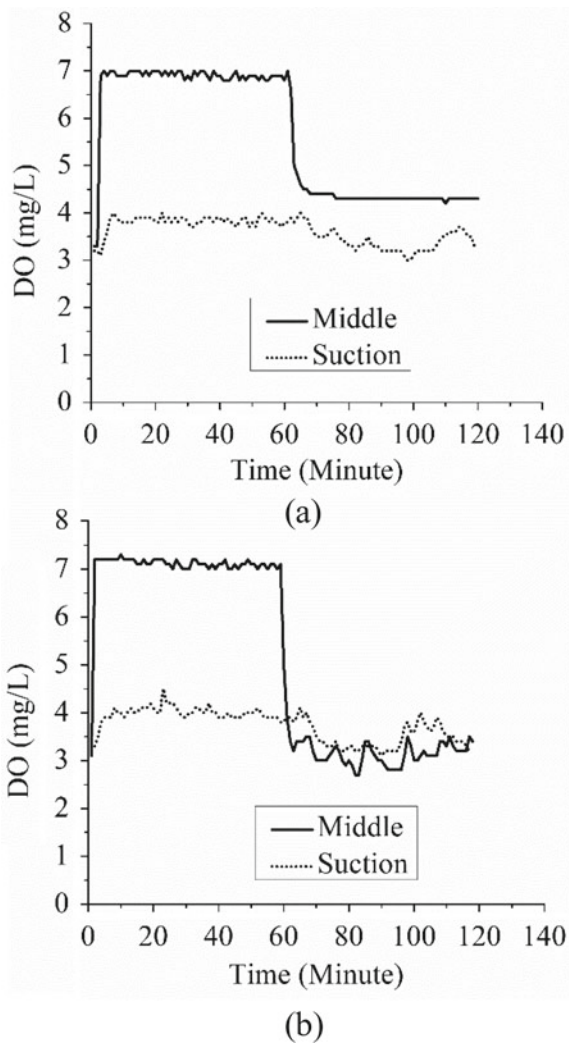
The optimum airflow rate was then used to compare reactor performance between continuous and intermittent operations of MBG. The intermittent operation was conducted by switching the MBG pump on and off manually to keep the DO > 1 mg/L. Both conditions of MBG operation were observed for 6 h, and the power consumed was measured by an energy metre. At the end of the DO observation period, we measured the soluble chemical oxygen demand (sCOD) for each operating condition.

### 3 Results and Discussion

#### 3.1 Selection of Reactor Configuration

Figure 2 shows the result of experiment using tap water. In Fig. 2, Tank A (Fig. 1b) merely reached high DO in the middle of the tank, while the suction area of the tank was not equally well aerated. This trend was observed at  $Q_g$  values of 0.8 and 1.65 L/min. This phenomenon might be caused by bubble breakdown at the coconut husk layer to produce smaller bubbles which led to better oxygen dissolution. On the

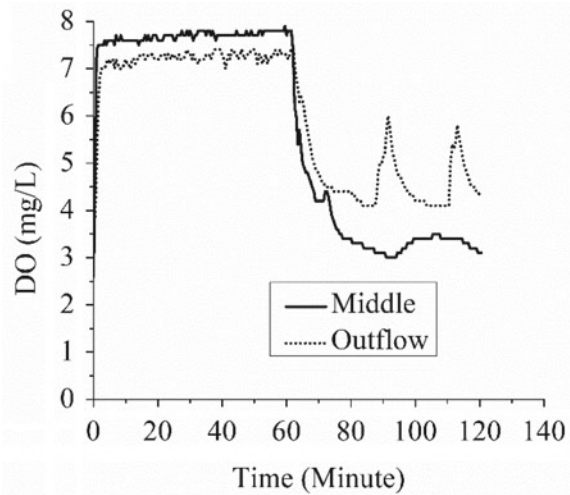
**Fig. 2** DO profile in the reactor for Tank A configuration presented in Fig. 1b at  $Q_g$  of 0.8 L/min (a) and  $Q_g$  of 1.65 L/min (b)



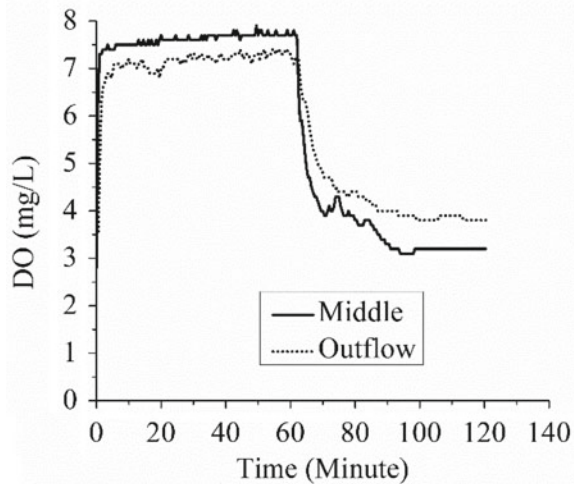
other hand, water circulation through the coconut husk and pumice stones failed to distribute bubbles to the bottom areas of the tank. The lack of bubbles at the bottom of the tank caused low DO value at those positions.

Figure 3 shows the performance of Tank B (Fig. 1c). This tank configuration successfully distributed the bubbles evenly to the entire tank so that the DO values were equal in both the middle and outflow areas of the tank. Elimination of coconut husk

**Fig. 3** DO profile in the reactor for Tank B configuration presented in Fig. 1c at  $Q_g$  0.8 L/min (a) and  $Q_g$  1.65 L/min (b)



(a)



(b)

and modification of pumice stone arrangement gave a significant effect because it prevented bubble collision that caused uneven DO distribution. In Tank B configuration, the probable bubble flow pattern was presented in Fig. 1d.

Compared to Tank A, Tank B performed better in terms of providing relatively homogeneous DO in the entire tank for the bacteria to degrade organic material in the greywater. Higher efficiency of organic material removal can be reached so that the configuration of Tank B was chosen to conduct the next experiment.

### 3.2 Evaluation of Aerobic Digestion in Selected Configuration (Tank B)

Figure 4a shows that in the tank filled with tap water, the saturated condition was achieved at DO value of 7.7 mg/L at the middle and 7.2 mg/L at the outflow. Figure 4b shows that when the MBG was operated in a bioreactor containing synthetic greywater with Tank B configuration (Fig. 1c), the maximum DO value was 3.3 mg/L in the middle and 4.7 mg/L at the outflow area. In the experiment with synthetic greywater, the aerator was turned on for only 30 min because it had reached constant DO value, in contrast to the experiment with tap water in which the MBG was turned on for 60 min to reach constant DO value. In the synthetic greywater tank, the maximum DO value was slightly higher at the outflow area. This indicates that the microbial activity, which consumed oxygen, might be higher in the middle of the tank, and the outflow area might be less occupied by the microbes and hence showed less oxygen consumption.

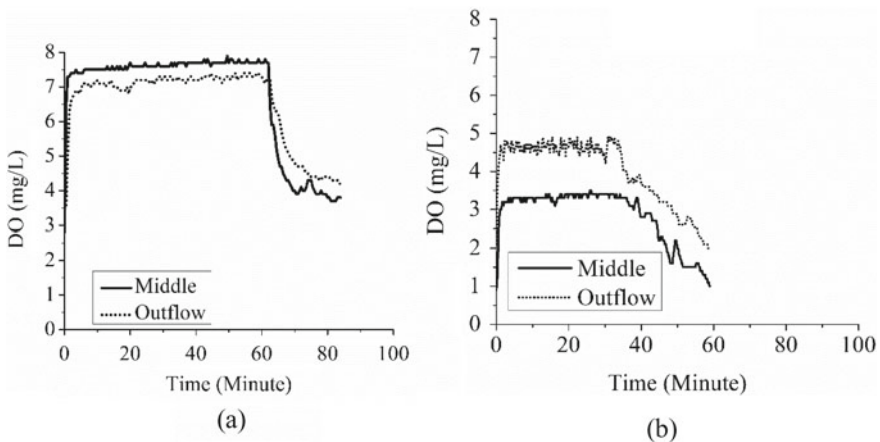


**Fig. 4** Comparison of DO profile in the tank between the experiment with tap water when the aeration was switched off after 60 min (a) and greywater and attached culture with the aeration switched off after 30 min (b)

The different trends of the highest DO concentrations between the experiment conducted in tap water and synthetic greywater represent the oxygen consumption rate by aerobic bacteria. In aerobic digestion, the DO value was usually maintained at the level of at least 2 mg/L. This study showed that MBG was able to sufficiently supply the oxygen required by the bacteria in this aerated tank. However, the excess DO provided by the MBG was still necessary to anticipate the possible COD concentrations fluctuations in the bioreactor feed.

### 3.3 $Q_g$ Optimization

Variation in  $Q_g$  values was required to be at least maintaining the minimum concentration of DO for aerobic biological activity, i.e. 2 mg/L (Tchobanoglous et al. 2003). The results of DO profiles with the variation of  $Q_g$  values in Tank B configuration filled with greywater are presented in Fig. 5a–c. The results of the  $Q_g$  optimization

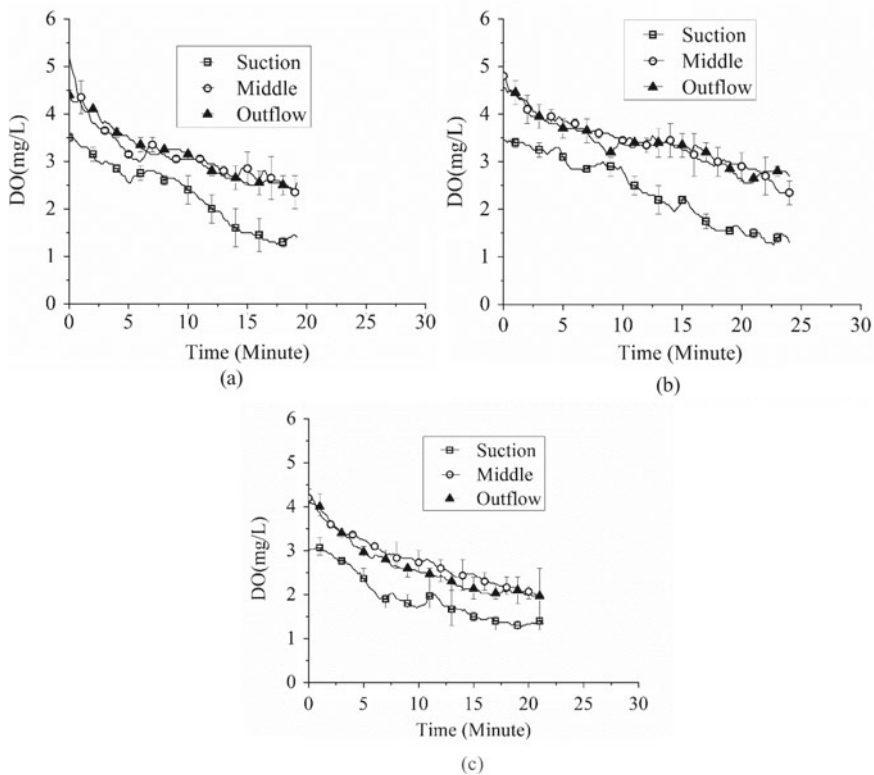


**Fig. 5** DO concentration profile at  $Q_g$  3.3 mg/L (a),  $Q_g$  1.65 mg/L (b),  $Q_g$  0.8 mg/L (c)

**Table 1** DO concentration distribution on varied airflow rates in two replicates

$Q_g$ (L/min)	Measurement (duplicate)	Saturated DO (mg/L) <sup>b</sup>			Time of DO decrease to 1 mg/L/min <sup>a</sup>
		Suction	Middle	Outflow	
3.3	(1)	3.4	5.1	4.1	30
	(2)	3.6	5.3	4.3	19
1.65	(1)	3.6	5.1	4.7	26
	(2)	3.3	4.5	4.2	24
0.8	(1)	3.2	4.4	3.9	35
	(2)	2.9	4.1	3.8	29

<sup>a</sup>The position of suction, middle, and outflow was presented in Fig. 1d

<sup>b</sup>After the MBG was switched off

experiment are listed in Table 1. Table 1 shows that DO values are smaller at lower  $Q_g$  in all regions of the reactor. In a previous study, it had been shown that the smaller  $Q_g$  led to a longer time for DO concentration to be maintained when the aeration was off before it started to decrease (Sadatomi et al. 2012). Gas dissolution is also higher when the bubble size is smaller (Khuntia and Majumder 2012). The smaller size of microbubble caused slower terminal velocity, higher internal pressure, and wider interfacial area which were all beneficial for bubble dissolution (Liu et al. 2012).

The longest time needed to reach DO value of 1 mg/L after the MBG was switched off was 35 min. This condition was achieved at the first measurement at  $Q_g$  0.8 L/min. However, in the second measurement, the time required to reach the DO value of 1 mg/L was shorter than the first measurement. The inconsistent DO values in the two measurements indicated unstable bubble supply. Even though smaller  $Q_g$  promotes greater dissolution of the gas, smaller  $Q_g$  injects less air into the system. The less amount of air injected into the system at the  $Q_g$  value of 0.8 L/min compared to higher  $Q_g$  values causes the DO value decreased more quickly. Therefore, a  $Q_g$  value of 1.65 L/min which exhibited better stability, with relatively values of DO on two measurements, was selected for intermittent operation.

The data of the MBG suction position in Fig. 5a–c are those taken at the middle-side of the tank (see the configuration in Fig. 1d). This suction side of the tank is the area that is not reached by the MBG outlet flow. Thus, this area becomes a “dead zone” with the lowest DO level as shown in Fig. 1d. In all  $Q_g$  variations, the level of DO at the suction position is always lower compared to the middle-centre and outflow position of the tank. MBG suction was intentionally placed on the dead zone location to make sure that all liquids were well mixed in the tank. As expected and shown in Fig. 5a–c, the DO levels at the middle-centre and outflow of the tank are quite the same in all  $Q_g$  values. This is an indication that the MBG successfully distributes dissolved oxygen from the point of the MBG downward and back upward after it hits the bottom of the tank, except for the aforementioned dead zone. The flow profile in the tank is illustrated in Fig. 1d. Nevertheless, by positioning the MBG suction close to the dead zone, the liquid in this position is forced to mix with the rest of it in the tank.



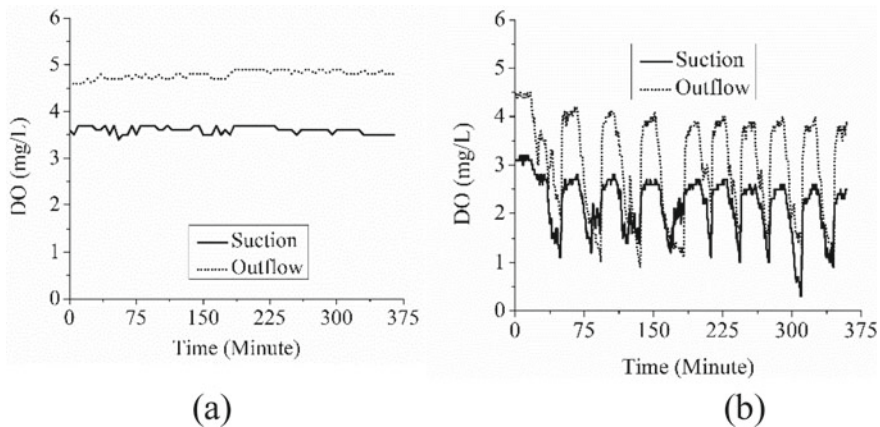


**Fig. 6** DO profile in Tank B filled with greywater in continuous operation (a) and intermittent operation (b)

### 3.4 Intermittent Operation

The objective of this experiment was to find an optimal operating condition with minimal energy consumption. The intermittent experiment was conducted after the process with non-stop aeration at a  $Q_g$  value of 1.65 L/min. The tank aerated continuously exhibits a stable DO profile as shown in Fig. 6a. Figure 6b shows that in intermittent aeration mode, the tank needed some time to reach constant DO value. In the first 3 h, there were four on–off cycles with highest DO value tend to decrease. In the next 3 h, there were five on–off cycles with steady DO value. Steady-state saturated DO is defined as the condition when the oxygen supply rate from the MBG equals oxygen consumption rate by the aerobic bacteria. Figure 6a indicates that there was excess oxygen in the reactor for bacteria in continuous operation. In Fig. 6a, DO increases significantly and reaches constant condition in 7 min after the MBG pump is switched on. This implies good oxygen mass transfer from the microbubbles to the bulk liquid.

Figure 6b shows the results of the intermittent experiment in Tank B filled with greywater in nine cycles. In the first four cycles, the highest DO value was still fluctuating, whereas in the next five cycles, the highest DO values were relatively stable. This experiment revealed that during the intermittent operation, the maximum off-time to maintain minimum DO value for bacteria was 15 min. It should be noted that the optimum intermittent on–off duration depends on COD concentration fed into the reactor. As for the situation in this experiment with tap water, the intermittent on–off cycle was optimum at 15 min on and 15 min off. The performances of the aerated tank in both operation modes were measured as sCOD removal and presented in Table 2.

Table 2 shows that the difference of sCOD removal between non-stop and intermittent aeration was not significant. This confirms that intermittent aeration does not

**Table 2** sCOD removal in non-stop and intermittent aeration

Aeration	COD feed (mg/L)	sCOD (mg/L)	% removal
Non-stop	309	39	87
Intermittent	309	31	90

**Table 3** Comparison of DO/power ratio and %COD removal/power ratio between non-stop and intermittent aeration (Damarjati 2019)

Aeration	DO/power ratio (mg/L kWh <sup>-1</sup> )	g sCOD removal/power ratio (g/kWh)
Non-stop	7.9	230
Intermittent	9.9	504

inhibit bacteria to degrade organic material from the substrate. The effectiveness of the intermittent aeration in reducing energy consumption is represented as DO/Power Ratio and sCOD Removal/Power in Table 3.

Although the intermittent process caused lower DO in the bioreactor compared to the non-stop aeration, it could still maintain a higher DO/power ratio than the non-stop aeration because of its lower energy consumption. The intermittent aeration reached 2.2 times higher of COD removal/power ratio compared with the non-stop aeration.

## 4 Conclusions

This study confirmed that three factors are essential for the application of an MBG-aerated tank for decentralized greywater treatment, namely: internal configuration of the tank, airflow rate ( $Q_g$ ), and the optimized on- and off-duration of the MBG for energy saving. Between the two configurations tested in this study, better performance was shown by the configuration with fewer obstacles for the bubbles. Concerning  $Q_g$  consideration, lower  $Q_g$  resulted in lower DO drop rate after the MBG was switched off, but on the other hand, it supplied less amount of oxygen. Therefore, the airflow rates must be selected carefully so that the oxygen demand of the bacteria can be fulfilled. Intermittent cycle duration depends on the COD level of the greywater. In this experiment with typical greywater composition, the on-off cycle was optimum at 15 min on and 15 min off. The intermittent operation did not inhibit bacteria performance as long as the DO value was maintained higher than the minimum requirement of the bacteria. Also, the intermittent aeration exhibited higher DO/power ratio and more than twice sCOD removal/power ratio to be compared to non-stop aeration. As the cost of electricity is a very important consideration of the prospective users of this technology, more efficient consumption of power in intermittent aeration by the MBG makes this system very promising as low-cost greywater treatment technology.

**Acknowledgements** This work was supported by Indonesia Infrastructure Finance Research Grant 2018 and Chemical Engineering Department UGM. A. Paramesti acknowledges Lembaga Pengelola Dana Pendidikan for the scholarship.

## References

- Budhijanto, W., Deendarlianto, Kristiyani, H., & Satriawan, D. (2015). Enhancement of aerobic wastewater treatment by the application of attached growth microorganisms and microbubble generator. *International Journal of Technology*, 6(7), 1101–1109. <https://doi.org/10.14716/ijtech.v6i7.1240>.
- Chan, Y. J., Chong, M. F., Law, C. L., & Hassell, D. G. (2009). A review on anaerobic-aerobic treatment of industrial and municipal wastewater. *Chemical Engineering Journal*, 155(1–2), 1–18. <https://doi.org/10.1016/j.cej.2009.06.041>.
- Chanakya, H. N., & Khuntia, H. K. (2013). Treatment of gray water using anaerobic biofilms created on synthetic and natural fibers. *Process Safety and Environmental Protection*, 92(2), 186–192. <https://doi.org/10.1016/j.psep.2012.12.004>.
- Damarjati, B. A. (2019). *Rancang Bangun Reaktor Aerob Tertutup Dan Optimasi Kondisi Operasi Microbubble Generator Dalam Sistem Pengolahan Limbah*. Universitas Gadjah Mada.
- Deendarlianto, Wiratni, Tontowi, A. E., Indarto, & Iriawan, A. G. (2015). The implementation of a developed microbubble generator on the aerobic wastewater treatment. *International Journal of Technology*, 6, 924–930.
- Donlan, R. M. (2002). Biofilms: Microbial life on surfaces. *Emerging Infectious Diseases*, 8(9), 881–890. <https://doi.org/10.3201/eid0809.020063>.
- Ebrahimi, S., & Borghai, M. (2011). Formaldehyde biodegradation using an immobilized bed aerobic bioreactor with pumice stone as a support. *Scientia Iranica*, 18(6), 1372–1376. <https://doi.org/10.1016/j.scient.2011.01.001>.
- Gerardi, M. H. (2006). *Wastewater bacteria*. New Jersey: Wiley.
- Kawahara, A., Sadatomi, M., Matsuyama, F., Matsuura, H., Tominaga, M., & Noguchi, M. (2009). Prediction of micro-bubble dissolution characteristics in water and seawater. *Experimental Thermal and Fluid Science*, 33(5), 883–894. <https://doi.org/10.1016/j.expthermflusci.2009.03.004>.
- Khuntia, S., & Majumder, S. K. (2012, January). Microbubble-aided water and wastewater purification: A review. *Reviews in Chemical Engineering*, 28, 191–221. <https://doi.org/10.1515/revce-2012-0007>.
- Liu, C., Tanaka, H., Ma, J., Zhang, L., Zhang, J., Huang, X., et al. (2012). Effect of microbubble and its generation process on mixed liquor properties of activated sludge using Shirasu porous glass (SPG) membrane system. *Water Research*, 46(18), 6051–6058. <https://doi.org/10.1016/j.watres.2012.08.032>.
- Lockwood, J. P., & Hazzlet, R. (2010). *Volcanoes global perspective* (1st ed.). West Sussex: Wiley.
- Morel, A., & Diener, S. (2006). *Greywater management in low and middle-income countries*. Swiss Federal Institute of Aquatic Science and Technology (Eawag): Dübendorf, Switzerland.
- Pradana, M. A., Fitriyadi, N., Hans, A., Dridya, M. A., Deendarlianto, Wiratni, & Majid, A. I. (2016). Pengujian Kapabilitas dan Konsumsi Energi Micro-bubble Generator pada Pengujian Kapabilitas dan Konsumsi Energi Micro-bubble Generator pada Proses Pengolahan Air Limbah Lindi di TPST Piyungan, Bantul, Yogyakarta. In *Thermofluid*. Yogyakarta.
- Sadatomi, M., Kawahara, A., Matsuura, H., & Shikatani, S. (2012). Micro-bubble generation rate, and bubble dissolution rate into the water by a simple multi-fluid mixer with orifice and porous tube. *Experimental Thermal and Fluid Science*, 41, 23–30. <https://doi.org/10.1016/j.expthermflusci.2012.03.002>.

- Shalindry, R. O., Rohmadi, R., & Budhijanto, W. (2015). Penguraian Limbah Organik secara Aerobik dengan Aerasi Menggunakan Microbubble Generator dalam Kolam dengan Imobilisasi Bakteri. *Jurnal Rekayasa Proses*, 9(2), 24–30.
- Soleimani, H., Mahvi, A. H., Yaghmaeian, K., Abbasnia, A., Sharafi, K., Alimohammadi, M., & Zamanzadeh, M. (2019). Effect of modification by five different acids on pumice stone as natural and low-cost adsorbent for removal of humic acid from aqueous solutions—Application of response surface methodology.pdf. *Journal of Molecular Liquids*, 290, 111181. <https://doi.org/10.1016/j.molliq.2019.111181>.
- Sumiyati, S., Purwanto, P., & Sutrisno, E. (2018). Biodegradation of COD in household wastewater with aerobic biofilm technology by adding sediment drainage sewerage. *E3S Web of Conferences*, 31, 03015.
- Tchobanoglous, G., Burton, F., & Stensel, H. D. (2003). In Metcalf, & Eddy (Eds.), *Wastewater engineering : Treatment and reuse* (4th ed.). New York: McGraw-Hill Companies.
- Tomaszek, J. A., & Maslon, A. (2015). A study on the use of the BioBall Ò as a biofilm carrier in a sequencing batch reactor. *Bioresource Technology*, 196, 577–585. <https://doi.org/10.1016/j.biortech.2015.08.020>.
- Tsuke, H. (2015). In H. Tsuke (Ed.), *Micro- and nanobubbles, fundamental and application*. Florida: Taylor & Francis Group.
- UN Inter-agency Group. (2017). *WHO Levels and trends in child mortality 2017*. Available at: [https://www.unicef.org/publications/files/Child\\_Mortality\\_Report\\_2017.pdf](https://www.unicef.org/publications/files/Child_Mortality_Report_2017.pdf).

# Management of Biodegradable Plastic Waste: A Review



Sariah Saalah, Suryani Saallah, Mariani Rajin, and Abu Zahrim Yaser

**Abstract** The development and utilization of biodegradable plastics are currently being promoted as a solution to ecological and environmental impacts associated with the conventional petrochemical-based plastics. Biodegradation processes have opened an unprecedented opportunity for sustainable management of plastic waste. However, definite answers to a few significant issues related to the choice of plastics, their biodegradability and role in waste management are limited. Since the physical appearance of plastics made from either biodegradable or non-biodegradable materials is indistinguishable, labelling and identification of biodegradable plastics in a sensible and easily recognizable way are necessary. Biodegradable plastics can benefit the waste management only if efficient collection and sorting systems is implemented. Successful implementation of sustainable waste management by the use of biodegradable plastics requires thorough understanding on the end-of-life management options and the environmental impact of these polymers, which call for the integration in policies, regulation and standards. This review addresses the current scenario, opportunities and challenges in the management of biodegradable plastic waste.

**Keywords** Biodegradable plastic waste · Recycling · Composting · Incineration · Landfill

## 1 Introduction

Plastics are extensively produced worldwide for a wide range of domestic and industrial applications, especially in packaging of food, beverage, cosmetics and pharmaceutical products. Despite their usefulness, extensive utilization of conventional

---

S. Saalah (✉) · M. Rajin · A. Z. Yaser  
Chemical Engineering Programme, Faculty of Engineering, Universiti Malaysia Sabah, Jalan UMS, 88400 Kota Kinabalu, Sabah, Malaysia  
e-mail: [s\\_sariah@ums.edu.my](mailto:s_sariah@ums.edu.my)

S. Saallah  
Biotechnology Research Institute, Universiti Malaysia Sabah, Jalan UMS, 88400 Kota Kinabalu, Sabah, Malaysia

petroleum-based plastics becomes a threat to the environment due to their recalcitrant nature. Accumulation of these materials in the environment causes ecological threat to terrestrial and marine wildlife. For this reason, biodegradable plastics become the new alternative in packaging as it serves a good performance during use and have biodegradable properties at the end of their useful life (Pattanasuttichonlakul et al. 2018).

Currently, bioplastics represent about one percent of the approximately 335 million tonnes of annual plastic production and forecasted to grow from 2.11 million tonnes in 2018 to about 2.62 million tonnes in 2023 (Fig. 1). Innovative bioplastics such as PLA (polylactic acid) and PHAs (polyhydroxyalkanoates) are the key drivers of this growth (Fig. 2). These polyesters are completely bio-based and biodegradable and feature a wide array of physical and mechanical properties depending on their chemical composition. PLA features excellent barrier properties and is available in high-performance grades that can be an excellent alternative to conventional polymers made from PS (polystyrene), PP (polypropylene) and ABS (acrylonitrile butadiene styrene) in more demanding applications. Packaging accounts for almost 65% (1.2 million tonnes) of the total bioplastics market in 2018 (European Bioplastics 2018).

Extensive studies have been done on the utilization of different lignocellulosic materials from wood and agricultural residue as fillers or reinforcers in thermoplastic composites. These materials such as wood, hemp, cotton, wheat straw, rice husk, leaf, oil palm, banana fibres and many others have gained popularity in thermoplastic industry due to their biodegradable and eco-friendly nature, low density, low cost and ease of processing (Karakus et al. 2016). Chattopadhyay et al. (2011) investigated

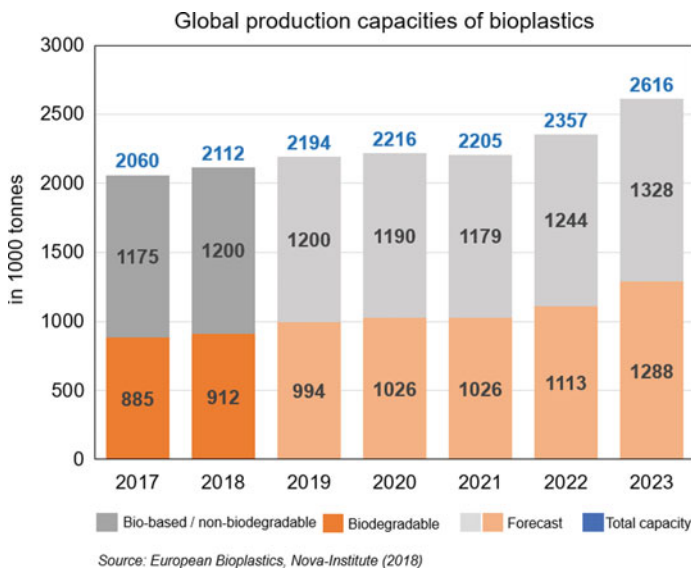


**Fig. 1** Global production capacities of bioplastics (European Bioplastics 2018)

### Global production capacities of bioplastics 2018 (by material type)

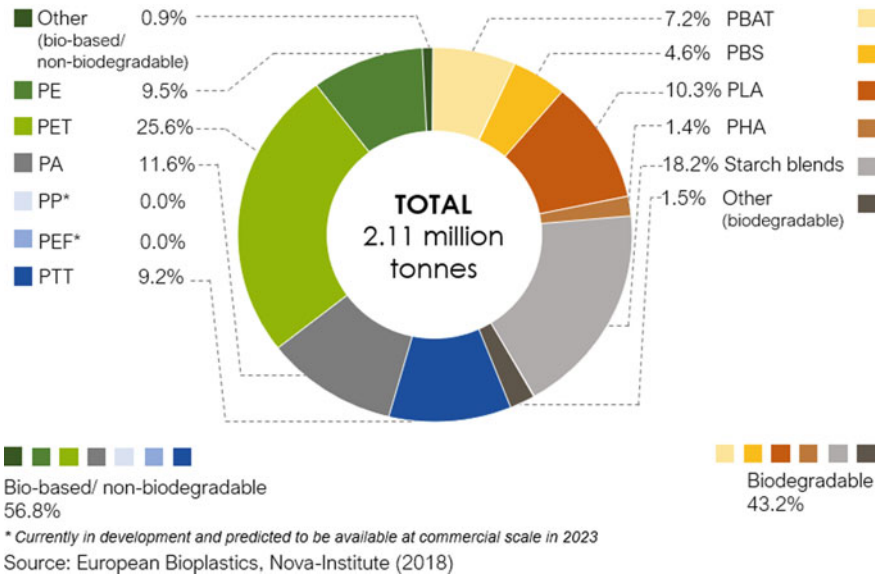


**Fig. 2** Global production capacities of bioplastics by material type (European Bioplastics 2018)

the biodegradability of various composites of polypropylene (PP) and natural fibres (10–50% volume fractions) of various sources such as pineapple leaf, banana and bamboo. Unfortunately, the composites were only exhibited partial biodegradation in the range of 5–15% depending on the fibre content. This is in agreement with the findings reported by Nakamura et al. (2005) which concluded that incorporation of biodegradable starch in low density polyethylene (LDPE) was not able to enhance the biodegradation of the polymer matrix significantly. On the bright side, incorporation of biodegradable material in conventional plastic composite could address to the management of waste plastics by reducing the amount of polymer content used that, in turn, will reduce the generation of non-biodegradable polymeric wastes.

It should be noted that not all bio-based plastics are biodegradable. As can be seen in Fig. 2, only about 43.2% of total bioplastics produced in 2018 are biodegradable. Bio-based, non-biodegradable plastics, including the drop-in solutions bio-based PE (polyethylene) and bio-based PET (polyethylene terephthalate), as well as bio-based PA (polyamides), currently make up for around 48% (1 million tonnes) of the global bioplastics production capacities. As the term “bioplastics” is often used interchangeably for “bio-based” and “biodegradable” plastics, in this paper, the definition of biodegradable plastics and certification standard for biodegradability will be highlighted followed by discussion on technologies available for the management of biodegradable plastics waste.

## 2 Definitions of Biodegradable Plastics

### 2.1 Bioplastics

The term bioplastics, bio-based plastics and biodegradable plastics are considered being related but require further clarification to avoid misconception throughout the value chain. According to The Society of Plastic Industry (SPI), lack of understanding and confusion around terminology is one of the major challenges in the growth of the bioplastic industry. This is due to the fact that bioplastics vaguely represent a large group of different kind of polymers which can be classified based on their origin or biodegradability. By referring to the material coordinate system of bioplastics in Fig. 3, bioplastics encompass (a) bio-based and biodegradable plastics, (b) fossil-based biodegradable plastics and (c) bio-based but non-biodegradable plastics (Dilkes-Hoffman et al. 2019).

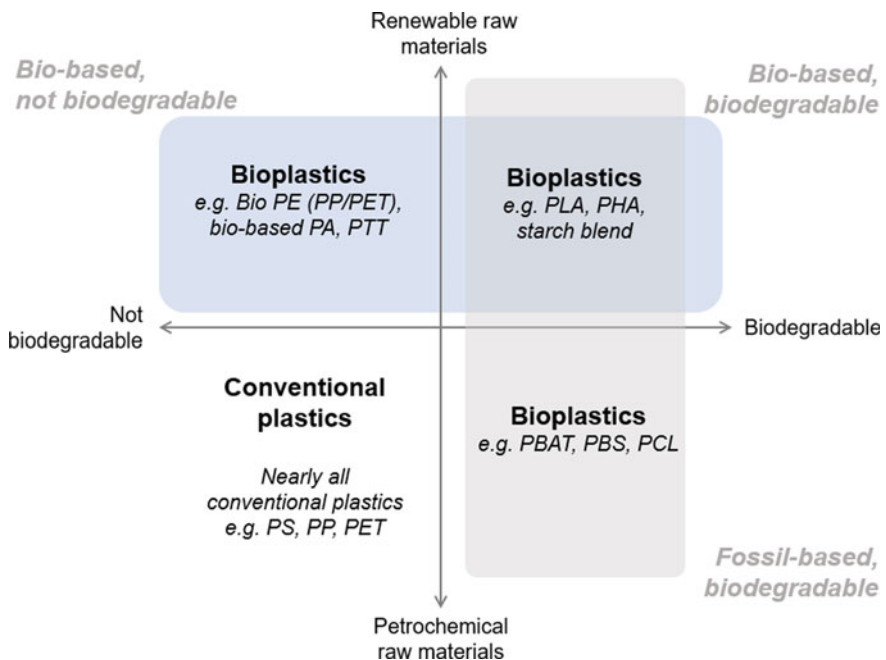


Fig. 3 Material coordinate system of bioplastics



## 2.2 *Bio-based Versus Fossil-Based Plastics*

Bio-based plastics are derived in whole or partially from renewable resources such as plants and microorganisms. Cellulose and starch are the most commonly used polysaccharides to produce bio-based plastics owing to their abundance in nature, inexpensiveness and biodegradability under certain environmental conditions. The so-called “drop-in bioplastics” such as bio-based polyethylene (Bio-PE) and polyethylene terephthalate (Bio-PET) have identical physical and chemical properties to their fossil-based PE and PET counterpart but differ in the way they are produced. Bio-based plastics also cover natural rubber and certain polyesters such as polyhydroxyalkanoates (PHA), poly-3-hydroxy-butyrate (PHB) and polylactic acid (PLA). These types of plastics are expected to compete with fossil-based plastics in terms of price and performance. Polyethylene furanoate (PEF) is a new type of bio-based plastic that receives growing attention especially for packaging of carbonated beverages. Note that bio-based plastics do not necessarily mean the product is biodegradable or compostable.

Fossil-based plastics are referring to those polymers obtained from the derivatives of hydrocarbon and petroleum (petrochemicals), particularly that of the five main commodity plastics which include polystyrene (PS), polypropylene (PP), polyethylene (PE), polyethylene terephthalate (PET) and polyvinyl chloride (PVC). Although most fossil-based plastics are non-biodegradable, some aliphatic polyesters such as polycaprolactone (PCL) and aromatic copolyesters such as polyvinyl alcohol (PVA) possess certain degrees of inherent biodegradability.

## 2.3 *Biodegradable Plastics*

Biodegradable plastics were produced commercially since 1990. When this kind of plastics started entering the market, there were a series of misconceptions about the term degradable and biodegradable. Many plastics entered the market with biodegradable labelling but only disintegrated and did not completely biodegrade (Mohee et al. 2008). Moreover, even when plastic is biodegradable, this does by no means imply that the material degrades in the environment in a short period of time (Verma and Fortunati 2019). For instance, PLA which is the most widely known biodegradable polymer can be fully biologically degraded within 6–24 months (Janczak et al. 2018). In order to avoid such misconceptions and to gain maximum benefit from plastics waste management, several standards in the area of degradable as well as biodegradable plastics have been developed by national standard bodies, including the USA (ASTM), Europe (CEN), Germany (DIN), Japan (JIS) and the International Organization for Standardization (ISO).

Different methods of assessment for biodegradability will give a different result. For instance, a commercially available biodegradable plastics Mater-Bi Novamont (MB) composed of 60% or more starch and starch derivatives and of about 40%

hydrophilic and biodegradable synthetic resin reported achieving 92% biodegradability after 100 days under aerobic composting liquid medium based on ISO 14852. However, aerobic composting of MB conducted by Mohee et al. (2008) shows that only 27% degradation achieved in 72 days. This suggested that the environmental degradability of plastics is a complex process that is influenced by the nature of the plastics and the conditions to which they are exposed.

According to ASTM standard D5988-03, biodegradable plastics are those that are capable of undergoing decomposition into carbon dioxide, methane, water, inorganic compounds or biomass as a result of the natural action of microorganisms such as bacteria, fungi and algae. The standard requires 60–90% decomposition of the plastic within 60–180 days in a composting environment (Mohee et al. 2008).

On the other hand, with referring to ASTM and ISO, degradable plastic is defined as a plastic designed to undergo a significant change in its chemical structure under specific environmental conditions, resulting in a loss of some properties that may vary as measured by standard test methods appropriate to the plastic and the application over a period of time that determines its classification (Song et al. 2009).

Degradation differs from biodegradation as degradable stage stops at the fragmentation of polymers. This occurs by the action of heat, moisture, sunlight and/or enzymes that shorten and weaken the polymer chains resulting in fragmentation residues and cross-linking to create more intractable persistent residues. Polymer is biodegradable only if the fragments are consumed by microorganisms as food and an energy source (Song et al. 2009).

From the definitions, it should be highlighted that the term “biodegradable” focuses solely on the way the degradation process occurs, regardless the source of the materials. Therefore, bio-based as well as fossil-based plastics can be biodegradable (Hermann et al. 2011). Fossil-based plastics that are biodegradable include aliphatic polyesters such as polyglycolic acid, polybutylene succinate and polycaprolactone (PCL), as well as aromatic copolyesters such as polybutylene succinate terephthalate and polyvinyl alcohol (PVA). These products are synthesized from monomers derived from petrochemical refining, which possess certain degrees of inherent biodegradability (Song et al. 2009). Figure 4 shows the chemical structure of selected biodegradable plastics.

Many commercial biodegradable plastics formulations combine materials from both classes to reduce cost and/or enhance performance. Biodegradable plastics, therefore, often comprise polymer blends that contain partly biogenic (renewable) carbon derived from biomass and partly petrochemical carbon (Song et al. 2009). Emadian et al. (2017) reviewed some studies conducted to improve the biodegradability of bioplastics in a compost environment. Increasing the content of soluble sugar in the biocomposites through the addition of materials containing high protein content enhanced the biodegradability of bioplastics. The presence of soy meal and canola meal, bio-based fillers derived from co-products of biofuel reported to improve biodegradation of PBS bioplastic composite, which was attributed to the high concentration of soluble sugars in the fillers. Incorporation of corn in PLA/corn blend bioplastic seemed to enhance the biodegradation in compost due to highly biodegradable nature of corn.

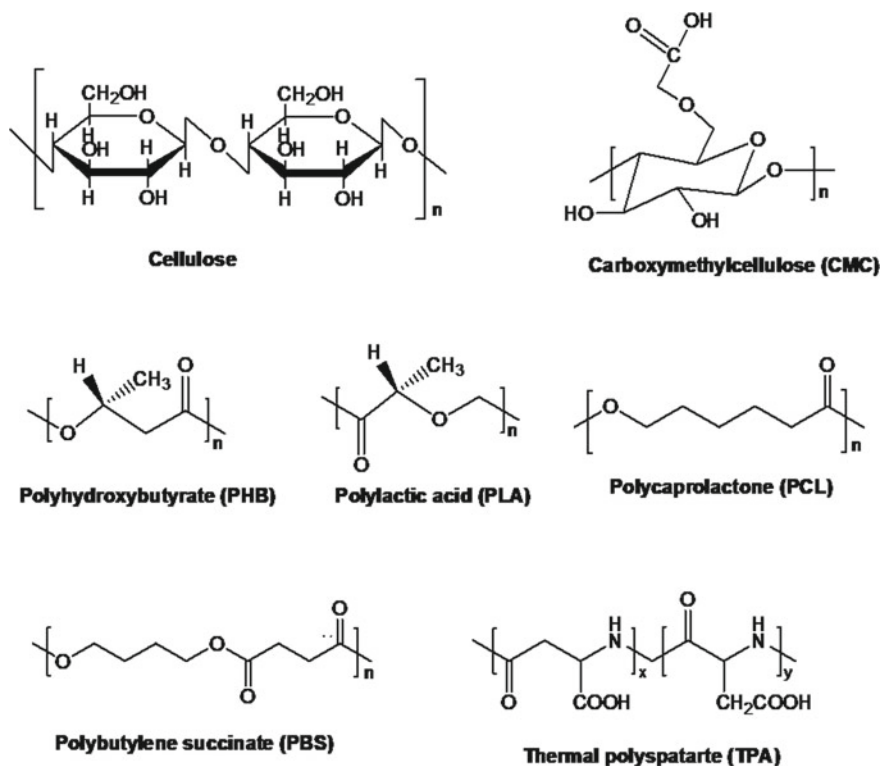
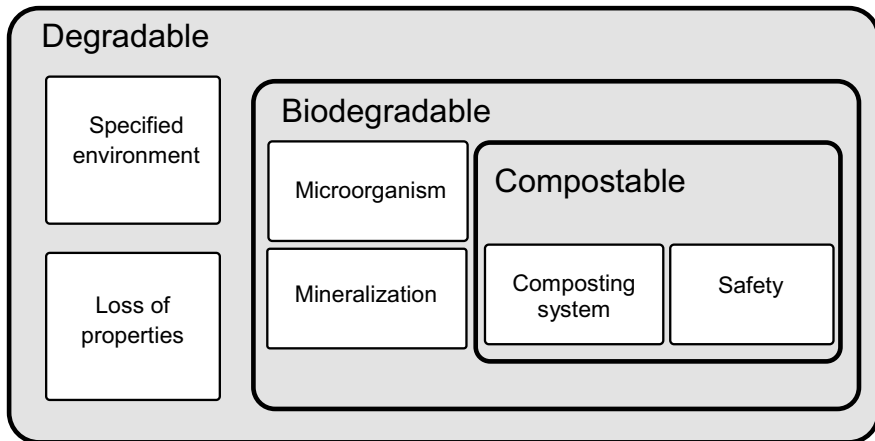


Fig. 4 Chemical structure of selected biodegradable plastics. Adapted from Álvarez-Chávez et al. (2012)

## 2.4 Compostable Plastics

ASTM D6400 and ISO 17088 define compostable plastics as “a plastic that undergoes degradation by biological processes during composting to yield CO<sub>2</sub>, water, inorganic compounds and biomass at a rate consistent with other compostable materials and leaves no visible, distinguishable or toxic residue”. The “residue” clause is an important distinction that favours truly biodegradable plastics rather than blended materials that disintegrate or partially biodegrade (Mooney 2009).

Plastics can be degradable and even biodegradable without being compostable. The biodegradable plastics and compostable plastics differ in additional requirements related to the latter. Besides undergoing biodegradation to yield CO<sub>2</sub>, water, inorganic compounds and biomass, the compostable polymers must also fulfil other criteria including compatibility with the composting facility, no negative effect to the compost's quality and degradation occur at a rate consistent with other known composting materials. The relationship between degradable, biodegradable and compostable plastics is illustrated in Fig. 5.



**Fig. 5** Relationship between degradable, biodegradable and compostable plastics. Adapted from Rudnik (2019)

### 3 Certification Standards for Biodegradability

The fact that biodegradable plastics are not readily distinguishable from regular plastics necessitates a mechanism to ensure their quality, proper labelling, as well as to promote the use of biodegradable plastics. This can be done through a standardization and certification system.

Various countries have implemented certification standards for biodegradability and compostability. Standard product testing to achieve certification for labelling based on the ASTM/CEN system of classification has been enforced in Europe, North America and some countries in Asia. The ASTM 6400-99 designation covers “standard specification for compostable plastics”, and EN 13432 covers “proof of compostability of plastic products”.

The certification process for compostability according to EN 13432/14995 is offered by Belgian certifier TUV Austria and German certifier DIN CERTCO. The “Seedling” is a reliable label for compostability and becomes an established identifier in Belgium, Switzerland, Poland, United Kingdom and many other countries. The logo printed on the product helps to assist in the decision on purchasing and disposing of a product. A certified compostable logo based on countries is presented in Fig. 6.

In Malaysia, certification for “SIRIM ECO 001:2018 Biodegradable and compostable plastics and bioplastic” is offered by SIRIM QAS since 2018. This is the revision of SIRIM ECO 001-2016 and AMD 1:2017 for “degradable and compostable plastic packaging”. The certification is based on EN 13432, ASTM and ISO criteria. These enable products to be certified under SIRIM Eco-Labeling Scheme as environmentally friendly and can further boost green consumerism as well as sustainable development in Malaysia. Figure 7 shows the eco-label offered by SIRIM QAS.



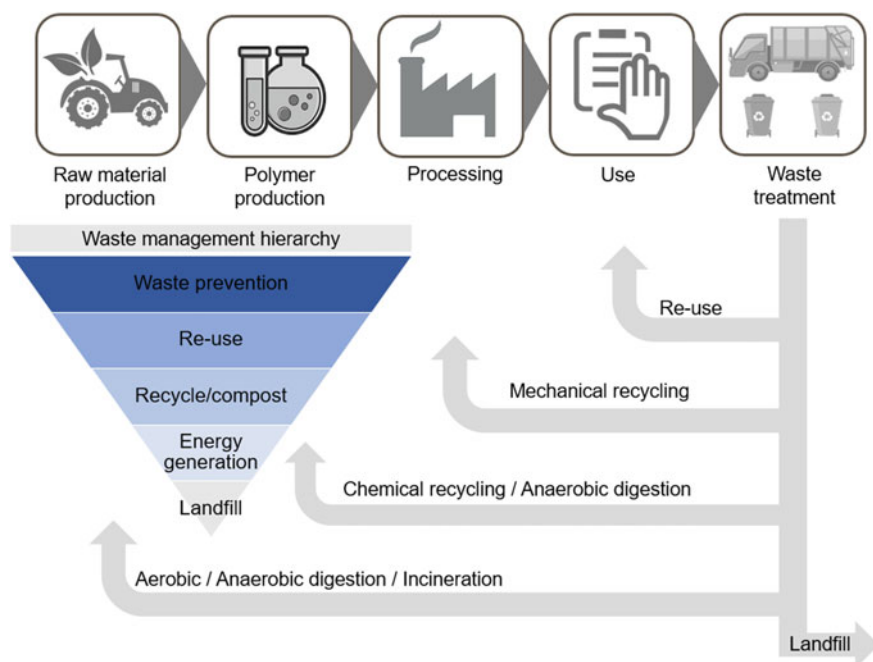
Fig. 6 Certified compostable logo

Fig. 7 Eco-label logo offered by SIRIM QAS



#### 4 Management of Biodegradable Plastic Waste

Based on the widely used “waste hierarchy”, there are several options available for end-of-life management of plastic waste with prevention and reuse are ranked at top of the hierarchy, followed by recycling and composting, energy recovery and the least preferred option, disposal to the landfill. Biodegradability has paved the way to the sustainable end-of-life management options for bioplastics such as composting and anaerobic digestion which is not applicable to non-degradable plastics. The life cycle of bioplastics and loop of different waste treatment options is presented in Fig. 8 and discussed further in the following sections.



**Fig. 8** Life cycle of bioplastics, loop and hierarchy of different waste treatment options. Adapted from Spierling et al. (2018)

## 4.1 Recycling

Recycling is one of the primary options available in the management of plastic waste. However, for biodegradable plastics, the opportunities for conserving resources, reducing environmental impacts and minimizing landfill deposition of the associated waste through recycling are rarely addressed. In principle, recycling of some of bio-based biodegradable polymers such as PLA and PHA through conventional mechanical means is technically feasible. According to Andrade et al. (2016), the life cycle analysis of PLA showed that mechanical recycling presented the lowest environmental impact compared to chemical recycling and composting. Nevertheless, from an economic point of view, the sorting of recyclable plastics that enter the municipal waste stream can be challenging and involving extensive labour costs (Dilkes-Hoffman et al. 2019). The sorting process is crucial to ensure purity of the feedstock as it affects the quality of the recycled products. Contamination of the conventional plastic recycling stream (e.g. PET) by bioplastic (e.g. PLA) may complicate the recycling process, thus reducing the yield. For certain applications such as food packaging, multilayer lamination of different biopolymers to enhance barrier properties will compromise recyclability of the scrap during packaging manufacture and of post-consumer waste (Song et al. 2009).

Besides efficient sorting, commercial success of bioplastics recycling also relies on continuous supply of bioplastic polymer waste in large quantities. A critical mass of biopolymers that are required to justify independent recycling stream and ensure profitability is about 200 million kg per year (Niaounakis 2013). To sum up, for bioplastics recycling to be both technically and economically feasible, Cornell (2007) suggested that the following criteria should be met:

- i. Availability of collection infrastructure
- ii. Investors for the market
- iii. Profitable applications for biodegradable plastics
- iv. Access to enough materials in the recycling stream.

Research into the recycling of bioplastics is still in infancy and requires an in-depth understanding and investigation of the factors affecting the process efficiency and economic considerations. Furthermore, as the process results in shortening of the polymer chains and alteration of the chemical properties, the desirable properties of the original materials such as strength and durability are compromised, making it inappropriate for high-end use (Dilkes-Hoffman et al. 2019).

## 4.2 Incineration

Incineration has become a popular waste management technique mainly applied to reduce the footprint of landfill facilities. If conducted in properly controlled facilities, the energy content of the materials can be recovered and exploited to generate maximum benefit at a justifiable amount of effort and expense (Dilkes-Hoffman et al. 2019). In fact, several countries including China, Japan, Sweden and Denmark have established an extensive incinerator infrastructure for dealing with solid waste (Lambert 2015).

Biodegradable plastics can be incinerated in the same manner as the non-biodegradable plastics. The incineration process of these bio-derived materials involves a close-loop system and generates less CO<sub>2</sub> as opposed to those of petrochemical-based plastics. Energy recovery by incineration of bioplastic polymers is considered as a suitable option to contribute to renewable energy (Dilkes-Hoffman et al. 2019). However, lack of scientific data on Gross Calorific Value (GCV) of bioplastics polymer makes it difficult to accurately determine the amount of energy recovered by incineration. Based on the study done by Endres and Rath (2011), the calorific value of biopolymers is not source dependent but exclusively based on their stoichiometric composition. For example, the calorific value of bio-based PET is equal to that of the petrochemical-based PET (Fig. 9) due to the same elementary composition of both materials. They concluded that the existing incineration facilities for conventional plastics can be applied for incinerating bioplastics without modifications or adaptations.

It is well known that incineration of conventional plastics may generate greenhouse gases and release toxic pollutants such as dioxins, polychlorinated biphenyls

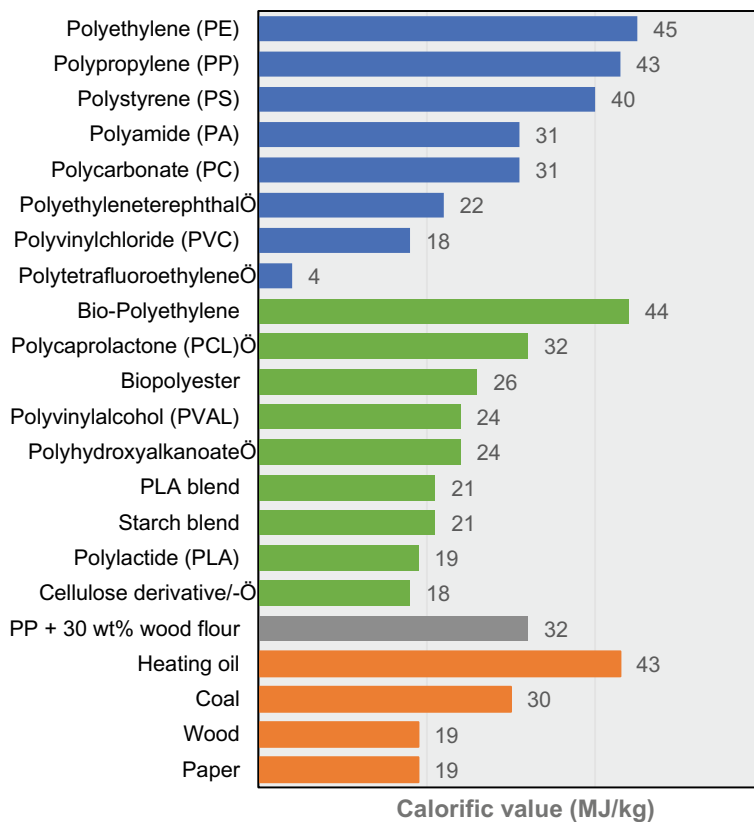


**Fig. 9** Calorific values of biopolymers (green) as opposed to conventional plastics (blue), polymer blend (grey) and petrochemical energy sources (orange). Adapted from Endres and Raths (2011)

and furans into the atmosphere. For bioplastics, energy generation is CO<sub>2</sub> neutral, and low pollutant potential is expected due to their “bio-based” composition. Certified compostable plastics e.g. according to EN 13432 may have lower environmental impacts upon incineration due to the controlled low levels of heavy metals and other ecologically harmful components (Endres and Raths 2011; Dilkes-Hoffman et al. 2019).

### 4.3 Composting

Composting has been identified as the most relevant waste treatment technology available for biodegradable plastics. Interestingly, it was reported that PCL which is a biodegradable plastic has the characteristic of being not only compostable but also of being able to suppress NH<sub>3</sub> emission during composting (Nakasaki et al.



2000). As previously stated in the preceding section, internationally implemented certifications for biodegradable plastics are based on their compostability. On top of that, the success of biodegradable plastics will be decided by the availability of composting or digestion facilities (Ren 2002). The economic viability of composting depends on a few factors. Mixed wastes composting has a large negative effect on the quality and marketability of the compost. Therefore, it is necessary to enhance separate collection of organic wastes and recovery of non-compostable wastes. Other than that, there must be a market or use for the compost. This market does not have to produce net income, but it must be factored into the cost of composting. The closer the market, the more likely that composting is sustainable (Ren 2002).

To ensure the success of composting and provide guarantee of the biodegradable plastics, the reduction of contaminant level is very important. Various approach to be considered in management of waste to obtain a high quality compost (Verma and Fortunati 2019):

- i. Reduce or eliminate contaminants in product design to facilitate the after-use disposal and improve the quality of recycled products, such as compost. It calls for life cycle consideration beyond waste management system to design, production and consumption.
- ii. Source separation of waste by households and commercial consumers into recyclables, compostable (organic wastes and non-recyclable papers, etc.) and wastes for final disposal.
- iii. Sorting at a centralized facility after collection and prior to composting is included in most of the modern municipal waste composting facilities.
- iv. To separate contaminants after composting, traditional practice of municipal waste composting.

Figure 10 shows the classification of biological waste treatment of biodegradable

Temperature	Biological treatment			
	Anaerobic (Bacteria, no fungi)		Aerobic (Bacteria and fungi)	
≤ 35 °C	Chemical pulp Starch Starch/PCL PHA	Mesophilic digestion	Home composting	Chemical pulp Mechanical pulp Starch, Starch/PCL PHA PBAT
50 —60 °C	Chemical pulp Starch PLA Starch/PCL PHA	Thermophilic digestion	Industrial composting	Chemical pulp Mechanical pulp Starch PLA Starch/PCL PHA PBAT

Fig. 10 Biological treatment of biodegradable plastics. Adapted from Hermann et al. (2011)

plastics. Composting involves aerobic treatment to generate carbon and nutrient-rich compost for addition to soil. Industrial composting occurs when bacteria and fungi degrade biomass under aerobic conditions and at high temperatures (50–60 °C). This condition is known as thermophilic phase, which is crucial to ensure the destruction of thermosensitive human and plant pathogens, fly larvae and weed seeds. According to regulations by the US Environmental Protection Agency, significant reduction of pathogens during composting can be achieved by exposing the compost at minimum operating temperature of 40 °C for 5 days, with temperatures exceeding 55 °C for at least 4 h of this period (Song et al. 2009). The biomass involved is also mixed more frequent to ensure higher homogeneity and thus faster degradation.

The metabolism of biodegradable plastics during the industrial composting process resulted in emission of carbon, mainly in the form of carbon dioxide (CO<sub>2</sub>), thus may increase the global warming potential (GWP). It has been reported that industrial composting and landfill caused the worst environmental impacts for biodegradable polymers (Dilkes-Hoffman et al. 2019). Nevertheless, the accusation was made solely based on the comparison of carbon footprint. Emissions of methane are rather exceptional and are small when they do occur, and interestingly, nitrous oxide emissions are much lower (Hermann et al. 2011). Moreover, compost also provides beneficial effects in term of:

- i. Long-term carbon storage in the soil to replace the continuous loss of carbon from agricultural activities
- ii. Nitrogen contained in composed can be utilized as organic fertilizer
- iii. Compost can be used as soil conditioner to improve soil structure.

On the other hand, home composting occurs when bacteria and fungi degrade biomass under aerobic conditions at ambient temperatures ( $\leq 35$  °C). Due to a low temperature and less frequent mixing, biomass degrades slowly as compared to industrial composting. Under such conditions, certain compostable materials certified for industrial composting (EN 13432) may not biodegrade sufficiently. In addition, regulating a home composting is difficult, and there is a tendency of releasing methane as a result of anaerobic composting conditions occurring in poorly managed systems.

TUV Austria offers certification for compostable plastics for industrial composting as well as home composting, and the label is shown in Fig. 11. Some bioplastic polymers, particularly used as bags and pots for horticulture or waste collection bag applications, have been certified by the OK Compost Home scheme, while others



**Fig. 11** Labelling for *OK compost INDUSTRIAL* and *OK compost HOME*

passed only “OK Compost” standard for industrial composting and are not suitable for home. The label used for both certifications is important to assist consumers in disposal procedure.

#### **4.4 Landfill**

Like other municipal solid waste, landfill of waste plastics has been the easiest and cheapest method as it does not require separation, cleaning or treatment. However, there is a challenge faced especially in modern and developing country in providing a suitable site for landfill as the space becomes limited over time. On the other hand, the public becomes more concerned about the impact of landfill on the environment and health due to the release of toxic materials in land-filled municipal waste. In this regard, reducing the quantities of waste that ultimately ends up in landfill has become an explicit government policy. The landfill of biodegradable materials including bioplastic polymers, garden and kitchen waste presents a problem due to the release of methane. Methane is a greenhouse gas with 25 times the effect of CO<sub>2</sub>, produced under anaerobic conditions. While such a “landfill gas” can and is captured and used as energy source, the Landfill Directive (99/31/EC) in UK seeks to reduce the total amount of biodegradable municipal waste (BMW) going to landfill in three successive stages eventually to 35% of the 1995 total of BMW by 2020 (Song et al. 2009).

Tokiwa and Jarerat (2004) reported the microbial degradation of some biodegradable plastics in soil environments, decreasing in the following order: Polyhydroxybutyrate (PHB) = Polycaprolactone (PCL) > Polybutylene succinate (PBS) > PLA. The degradation rate of polymers depends on their molecular weight. Polymers with high molecular weights had slower degradation rate than those with low molecular weights. The biodegradability of polymers can be changed by exposure to abiotic factors (e.g. mechanical, light, thermal and chemicals), and these factors are useful for initiating the biodegradation process (Lucas et al. 2008; Pattanasuttichonlakul et al. 2018). The use of plant growth promoting microorganisms was reported capable to accelerate the biodegradation process, for instance, application of rhizosphere microorganism for PLA (Janczak et al. 2018). Recently, it has been reported that complete degradation of PLA sheets was achieved after 15 days of burial in the soil with dairy wastewater sludge, having high total nitrogen content (Pattanasuttichonlakul et al. 2018).

## **5 Conclusions**

Biodegradable plastics and other biowastes like paper, food and garden waste are generally unsuitable for landfill due to their potential to release methane under anaerobic conditions. Separation of such waste from non-compostable materials is necessary

at the household level. Certification and labelling of biodegradable plastics have been available worldwide and continuously implemented in modern and developed countries. Further steps should be on educating the public on proper disposal of biodegradable plastic waste according to the labelling. Compostable plastics will biodegrade well in industrial composting system, but home composting seems not relevant in most countries as most certification relevant to biodegradation under thermophilic temperature.

## References

- Álvarez-Chávez, C. R., Edwards, S., Moure-Eraso, R., & Geiser, K. (2012). Sustainability of bio-based plastics: General comparative analysis and recommendations for improvement. *Journal of Cleaner Production*, 23(1), 47–56. <https://doi.org/10.1016/j.jclepro.2011.10.003>.
- Chattopadhyay, S. K., Singh, S., Pramanik, N., Niyogi, U., Khandal, R., Uppaluri, R., et al. (2011). Biodegradability studies on natural fibers reinforced polypropylene composites. *Journal of Applied Polymer Science*, 121(4), 2226–2232. <https://doi.org/10.1002/app.33828>.
- Cornell, D. D. (2007). Biopolymers in the existing postconsumer plastics recycling stream. *Journal of Polymers and the Environment*, 15(4), 295–299.
- de Andrade, M. F. C., Souza, P. M. S., Cavalett, O., & Morales, A. R. (2016). Life cycle assessment of Poly(Lactic Acid) (PLA): Comparison between chemical recycling, mechanical recycling and composting. *Journal of Polymers and the Environment*, 24(4), 372–384.
- Dilkes-Hoffman, L. S., Pratt, S., Lant, P. A., & Laycock, B. (2019). The role of biodegradable plastic in solving plastic solid waste accumulation. *Plastics to Energy*, 469–505. <https://doi.org/10.1016/b978-0-12-813140-4.00019-4>.
- Emadian, S. M., Onay, T. T., & Demirel, B. (2017). Biodegradation of bioplastics in natural environments. *Waste Management*, 59, 526–536. <https://doi.org/10.1016/j.wasman.2016.10.006>.
- Endres, H.-J., & Raths, A.-S. (2011). End-of-life options for biopolymers. In H.-J. Endres & A.-S. Raths (Eds.), *Engineering Biopolymers*, Hanser (pp. 225–243).
- European Bioplastics. (2018). Bioplastic market data 2018. In *European Bioplastics*.
- Gross, R. A., & Kalra, B. (2002). Biodegradable polymers for the environment. *Science*, 297(5582), 803–807. <https://doi.org/10.1126/science.297.5582.803>.
- Hermann, B. G., Debeer, L., De Wilde, B., Blok, K., & Patel, M. K. (2011). To compost or not to compost: Carbon and energy footprints of biodegradable materials' waste treatment. *Polymer Degradation and Stability*, 96(6), 1159–1171. <https://doi.org/10.1016/j.polymdegradstab.2010.12.026>.
- Janczak, K., Hryniewicz, K., Znajewska, Z., & Dąbrowska, G. (2018). Use of rhizosphere microorganisms in the biodegradation of PLA and PET polymers in compost soil. *International Biodeterioration and Biodegradation*, 130(March), 65–75. <https://doi.org/10.1016/j.ibiod.2018.03.017>.
- Karakus, K., Birbilen, Y., & Mengeloğlu, F. (2016). Assessment of selected properties of LDPE composites reinforced with sugar beet pulp. *Measurement: Journal of the International Measurement Confederation*, 88, 137–146. <https://doi.org/10.1016/j.measurement.2016.03.039>.
- Lambert, S. (2015). Biopolymers and their application as biodegradable plastics. *Microbial Factories* 1–9. [https://doi.org/10.1007/978-81-322-2595-9\\_1](https://doi.org/10.1007/978-81-322-2595-9_1).
- Lucas, N., Bienaime, C., Belloy, C., Queneudec, M., Silvestre, F., Nava-Saucedo, J. E. (2008). Polymer biodegradation: Mechanisms and estimation techniques—A review. *Chemosphere*, 73(4), 429–442.

- Mohee, R., et al. (2008). Biodegradability of biodegradable/degradable plastic materials under aerobic and anaerobic conditions. *Waste Management*, 28(9), 1624–1629. <https://doi.org/10.1016/j.wasman.2007.07.003>.
- Mooney, B. P. (2009). The second green revolution? Production of plant-based biodegradable plastics. *Biochemical Journal*. <https://doi.org/10.1042/BJ20081769>.
- Nakamura, E. M., et al. (2005). Study and development of LDPE/starch partially biodegradable compounds. *Journal of Materials Processing Technology*, 162–163(SPEC. ISS.), 236–241. <https://doi.org/10.1016/j.jmatprotec.2005.02.007>.
- Nakasaki, K., Ohtaki, A., & Takano, H. (2000). Biodegradable plastic reduces ammonia emission during composting. *Polymer Degradation and Stability*, 70(2), 185–188. [https://doi.org/10.1016/S0141-3910\(00\)00104-X](https://doi.org/10.1016/S0141-3910(00)00104-X).
- Niaounakis, M. (2013). Physical recycling. *Biopolymers Reuse, Recycling, and Disposal*, 151–166.
- Pattanasuttichonlakul, W., Sombatsompop, N., & Prapagdee, B. (2018). Accelerating biodegradation of PLA using microbial consortium from dairy wastewater sludge combined with PLA-degrading bacterium. *International Biodeterioration and Biodegradation*, 132(March), 74–83. <https://doi.org/10.1016/j.ibiod.2018.05.014>.
- Ren, X. (2002). Biodegradable plastics: A solution or a challenge? *Journal of Cleaner Production*, 11(1), 27–40. [https://doi.org/10.1016/S0959-6526\(02\)00020-3](https://doi.org/10.1016/S0959-6526(02)00020-3).
- Rudnik, E. (2019). Chapter 2—Compostable polymer materials—Definitions, structures and methods of preparation. In E. Rudnik (Ed.), *Compostable Polymer Materials* (2nd ed., pp. 11–48), Elsevier. ISBN 9780080994383, <https://doi.org/10.1016/B978-0-08-099438-3.00002-1>.
- Song, J. H., Murphy, R. J., Narayan, R., & Davies, G. B. H. (2009). Biodegradable and compostable alternatives to conventional plastics. *Philosophical Transactions of the Royal Society B: Biological Sciences*, 364(1526), 2127–2139. <https://doi.org/10.1098/rstb.2008.0289>.
- Spierling, S., Venkatachalam, V., Behnsen, H., Herrmann, C., & Endres, H.-J. (2018). Bioplastics and circular economy—Performance indicators to identify optimal pathways. *Progress in Life Cycle Assessment*, 147–154. [https://doi.org/10.1007/978-3-319-92237-9\\_16](https://doi.org/10.1007/978-3-319-92237-9_16).
- Tokiwa, Y., & Jarerat, A. (2004). Biodegradation of poly(l-lactide). *Biotechnology Letters*, 26(10), 771–777.
- Verma, D., & Fortunati, E. (2019). Biobased and biodegradable plastics. In *Handbook of ecomaterials* (vol. 4). [https://doi.org/10.1007/978-3-319-68255-6\\_103](https://doi.org/10.1007/978-3-319-68255-6_103).

# Challenges and Current State-of-Art of the *Volvariella volvacea* Cultivation Using Agriculture Waste: A Brief Review



N. A. Umor, S. Abdullah, A. Mohamad, S. Ismail, S. I. Ismail, and A. Misran

**Abstract** Agriculture waste has been used for the cultivation of commercial mushroom from historical years. Yet some limitations in producing efficient yield of the harvest especially for *Volvariella volvacea* cultivation remain unresolved. With different types of substrate used in the commercial farming of this mushroom, the biological efficiency of the mushroom is considered low compared to other species such as *Lentinus* sp., *Pleurotus* sp. and *Agaricus* sp. Thus, over the years, many attempts have been conducted to improve its biological efficiency using different approaches. In this brief review, major factors that limit the conversion of substrate to fruiting bodies will be discussed, while the current state-of-art for the cultivation practise for *Volvariella volvacea* will also be layout.

**Keywords** *Volvariella volvacea* · Biological efficiency · Treatment

## 1 Introduction

The past decades have seen the rapid development in agriculture industry simultaneously with the increment of population. As a result, the industry produces vast amount of agrowastes that are potentially causing environmental problems if not properly managed. To date, it is estimated more than 100 billion metric tons of biomass produced yearly with majority of it coming from agriculture field including

---

N. A. Umor (✉) · S. Abdullah · S. I. Ismail · A. Misran  
Faculty of Agriculture, Universiti Putra Malaysia, Serdang, 43400 Seri Kembangan, Selangor, Malaysia  
e-mail: [noorazrimi@gmail.com](mailto:noorazrimi@gmail.com)

N. A. Umor  
Faculty of Applied Sciences, Universiti Teknologi MARA Cawangan Negeri Sembilan, Kampus, 72100 Kuala Pilah, Negeri Sembilan, Malaysia

A. Mohamad  
Malaysia Nuclear Agency, Bangi (Dengkil Road Complex), Kampung Sungai Buah, 43800 Dengkil, Selangor, Malaysia

S. Ismail  
Universiti Malaysia Terengganu, 21030, Kuala Nerus, Terengganu, Malaysia

© Springer Nature Singapore Pte Ltd. 2020  
A. Z. Yaser (ed.), *Advances in Waste Processing Technology*,  
[https://doi.org/10.1007/978-981-15-4821-5\\_9](https://doi.org/10.1007/978-981-15-4821-5_9)

wood residue and oil palm, agriculture waste (Belewu and Babalola 2009; Field et al. 1998). This organic waste provides highly potential feedstock or substrate in plethora of industry including for mushrooms cultivation, renewable energy production and biofertilizers.

Mushroom cultivation is fast becoming one of the real solutions of utilizing abundance of agrowaste specifically ligno-cellulolytic waste for good harvest. With over 2000 species known to exist in nature, yet only 30 reported to be edible while 10 are grown systematically (Prasad et al. 2017; Valverde et al. 2015). This provided various opportunity for new exploration. Many species including *Agaricus*, *Pleurotus*, *Agrocybe* and *Volvariella* have been widely commercial using different types of agrowaste (Oseni et al. 2012).

*Volvariella volvacea* is a type of edible mushroom regularly grown in China, India and South East Asian country such as Indonesia, Malaysia and Thailand. It accounts for 16% of total production of cultivated mushrooms in the world (Singh et al. 2018). It belongs to the family Pluteaceae of the Basidiomycetes. This mushroom is first cultivated in China in 1822 (Chang and Miles 1989). Also known as paddy straw mushroom, it is a type of “warm mushroom” as it grows at relatively high temperature. It is a fast growing mushroom, and under favourable growing conditions, the total crop cycle is completed within 4–5 weeks time. This mushroom can use wide range of cellulosic materials, and the C:N ratio needed is 40–60 and considered as easy growing mushroom.

It also can be cultivated on uncomposed substrates such as paddy straw and cotton waste or other cellulosic organic waste materials within short period of time (Ahlawat and Kumar 2005). Although this mushroom has a long history of cultivation, the low yield efficiency remained to be an unsolved obstacle in the commercial practise.

Thus, this paper will review the research conducted about cultivation of *V. volvacea* with highlighting on the factor that involved for producing fruiting bodies and current state-of-the-art of the cultivation process of this mushroom. The aim of this review paper is to highlight the limitation of the cultivation process which mainly due to low conversion of substrate and discussed the recent development of *V. volvacea* cultivation (Fig. 1).

**Fig. 1** *Volvariella volvacea* grown on oil palm empty fruit bunch fibre



## 2 Various Substrate for *Volvariella volvacea* Cultivation

The cultivation of *V. volvacea* is believed to begin 1822 in China. *V. volvacea* is also known as rice paddy straw mushroom as it is commonly grown using this substrate. However, various substrate had also been used to cultivate this mushroom which includes paddy straw, water hyacinth, oil palm bunch, oil palm pericarp waste, banana leaves, saw dust, cotton waste and sugarcane bagasse (Chang and Miles 1989).

The cultivation of *Volvariella* is easy and less complicated comparing to other types of mushroom and economically potential. Before 1970, it was only paddy straw used as substrate for this mushroom cultivation. However, the introduction of ginning mill waste (cotton waste) as heating material in 1971 has revolutionized new method for paddy straw mushroom as it was found to be a good replacement to paddy straw and yielded better (30–40%). After adoption of cotton waste, the cultivation of paddy straw mushroom has become semi-industrialized in Hong Kong, Taiwan, Indonesia, China and Thailand.

Empty fruit bunch meanwhile is not a commercial substrate for *Volvariella* industry, but the previous work suggests its potential to be as replacement with comparable yield. Many reports from previous researcher suggest the substrate as highly potential for *Volvariella* sp. cultivation due to its properties and abundance. However, with certain pre-treatment especially during composting and additional of supplement during growth stages, this substrate can be a suitable media for the cultivation (Biswas 2014; Thiribhuvanamala 2012) (Table 1).

### 2.1 Rice Straw

Historically, the *V. volvacea* mushroom is grown using paddy straw as main substrate and before 1970, it was practically the only substrate used for growing of this mushroom under natural environment conditions. The biological efficiency (B.E.) under natural conditions varied from 1.5 to 14.0%. The nature of *V. volvacea* growth

**Table 1** Substrate for *Volvariella volvacea* cultivation

Substrate	Yield efficiency (%)	References
Rice straw	10.2	Biswas (2014)
Banana leaf	15.2	Chiu et al. (2000)
Oil palm empty fruit bunch	6–7	Azhar et al. (2018)
Cotton waste	30–40	Chang and Miles (1989)
Sugar cane bagasse	12.4	Hu et al. (1973)
Cassava peel	2.1	Fasidi (1994)



prefers high cellulose, hemicellulose and low lignin containing substrate as due to its ability to excrete various cellulolytic enzymes (Ahlawat and Kumar 2005). Composting step involves the addition of 2% CaCO<sub>3</sub> solution in wetted dried paddy straw for couples of hour (2–6 h) before the excess water is drained off. Next, a thin layer of this substrate is spread over clean cement floor or any platform before adding urea (1%) and gypsum (5%) to mix well. Then, the compost heap was built out of this substrate and covered with polythene tarp for six days. The compost then divided into bed prior to spawning. Usually, the first harvest appears between 11 and 13 days after spawning. Maximum B.E for *V. volvacea* cultivation recorded at 21.8% when applying booster and mixture of alternative substrate such as oil palm empty fruit bunch fibre in the rice straw compost (Thiribhuvanamala 2012). While another study noted that bed method is preferable for cultivation of paddy straw mushroom as it produces higher yield compared to spiral and heap method (Biswas 2014).

## 2.2 Cotton Waste

Cotton waste first used as substrate for the production of *V. volvacea* beginning in 1971 (Chang and Miles 1989). It proved to be efficient for the cultivation as it does not require composting process yet the yield reported was higher compared to other types of substrate. In Taiwan, local growers used a mixture of 2:1 cotton waste and rice straw due to availability of the substrate. Some practise in using cotton waste for mushroom substrate involved the addition of the spent compost of *Agaricus bisporus* as part of substrate mixture, whereby the spent compost is placed at the bottom layer and wetted cotton on the upper side before being pasteurized at 70 °C for 12 h. Spawning is carried out after cooling down to 35 °C. During spawning and cropping, proper amounts of fresh air and light are provided to ensure normal development of the champignon. First flush is expected to be from 12 to 15 days afterwards. Yield up to 40% can be harvested for 15–20 days of fruiting. Another interesting practise was the growers kept the spent cotton wastes and rice straw compost after each crop, to be used for next cycle of *V. volvacea* crop. This is done just by layering new wetted cotton on the surface of the old compost. By the way, this practise helps to maintain the mushroom bed at required temperature while saving both labour cost in removing the used compost and energy cost for pasteurization. The final spent compost of cotton waste and rice straw can be utilized as organic fertilizer mixture or soil conditioner.

## 2.3 Oil Palm Empty Fruit Bunch (EFB)

In a typical palm oil mill, empty fruit bunches are available in abundance as fibrous material of purely biological origin. EFB contains neither chemical nor mineral additives, and depending on proper handling operations at the mill, it is free from

foreign elements such as gravel, nails, wood residues, waste and others (MPOB 2017). However, it is saturated with water due to the biological growth combined with the steam sterilization at the mill. The use of EFB as mushroom compost specifically *V. volvacea* is still new and requires further research. One of the challenges is the composition of EFB itself as the main substrate for cultivating *V. volvacea*.

Previous study shown the penetration ratio for conversion of substrate to product is low, and pre-treatment strategies are suggested. Current practice of *V. volvacea* cultivation using whole EFB is by composting it prior to spawning. Composting remains the vital process in mushroom cultivation, whereas it acts as to decompose polymers in growth media, such as hemicellulose and cellulose into simpler monomers, such as xylose and glucose, whereby monomers are used as nutrients on compost for metabolism and fruit body formation (Chang and Miles 1989). The common steps involved from the composting followed by spawning then pinning and harvesting of fruiting bodies at egg stage. During spawning, the humidity is provided at the beginning of the process and is controlled by tightly covered the growth bed to prevent loss of water while providing high CO<sub>2</sub> environment. Growth of *V. volvacea* mycelium required high CO<sub>2</sub> concentration, while in the pinning stage that is the beginning of fruitification of mushroom, oxygen is needed. The first harvest may appear between 12 and 17 days later after inoculation of the mushroom spawn (Triyono et al. 2019). Fruiting bodies appear for 2 or 3 flushes that last between 10 and 15 day. Biological efficiency of EFB for *V. volvacea* as reported in the literature by previous research was in the range from 5 to 7.6% (Azhar et al. 2018; Triyono et al. 2019). B.E. of *Volvariella* cultivation can be improved if the whole bunch EFB is replaced with the EFB fibre. EFB fibre is produced through screwpressing and grinding process that remove 60–70% of water content thus reduce the weight of substrate while maintaining majority of the nutrient substance. Although not many work related on using EFB fibre for *Volvariella* cultivation reported, the use of it for other types of mushroom such as *Pleurotus* sp. proves to be successful with yield up 100% achieved (Kavitha et al. 2013).

### 3 Challenges in *Volvariella volvacea* Cultivation

In general *V. volvacea*, productivity is attributed to the hydrolytic enzyme production potential of the mushroom quality of the substrate used, substrate preparation method and growing conditions (Ahlawat and Tewari 2007). Environmental factors particularly related with temperature and humidity of the growth bed must be suitable to grow the mushrooms as changes of this component may contribute to the negative effect. Either in closed door system or outdoor growing style, both factors effect directly to the yield. While in Malaysia most of the growers using outdoor cultivation system that are more cheaper and easy but with some limitation as this system produced low yield for subsequent growing season due to high number of contamination (Azhar et al. 2018). As far as concerned, the development of cultivation methodology of mushroom to suit the local substrate feedstock and location

**Table 2** Common problem in *Volvariella volvacea* cultivation (Ahlawat and Tewari 2007)

Types of problems	Reasons	Effect
Presence of contaminants	Composting and pasteurization process incomplete	Loss of yield and need to be discarded to avoid spread
Dry out/dehydration	Less humidity, too much ventilation	Growth retarded
Suspended growth	Light deficiency, low quality spawn	Loss of yield
Death at early stages	Low quality spawn, insect infestation, low oxygen and high CO <sub>2</sub> , diseases from fungi or virus	Loss of yield
Growth of <i>Coprinus</i>	High nitrogen content, low quality substrate and excess heat of the compost bed	Loss of yield due to competition growth

factor is ongoing. For Malaysia's scenario, lack of proper design and construction of mushroom house for small, medium and commercial-scale indoor cultivation of *V. volvacea* limited the growers to opt for this mushroom. With the fact oyster mushroom continues to dominate the local production with more than 90% while less than 1% for *Volvariella*, a lot of work need to be done to improve its production (Rosmiza et al. 2016). Meanwhile, commercial cultivation of *V. volvacea* is done in controlled mushroom house in China, Hong Kong and Indonesia which are readily established. Common problems may be caused by external factor such as pest infestation or contamination (Table 2).

### 3.1 Biological Efficiency

Biological efficiency is the common measurement for the efficiency of the mushroom cultivation, whereas it compares the weight of the harvest to the dry weight of mushroom compost. Higher yield increases the biological efficiency. One crucial factor for the creation of a fruiting body in mushroom cultivation is the environmental condition (Scrase and Elliott 1998), whereby induction from drastic environmental shift may provide ideal condition for mycelial growth and subsequent fruiting. However, every mushroom has a different behaviour regarding fructification stage, and there is no general set of condition in all mushrooms.

Substrate component in *V. volvacea* compost bed is important subject of study for increasing of yield. There are a lot of research is being carried out to test the set of conditions for high yield mushroom cultivation; however, it only focuses on a certain mushroom species (Belewu and Babalola 2009; Biswas 2014; Oseni et al. 2012; Philippoussis and Zervakis 2001). For fruiting body formation, a slightly higher concentration of nitrogen is needed than the concentration supporting mycelial

growth. Meanwhile, the cellulose/lignin ratios in substrates are found to be positively correlated to mycelial growth rates and mushroom yields.

For example, a study had reported an increased of biological efficiency up to 24.5% when supplementation of beds with horse gram and tamarind seed powder (1:1 w/w) at 2% level (Nannapaneni and Subbiah 2016). While in the beds of mustard straw + paddy straw (1:1), the presence of more lignin and volatile components in mustard straw, nematodes and moulds attack could be the reasons for slower *V. volvacea*'s spawn run, poor yields and biological performance. All of this factor is worth to be investigated in order to determine the best formulation for higher yield.

### 3.2 *Enzymatic Activities During Volvariella volvacea Growth*

Growth of mushroom relies on the metabolism of the substrate for conversion to nutrient facilitated by the enzymatic process. The activities of enzymes differ in stages contribute to the physiological changes in both environmental condition and cellulosic level. For the development of any mushroom fruiting body, it is affected by the different nutrients and physical factors changes caused by extracellular enzymes such as cellulases, hemicellulases and lignases (Thiribhuvanamala 2012). Cellulases play a critical role during substrate colonization, while laccase dominates during sporophore development. Mannitol dehydrogenase, tyrosinase and water activity were found to be expressed disparately with different morphogenic stages and strains of *V. volvacea*.

While *V. volvacea* is generally considered a straw-degrading fungus, this mushroom however has a low biological substrate conversion rate. It was due to lacking of an active ligninolytic enzyme system involving isoenzyme combinations of three heme peroxidases: lignin peroxidases (LiPs), manganese peroxidases (MnPs) and hybrid enzymes known as polyvalent peroxidases (VPs) (Bao et al. 2013). thus inhibit further enzymatic conversion in the cellulosic substrate to fruiting bodies of *Volvariella volvacea*. Some strategy implemented to boost the enzymatic activities is by adding micronutrient such as sodium acetate and mixture of other chemicals to the compost bed via spraying or soaking (Thiribhuvanamala 2012; Hou et al. 2017). This strategy produces better result yet still low compared to other type of mushroom such as *Pleurotus* sp.

## 4 Recent Development in Cultivation Process

The cultivation of *V. volvacea* had been around for more than hundred years which established steadily. However, the research on utilizing various agriculture waste to grow this mushroom is ongoing with attempt to improve the biological efficiency. Some of the recent development regarding the process is presented here.

## 4.1 Pre-treatment Process

The aim of pre-treatment process in mushroom cultivation is to prepare the substrate to be readily available as well as facilitating cell's nutrient uptake and also eliminating contaminants and pathogens in the compost that may effect the yield (Nannapaneni and Subbiah 2016). There have been many studies on the pre-treatment of ligno-cellulosic biomass content, whether physical, chemical or biological. Composting is considered the most common biological method applied. Even though it was proven to increase the yield yet in the end, the conversion from substrate to fruiting bodies is still low. However, different strategies in composting may provide better solution to increase availability of nutrient for mushroom growth. For example, the augmentation of specialized microorganisms instead of indigenous could be a good way to boost degradability of substrate especially in removing the lignin part. Another study showed that the application of effective microorganisms prior to spawning had improved the mycelia cell growth of *Pleurotus* sp. while also reduced the contamination (Vetayasuporn 2004). While in another report, application of laccase-producing *Trichoderma* sp. in fermentation substrate successfully remove the lignin component (Bagewadi et al. 2017).

Meanwhile, in the chemical pre-treatment, the method tends to specify to the target component. For example, method using acid will target hemicelluloses, while in alkali-catalyzed pre-treatment, mainly lignin is removed (Hahn-Hagerdal et al. 2006). Both methods involved the disruption of cell wall through breaking down of bond and linkages which finally solubilized the wall, thus increasing the enzymatic digestibility of cellulose. But as far as concerned, these methods are more likely to be used for generation of renewable energy such as biogas and bio-ethanol other than for mushroom cultivation due to the cost involved. Until recently, there has been no standard pre-treatment to be applied for the substrate in *V. volvacea* cultivation as different types of agriculture wastes are used in different region. The research on this field is still ongoing.

## 4.2 Organic Supplementation

As discussed previously, a common strategy to improve yield in *V. volvacea* cultivation is by supplementing the compost bed with additional sources of *C* and *N* plus the micronutrient. This strategy effectively increases the enzymatic activities while in the same time fasten the forming of fruiting bodies. There is a large volume of published studies describing the role of organic amendment in *V. volvacea* mushroom compost including the cotton seed cake, cotton waste, neem cake, soyabean meal, deoiled rice bran, mustard cake, wheat bran, gram dal powder (Ahlawat and Tewari 2007; Belewu and Babalola 2009; Thiribhuvanamala 2012). The increment however only reaches to the extent of 30–40% and only applied to the cotton waste, while for other type of substrates, it is lower.

**Table 3** Effect of supplementation in the compost media for *Volvariella volvacea* cultivation

Supplements	Methods of application	Biological efficiency (%)	References
Sodium acetate	1.48 L/m <sup>2</sup> of 0.02% sodium acetate solution applied after 3 days spawning	16.71	Hou et al. (2017)
Liquid organic fertilizer	2 L liquid organic fertilizer solution at 0.25% added during composting of substrate	7.06	Singh et al. (2018)
Micronutrient (mixture)	Spraying during pinning stage at 600 ppm	25.3	Thiribhuvanamala (2012)
Horsegram + tamarind seed powder	20 g of each pre-sterilized supplement was sprinkled in each layer over the spawn at 2% level (in dry weight basis)	24	Li et al. (1992)

An increment of 156% on the mycelial growth of *V. volvacea* was recorded when Tween 80 is applied in the growth culture (Li et al. 1992). The addition of lipid substances in the growth media assumably stimulates enzyme levels activities and support biomass production. In which can be observed by higher yield in Tween 80 supplemented culture compared to non supplemented. These however did not necessarily reflect directly to the yield as fruitification stage required different condition. Unfortunately, none of the research had been conducted to study the effect lipid compound to the yield of *Volvariella* (Table 3).

### 4.3 *Biotechnology and Nanotechnology Application in Volvariella volvacea Cultivation*

Interesting development in the field of nanotechnology provides future sight on the new frontier in better agriculture economy. In conjunction with mushroom cultivation, nanoparticle synthesis regains much attention as proved by increment reports in this particular subject (Prasad et al. 2017). The process of nanoparticle biosynthesis by the means of fungi mediated is far more clean and safe to the environment compared to the use of chemicals. In recent years, many species have been reported to have ability in synthesizing nanoparticle either intracellularly or extracellularly

(Khandel and Kumar 2018). However, as far as concerned, none of the report suggests the synthesis by *V. volvacea*. Nevertheless, there are possibilities for it looking to the increment trend for this research.

Bioinoculant application in mushroom cultivation can be a way forward to increase growth of this mushroom at all stages for crop yield. Introduction of specific microbiota such as bacteria of genera *Azotobacter*, *Bacillus* and *Pseudomonas* has been reported to develop antireaction towards competitive mould while also supporting the degradation of cellulolytic component (Singh et al. 2018).

A research on *V. volvacea* genome had provided insight knowledge to understand the behaviour of this mushroom during degradation of the cultivating compost, the sexual reproduction mechanism and its sensitivity to low temperatures at the molecular level (Bao et al. 2013). The knowledge can be applied to improve cultivation practise. In addition, the insertion of multi-functional cellulase gene in *V. volvacea* via transgenic strain successfully increases the cellulase activities and yield of fruiting bodies (Zhao et al. 2010).

## 5 Conclusion

Although the cultivation of *V. volvacea* is considered easy and requires less technology, but still the current practises are lacking in terms of producing high yield in comparable with other commercial mushroom. To date, research on *V. volvacea* is considered inadequate to answer the related issues regarding its low yield. Implementation of biotechnology and nanotechnology could be a possible breakthrough for improving biological efficiency. As through genetic engineering, there are possible way to boost cell's degradation ability with manipulation of specific genes. Following this, in depth understanding on the mechanisms of enzymatic activities would perhaps overcome the barrier for efficient bioconversion of the cellulolytic substrate to fruiting bodies of *V. volvacea*. Another possible solution is to design a suitable compost that may comprise variety component of main substrate supplemented with organic compound or nutrient.

Furthermore, it is suggested here that future work may be focused on new cultivation technique by applying modern technology such as automation controlled system that can create optimum condition for higher yield. As a conclusion, the improvement of *V. volvacea* will contribute to significant socio-economic growth and support the green economic policy.

**Acknowledgements** The author would like to express gratitude to Southeast Asian Regional Centre for Graduate Study and Research in Agriculture (SEARCA) as the main sponsor for this Ph.D. study, the host institution of UPM Serdang and UiTM Malaysia while Malaysia Nuclear Agency, Bangi, for facilities including the mushroom spawn and plot to cultivate the mushroom. Thank you.

## References

- Ahlawat, O. P., & Kumar, S. (2005). Traditional and modern cultivation technologies for the paddy straw mushroom (*Volvariella* spp.). *Frontiers in Mushroom Biotechnology* 157–161.
- Ahlawat, O. P., & Tewari, R. P. (2007). Cultivation technology of paddy straw mushroom (*Volvariella volvacea*), pp. 14–26. National Research Centre for Mushroom (Indian Council of Agricultural Research).
- Azhar, H., Yuzaidi, M., & Nur Hafizah, S. (2018). Teknologi Penanaman Cendawan *Volvariella* (pp. 5–15). Malaysia: Penerbit Agensi Nuklear.
- Bagewadi, Z. K., Mulla, S. I., & Ninnekar, H. Z. (2017). Optimization of laccase production and its application in delignification of biomass. *International Journal Recycling Organic Waste Agriculture*, 6, 351–365. <https://doi.org/10.1007/s40093-017-0184-4>.
- Bao, D., Gong, M., Zheng, H., Chen, M., Zhang, L., Wang, H., & Tan, Q. (2013). Sequencing and comparative analysis of the straw mushroom (*Volvariella volvacea*) Genome. *PLoS ONE*, 8(3). <https://doi.org/10.1371/journal.pone.0058294>.
- Belewu, M. A., & Babalola, F. T. (2009). Nutrient enrichment of waste agricultural residues after solid state fermentation using *Rhizopus oligosporus*. *Journal of Applied Bioscience*, 695–699.
- Biswas, M. K. (2014). Techniques for increasing the biological efficiency of paddy straw mushroom (*Volvariella volvacea*) in Eastern India mushroom project (AICMIP). *Food Science and Technology*, 2(4), 52–57. <https://doi.org/10.13189/fst.2014.020402>.
- Chang, S. T., & Miles, P. G. (1989). *Edible mushrooms and their cultivation* (pp. 285–295). New York: CRC Press.
- Chiu, S. W., Law, S. C., Ching, M. L., Cheung, K. W., & Chen, M. J. (2000). Themes for mushroom exploitation in the 21st century: Sustainability, waste management, and conservation. *Journal of General and Applied Microbiology*, 46, 269–282.
- Fasidi, I. (1994). Studies on *Volvariella esculenta* (mass) singer: Cultivation on agricultural wastes and proximate composition of stored mushrooms. *Food Chemistry*, 55(2), 161–163.
- Field, C. B., Behrenfeld, M. J., Randerson, J. T., & Falkowski, P. (1998). Primary production of the biosphere: Integrating terrestrial and oceanic components. *Science*, 281(5374), 237–240.
- Hahn-Hagerdal, B., Galbe, M., Gorwa-Grauslund, M. F., Liden, G., & Zacchi, G. (2006). Bio-ethanol the fuel of tomorrow from the residues of today. *Trends in Biotechnology*, 24, 549–556.
- Hou, L., Li, Y., Chen, M., & Li, Z. (2017). Improved fruiting of the straw mushroom (*Volvariella volvacea*) on cotton waste supplemented with sodium acetate. *Applied Microbiology and Biotechnology*, 101(23–24), 8533–8541. <https://doi.org/10.1007/s00253-017-8476-1>.
- Hu, K. H., Song, S. F., & Liu, P. (1973). Experiments on Chinese mushroom cultivation. I. The comparison of cultivating materials. II. Investigation on sugar cane rubbish for Chinese mushroom cultivation and its growth factors. *Agriculture Research*, 22, 145–154.
- Kavitha, B., Rajannan, G., & Jothimani, P. (2013). Utilization of empty fruit bunch of oil palm as alternate substrate for the cultivation of mushroom. *International Journal of Science*, 2(5), 839–846.
- Khandel, P., & Kumar, S. (2018). Mycogenic nanoparticles and their bio-prospective applications: Current status and future challenges. *Journal of Nanostructure in Chemistry*, 8(4), 369–391. <https://doi.org/10.1007/s40097-018-0285-2>.
- Li, Y., Cho, K. Y., Wu, Y. Z., & Nair, N. G. (1992). The effect of lipids and temperature on the physiology and growth of *Volvariella volvacea*. *World Journal of Microbiology and Biotechnology*, 8, 621–626.
- MPOB. (2017). MPOB coordinators, pocketbook of oil palm uses (pp. 10). Malaysia: Malaysian Palm Oil Board.
- Nannapaneni, K. K., & Subbiah, K. A. (2016). Influence of organic nitrogen supplementation on yield of paddy straw mushroom, *Volvariella volvacea* (Bull. Ex Fr.) Sing. *International Journal of Green Pharmacy*, 10(4), 237–241. <https://doi.org/10.22377/ijgp.v10i04.789>.



- Oseni, T. O., Dlamini, S. O., Earnshaw, D. M., & Masarirambi, M. T. (2012). Effect of substrate pre-treatment methods on oyster mushroom (*Pleurotus ostreatus*) production. *International Journal of Agriculture and Biology*, 14(2), 251–255.
- Philippoussis, A., & Zervakis, G. (2001). Diamantopoulou, bioconversion of agricultural lignocellulosic wastes through the cultivation of the edible mushrooms *Agrocybe aegerita*, *Volvariella volvacea* and *Pleurotus* spp. *World Journal of Microbiology and Biotechnology*, 17, 191–200. <https://doi.org/10.1023/A:1016685530312>.
- Prasad, R., Bhattacharyya, A., & Nguyen, Q. D. (2017). Nanotechnology in sustainable agriculture: Recent developments, challenges, and perspectives. *Frontiers in Microbiology*, 8, p1–13. <https://doi.org/10.3389/fmicb.2017.01014>.
- Rosmiza, M., Davies, W., Aznie, R. C., Jabil, M., & Mazdi, M. (2016). Prospects for increasing commercial mushroom production in Malaysia: Challenges and opportunities. *Mediterranean Journal of Social Sciences*, 406–414. <https://doi.org/10.5901/mjss.2016.v7n1s1p406>.
- Scrase, R. J., & Elliott, T. J. (1998). *Microbiology of fermented food, biology and technology for mushroom culture* (pp. 543–582). New York: Springer.
- Singh, K., Dey, I., & Kumar, S. (2018). Paddy straw mushroom (*Volvariella* spp.): A natural scavengers who help in malnutrition and environment protection. *International Journal of Microbiology Research*, 10(5), 1183–1185. <https://doi.org/10.9735/0975-5276.10.5>.
- Thiribhuvanamala, G. (2012). Improved techniques to enhance the yield of paddy straw mushroom (*Volvariella volvacea*) for commercial cultivation. *African Journal of Biotechnology*, 11(64), 12740–12748. <https://doi.org/10.5897/AJB11.4066>.
- Triyono, S., Haryanto, A., Telaumbanua, M., Dermiyati, D., Lumbanraja, J., & To, F. (2019). Cultivation of straw mushroom (*Volvariella volvacea*) on oil palm empty fruit bunch growth medium. *International Journal of Recycling of Organic Waste in Agriculture*, 1–12. <https://doi.org/10.1007/s40093-019-0259-5>.
- Valverde, M. E., Hernández-pérez, T., & Paredes-lópez, O. (2015). Edible mushrooms: Improving human health and promoting quality life. *International Journal of Microbiology*, 1–15. <https://doi.org/10.1155/2015/376387>.
- Vetayasuporn, S. (2004). Effective microorganism for enhancing *Pleurotus ostreatus* (Fr.) Kummer production. *Journal of Biosciences*, 4(6), 706–710.
- Zhao, F. Y., Lin, J. F., Zeng, X. L., Guo, L. Q., Wang, Y. H., & You, L. R. (2010). Improvement in fruiting body yield by introduction of the *Ampullaria crosseana* multi-functional cellulase gene into *Volvariella volvacea*. *Bioresource Technology*, 101(16), 6482–6486. <https://doi.org/10.1016/j.biortech.2010.03.03>.

# Microbial Degradation of Hydrocarbons from Petrochemical Waste Using Food Waste Amendments



Fazilah Ariffin, Cheah Jin Min, Gan Sik Ze, Sabariah Yussof, and Noraznawati Ismail

**Abstract** Polycyclic aromatic hydrocarbons (PAHs) are an organic pollutant that is abundant in petrochemical waste. Bioremediation can be an alternative way for the remediation of such hydrocarbon-contaminated soil. Therefore, this study determined the PAHs degradation activity by soil bacteria amended with food waste in a shake flask system. Diesel oil that was amended with various types of food wastes was inoculated with hydrocarbon-contaminated soil and incubated for 5 weeks at 30 °C, 150 rpm. The PAH extraction was conducted by using a liquid–liquid extraction procedure, and the diesel oil degradation compound was analyzed using gas chromatography–mass spectrometry (GC-MS). Bacteria from the enrichment culture flasks were isolated and identified based on colony morphology and biochemical tests using the BBL Crystal Identification Kit. As a result, the degradation rates of diesel oil compounds were higher in the flasks amended with food wastes as compared to the flask unamended with food wastes. A total of 11 hydrocarbon-degrading bacteria were successfully isolated and preliminary identified to be *Acinetobacter baumannii*, *Pseudomonas aeruginosa*, *Stenotrophomonas maltophilia*, *Pseudomonas fluorescens*, *Klebsiella pneumoniae*, *Shewanella putrefaciens*, *Enterobacter aerogenes*, *Brevibacillus brevis*, *Bacillus cereus*, *Staphylococcus saprophyticus* and *Corynebacterium* sp. The results of this study demonstrated the potential of food wastes to be harnessed for enhancing the bioremediation of diesel-contaminated soil instead of being disposed of as a waste.

**Keywords** Bioremediation · Polycyclic aromatic hydrocarbons · Food waste · Hydrocarbon-degrading bacteria

---

F. Ariffin (✉) · C. J. Min · G. S. Ze · S. Yussof  
Faculty Science and Marine Environment, Universiti Malaysia Terengganu, 21030 Kuala Nerus,  
Terengganu, Malaysia  
e-mail: [fazilah@umt.edu.my](mailto:fazilah@umt.edu.my)

N. Ismail  
Institute Marine Biotechnology, Universiti Malaysia Terengganu, 21030 Kuala Nerus,  
Terengganu, Malaysia

## 1 Introduction

Polycyclic aromatic hydrocarbons (PAHs) are major cause of concern as it tends to contribute negatively to the environment and human health. Naturally, PAHs and its derivatives are formed by incomplete combustion and natural combustion such as volcanic eruptions and forest fires. However, anthropogenic activities such as industrial production, gasification, vehicular emissions, municipal waste, incineration of solid waste and residential wood burning contribute to a large amount of PAHs released into the surroundings (Deka and Lahkar 2016; Ravindra 2008). PAHs are categorized as complex organic chemicals with at least two fused benzene rings that include carbon and hydrogen. PAHs with two to three benzene rings are known as low molecular weight (LMW) PAHs, whereas those with more than 3 benzene rings are considered as high molecular weight (HMW).

PAHs have low solubility of water and low vapor pressures that make them tend to adsorb tightly to organic matter in soil, resulting in them being less susceptible to biological and chemical degradation (Lau et al. 2010; Keshavarzifard et al. 2014). According to Deka and Lahkar (2016), about 16 out of 130 PAHs are classified as organic pollutants that are carcinogenic and mutagenic to humans. It has been reported that benzo(*a*)pyrene is the most toxic PAHs due to its molecular structure while other PAHs that also have teratogenicity and carcinogenic properties are benz(*a*)anthracene, chrysene[C<sub>18</sub>H<sub>12</sub>], dibenz[*a,h*]anthracene [C<sub>20</sub>H<sub>14</sub>] and indeno[1,2,3-*cd*]pyrene [C<sub>22</sub>H<sub>12</sub>] (Haritash and Kaushik 2007).

Bioremediation has the potential to be an effective way to remove PAHs and reduce their toxicity to the environment. Bioremediation can be defined as the breakdown of hazardous substances to less toxic substances by using microorganisms to degrade contaminants naturally. This technique includes nutrient supplementation or bio-stimulation which provides suitable nutrients and conditions for both indigenous and exogenous microbes. It has become a viable approach in cases where the microbial population has adapted due to exposure to hydrocarbons at contaminated sites (Tyagi et al. 2010; Delille et al. 2007).

Several soil microorganisms play a crucial role in degrading PAHs in the soil as the bacterial enzymes are highly efficient in breaking resonance structures either in aerobic or anaerobic conditions (Sinha et al. 2012; Diaz 2004). For instance, the common genera that are involved in oil degradation are *Pseudomonas*, *Acinetobacter*, *Mycobacterium* and *Bacillus* and these bacteria can survive throughout the whole bio-treatment (Haritash and Kaushik 2007). However, the degradation might not be completely accomplished due to the lack of essential nutrients such as nitrogen and phosphorus for the bacteria to completely degrade the PAHs in soil. Therefore, the application of food waste as potential amendments for enhanced bioremediation by bacteria isolated from contaminated soil would be an alternative towards the greater degradation of the pollutants (Abioye et al. 2012). Additionally, the solid waste production in Malaysia was projected to face a drastic increment from about 9.0 million tons in 2000 to 10.9 million tons in 2010 and it will be about 15.6 million tons in 2020 (Agamuthu and Victor 2011). Hamid et al. (2015) states that food waste

has the highest proportion compared to other types of wastes such as plastic, paper and glass. Indirectly, the application of food waste in bioremediation projects may reduce the accumulation of food waste in the environment.

## **2 Methods**

### ***2.1 Collection of Soil Samples***

The soil samples were collected from selected locations which have been exposed to petrochemical waste containing a mixture of various PAHs. For each sampling area, around five random soil samples were collected from a layer 0–10 cm deep with the temperature and pH of the soil being measured before being stored at 4 °C. The soil samples then undergo further physiochemical analysis and isolation of potential PAH-degrading bacteria. Food wastes such as sugarcane bagasse (SB), banana skin (BS), fish bone (FB), chicken bone (CB), rotten vegetables (RV) and expired bread (EB) were collected around canteens at the Universiti Malaysia Terengganu (UMT) while diesel oil was obtained at from a commercial petrol station. The food wastes were dried at 90 °C and blended to make a powder.

### ***2.2 Enrichment of Diesel Oil-Degrading Bacteria***

Minimal salt medium (MSM) was used as an enrichment medium for the isolation of diesel oil-degrading bacteria. MSM contained (g/L): 1.0 g  $(\text{NH}_4)_2\text{SO}_4$ , 0.1 g  $\text{CaCl}_2 \cdot 2\text{H}_2\text{O}$ , 0.8 g  $\text{K}_2\text{HPO}_4$ , 0.2 g  $\text{KH}_2\text{PO}_4$ , 0.012 g  $\text{FeSO}_4 \cdot 7\text{H}_2\text{O}$ , 0.003 g  $\text{MnSO}_4 \cdot 7\text{H}_2\text{O}$ , 0.003 g  $\text{ZnSO}_4 \cdot 7\text{H}_2\text{O}$  in 1 L of distilled water (modified from Kim et al. 2005). The diesel oil-degrading bacteria were enriched in Erlenmeyer flasks containing MSM, soil sample and diesel oil. The pH of the medium was adjusted to pH 7.0. The flasks were incubated for 2 days at 30 °C in an orbital shaker at 150 rpm. The dried powdered food wastes (SB, BS, FB, CB, EB and RV) were introduced after 2 days of incubation into each of the prepared flasks separately and were then mixed thoroughly. Meanwhile, the flask labelled as C was left as the control which contained only MSM, soil sample and diesel oil (Abioye et al. 2012).

### ***2.3 Diesel Oil Extraction from Medium***

The diesel oil in the enrichment culture (EC) was extracted at every 7 days intervals for 35 days. The diesel oil extraction was determined by using the mechanical

shaking/liquid–liquid extraction procedure. Initially, the enrichment culture was suspended in hexane with a ratio of 1:1. The suspension was homogenized on the orbital shaker for 1 h at room temperature and then centrifuged for 5 min at 150 rpm. The resulting supernatant was then suspended in *n*-hexane at a 1:1 ratio of supernatant to *n*-hexane. The lower phase was released, and the supernatant was evaporated using a rotary evaporator. The extracted diesel oil extracted was stored at 4 °C for further analysis (Lau et al. 2010). Procedures for the extraction are also described in EPA, 1983 method 4181.

## 2.4 Enumeration of Diesel Oil-Degrading Bacteria

Samples from the enrichment culture (EC) were collected every 7 days for the enumeration of diesel oil-degrading bacteria. The EC samples were serially diluted, and 0.1 mL of the diluted samples was transferred to nutrient agar (NA) plates using the spread plate method. For the working stock culture of the bacteria, single colonies of diesel oil-degrading bacterial isolates were sub-cultured and preserved in MSM and NA agar slants and stored at 4 °C. For long-term storage, the diesel oil-degrading bacterial cultures were preserved in 15% (v/v) glycerol. The CFU/mL of the bacteria samples was calculated using the formula:

$$\text{Total number of bacteria} = \frac{\text{Number of Colonies}}{\text{Dilution} \times \text{Actual Volume Plated}}$$

## 2.5 Identification of the Potential Diesel Oil-Degrading Bacteria

Identification and characterization of potential diesel oil-degrading bacteria were based on macroscopic and microscopic observations. The morphology of the bacterial isolates was observed by using the gram-staining technique. The objective of this experiment was to confirm the purity of the bacterial isolates. The bacterial cultures were streaked onto NA plates and incubated overnight at 37 °C. The important features of the colony such as the shape, elevation and the pattern of the colonies were observed. Further, characterization was performed using the standard biochemical tests of the BBL Crystal Identification Kit (Jackson et al. 2004). This method was developed to allow rapid identification to a species level based upon reactions to panels of biochemical tests (Miller and Shah 1999).

## 2.6 Diesel Oil Biodegradation Using Gas Chromatography–Mass Spectrometry (GC-MS) Analysis

The diesel residue extractions were filtered using 0.45  $\mu\text{m}$  PTFE membrane filters before injecting them into the GC-MS (QP2010 ultra). This machine operated automatically and followed standardized conditions (Table 1). The temperature of the injector and detector were set at 300  $^{\circ}\text{C}$ . The volume of injected sample was 1  $\mu\text{L}$ , and the analysis of each of the sample was about 1 h per sample injection. Procedures for the degradation analysis are described in EPA, 1992 method 1663. The concentration of diesel extract was determined by comparing the peak area of diesel external standard to the peak area of the sample by using the following formula (Deng et al. 2014):

$$\text{Concentration of } C_n \text{ in sample solution} = \frac{\text{PA}}{\text{PA}'} \times \frac{\text{Final volume of standard}}{\text{Weight of analysed sample}}$$

where

PA Peak area of  $C_n$  in sample solution

**Table 1** Analysis conditions of GC-MS

GC-MS	GCMS-QP2010 ultra
<i>[GC]</i>	
Column	Rtx-5MS 0.25 $\times$ 30 m df = 0.25 $\mu\text{m}$
Inlet mode	Split less
Column oven temperature	50 $^{\circ}\text{C}$ (1 min) * 300 $^{\circ}\text{C}$ (5 min)
Carrier gas	Helium
Control mode	Constant linear velocity 35.5 cm/s
High-pressure injection	150 kPa (1.00 min)
Purge flow rate	3.0 mL/min
Injection rate	1 $\mu\text{L}$
<i>[MS]</i>	
Interface temperature	300 $^{\circ}\text{C}$
Ion surface temperature	200 $^{\circ}\text{C}$
Data sampling time	1.0 min
Measurement mode	Scan
Mass range	m/z 50–600
Event time	0.05 s

PA' Peak area of  $C_n$  in standard solution (diesel).

The degradation rate of diesel oil was calculated using the equation:

$$Rd = \frac{W0 - W5}{W0}$$

where

Rd Degradation rate of diesel oil

W0 Diesel oil hydrocarbon concentration on Week 0

W5 Diesel oil hydrocarbon concentration on Week 5.

### 3 Results and Discussion

The properties of the food wastes used in the present study are shown in Table 2. Rotten vegetables (RT) had the highest moisture content of 16.41% among the five food wastes tested. This parameter may be responsible for bio stimulating some important microorganisms that will contribute positively to the biodegradation of diesel oil in the soil. The pH of food wastes was slightly neutral in the range of pH 7.8–8.4, which may contribute to the effectiveness the bioremediation processes. All of the food wastes had an organic matter content of above 90% which is beneficial as they function as supplemental nutrients during the bioremediation process. The total carbon and nitrogen content of chicken bone (65.76% and 60.06%, respectively) and fish bone (2.33% and 2.40%, respectively) were higher than those of banana skin, rotten vegetables, sugarcane bagasse and expired bread. This parameter might promote the growth of some important microorganisms that will contribute positively to the biodegradation of diesel oil in the soil.

Phosphorus and potassium play an important role in the physiological function of the bacteria cell. Rotten vegetables had the highest phosphorus and potassium content (0.43 and 7.21%) while banana skin had 6.41% of potassium content. Chicken bone and fish bone had the highest calcium content of 14.56 and 14.46%. Meanwhile, the magnesium content was higher in rotten vegetables (0.56%). Magnesium is involved in the synthesis of bacterial protoplasm as well as cell division and could enhance the degradation rate of diesel oil. Calcium is important for the maintenance of the bacterial cell structure, sufficiently enough to enhance the degradation of the crude oil (Kumar and Gopal 2015).

**Table 2** Food waste composition analysis

Food waste/content analysis	Moisture	pH	Organic matter (%)	Total-C (%)	Total-N (%)	P (%)	K (%)	Ca (%)	Mg (%)
Banana skin (BS)	11.28	8.1	93.34	53.57	2.04	0.25	6.41	0.23	0.35
Rotten vegetables (RT)	16.41	8.2	93.15	50.38	2.17	0.43	7.21	1.40	0.56
Sugarcane bagasse (SB)	10.73	8.4	90.20	51.57	1.74	0.29	0.30	0.12	0.04
Chicken bone (CB)	5.84	7.8	99.71	65.76	2.33	0.24	0.04	14.56	0.37
Expired bread (EB)	9.41	8.4	90.74	52.33	1.82	0.27	0.15	0.22	0.04
Fish bone (FB)	7.76	8.0	98.82	60.06	2.40	0.28	0.05	14.46	0.33



### 3.1 Effect of Bacteria Growth in the Flask System Amended with Food Wastes

Figure 1 shows the viable cell count in the flask system amended with food wastes after 5 weeks of cultivation. From the graph, the average viable cell count in the enrichment cultures containing expired bread (EB), rotten vegetables (RT), chicken bone (CB) and banana skin (BS) increased slightly from 9.5 CFU/mL (log) to 12.4 CFU/mL (log) at the first 2 weeks of cultivation. However, after week 3, it decreased to 11.11 CFU/mL (log). Figure 1 shows that the average viable cell count in enrichment cultures containing fish bone (FB) and sugarcane bagasse (SB) increased from 9.5 CFU/mL (log) to 12.4 CFU/mL (log) at the first 3 weeks of cultivation. The bacteria growth remained constant until week 5. Meanwhile, the result showed that the control culture unamended with food wastes had the lowest viable cell count as compared to the other flasks amended with food wastes.

According to Fig. 1, the growth curves of the bacteria in the flask systems showed a normal growth variation which began with a lag phase, followed by log phase, stationary phase and some of the treatments ended with a death phase. During week 1, the bacteria were adapting to the environment. Then, the bacteria grew exponentially at weeks 2 and 3 because the bacteria had adapted to the environment and were able to utilize the nutrient surroundings. It can be observed that the control culture showed the lowest growth rate, suggesting that it had the lowest ability to enhance

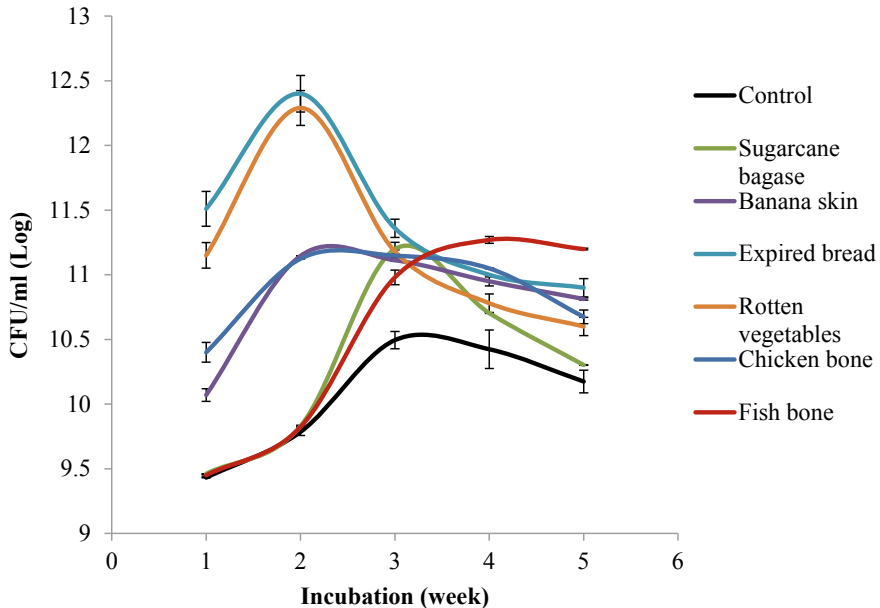


**Fig. 1** Profile of viable cell count (CFU/mL) in flask systems containing food waste and a control without food waste after 5 weeks of cultivation

the growth of bacteria in the flask system. Unlike bacteria in the enrichment cultures that contained food waste, bacteria in the control culture without food waste grew slower because there were no additional nutrients. The viable cell counts at week 4 and week 5 decreased because the bacteria were moving to the death phase where the nutrient supply was becoming limited. Table 2 shows that the nutrient enhancement provided by food waste can stimulate and increase cell growth which is in agreement with similar observations by other researches (Victor et al. 2015). The higher viable cell count in flasks amended with banana skin was due to the high nutrient content in banana skin. Studies revealed that banana skin is rich in nitrogen and macronutrients such as potassium, calcium and phosphorus which are important nutrients that can enhance the bacterial growth (Panwar 2015). The availability of nutrients, especially nitrogen and phosphorus, can significantly control microbial activities (Margesin et al. 2000), and these nutrients are necessary to enhance the biodegradation of oil pollutants. Moreover, researches also proved that chicken bone and fish bone contain high calcium and phosphorus content which can stimulate the growth of bacteria (Suchý et al. 2009; Kumar and Gopal 2015). The sugarcane bagasse and fish bone also provide additional nutrients for the bacteria to grow. Sugarcane bagasse is made up of 40% cellulose, 35% hemicellulose and 15% lignin which means that it is a carbon source for bacteria (Alves Da Costa et al. 2015). Since sugarcane bagasse had been blended into a powdered form, it can be easily utilized by the bacteria to grow. The viable cell count of all flasks amended with food waste decreased after week 3 as shown in Fig. 1. This is due to the accumulation of toxic material and exhaustion of oxygen in the medium resulting in bacterial death (Schaechter et al. 2007). In addition, similar results were also reported in previous studies where the depletion of nutrients towards the end of the experiment reduced the microbial activities and resulted in the reduction of the viable cell count (Nwogu et al. 2015).

### 3.2 Identification of Bacteria Isolated from Soil Sample

In this study, a total of 11 bacterial isolates were obtained from the soil samples and were identified by using the BBL Crystal Identical System. The isolates were grown on nutrient agar, and the physiological characteristics of the isolates are shown in Table 3. From Table 3, the results showed that 7 isolates were gram-negative bacteria, whereas 4 isolates were gram-positive bacteria. The isolates were identified, and the results are shown in Table 4. Based on Table 4, these isolates showed high confidence factors of above 0.95 to be *Acinetobacter baumannii*, *Pseudomonas aeruginosa*, *Stenotrophomonas maltophilia*, *Pseudomonas fluorescens*, *Klebsiella pneumoniae*, *Shewanella putrefaciens*, *Enterobacter aerogenes*, *Brevibacillus brevis*, *Bacillus cereus*, *Staphylococcus saprophyticus* and *Corynebacterium* sp. All of these bacterial isolates are hydrocarbon-degrading, and similar bacteria have been reported by other studies related to hydrocarbon biodegradation (Van Hamme et al. 2003; Rifaldi et al. 2006; Akpe et al. 2015). The higher occurrence of gram-negative over gram-positive bacteria in this study is in agreement with earlier reports that both

**Table 3** Physiological characteristics of isolated bacteria from enrichment culture containing food waste

Characteristic	Form	Pigmentation	Elevation	Margin	Gram Stain	Cell morphology
Isolate 1	Circular	White	Raised	Entire	–	Cocci
Isolate 2	Circular	Greenish	Raised	Irregular	–	Bacilli
Isolate 3	Circular	White	Convex		–	Bacilli
Isolate 4	Circular	Shiny white	Convex	Entire	–	Bacilli
Isolate 5	Circular	White	Raised	Irregular	–	Bacilli
Isolate 6	Circular	White	Convex	Entire	–	Bacilli
Isolate 7	Circular	Shiny white	Convex	Entire	–	Bacilli
Isolate 8	Circular	White	Flat	Undulate	+	Bacilli
Isolate 9	Circular	White	Flat	Undulate	+	Bacilli
Isolate 10	Circular	White	Raised	Entire	+	Cocci
Isolate 11	Circular	White	Flat	Undulate	+	Bacilli

**Table 4** Specimen report of BBL crystal MIND

Isolate	Bacteria species
1	<i>Acinetobacter baumannii</i>
2	<i>Pseudomonas aeruginosa</i>
3	<i>Stenotrophomonas maltophilia</i>
4	<i>Enterobacter aerogenes</i>
5	<i>Shewanella putrefaciens</i>
6	<i>Pseudomonas fluorescens</i>
7	<i>Klebsiella pneumoniae</i>
8	<i>Bacillus cereus</i>
9	<i>Brevibacillus brevis</i>
10	<i>Staphylococcus saprophyticus</i>
11	<i>Corynebacterium</i> sp.

gram-positive and gram-negative bacteria are encountered in the degradation of contaminants, but with gram-negative bacteria dominating. Our findings also correlate with the reports of previous workers (Foght and Westlake 1987; Abbasian et al. 2016) who isolated more gram-negative organisms, suggesting that they are better degraders of crude oil when compared with their gram-positive counterparts. Kaplan and Kitts (2004) reported that oil-polluted soil is often dominated with gram-negative bacteria such as *Pseudomonas* sp. and *Klebsiella* sp. that contribute to the hydrocarbon degradation process. According to a previous study (Nwinyi et al. 2014), there are some specific microorganisms that are able to degrade diesel oil such as *Arthrobacter*, *Bacillus* sp., *Corynebacterium* sp., *Klebsiella* sp., *Flavobacterium* sp. and *Nocardium*. *S. maltophilia* has been proved to degrade hydrocarbons in the

*n*-alkanes range from petroleum hydrocarbon-rich industrial wastewaters with an efficiency rate of more than 70% (Aris et al. 2014). In addition, *B. brevis* has been characterized as a petroleum hydrocarbon-degrading microbe as a previous study proved that it showed a high degradation rate of diesel of about 96.8% (Ahamed et al. 2011). Furthermore, the widely distributed soil bacterium *B. cereus* is able to adapt to a wide range of environmental conditions. Previous research also showed that *B. cereus* is a good diesel degrader as it was able to degrade approximately 80% of diesel oil after 28 days of incubation in diesel-contaminated medium (Borah and Yadav 2014). *Bacillus* sp. has been reported to be capable of utilizing phenanthrene, anthracene and pyrene as carbon sources (Fazilah et al. 2016; Amodu et al. 2016).

### 3.3 Effect of Addition of Food Waste on pH Value in Flasks System

Based on Fig. 2, the pH value showed a slight decrease starting at week 3 of cultivation because the bacteria growth had reached their decline phase. This stage was attained due to the production of acidic by-products and metabolites such as organic acid, carbon dioxide and ketones during the degradation of diesel by the bacteria. This condition facilitates the bacteria to move on to the death phase. In addition, the reduction of pH value was also caused by cell lysis as cells became old and died at the end of the study. Furthermore, the accumulation of metabolite by-products, metabolic wastes, dead bacteria and toxic materials will also cause the environment to be acidic (Darsa et al. 2014).

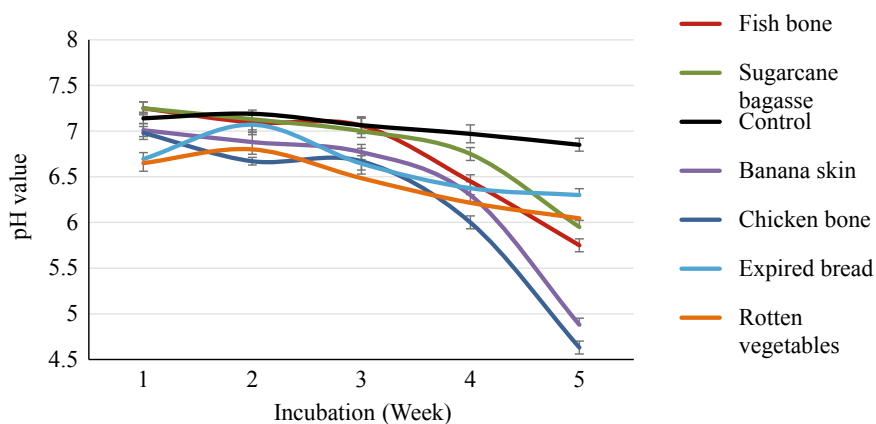


**Fig. 2** Profile of pH value in flask systems containing food wastes and a control without food waste after 5 weeks of cultivation

### 3.4 Diesel Oil Biodegradation Capacities of the Flask System

In this study, all of the bacteria isolated from the soil samples were capable of degrading diesel oil as the results showed decreasing concentrations of diesel oil compounds. This was due to the degradation process by the bacteria that utilized the diesel oil as a source of carbon and energy for growth. The degradation of selected PAHs was proven by using the GC-MS analytical method (Passarini et al. 2011). GC-MS analyses of diesel oil extracted after the incubation revealed the fraction of selected diesel components that were degraded. The gas chromatogram obtained at different retention times clearly illustrated the decrease of the selected hydrocarbon compounds in the diesel oil by Week 5. Nine components were found to be present in the enrichment cultures containing food waste which were decane, styrene, ethanol-2-butoxy, 1-ethyl-2, 3-dimethyl, benzene, 2-ethyl-1,4-dimethyl, 1,2,3,4-tetramethyl, heptasiloxane hexadecamethyl and cyclononasiloxane octadecamethyl (Fig. 3). The comparison of the degradation rate was selected from the week 0 to week 5 of the incubation period for each of the flask systems. The percentage degradation of diesel oil compounds in the samples decreased at various degradation rates, with the highest reduction in samples occurred in the cultures amended with banana skin (74.27%) followed by chicken bone (65.29%) and expired bread (62.62%). This pattern of degradation rates may be due to the high percentage of nutrients content (Table 2) and bioavailability of the nutrients to the bacterial species in the samples. This result is in agreement with previous studies on the effectiveness of food wastes

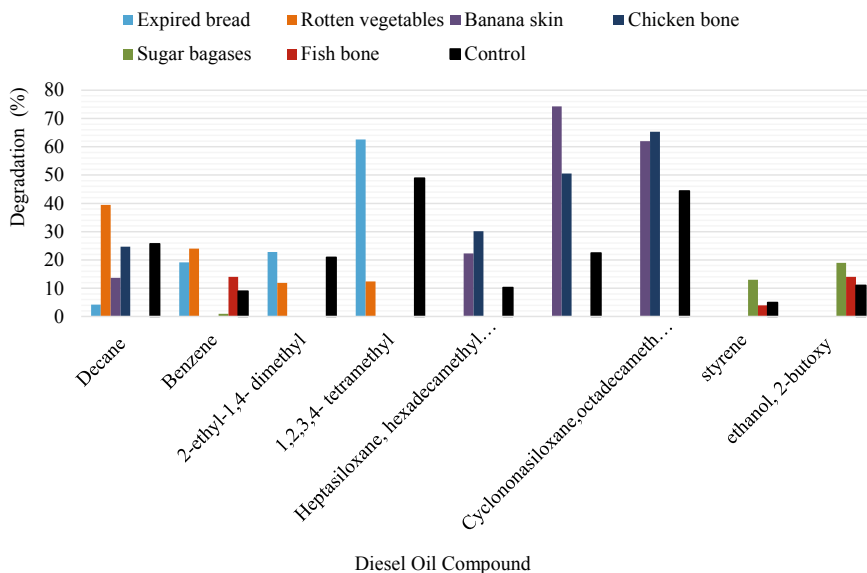


**Fig. 3** Degradation percentage (%) of the compounds in diesel oil by soil bacteria in the enrichment culture contain food waste after 5 weeks cultivation

such as banana skin in stimulating the degradation of hydrocarbons by hydrocarbon degraders (Omoni et al. 2015). Study done by Omoni et al. (2015) revealed that there was a remarkable degradation of total petroleum hydrocarbon (TPH) during the studied period in soil supplemented with banana peels with 35.67% after 14 days. Furthermore, Abioye et al., (2012) demonstrated that at the end of 28 days in soil contaminated with 15% oil, there was 24% total petroleum hydrocarbon (TPH) degradation in soil amended with banana skin. It is proved that banana skin can provide P and N to bacteria to stimulate their growth and eventually enhance the degradation process (Abioye et al. 2010).

Meanwhile, chicken bone contains high K and Ca which are vital nutrients for bacterial growth.

Bone meal contains K, Ca, Mg and O (Jeng et al. 2004), and these features make it a stable source of nutrients with enhanced activity of soil microbes.

Moreover, previous researcher also reported that the higher degradation rate in flasks amended with food wastes is believed to be due to the availability of nutrients in food wastes to the bacterial cell in the oil-polluted soil (Onuoha 2013). Liu et al. (2019) reported that also the percentage of diesel oil degradation by bone meal amendment was more than 77% during the first 28 days of treatment.

The degradation rate of all diesel oil compounds in the control flask was the lowest as shown in Fig. 3. This finding showed that food waste can enhance the biodegradation of diesel oil. From the result, the degradation rate of styrene, ethanol-2-butoxy and benzene was the lowest as compared to other compounds. This is might be due to the incomplete degradation of short-chain alkanes that are caused by limited dissolved oxygen and substrate toxicity (Hamzah et al. 2013). Furthermore, Atlas (1975) found that factors such as the temperature, viscosity of the oil and the volatility of the toxic low molecular weight hydrocarbons can affect the biodegradation process.

## 4 Conclusion

The use of food waste significantly improved the rate of diesel oil biodegradation in our shake flasks system. The results also showed that hydrocarbon-degrading bacteria were naturally present in the enrichment cultures amended with food waste. The food waste was thereby supplying not only nutrients but also enhanced the biodegradation of hydrocarbons by the bacteria. The increase in the rate of degradation percentage of diesel oil compounds was parallel with the increase in microbial count. This indicates that the food wastes provided additional nutrients such as N, P and Ca which are important components for bacterial growth. In addition, the reduction of the diesel oil components as proven by GC-MS, indicates that these bacteria are hydrocarbon degraders with the ability to degrade diesel oil. The bacterial species identified in this study can be used for bio-augmentation of hydrocarbons biodegradation processes. Therefore, instead of disposing food waste into the environment, it can be harnessed and used as enhancers of bioremediation in sites polluted with diesel oil.

## References

- Abbasian, F., Lockington, R., Megharaj, M., & Naidu, R. (2016). The biodiversity changes in the microbial population of soils contaminated with crude oil. *Current Microbiology*, 72(6), 663–670.
- Abioye, P. O., Abdul Aziz, A., & Agamuthu, P. (2010). Enhanced biodegradation of used engine oil in soil amended with organic wastes. *Water, Air, and Soil pollution*, 209(1–4), 173–179.
- Abioye, O. P., Agamuthu, P., & Abdul Aziz, A. R. (2012). Biodegradation of used motor oil in soil using organic waste amendments. *Biotechnology Research International*, 2012, 1–8.
- Agamuthu, P., & Victor, D. (2011). Policy trends of extended producer responsibility in Malaysia. *Waste Management and Research*, 29(9), 945–953.
- Ahamed, F., Hasibullah, M., Ferdouse, J., & Anwar, M. N. (2011). Microbial degradation of petroleum hydrocarbon. *Bangladesh Journal of Microbiology*, 27(1), 10–13. <https://doi.org/10.3329/bjm.v27i1.9161>.
- Akpe, R., Ekundayo, A. O., Aigere, S. P., & Okwu, G. I. (2015). Bacterial degradation of petroleum hydrocarbons in crude oil polluted soil amended with cassava peels. *American Journal of Research Communication*, 3(7), 99–118.
- Alves Da Costa, D., Lucas De Souza, C., De Oliveira, E., Saliba, S., Da, J., & Carneiro, C. (2015). By-products of sugarcane industry in ruminant nutrition. *IJAAR*, 3, 1–9.
- Amodu, O. S., Ojumu, T. V., & Ntwampe, K. O. (2016). Bioremediating silty soil contaminated by phenanthrene, pyrene, benz (a) anthracene, benzo (a) pyrene using *Bacillus* sp. and *Pseudomonas* sp.: Biosurfactant/Beta vulgaris agrowaste effects. *African Journal of Biotechnology*, 15(22), 1058–1068.
- Aris, A. Z., Ismail, T. T., Harun, R., Abdullah, A. M. & Ishak, M. Y. (2014). From sources to solution. In *Proceedings of the International Conference on Environment Forensics* (vol. 10, pp. 978–981).
- Atlas, R. M. (1975). Effects of temperature and crude oil composition on petroleum biodegradation. *Applied and Environment Microbiology*, 30(3), 396–403.
- Borah, D., & Yadav, R. N. S. (2014). Optimization of BH medium for efficient biodegradation of diesel, crude oil and used engine oil by a newly isolated *Bacillus cereus* strain DRDU1 from an automobile engine. *Biotechnology*, 13(4), 181–185.
- Darsa, K. V., Thatheyus, A. J., & Ramya, D. (2014). Biodegradation of petroleum compound using the bacterium *Bacillus subtilis*. *Science International*, 2(1), 20–25.
- Deka, H., & Lahkar, J. (2016). *Soil bacteria for polycyclic aromatic* (p. 291). *Soil and Microbes: Plant*.
- Delille, D., Coulon, F., & Pelletier, E. (2007). Long-term changes of bacterial abundance, hydrocarbon concentration and toxicity during a biostimulation treatment of oil-amended organic and mineral sub-Antarctic soils. *Polar Biology*, 30(7), 925–933.
- Deng, M. C., Li, J., Liang, F. R., Yi, M., Xu, X. M., Yuan, J. P., Peng, J., Wu, C. F., & Wang, J. H. (2014). Isolation and characterization of a novel hydrocarbon-degrading bacterium *Achromobacter* sp. HZ01 from the crude oil-contaminated seawater at the Daya Bay, southern China. *Marine Pollution Bulletin*, 83(1), 79–86.
- Diaz, E. (2004). Bacterial degradation of aromatic pollutants: A paradigm of metabolic versatility. *International Microbiology*, 7(3), 173–180.
- Fazilah, A., Darah, I., & Noraznawati, I. (2016). Bioremediation of phenanthrene by monocultures and mixed culture bacteria isolated from contaminated soil. *International Journal of Biological, Biomolecular, Agricultural, Food and Biotechnological Engineering*, 10(9), 495–498.
- Foght, J. M., & Westlake, D. W. S. (1987). Biodegradation of hydrocarbons in freshwater. In *Oil in freshwater: chemistry, biology, countermeasure technology* (pp. 217–230). Pergamon.
- Hamid, K. B. A., Ishak, M. Y., & Samah, M. A. A. (2015). Analysis of municipal solid waste generation and composition at administrative building café in Universiti Putra Malaysia: A case study. *Polish Journal of Environmental Studies*, 24(5), 1969–1982.
- Hamzah, A., Phan, C.-W., Abu Bakar, N. F., & Wong, K. K. (2013). Biodegradation of crude oil by constructed bacterial consortia and the constituent single bacteria isolated from Malaysia. *Bioremediation Journal*, 17(1), 1–10. <https://doi.org/10.1080/10889868.2012.731447>.

- Haritash, A., & Kaushik, C. (2007). Assessment of seasonal enrichment of heavy metals in respirable suspended particulate matter of a sub-urban Indian City. *Environmental Monitoring and Assessment*, 128(1–3), 411–420.
- Jackson, C. R., Fedorka-Cray, P. J., & Barrett, J. B. (2004). Use of a genus- and species-specific multiplex PCR for identification of enterococci. *Journal of Clinical Microbiology*, 42(8), 3558–3565.
- Jeng, A., Haraldsen, T., & Vagstad, N. (2004). Meat and bone meal as nitrogen fertilizer to cereals in Norway. *Agricultural and Food Science*, 13(3), 268–275.
- Kaplan, C. W., & Kitts, C. L. (2004). Bacterial succession in a petroleum land treatment unit. *Applied and Environment Microbiology*, 70(3), 1777–1786.
- Keshavarzifard, M., Zakaria, M. P., Tan, H. W., Ferdiusus M. Y., Mustafa, S., Vaezzadeh, V., et al. (2014). Baseline distributions and sources of Polycyclic Aromatic Hydrocarbons. *Marine Pollution Bulletin*, 88, 366–372.
- Kim, Y.-H., Freeman, J. P., Moody, J. D., Engesser, K.-H., & Cerniglia, C. E. (2005). Effects of pH on the degradation of phenanthrene and pyrene by *Mycobacterium vanbaalenii* PYR-1. *Applied Microbiology and Biotechnology*, 67(2), 275–285.
- Kumar, B. L., & Gopal, D. S. (2015). Effective role of indigenous microorganisms for sustainable environment. *Biotech*, 5(6), 867–876.
- Lau, E. V., Gan, S., & Ng, H. K. (2010). Extraction technique for polycyclic aromatic hydrocarbon in soil review article. *International Journal of Analytical Chemistry*, 1–9.
- Liu, X., Selonen, V., Steffen, K., Surakka, M., Rantalainen, A. L., Romantschuk, M., et al. (2019). Meat and bone meal as a novel biostimulation agent in hydrocarbon contaminated soils. *Chemosphere*, 225, 574–578.
- Margesin, R., Zimmerbauer, A., & Schinner, F. (2000). Monitoring of bioremediation by soil biological activities. *Chemosphere*, 40(4), 339–346.
- Miller, J. H., & Shah, S. (1999). Identification of clinically isolated vancomycin-resistant Enterococci: Comparison of API and BBL Crystal systems. *Journal of Medical Microbiology*, 48(7), 695–696.
- Nwinyi, O. C., Kanu, I. A., Tunde, A., & Ajanaku, K. O. (2014). Characterization of diesel degrading bacterial species from contaminated tropical ecosystem. *Brazilian Archives of Biology and Technology*, 57(5), 789–796.
- Nwogu, T. P., Azubuikwe, C. C., & Ogugbue, C. J. (2015). Enhanced bioremediation of soil artificially contaminated with petroleum hydrocarbons after amendment with *Capra aegagrus hircus* (Goat) Manure. *Biotechnology Research International*, 2015, 657349. <https://doi.org/10.1155/2015/657349>.
- Omoni, V. T., Aguoru, C. U., Edoh, E. O., & Makinde, O. (2015). Biostimulation of hydrocarbon utilizing bacteria in soil contaminated with spent engine oil using banana and plantain agrowastes. *Journal of soil science and environmental management*, 6(8), 225–233. <https://doi.org/10.5897/JSEM15.0505>.
- Onuoha, S. C. (2013). Stimulated biodegradation of spent lubricating motor oil in soil amended with animal droppings. *Journal of Natural Sciences Research*, 3(12), 106–116.
- Panwar, N. (2015). Studies on physicochemical characteristics and fertility of soil by addition of banana peels—Waste Management. *IJSRD—International Journal for Scientific Research and Development*, 3(1), 2321–2613.
- Passarini, M. R., Rodrigues, M. V., da Silva, M., & Sette, L. D. (2011). Marine-derived filamentous fungi and their potential application for polycyclic aromatic hydrocarbon bioremediation. *Marine Pollution Bulletin*, 62(2), 364–370.
- Ravindra, K. S. (2008). Atmospheric polycyclic aromatic: Source attribution, emission factors and regulation. *Atmospheric Environment*, 42(13), 2895–2921.
- Riffaldi, R., Levi-Minzi, R., Cardelli, R., Palumbo, S., & Saviozzi, A. (2006). Soil biological activities in monitoring the bioremediation of diesel oil-contaminated soil. *Water, air, and soil pollution*, 170(1–4), 3–15.



- Schaechter, M., Engleberg, C., DiRita, V. J., & Dermody, T. (2007). Schaechter's mechanisms of microbial disease. In W. Lippincott Williams, I. Sherameti, & A. Varma (Eds.), *Soil heavy metals*. Berlin: Springer.
- Sinha, S., Chattopadhyay, P., & Ken, S. K. (2012). Microbial degradation of xenobiotics. *Environmental Science and Engineering*, 3, 395–410.
- Suchý, P., Straková, E., Herzig, I., Steinhäuser, L., Králik, G., & Zapletal, D. (2009). Chemical composition of bone tissue in broiler chickens intended for slaughter. *Czech Journal of Animal Science*, 54(547), 324–330.
- Tyagi, M. D. F., Manuela, M. R., Carvalho, & Carla C. C. R. (2010). Bioaugmentation and biostimulation strategies to improve the effectiveness of bioremediation processes. *Biodegradation*, 22(2), 231–241.
- U.S. Environmental Protection Agency (EPA). (1983). *Method 4181—Chemical analyses of water and wastes*, Washington DC.
- U.S. Environmental Protection Agency (EPA). (1992). *Method 1663—Differentiation of diesel and crude oil by GC/FID*, Washington DC.
- Van Hamme, J. D., Singh, A., & Ward, O. P. (2003). Recent advances in petroleum microbiology. *Microbiology and Molecular Biology Reviews*, 67(4), 503–549.

# Model Optimization Using Artificial Intelligence Algorithms for Biological Food Waste Degradation



Norazwina Zainol, Abdul Sahli Fakharudin, and Nor Ilyya Syahira Zulaidi

**Abstract** Food waste is categorized as the largest degradable component in the waste stream. Degradation of food waste that involved aerobic bacteria is the most suitable approach to dispose of this waste. The main objective of this research is to evaluate the optimum condition of aerobic bacteria growth for food waste degradation by comparing the implementation of response surface method (RSM) and genetic algorithm. Preliminary experiment is conducted to determine the best time for aerobic bacteria growth. Then, evaluation of five factors such as temperature, time, type of nutrient, agitation rate and inoculum size is done by conducting experiments according to the experimental table that is constructed by using design expert software. Growth of aerobic bacteria can be determined by measuring the optical density (OD) of the bacteria. Aerobic bacteria at the best growth condition are mixed with the food waste for degradation process. The ability of aerobic bacteria to degrade food waste is determined by monitoring the pH, moisture content and ratio of volatile solid to total solid (VS/TS) of food waste on the first and twentieth days of degradation. The result analysis using RSM showed that the optimum condition for aerobic bacteria growth is at 37 °C and 200 rpm in commercial nutritional supplement (CNS) medium with 10% (v/v) of inoculum size for 20 h. At this optimum condition, the OD value was 2.264 while optimization using genetic algorithm generated the OD value at 2.643 where this is 14% improvement from the RSM.

**Keywords** Genetic algorithm · Response surface method · Optimization · Food waste degradation

---

N. Zainol  
CARIFF, Universiti Malaysia Pahang, 26300 Gambang, Pahang, Malaysia

A. S. Fakharudin (✉)  
Faculty of Computing, Universiti Malaysia Pahang, 26300 Gambang, Pahang, Malaysia  
e-mail: [sahli@ump.edu.my](mailto:sahli@ump.edu.my)

N. I. S. Zulaidi  
College of Engineering, Universiti Malaysia Pahang, 26300 Gambang, Pahang, Malaysia

## 1 Introduction

In recent years in Malaysia, environmental issues keep rising due to the increasing amount of food waste. Statistics from the Solid Waste Corporation of Malaysia (SWCorp) showed that in 2015, the food waste in Malaysia reached 15,000 tonnes daily (Komandai 2017). Degradation of food waste by using aerobic bacteria is one of the most promising approaches to manage food waste as this waste contains high organic matters which are easily biodegradable. Food waste can also be degraded under anaerobic condition but the process is slow and less efficient compared to the aerobic condition (Gill et al. 2014).

Tortora et al. (2016) stated that aerobic bacteria grow at its best at pH near neutral which is between 6.5 and 7.5. According to Haug (2018), aerobic bacteria required adequate amounts of oxygen to grow and degrade food waste. Oxygen should be well supplied during the degradation process to reduce the reaction time between food waste and aerobic bacteria. Other than that, moisture content is one of the factors that must be considered for food waste degradation. Excess amount of moisture in food waste is not good for degradation process because it can slow the process (Hamid et al. 2019). On the other hand, carbon-to-nitrogen ratio is also important in degradation process because it shows the quality of biofertilizer. Lin et al. (2019) stated that the degradation may be more effective when C/N ratio is between 30 and 40%. Other factors such as temperature, time, type of nutrients, agitation rate and inoculum size are also crucial for bacteria growth. Most of the previous studies did not focus on those five factors. Therefore, this study focused on those five affecting factors to aerobic bacteria growth for food waste degradation. Hence, the main objective of this research is to optimize the growth of aerobic bacteria for food waste degradation.

The modelling and optimization process done by (Dhanarajan et al. 2014) for production of marine bacterial lipopeptide from food waste had used artificial neural network (ANN) to model the production process, and particle swarm had been used to optimize the production output. The selected feedforward network architecture was 4-17-1 and the model training error of 0.000124 mean square error (MSE). The optimization of production output had used the particle swarm optimization produced a significant enhancement of lipopeptide production from waste by about 46% (w/v).

The modelling and optimization of anaerobic codigestion of potato waste and aquatic weed by response surface methodology and genetic algorithm by Jacob and Banerjee (2016) had produced higher methane yield around 6% improvement by the ANN-GA method when compared with the CCD-RSM method. The ANN topology for modelling had used 3-12-1 architecture and used Levenberg–Marquardt training algorithm to train the network. The MSE for ANN modelling with architecture of 3-12-1 was 0.14 while other ANN architectures produced higher modelling MSE compared to the 3-12-1 architecture. Genetic algorithm (GA) was also being used to determine the maximum biogas yield output from several ANN models which used back-propagation training, particle swarm optimization and evolutionary neural networks (Fakharudin et al. 2013).

## **2 Process Description of Optimization Using Response Surface Method**

### ***2.1 Materials***

The sample of food waste was collected from several cafeterias at Universiti Malaysia Pahang in Gambang, Pahang. Aerobic bacteria were purchased from Universiti Malaya, Kuala Lumpur. Nutrient broth, nutrient agar and sodium chloride (NaCl) were obtained from Sigma-Aldrich. Commercial nutritional supplement (CNS) was purchased from a local grocery shop.

### ***2.2 Preparation for Aerobic Bacteria Growth***

Aerobic bacteria were cultured on nutrient agar medium. Nutrient agar was prepared by dissolving 23 g of nutrient agar medium in 1000 ml distilled water. Then, the agar on agar plate was cooled and toughened in the refrigerator overnight. Saline solution was prepared by dissolving NaCl distilled water to produce NaCl solution with 0.85% concentration. NaCl is able to enhance bacteria growth and prevent cell damage. 0.5 g of aerobic bacteria was mixed with 10 ml of NaCl (Zhang et al. 2019). 0.1 ml of bacteria samples was spread evenly on the surface of agar by using triangle shape cell spreader. Aerobic bacteria were spread from the first quadrant until quadrant number 4 of agar before incubating it at 37 °C for 24 h. Aerobic bacteria on the agar were streaked by using inoculation loop and transferred to nutrient broth in conical flask. Then, the samples of bacteria in nutrient broth were incubated at 37 °C and 100 rpm for 24 h (Smarajit and Kenney 2018).

### ***2.3 Preliminary Experiment***

Preliminary experiment was conducted in order to determine the best time for aerobic bacteria growth. Nutrient broth was used as a growth medium of bacteria. Then, all samples were incubated at 37 °C and 100 rpm in stackable incubator shaker (Smarajit and Kenney 2018). Every two hours, Varian Spectrophotometer was used to determine optical density for each sample.

## 2.4 Experimental Set-up for Response Surface Method (RSM)

There were five selected factors that were studied in this research in order to optimize the OD value of aerobic bacteria sample. The factors were temperature, time, type of nutrient, agitation rate and inoculum size. Tables 1 and 2 show the design factors and levels were coded as  $-1$  (low level) and  $+1$  (high level) where low level indicates the lowest range of the factors and high level indicates the highest range of the factors. 16 runs of experiments were conducted in this study (Dzulkefli and Zainol 2018). The responses (optical density) of the experimental design were analyzed by using ANOVA based on the  $p$ -value with 95% of confidence level.

**Table 1** Information on selected factors

Factors	Level	
	$-1$	$+1$
Temperature ( $^{\circ}\text{C}$ )	Ambient	37
Time (h)	20	30
Type of nutrient	Nutrient broth	CNS
Agitation rate (rpm)	0	200
Inoculum size (% v/v)	10	20

**Table 2** Experimental design for RSM

Std	Factor 1	Factor 2	Factor 3	Factor 4	Factor 5	Response optical density (ABS)
1	$-1$	$+1$	$-1$	$-1$	$-1$	0.9295
2	$+1$	$-1$	$+1$	$+1$	$-1$	1.6902
3	$-1$	$+1$	$+1$	$-1$	$+1$	0.9914
4	$+1$	$+1$	$+1$	$+1$	$+1$	1.6457
5	$-1$	$+1$	$-1$	$+1$	$+1$	0.5115
6	$+1$	$+1$	$-1$	$+1$	$-1$	1.7866
7	$+1$	$-1$	$+1$	$-1$	$+1$	0.0673
8	$-1$	$-1$	$-1$	$-1$	$+1$	0.4252
9	$-1$	$-1$	$+1$	$-1$	$-1$	2.2994
10	$-1$	$+1$	$+1$	$+1$	$-1$	2.0610
11	$-1$	$-1$	$-1$	$+1$	$-1$	2.3488
12	$-1$	$-1$	$+1$	$+1$	$+1$	2.0461
13	$+1$	$+1$	$-1$	$-1$	$+1$	0.6873
14	$+1$	$-1$	$-1$	$-1$	$-1$	1.7078
15	$+1$	$+1$	$+1$	$-1$	$-1$	0.9649
16	$+1$	$-1$	$-1$	$+1$	$+1$	1.1496

## 2.5 *Sample Analysis*

The bacteria concentration in suspension was determined in terms of optical density by using Varian Spectrophotometer. Each sample was inserted into cuvette before locating it in sample holder. The wavelength of the spectrophotometer was set to 600 nm in order to get the absorbance from the samples. The optical density was expressed in absorbance unit (ABS) which is a dimensionless unit.

## 3 Genetic Algorithm Optimization Methodology

### 3.1 *Process Optimization Using Artificial Intelligence Techniques*

The model had used basic architecture of five input nodes for all five factors and one output node for the optical density. Only the output node used linear activation function while the hidden node used hyperbolic tangent activation function. Levenberg–Marquardt (LM) training algorithm was used to train the ANN model starting from the smallest number (2 hidden nodes) and will be increased until a significant ANN model can be generated through the training process. Only LM training algorithm was used because of the fast convergence and less epoch compared to other algorithm, and only this model was used for the optimization process. The training process will be stopped when the training error reaches 0.01. The implementation of the ANN modelling had used the ENCOG 3.3.0 (Heaton 2018) Java library with NetBeans 8.0.2 which was used to the development of IDE.

The data set was divided into 80:20 percent ratio—with 12 random samples of the data set were used as training and 4 samples were used as testing set. The data set was normalized between  $-1$  to  $1$  which followed the hyperbolic activation function range. The network performance will be measured using mean square error (MSE), and one model was selected to be optimized using the GA search. The generated ANN model architecture was 5-4-1 with 4 hidden nodes. The model training MSE was  $1.0881 \times 10^{-5}$ , and testing MSE was 0.1920. The model overall MSE was 0.0480.

### 3.2 *Genetic Algorithm Optimization Process*

The optimization of the neural network output was implemented using Jenetics 3.6.0 (Wilhelmstötter 2018) a Java library for genetic algorithm, evolutionary algorithm and genetic programming. A preliminary run was conducted to find the optimal parameter for crossover and mutation operators. The final value for the crossover probability was set to 0.1, and mutation probability was set to a small value of 0.01

**Table 3** Criteria for validation experiment

Criteria	Goal	Value
Temperature	Is in range	Ambient and 37 °C
Time	Is in range	20 and 30 h
Type of nutrient	Is in range	Nutrient broth and CNS
Agitation rate	Is in range	0 and 150–200 rpm
Inoculum size	Is in range	10 and 20% v/v
OD	Maximize	–

**Table 4** Suggested optimum condition for maximum OD value

Factors	Condition
Temperature (°C)	37
Time (h)	20
Type of nutrient	CNS
Agitation rate (rpm)	200
Inoculum size (% v/v)	10
Predicted OD (ABS)	2.264

based on the preliminary run which produced higher OD. The population size was set to 30 chromosomes with 100 generations for all the runs. The optimization run was also set to 10 runs, and the best (lowest) was selected as the optimized value. In this process, the generated model was used as the fitness function and the boundary followed the normalized range of  $-1$  to  $1$ .

## 4 Results and Discussion

### 4.1 Optimization by Response Surface Method

The criteria set-up to select optimum processing condition was given in Table 3. The suggested optimum condition is given in Table 4 and can be applied in the aerobic bacteria growth to be used for food waste degradation.

### 4.2 Optimization by Genetic Algorithm

The optimization results using the heuristic search of genetic algorithm are shown in Table 5. The neural network model was used as the fitness function for the genetic algorithm, and it searched for the maximum neural network output. The highest run was by run number 8 with the OD of 1.2578, and the lowest output was by run

**Table 5** GA optimization results

Run	Factor 1	Factor 2	Factor 3	Factor 4	Factor 5	OD (ABS)
1	0.9057	-0.9922	0.9258	-0.8945	-0.5432	1.2574
2	0.8911	-0.9316	0.9117	-0.9887	0.6078	1.2502
3	0.9857	-0.6274	0.9171	-0.8066	-0.6613	1.2489
4	0.8041	-0.9214	0.9344	-0.9588	0.5068	1.2298
5	0.8834	-0.8584	0.9962	-0.9908	-0.5517	1.2460
6	0.8048	-0.9425	0.9182	-0.9889	-0.3520	1.2310
7	0.9755	-0.8882	0.6854	-0.7930	0.1892	1.2454
8	0.9221	-0.9756	0.9592	-0.7313	-0.0514	1.2578
9	0.9298	-0.7521	0.6791	-0.9263	0.9449	1.2270
10	0.8363	-0.9706	0.7915	-0.6255	-0.8034	1.2238

number 10 with OD of 1.2238. Overall the OD optimization by GA has shown stable output with OD around 1.2.

The value in Table 4 was in normalized value and to get the actual value which can be compared with the response surface optimization the process of denormalized had been applied to the result. The best result which was the run number 8 had been denormalized and the actual value is shown in Table 6. For factors 1, 2, 3, the values were denormalized to the nearest condition but for factors 4 and 5, the values were denormalized using actual numbers. Table 7 shows the comparison of

**Table 6** Suggested optimum condition from GA

Factors	Condition
Temperature (°C)	37
Time (h)	20
Type of nutrient	CNS
Agitation rate (rpm)	26
Inoculum size (% v/v)	14
Predicted OD (ABS)	2.643

**Table 7** Comparison of optimum condition between GA and RSM model

Factors	Condition from RSM	Condition from GA
Temperature (°C)	37	37
Time (h)	20	20
Type of nutrient	CNS	CNS
Agitation rate (rpm)	200	26
Inoculum size (% v/v)	10	14
Predicted OD (ABS)	2.264	2.643



optimum conditions from RSM and GA for maximum OD value. The condition for temperature, reaction time and type of nutrient were the same from both optimization models. However, GA suggested a lower value of agitation at only 26 rpm compared to 200 rpm suggested by RSM. In terms of OD value, optimization using GA model yielded a value of 2.643, which is an improvement of 14% compared to the value yielded using RSM.

## 5 Conclusions

The optimization of OD using genetic algorithm yielded a value of 2.643 compared to 2.264 from RSM. This shows 14% improvement in OD value compared to RSM. The application of machine learning by using ANN and heuristic search of GA had produced improved OD.

**Acknowledgements** The authors wish to acknowledge the Universiti Malaysia Pahang for funding the project under grant RDU1803119 and RDU1703295.

## References

- Dhanarajan, G., Mandal, M., & Sen, R. (2014). A combined artificial neural network modeling–particle swarm optimization strategy for improved production of marine bacterial lipopeptide from food waste. *Biochemical Engineering Journal*, *84*, 59–65. <https://doi.org/10.1016/J.BEJ.2014.01.002>.
- Dzulkefli, N. A., & Zainol, N. (2018). Data on modeling mycelium growth in *Pleurotus sp.* cultivation by using agricultural wastes via two level factorial analysis. *Data in Brief*, *20*, 1710–1720. <https://doi.org/10.1016/j.dib.2018.09.008>.
- Fakharudin, A. S., Sulaiman, M. N., Salihon, J., & Zainol, N. (2013). Implementing artificial neural networks and genetic algorithms to solve modeling and optimization of biogas production. In *Proceedings of the 4th International Conference on Computing and Informatics, ICOCI 2013* (pp. 121–126), Sarawak, Malaysia. Universiti Utara Malaysia, August 28–30, 2013.
- Gill, S. S., Jana, A., & Shrivastav, A. (2014). Aerobic bacterial degradation of kitchen waste: A review. *Journal of Microbiology, Biotechnology and Food Sciences*, *3*(6), 477–483.
- Hamid, B., Jehangir, A., Baba, Z. A., & Fatima, S. (2019). Isolation and characterization of cold active bacterial species from municipal solid waste landfill site. *Research Journal of Environmental Sciences*, *13*, 1–9.
- Haug, R. (2018). *The practical handbook of compost engineering eBook*. New York: Routledge. <https://doi.org/10.1201/9780203736234>.
- Heaton, J. (2018). *Encog machine learning framework*. Retrieved May 15, 2018, from <https://github.com/encog/encog-java-core>.
- Jacob, S., & Banerjee, R. (2016). Modeling and optimization of anaerobic codigestion of potato waste and aquatic weed by response surface methodology and artificial neural network coupled genetic algorithm. *Bioresour Technol*, *214*, 386–395. <https://doi.org/10.1016/J.BIORTECH.2016.04.068>.

- Komandai, N. (2017). *Free Malaysia Today Corporation*. Retrieved from Free Malaysia Today Web site: <http://www.freemalaysiatoday.com/category/opinion/2017/08/29/food-wastage-management-crucial-for-a-better-environment/>.
- Lin, L., Xu, F., Ge, X., & Li, Y. (2019). Biological treatment of organic materials for energy and nutrients production—Anaerobic digestion and composting. In *Advances in Bioenergy* (Vol. 4, pp. 121–181). <https://doi.org/10.1016/bs.aibe.2019.04.002>.
- Smarajit, C., & Kenney, L. J. (2018). A new role of OmpR in acid and osmotic stress in *Salmonella* and *E. coli*. *Frontiers in Microbiology*, 9, 2656. <https://doi.org/10.3389/fmicb.2018.02656>.
- Tortora, G., Funke, B., & Case, C. (2016). *Microbiology: An Introduction* (12th ed.). San Fransisco: Pearson Benjamin Cummings.
- Wilhelmstötter, F. (2018). Jenetics. Retrieved May 15, 2018, from <http://jenetics.io/>.
- Zhang, F., Wang, X., Lu, W., Li, F., & Ma, C. (2019). Improved quality of corn silage when combining cellulose-decomposing bacteria and lactobacillus buchneri during silage fermentation. *BioMed Research International*, 1–11. <https://doi.org/10.1155/2019/4361358>.

# Anaerobic Digestion of Food Waste: The Effect of *Candida rugosa* Lipase Amount on the Digestive Activity



Mariani Rajin, Abu Zahrim Yaser, Sariah Saalah, Yogananthini Jagadeson, Siti Nazihah Ibrahim, and Muhammad Syah Azhar Mislahani

**Abstract** The large amount of food waste generated becomes one of the problems to the environment. Anaerobic digestion of food waste has been identified as an alternative to overcome this problem. The main constraint for the anaerobic digestion is the relatively slow hydrolysis of the substrate. Enzyme addition has been reporting to be applied in enhancing the hydrolysis. Therefore, in this work, *Candida rugosa* lipase is added to the system to facilitate the anaerobic digestion. The anaerobic digestion is conducted for 40 day, using 15 and 30 mg of lipase. The effect of lipase amount on the digestate has been studied. It was found that the *Candida rugosa* lipase added did not improve the moisture content achieved at the end of the digestion process. The samples with lipase obtained lower pH as compared to the control. Both lipase amount of 15 and 30 mg achieved identical pH value of 4.3. The samples with 30 mg of lipase have higher electrical conductivity values as compared to those with 15 mg lipase and control sample on day 30. At the end of the digestion process, the reduction of total organic carbon in the samples with 30 mg of lipase is higher in comparison with 15 mg and control samples. The organic matter loss achieved with 30 mg of lipase is found to be 30.2%. Food waste with higher concentration of lipase shows better degradation.

**Keywords** Anaerobic digestion · Enzyme · *Candida rugosa* lipase · Physiochemical properties

## 1 Introduction

Food waste which consists of both precooked and leftover is a biodegradable waste discarded from various sources including factories, kitchen scraps, food not sold in shops or restaurants, and plate waste. The amount of food waste is increasing due to the economic and growth of population in the world (Paritosh et al. 2017). It has been reported that from year 2005 to 2025, the urban food waste production could

---

M. Rajin (✉) · A. Z. Yaser · S. Saalah · Y. Jagadeson · S. N. Ibrahim · M. S. A. Mislahani  
Chemical Engineering Programme, Faculty of Engineering, Universiti Malaysia Sabah, Kota  
Kinabalu, Sabah, Malaysia  
e-mail: [mariani@ums.edu.my](mailto:mariani@ums.edu.my)

increase by 44% which is from 278 to 416 million tons per year in Asian countries (Melikoglu et al. 2013). There are around 1.4 billion ha of rich land which is 28% of the world's cultivated area is used per year to dispose food waste (Paritosh et al. 2017).

A proper management of food waste is crucial as it may lead to many environmental problems. Untreated food waste may cause contamination of soil, water, and air during its collection, transportation, and storage due to its easy decomposition (Xiao et al. 2018). There are several ways that can be used to manage the huge number of food waste generated every year, which are by landfills, incinerators, and anaerobic digestion (Paritosh et al. 2017). In Malaysia, open dumping and sanitary landfill are major methods for waste disposal. However, it is proven that the land-filling of biodegradable food waste is contributed to environmental problem due to the production of highly polluting leachate and methane gas (Tweib et al. 2011). On the other hand, food waste treatment by using incineration can cause the release of dioxins (Paritosh et al. 2017). Thus, anaerobic digestion has been considered as an attractive alternative to overcome these limitations.

Anaerobic digestion involved degradation process of organic matter by microbial in absence of oxygen. This technology is cost-effective and more environmental friendly. Furthermore, it is able to produce renewable energy such as biogas and reclaim nutrient rich fertilizer (Morales-Polo et al. 2018). Anaerobic digestion has been widely applied in waste management of organic waste including food waste (Yaser 2014; Rajin 2018).

There are four sequential stages in anaerobic digestion, namely hydrolysis, acidogenesis, acetogenesis, and methanogenesis. Among these stages, the hydrolysis has been identified as a bottleneck that can restrict the production of methane (Rajin 2018). During enzymatic hydrolysis, complex polymers are transformed into soluble monomers by extracellular microbial enzymes. It has been reported that the hydrolysis of carbohydrates, lipids, and proteins rich substrate is relatively slow thus becomes the rate limiting for anaerobic digestion process (Krishna and Kalamdhad 2014). Therefore, increasing the hydrolysis rate is crucial to improve the efficiency of the anaerobic digestion.

The addition of enzyme into the system is among the method that is suggested to accelerate the hydrolysis reaction (Pascale et al. 2019). Commercial enzymes including lipases have been used to improve hydrolysis of food waste. Various types of lipase have been identified as suitable to be used in food waste substrate. From the previous research, it was found that *Candida antarctica* lipase B has improved the moisture content and total organic carbon of the food waste digestate but has no effect on the pH and electrical conductivity (Rajin et al. 2020). However, the justification on the lipase performance is limited as the data is only based on single amount of lipase.

Lipase from *Candida rugosa*, known as hydrolase-based biocatalysis, has shown an enormous potential for biotechnological applications (Domínguez De María et al. 2006). As a lipase, it is suitable to assist the anaerobic digestion process for food waste which is rich in fats and carbohydrates. In previous report, it was shown that the pre-treatment using *Candida rugosa* lipase enhanced the hydrolysis and methane

production rate (Domingues et al. 2015; Meng et al. 2017). However, most of the previous work focused on the effect of lipase addition on then biogas production. Therefore, this research is conducted to further investigate the effect of lipase amount on the digestive activity and physicochemical properties of the food waste digestate.

## 2 Materials and Methods

### 2.1 Preparation of Substrate and Inoculum

The food waste was collected from cafeteria in Faculty of Engineering, Universiti Malaysia Sabah, Kota Kinabalu, Sabah. The food waste consists of leftover rice, noodles, bread, fruits, meat-based waste, chicken fat, and rotten part of vegetables. Inoculum was prepared through 50 days anaerobic digestion of food waste. The commercial enzyme used is *Candida rugosa* lipase (CRL) from Sigma-Aldrich Co. (Poland).

### 2.2 Anaerobic Digestion of Food Waste

The anaerobic digestion process was carried out by feeding 350 g of food waste into a 500 mL bottle as a batch reactor. Two different amounts of *Candida rugosa* lipase (CRL) were added into the reactors: 15 mg lipase/100 g of food waste and 30 mg lipase/100 g of food waste. Control reactors without lipase were also prepared. All reactors were sealed for 40 days. For each consecutive ten days, the sample of food waste digestate was collected for physicochemical analysis. All experiments were done in duplicates.

### 2.3 Physicochemical Analysis of Food Waste Digestate

The food waste samples for days 0, 10, 20, 30, and 40 were analyzed for moisture content, pH, conductivity, and total organic carbon (TOC). All analysis methods and calculation were adapted from Yaser et al. (2008).

#### 2.3.1 Moisture Content

The moisture content was determined as the loss in weight in an oven at 105 °C for 24 h. The mass of the sample on initial and final was recorded. The moisture content of the sample was calculated by using Eq. 1:

$$\text{Moisture Content} = \frac{\text{Initial Mass} - \text{Final Mass}}{\text{Initial Mass}} \times 100\% \quad (1)$$

### 2.3.2 pH and Conductivity

The pH and conductivity of food waste were measured at day 0, 10, 20, 30, and 40 for each ten days. 5 g of the food waste sample was dried in oven at 105 °C for 24 h. The dried samples were mixed with 50 ml of distilled water, stirred at 130 rpm for 24 h. The solution was then filtered to remove impurities and then analyzed by using pH meter and conductivity meter (HI 9811-5).

### 2.3.3 Total Organic Carbon (TOC)

The food waste sample was dried in the oven at 105 °C for 24 h. The dried samples were burned in the furnace at 550 °C for 4 h. The organic matter was determined as volatile solid. The percentage of ash and TOC was determined by using Eqs. 2 and 3, respectively.

$$\text{Ash Percentage} = \frac{\text{Weight crucible and sample after burning} - \text{Weight crucible}}{\text{Weight sample}} \times 100\% \quad (2)$$

and

$$\text{TOC} = \frac{\text{Ash Percentage}}{1.8} \quad (3)$$

## 3 Results and Discussions

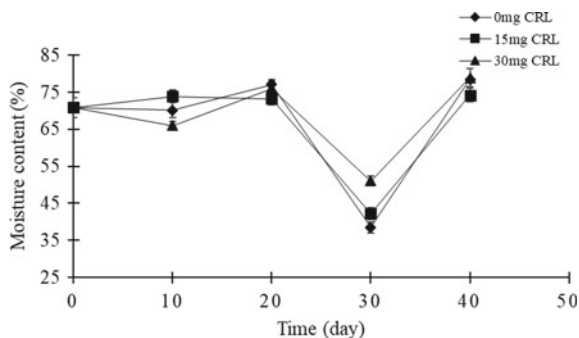
### 3.1 Effect of the Lipase Amount on Moisture Content

Figure 1 shows the effect of enzyme amount on the moisture content of the food waste digestate during the anaerobic digestion process.

Based on the moisture content profile in Fig. 1, similar trend is observed for all samples regardless the amount of the lipase added. The amount of lipase did not have significant effect on the moisture content of the food waste except for day 30 where the moisture content for samples with 30 and 15 mg of lipase is decreased as compared to the control.

The moisture content slightly increased for the first 20 days then reduced at day 30. The reduction of moisture content within day 20 and day 30 could be due to the

**Fig. 1** Moisture content profile of the food waste digestate



increase in temperature as anaerobic digestion is exothermic process. The soluble substrates are degraded easily during thermophilic phase. At this phase, the heat tolerant microorganism has hydrolyzed the complex substrate (Manu et al. 2017).

The increases in moisture content can be observed from day 30 to day 40 for all samples. The anaerobic digestion in the present work is conducted in a closed system. The evaporated and condensed water on the lid and reactor's wall were fell back in the mixture thus increase the moisture level in the system (Anjeena et al. 2017).

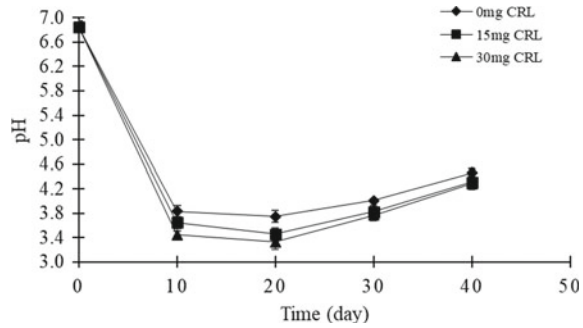
It was found that the average moisture contents of food waste digestate with all three different amounts of lipase were unstable throughout the anaerobic digestion process. This result was similar to previous study by Anjeena et al. (2017) and Narkhede et al. (2010). The unsteady moisture content is due to the fluctuating of microbial population. Moisture content is important to facilitate the movement and transport of the nutrient for the utilization of microorganisms (Ishak et al. 2014 and Manu et al. 2017). The optimum moisture content also enhances the growth of the microbes and consequently increases the biodegradation rate. However, it is difficult to maintain the same availability of water throughout the digestion cycle.

From the previous finding, it was found that the suggested moisture content is within 60–80% for highest methane production (Bouallagui et al. 2003). Meanwhile, Tanimu et al. (2014) claimed that moisture content of 95–97% is ideal for anaerobic digestion. The final moisture content obtained at the end of the anaerobic digestion process in the present work is 70.2–79.3%, within the range of the suggested moisture content suitable for anaerobic digestion, indicating that food waste is an easily biodegradable organic substrate.

### 3.2 Effect of the Lipase Amount on pH

One of the important parameter in anaerobic digestion is pH. The hydrogen ion concentration during anaerobic digestion changes the pH of the system (Ajay et al. 2011). Figure 2 shows the pH profile of the food waste digestate for 40 days. Based

**Fig. 2** pH profile of the food waste digestate



on Fig. 2, the initial pH value for all samples is found to be 6.8 which is approaching neutral phase. A sharp drop in the pH values was observed on day 10 for all samples. The reduction in the pH values throughout the process is due to the formation of organic acids such as acetic acid and butyric acid produced by the microorganisms (Yang et al. 2013).

From day 10 to day 40, all samples show a slightly increase in the pH. In this stage, the decomposition of nitrogen-containing organic matter is taking place. Alkaline  $\text{NH}_4^+$  is formed as the result of the accumulation of  $\text{NH}_3$  which dissolved in moisture. There are also possibilities for the organic wastes to be further degradable to form organic acids that eventually produce carbon dioxide and water. Moreover, the increase in pH also caused by the release of volatile ammonia and ammonium from the mineralization of proteins, amino acids, and peptide (Lin 2008).

At day 40, all samples show acidic condition with pH within 4.3–4.5. The pH of food waste should be in the acidic range, which is 3.6–6.0 (Carucci et al. 2005). The optimal range of pH to produce high biogas yield is between 6.6 and 7.6 (Polprasert 2007). The pH at the end of the digestion process for samples with lipase is slightly lower as compared to the control sample. However, the amount of lipase did not affect the pH where both lipase amounts achieved identical pH value of 4.3.

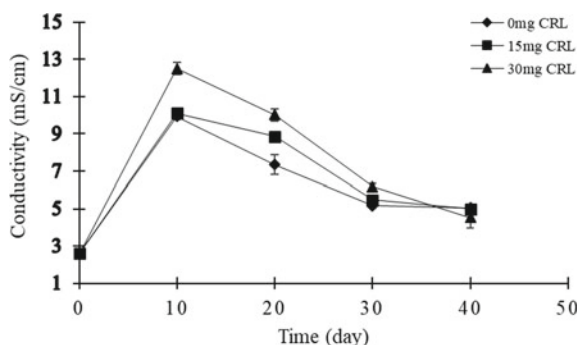
### 3.3 Effect of the Lipase Amount on Electrical Conductivity

Figure 3 shows the electrical conductivity profile for the food waste digestate. Electrical conductivity (EC) measurement determines the total soluble salts in the anaerobic digestate of food waste. The value of EC indicates the suitability of the digestate to be directly used as a fertilizer.

It is observed that all samples show similar trend on the EC value, regardless of the amount of lipase added. The electrical conductivity increased during the first 10 days of anaerobic digestion. The increase in EC is caused by the released of mineral salts such as phosphate and ammonium in the food waste during the decomposition of organic substances (Lin 2008). The presence of basic ions after the degradation process also may led to the increase in electrical conductivity (Fang and Wong 1999).



**Fig. 3** Electrical conductivity profile of the food waste digestate



At the day 20, the value of electrical conductivity for 30 mg lipase, 15 mg lipase and without lipase is then gradually decreased to 7.35 mS/cm, 8.86 mS/cm, and 10.01 mS/cm, respectively. From day 20 to day 40, the EC values are further reduced for all samples. The reduction in EC value is caused by the evaporation of ammonium ion and reduction of other basic ions (Wong et al. 1995). Other than that, volatilization of ammonia and the precipitation of mineral salts precipitation could reduce the EC as reported by Ishak et al. (2014).

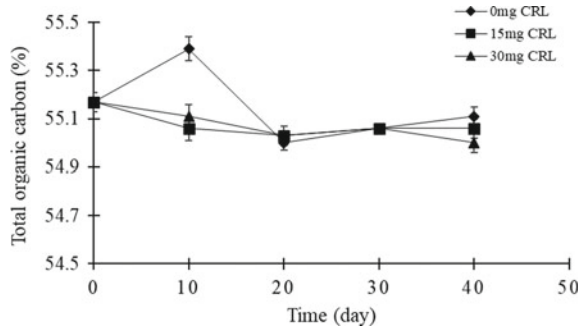
In comparison, based on the EC profile, from day 10 to day 30, the higher amount of lipase addition (30 mg) has higher EC values as compared to 15 mg of lipase and control sample. This finding shows that the lipase added facilitates the hydrolysis of fats and oils; thus, enhance the degradation rate of the food waste. Higher amount of lipase added led to higher release of mineral salts, such as ammonium and magnesium ions and/or to sulfates and phosphates into the medium, which indicates progressive mineralization of organic matter (Cáceres et al. 2006; Al-Alawi et al. 2019).

The final electrical conductivity values achieved at the end of digestion process are in the range of 4.5–5 mS/cm. The higher the value of EC the higher the amount of nutrient contained in the digestate. However, to be directly used as fertilizer, the EC suggested should be in between 2.5 and 4 mS/cm. The EC more than 4 mS/cm will cause negative impact on plant growth (Himanen and Hänninen 2011). The EC obtained in this present work is out of the range of the ideal EC for safe plant growth. Further pre-treatment can be conducted to lower down the EC value prior using as fertilizer as suggested by (Ishak et al. 2014).

### 3.4 Effect of the Enzyme Addition on the Total Organic Carbon (TOC)

Total organic carbon (TOC) is used as the energy source for microorganisms during digestion process. The level of digestate maturity can be indicated by the degradation of carbon (Zhang et al. 2017). The reduction in total organic carbon is related to the microbial degradation and respiration (Kulikowska 2016; Kulcu and Yaldiz 2004).

**Fig. 4** Total organic carbon profile of the food waste digestate



The larger the reduction in total organic carbon the higher the degradation and carbon utilization by microorganisms.

Figure 4 shows the TOC profile of the digestate is obtained in the present work. It can be observed that the average TOC value is unsteady throughout the digestion process. Overall, from day 0 to day 40, the TOC for all samples is slightly decreased. The small reduction in TOC is due to the presence of hardly degradable substances in the food waste (Petric and Mustafić 2015). On the other hand, during the anaerobic digestion process, the microbial population is fluctuating. When the population of microorganism increases, the degradation process becomes more rapid. Consequently, more residues are produced in the form of carbon source material resulting in the increase of carbon content at the end of the digestion process (Narkhede et al. 2010).

The reduction of TOC in samples with 30 mg of lipase is higher as compared to 15 mg and control samples. The organic matter loss for samples with 15 mg lipase and 30 mg lipase is found to be 22.4% and 30.2%, respectively. This finding shows that the addition of lipase enhanced the degradation rate. Previous research shown that lipase has shorten the degradation time and increased the methane yield (Meng et al. 2017). The lipase added has facilitated the hydrolysis of carbohydrates, proteins, and lipids in the food waste producing simpler molecules that can be easily utilized by the microorganism.

Total organic carbon (TOC) and organic matter loss (OM) are directly related. The decreasing trend of TOC will lead to increasing trend of organic matter loss. Thus, increasing trend of organic matter loss profile indicates the increased trend of easily degradable fractions of organic wastes. The decreasing trend of organic matter loss is may be due to the influence of hardly degradable fractions (Petric and Mustafić 2015). Furthermore, the increase amount of organic acids in the mixture reduced the pH of the system which eventually hinders the microorganism activities (Wang et al. 2016).

## 4 Conclusion

The anaerobic digestion of food waste has been conducted. The effects of *Candida rugosa* lipase addition on the moisture content, pH, electrical conductivity, and total organic carbon (TOC) have been investigated. The higher amount of lipase the higher values in electrical conductivity. The samples with higher amount of lipase also show better degradation and higher reduction in total organic carbon with organic matter loss of 30.2%. In terms of pH, both lipase amount of 15 and 30 mg achieved identical pH value of 4.3, which is lower as compared to the control. However, there is no significant improvement of lipase addition on the moisture content.

## References

- Ajay, K. J., Jianzheng, L., Loring, N., & Liguó, Z. (2011). Research advances in dry anaerobic digestion process of solid organic wastes. *African Journal of Biotechnology*, 10(65), 14242–14253.
- Al-Alawi, M., Szegi, T., El Fels, L., Hafidi, M., Simon, B., & Gulyas, M. (2019). Green waste composting under GORE(R) cover membrane at industrial scale: Physico-chemical properties and spectroscopic assessment. *International Journal of Recycling of Organic Waste in Agriculture*, 8, 385–397.
- Anjeena, S., Mudhoo, A., & Kumar, S. (2017). Bioresource technology co-composting of vegetable wastes and carton: Effect of carton composition and parameter variations. *Bioresource Technology*, 227, 171–178.
- Bouallagui, H., Ben Cheikh, R., Marouani, L., & Hamdi, M. (2003). Mesophilic biogas production from fruit and vegetable waste in a tubular digester. *Bioresource Technology*, 86(1), 85–89.
- Cáceres, R., Flotats, X., & Marfà, O. (2006). Changes in the chemical and physicochemical properties of the solid fraction of cattle slurry during composting using different aeration strategies. *Waste Management*, 26, 1081–1091.
- Carucci, G., Carrasco, F., Trifoni, F., Majone, M., & Beccari, M. (2005). Anaerobic digestion of food industry wastes: Effect of codigestion on methane yield. *Journal of Environmental Engineering*, 131(7), 1037–1045.
- Domingues, R. F., Sanches, T., Silva, G. S., Bueno, B. E., Ribeiro, R., Kamimura, E. S., et al. (2015). Effect of enzymatic pretreatment on the anaerobic digestion of milk fat for biogas production. *Food Research International*, 73, 26–30.
- Domínguez De María, P., Sánchez-Montero, J. M., Sinisterra, J. V., & Alcántara, A. R. (2006). Understanding candida rugosa lipases: An overview. *Biotechnology Advances*, 24(2), 180–196.
- Fang, M., & Wong, J. W. C. (1999). Effects of lime amendment on availability of heavy metals and maturation in sewage sludge composting. *Environmental Pollution*, 106(1), 83–89.
- Himanen, M., & Hänninen, K. (2011). Composting of bio-waste, aerobic and anaerobic sludges—Effect of feedstock on the process and quality of compost. *Bioresource Technology*, 102(3), 2842–2852.
- Ishak, N. F., Ahmad, A. L., & Ismail, S. (2014). Feasibility of anaerobic co-composting empty fruit bunch with activated sludge from palm oil mill wastes for soil conditioner. *Journal of Physical Science*, 25(1), 77–92.
- Krishna, D., & Kalamdhad, A. S. (2014). Pre-treatment and anaerobic digestion of food waste for high rate methane production—A review. *Journal of Environmental Chemical Engineering*, 2(3), 1821–1830.

- Kulcu, R., & Yaldiz, O. (2004). Determination of aeration rate and kinetics of composting some agricultural wastes. *Bioresource Technology*, 93(1), 49–57.
- Kulikowska, D. (2016). Kinetics of organic matter removal and humification progress during sewage sludge composting. *Waste Management*, 49, 196–203.
- Lin, C. (2008). A negative-pressure aeration system for composting food wastes. *Bioresource Technology*, 99(16), 7651–7656.
- Manu, M. K., Kumar, R., & Garg, A. (2017). Bioresource technology performance assessment of improved composting system for food waste with varying aeration and use of microbial inoculum. *Bioresource Technology*, 234, 167–177.
- Melikoglu, M., Sze, C., Lin, K., & Webb, C. (2013). *Analysing global food waste problem: Pinpointing the facts and estimating the energy content*, 3(2), 157–164.
- Meng, Y., Luan, F., Yuan, H., Chen, X., & Li, X. (2017). Bioresource technology enhancing anaerobic digestion performance of crude lipid in food waste by enzymatic pretreatment. *Bioresource Technology*, 224, 48–55.
- Morales-Polo, C., Cledera-Castro, M. D., & Moratilla Soria, B. Y. (2018). Reviewing the anaerobic digestion of food waste: From waste generation and anaerobic process to its perspectives. *Applied Sciences*, 8(10), 1804–1839.
- Narkhede, S., Attarde, S. B., & Ingle, S. T. (2010). Combined Aerobic Composting of Municipal Solid Waste and Sewage Sludge. *Global Journal of Environmental Research*, 4(80), 109–112.
- Paritosh, K., Kushwaha, S. K., Yadav, M., Pareek, N., Chawade, A., & Vivekanand, V. (2017). *Food waste to energy: An overview of sustainable approaches for food waste management and nutrient recycling*.
- Pascalle, N. C., Chastinet, J. J., Bila, D. M., Sant'Anna, G. L., Quitério, S. L., & Vendramel, S. M. R. (2019). Enzymatic hydrolysis of floatable fatty wastes from dairy and meat food-processing industries and further anaerobic digestion. *Water Science and Technology*, 79(5), 985–992.
- Petric, I., & Mustafić, N. (2015). Dynamic modeling of the composting process of the mixture of poultry manure and wheat straw. *Journal of Environmental Management*, 161, 392–401.
- Polprasert, C. (2007). *Organic waste recycling—Technology and management*.
- Rajin, M. (2018). A current review on the application of enzymes in anaerobic digestion. In N. Horan, A. Yaser, & N. Wid (Eds.), *Anaerobic digestion processes. Green energy and technology*. Singapore: Springer.
- Rajin, M., Yaser, A. Z., Saalah, S., Jagadeson, Y., & Ag, Duraim M. (2020). The effect of enzyme addition on the anaerobic digestion of food waste. In A. Yaser (Ed.), *Green engineering for campus sustainability*. Singapore: Springer.
- Tanimu, M. I., et al. (2014). Effect of carbon to nitrogen ratio of food waste on biogas methane production in a batch mesophilic anaerobic digester. *International Journal of Innovation, Management and Technology*, 5(2), 116–119.
- Tweib, S. A., Rahman, R. A., & Khalil, M. S. (2011). Composting of Solid Waste from Wet Market of Bandar Baru Bangi Malaysia. *Australian Journal of Basic and Applied Science*, 5(5), 975–983.
- Wang, X., Selvam, A., & Wong, J. W. C. (2016). Influence of lime on struvite formation and nitrogen conservation during food waste composting. *Bioresource Technology*, 217, 227–232.
- Wong, J. W. C., Li, S. W. Y., & Wong, M. H. (1995). Coal fly ash as a composting material for sewage sludge: Effects on microbial activities. *Environmental Technology*, 16(6), 527–537.
- Xiao, B., Qin, Y., Zhang, W., Wu, J., Qiang, H., Liu, J., et al. (2018). Temperature-phased anaerobic digestion of food waste: A comparison with single-stage digestions based on performance and energy balance. *Bioresource Technology*, 249, 826–834.
- Yang, F., Li, G. X., Yang, Q. Y., & Luo, W. H. (2013). Effect of bulking agents on maturity and gaseous emissions during kitchen waste composting. *Chemosphere*, 93(7), 1393–1399.
- Yaser, A. Z. (2014). Current advances in anaerobic digestion of highly concentrated dye effluent. In J. Fu (Ed.), *Dyeing: Processes, techniques and applications* (pp. 217–227). Nova Publisher.

- Yaser, A., Rahman, R., & Kalil, M. (2008). Co-composting of palm oil mill sludge-sawdust. *Pakistan Journal of Biological Sciences*, *10*, 4473–4478.
- Zhang, L., et al. (2017). The impact of silver nanoparticles on the co-composting of sewage sludge and agricultural waste: Evolutions of organic matter and nitrogen. *Bioresource Technology*, *230*, 132–139.

# Recycled Materials and Warm Mix Asphalt Technology: A Green Approach in Pavement Modification



Lillian Gungat, Nurul Ariqah Ispal, Ng Chee Hiong,  
and Meor Othman Hamzah

**Abstract** Increasing amount of waste and depletion of natural resources has encouraged recycling of materials in road construction. In this study, two types of recycled materials incorporated in road pavement construction, namely reclaimed asphalt pavement (RAP) and crumb rubber warm mix asphalt (CRWMA) were investigated. Both materials were incorporated with asphalt materials at various contents. The evaluation assesses the effects of compaction temperature during mix design, resilient modulus and the effects of moisture to pavement with recycled materials. Based on the analysis of compaction temperature effects, it shows that the warm mix additive can reduce the compaction temperature of the recycled asphalt mixture which is found to be environmentally beneficial. In terms of resilient modulus, the addition of recycled materials increases the resilient modulus. It was found that recycled material contents are the crumb rubber and RAP has significant effects on the resilient modulus. The incorporation of crumb rubber slightly reduced the moisture resistance. It is proposed to treat the crumb prior incorporation into asphalt mixture. The addition of WMA into RAP showed improvement in fatigue resistance. From the study, the recycled materials showed some environmental benefits and improved the resilient modulus. Hence, it has the potential to be used as green construction with some treatment.

---

L. Gungat (✉) · N. A. Ispal  
Civil Engineering Program, Faculty of Engineering, Universiti Malaysia Sabah,  
88400 Kota Kinabalu, Sabah, Malaysia  
e-mail: [lillian@ums.edu.my](mailto:lillian@ums.edu.my)

N. A. Ispal  
e-mail: [nurulariqahispal@gmail.com](mailto:nurulariqahispal@gmail.com)

N. C. Hiong  
Hoyu Recycling and Retreading Sdn. Bhd, Kota Kinabalu Industrial Park,  
88460 Kota Kinabalu, Sabah, Malaysia  
e-mail: [anthony.hoyu@gmail.com](mailto:anthony.hoyu@gmail.com)

M. O. Hamzah  
School of Civil Engineering, Universiti Sains Malaysia, Engineering Campus, 14300 Nibong  
Tebal, Seberang Prai, Penang, Malaysia  
e-mail: [cemeor@usm.my](mailto:cemeor@usm.my)

**Keywords** Recycled materials · Reclaimed asphalt pavement · Crumb rubber · Warm mix asphalt

## 1 Introduction

Industrial countries are producing a considerable amount of wastes and improper waste management that leads to negative impact on environment and communities. In line with sustainable goal, government agencies are promoting waste reuse and recycling. This provides a substantial opportunity to recycle wastes produced as precious raw materials, for example, in road pavements. Depletion of natural resources around the globe has triggered the exploration of using recycled materials replacing the virgin construction materials in the construction industries. Many studies have been conducted to investigate the environmental benefits, cost benefits, and performance of the recycled materials in road construction. Various types of waste materials have been successfully utilized in road pavements. Examples of recycled materials in road construction are reclaimed asphalt pavement (RAP), used tires, steel slag, plastic waste, etc.

The motivation for recycling in pavements is twofold: either to save resources or to improve material properties. Green pavement approaches such as recycling of used pavement and recycled tires in pavement emphasized the resources conservation and improvement of material properties through pavement modification. The utilization of RAP shows comparable properties with the conventional mixtures if the RAP materials are treated properly (Zaumanis and Mallick 2015). In terms of recycled tire usage, previous researches have proven that the usage of recycled tires in the form of crumb rubber in the pavement led to more environment-friendly road construction (Gheni et al. 2017).

Aggregate, bitumen, and filler are the main materials in flexible pavement construction. These materials should be carefully examined for its compliance with the established standard particularly when incorporating recycled materials. Increasing number of vehicles and continuous development brings newer road constructions. Hence, it requires a substantial amount of aggregates, bituminous, and filler as well as performance-enhancing additives to withstand the ever-increasing demands in terms of axle loads and frequency of traffic. At the same time, with the increase of heavy vehicles on the road and scarcity of raw materials depending on the region, the road pavement industry is facing new challenges in terms of resources and mechanical performances that must be met.

### *1.1 Recycled Tire for Road Construction*

Tires, of everyday use, are designed to be abrasive, load carrying, indestructible manufactured to stringent quality standards to ensure safe ride and long service

life. Such properties of tires have in return resulted in a difficult task to dispose of them annually, making it the largest and most problematic sources of waste due to the large volume produced. Thus, used tires occupy a great volume of the landfill spaces; landfills without proper treatment facilities have started to reject the dumping of used tires, as they are not compactable, and the disintegration rate is very slow. From the past to date, apart from disposal at limited landfills, used tires are either temporarily stored in company yards, disposed secretly at illegal dump sites, or even ended up along unknown routes in certain cases. Nonetheless, recycling of used tires in various degrees has become more prominent today.

Over the past, high used tire volume consuming options include artificial reef construction to rubberized asphalt road surfacing. These have been, however, discouraged by several factors. As the world pushes forward the concept of sustainability and social responsibility, it has become so crucial than ever to better manage the increasing used tires from year to year.

Utilizing recycled tire is an inexpensive sustainable technology which would transform unwanted trade waste into a new bituminous mixture with improved engineering properties. Many researches to date have provided more than enough yet strong justifications for recycled tires to be incorporated into the so-called innovative pavement construction. [Praticò et al. \(2015\)](#) have in fact commented that asphalt concrete incorporating recycled tires has the potential for constructing innovative urban and rural infrastructures. Used tires can be recycled into rubber granules that are less than or equal to six millimeters in size and named as crumb rubber. It is proposed for the pavement as it is a waste material, and crumb rubbers modified asphalt pavement shows excellent performance. The effects of the addition of crumb rubber on the properties of crumb rubber asphalts have been investigated by many researchers in the past. The process of asphalt modification involving natural and synthetic rubber was introduced as early as 1840s. In Malaysia, rubber additives for road construction had been used since the 1940s but evidence available started to be recorded in the early 1980s. [Table 1](#) shows that history of rubberized road pavements in Malaysia starting from 1950.

The usage of crumb rubber in road construction has a multiple benefits since it has started to be implemented in real road construction. Rubber Pavement Association found that using tire rubber in open-graded mixture binder could decrease tire noise by approximately 50%; not only so, in spray applications, rubber particles of multiple sizes have better sound absorption ([Mashaan et al. 2011](#)). Moreover, other benefits of using crumb rubber modified asphalt are lower susceptibility to varying temperatures on a daily basis, more resistance to deformation at higher pavement temperature, proved age resistance properties, higher fatigue life for mixtures, and better adhesion between aggregate and binder ([Mashaan et al. 2014](#)). It was proven that the inclusion of crumb rubber to asphalt binder has increased the rheological properties of the binder ([Xiao et al. 2006](#)), where the surface-initiated cracks resistance found to be improved, fatigue cracking reduced, temperature susceptibility reduced and durability improved, resulted from the experimental findings, and it was also found that the maintenance cost of road pavement can be reduced ([Liu et al. 2009](#)).



**Table 1** Rubberized roads in Malaysia

Year	Location	Rubber used (wet process)
1950	Kota Bharu–Kuala Krai (90 m)	Crumb rubber and latex (5%)
1968	Klang	1.5% crumb rubber and 8.3% latex
1993	Rembau–Tampin (1 km)	Crumb rubber and latex
1996	Sungai Buluh (3 km)	Crumb rubber
1996	KLIA (50 km)	Crumb rubber
2003	Jalan Kuantan–Gambang (4 km)	Crumb rubber
2010	Bukit Kuantan (0.6 km)	Crumb rubber
2015	Kota Tinggi, Johor (1 km)	Cup lump (5%)
2016–2017	Rubberized asphalt pilot projects in Negeri Sembilan, Pahang, Kedah, Kelantan and Johor	Cup lump (5%)

Source Hassan (2017)

The cost of using recycled tires into road construction depends on a few factors, from the source of end-of-use tires to the mechanism of recycling tires, the involvement of governmental policies as well as the collaborations among various stakeholders' inclusive developers and road builders. With the rising price of non-renewable natural aggregates, the overall cost to integrate recycled tires into pavement could then be possibly cheaper if not comparable to that of the conventional road construction. When and if used tires are extensively recycled and utilized as partial replacement to natural aggregates in asphalt concrete production, it will not only resolve the adverse environmental issues but also present a green approach to pavement construction and maintenance industry.

## 1.2 Reclaimed Asphalt Pavement

In the road industry, the recycling of asphalt started since the mid 1970s due to the significant increase in asphalt prices as a result of Arab oil embargo (Karlsson and Isacson 2006). Initially, the implementation of asphalt recycling in road construction and maintenance was limited to the inclusion of a low percent of reclaimed asphalt pavement (RAP) content. According to the Asphalt Recycling and Reclamation Association (ARRA), recycling of Hot Mix Asphalt (HMA) can be categorized into cold planning, hot recycling, hot in-place recycling, cold in-place recycling, and full depth reclamation (ARRA 2001). The most commonly implemented method of recycling is hot recycling due to its proven cost effectiveness and environmentally friendly in comparison to other techniques. In the hot recycling process, the old road surfacing is milled, processed, and combined with a new/virgin binder, aggregate and/or recycling agent in an asphalt plant. The removed and processed materials are defined as RAP. RAP comprises of valuable asphalt binder and aggregates and they

are properly stored in the recycling plant before mixing with the virgin materials (Miliutenko et al. 2013).

The application of RAP in road construction and maintenance had gained attention among scientists and paving engineers due to its cost effectiveness and environmental benefits. According to Aurangzeb et al. (2014), hybrid life-cycle assessment (LCA) which is a combination of LCA and Input–Output LCA on high RAP content showed a significant reduction in energy consumption and greenhouse gasses (GHG) emissions with increased RAP content. The results of comparative LCA on the use of RAP materials in the base and sub-base layers of pavements show a potential reduction of global warming (20%), energy consumption (16%), water consumption (11%), life-cycle costs (21%), and hazardous waste generation (11%) (Lee et al. 2010). In addition, this also reduced 23% eco-burden of the landfill (Chiu et al. 2008). The utilization of RAP will benefit more on the material costs as 70% of the expenses to produce HMA are from materials (Copeland 2011). In the USA, the use of reclaimed materials alone conserved about 3.7 million tons of virgin asphalt binder which translates savings up to USD 2.2 billion (NAPA 2013). The key variable for evaluating the amount of cost saving of virgin materials due to the addition of RAP is the amount of effective asphalt binder content within the RAP (Howard et al. 2009). Although the practical use of high RAP is limited, the highway agency and paving industry have considered the high amount of RAP in asphalt paving mixtures to offset the rising cost of asphalt binder (West et al. 2013). In some European countries, the utilization of the valuable RAP results in more cost saving especially in countries where aggregates are mostly imported (Dinis-Almeida et al. 2012; Zaumanis and Mallick 2015).

Many countries were reluctant to use RAP in quantities of more than 30% for road surface courses due to the lack of guidelines for implementation (FHWA 2008). With the continued evolution of RAP usage through research and development, the maximum allowable RAP amount increases to more than 30%. Other studies have suggested that the homogeneity of RAP affects the limit of RAP content for incorporation into HMA (Mucinis et al. 2009). Many studies were conducted to identify the possibility of incorporating higher RAP content for its environmental and economic benefits. A paradigm shift from low to high RAP contents and even 100% RAP is necessary to sustain the tremendous demands of civil engineering infrastructure.

West et al. (2013) revised the mix design involving high RAP content and recommended some additional tests to further evaluate the asphalt mixtures. Utilization of RAP should meet the two guiding principles, namely the mixtures containing RAP should meet the requirements as for virgin materials and the performance at least equal to or better than conventional HMA. The performance of asphalt mixtures with high RAP content can be improved by modifying the mixture such as using a softer binder grade, incorporating WMA additive, utilizing rejuvenators, and adding anti-stripping agents (West et al. 2013; Shen et al. 2007). McDaniel and Anderson (2001) demonstrated that properly designed and constructed RAP showed a comparable performance with the conventional asphalt mixtures. However, higher production temperature due to RAP stiffness becomes the main concern in the production of RAP as this will further age the RAP binder.

### 1.3 Warm Mix Asphalt Technology

Energy consumption in asphalt production comes from the energy needed to manufacture asphalt binders in oil refineries and carbon-based energy carriers that are utilized as industrial fuels in asphalt mixing plants. Based on the estimation carried out by the Environmental Protection Agency (EPA), on average, a drum mix asphalt plant that produced 200,000 tons of asphalt mixture in a year results in the emissions of approximately 14 tons of carbon monoxide (CO), 5.0 tons of volatile organic compounds, 1.1 tons of sulfur dioxides, 5.5 tons of nitrogen oxides, and 1.0 tons of total hazardous air pollutants (HAP) (US EPA Report 2000). Therefore, in response to combating global warming as well as encouraging sustainable practices, the asphalt industries have made considerable efforts to minimize the GHG emissions and the excessive consumptions of fossil fuel. This can be achieved by reducing the production temperature of the asphalt mixtures without adversely affecting its properties by using warm mix asphalt technology.

Warm mix asphalt (WMA) is an advancement of asphalt technology after the HMA technology. According to Zaumanis and State (2015), the modern warm mix asphalt originated in Germany by the mid 1990s. The technology was then started to be developed widely by the European countries, followed in 2002 by the USA (D'Angelo et al. 2008). Now in this recent year, the technology of WMA is starting to revolve in the highway engineering industry all over the globe. Gungat et al. (2016), stated that, in comparison with the HMA, the production of asphalt mix using WMA reduces temperature by 30–50 °C. Thus, the production of these mixtures ranged between 110 and 140 °C (Dinis-Almeida and Afonso 2015; Capitaio et al. 2012; D'Angelo et al. 2008). The advanced technology of WMA allows the reduction in mixing temperature yet improves better workability and compaction compared with the HMA (Zaumanis and State 2015). Therefore, the level of mechanical performance of the asphalt would not be reduced when the temperature for mixing is slightly lower than that of the HMA technology.

Apart from better workability and compaction, several significances of WMA include reduced greenhouse gas emissions, better working conditions, lower energy consumption, longer hauling distances, etc. (Guo et al. 2014). However, according to Abdullah et al. (2014), the specific advantages of WMA technology can be detailed as in the environmental benefits, economic benefits, construction benefits, and recycling benefits. The following are the conveniences of WMA based on the classification as stated:

- i. Environmental benefits: Saves production energy and electric usage that eventually reduces the gaseous emissions that will pollute the environment like CO<sub>2</sub>, SO<sub>2</sub>, NO<sub>x</sub>, CO, and dust.
- ii. Economic benefits: Reduces cost in terms of the plant maintenance and energy consumption because of the reduction of temperature.
- iii. Construction benefits: Reduces the need for compaction as WMA has better workability due to the improved aggregate coating. Another situation is that it

creates longer hauling distances between construction site and plant that suits for the cold weather.

- iv. Recycling benefits: Allows even more production of reclaimed asphalt.
- v. Pavement (RAP) with less aging of binder properties in WMA mixtures.

#### ***1.4 Crumb Rubber Warm Mix Asphalt***

In Early mid 1960s, rubber has been used in asphalt mixtures when it was pioneered by the city of Phoenix, Arizona, to be used in their chip seal program for the city's streets. Since Arizona DOT fully implemented their rubber asphalt program in 1988, they have used more than 4.2 million tons of asphalt rubber which results in the recycling of 15 million old tires (Hicks 2010).

According to Hicks (2010), the use of asphalt rubber has been proven to reduce the traffic noise level which deducted, and obtained noise readings have shown that a noise reduction of four decibels can be attained. Other than noise reduction, Hicks (2010) found that addition of rubber improves the fatigue resistance. The study concluded that insertion of rubber into the WMA was a beneficial combination that improved the rheological properties of binders. The fatigue life is greater for warm mix mixtures that included crumb rubber than the control RHMA mixture. The study also found that the fatigue life, stiffness, and cumulative dissipated energy in asphalt mixtures depend on the type of aggregates used. The production and compaction temperatures of asphalt rubber incorporated with WMA can be reduced considerably, hence it helps reducing the odor and smoke coming from the asphalt mixture. It will also help to cut the cost of the burner fuel due to reduced usage of fuel and reduces the emissions, thus allowing more asphalt rubber to be produced without exceeding the maximum allowable emissions.

There are a lot of advantages of using crumb rubber in road pavements. The researches and applications of crumb rubber modified asphalt binders in various countries have reported that the crumb rubber modified asphalt binder has many advantages such as improved resistance to rutting due to high viscosity, high softening point, and better resilience (Fontes et al. 2010; Katman et al. 2011). Earlier works also have indicated that crumb rubber modified (CRM) asphalt binders may even be employed in porous mixes (Ibrahim et al. 2007; Katman et al. 2005).

Addition of crumb rubber to virgin asphalt produces binders with improved resistance to fatigue cracking reducing the thickness of asphalt overlays (Xiao et al. 2010). Putman and Amirkhanian (2006) proved that addition of crumb rubber to asphalt binders increases the rheological properties of the binders. Based on experimental findings, the addition of crumb rubber also improved asphalt resistance to surface initiated cracks, the reduction of fatigue cracking, the reduction of temperature susceptibility, improved durability as well as the reduction in road pavement maintenance costs (Liu et al. 2009).

Another study has shown the significant effect of crumb rubber modified concentration on physical and rheological properties of rubberized asphalt binder (Mashaan et al. 2011). From the rutting evaluation by Abdul Hassan et al. (2014), the rubberized dense-graded asphalt mixtures showed higher rutting resistance compared to the conventional dense-graded mixture which resulted from the elastic recovery of the rubber particles. Furthermore, Asadi et al. (2016) in their study also mentioned that addition of rubber to the asphalt will also reduce some environmental pollution due to the rubber.

### ***1.5 Reclaimed Asphalt Pavement and Warm Mix Asphalt***

Warm mix asphalt technology with RAP mixtures was used since 1980s for low volume roads (Roberts et al. 1984). The first field constructability assessment was conducted at the National Center for Asphalt Technology (NCAT) test track containing 45% RAP with 1.5% Sasobit (West et al. 2009). Furthermore, a plant produced RAP–WMA in Florida, USA was tested in collaboration with NCAT (Copeland et al. 2010). Intensive studies have also been conducted on the performance of asphalt mixtures with high RAP content, as well as various types of WMA additives and conditioning effects to simulate field situations (Mogawer et al. 2011; Doyle and Howard 2011; Shu et al. 2012; Doyle and Howard 2013). The increasing number of studies on high RAP usage has also led to the publication of established guidelines for RAP incorporated with WMA (Solaimanian et al. 2011; West et al. 2013).

An economic evaluation of the use of RAP combined with WMA indicated positive findings and concluded that this new technology may save costs (Howard et al. 2009). In addition to economic evaluation, an environmental assessment was also performed on emissions during the production of RAP–WMA mixtures (Middleton and Forfylyow 2009). The LCA concluded that potential savings may be made through the use of high RAP (Vidal et al. 2013). Based on a survey by National Asphalt Pavement Association (NAPA) on the usage of RAP and WMA in the USA, the amount of RAP utilization is approximately 68.3 million tons in 2012 with USD 2.04 billion estimated spent on asphalt binder (Hansen et al. 2013). There are two main benefits of WMA additives on RAP mixtures which are reduced production temperature and improved blending and workability.

High RAP content increases the mixture stiffness and hence requires high production temperature. Integration of WMA technology is able to reduce the viscosity of RAP mixtures and thus the production temperature can be lowered. The benefits of low production temperature for RAP and WMA additive (RAP–WMA) include minimizing further aging of RAP due to the heating temperature, aiding compaction, limiting emissions during production at asphalt plants, shortening construction duration, and increasing cost savings. According to Hill (2011), other than the reduction of viscosities, the chemical composition of the WMA additives also affected the reduction of production temperature.

Workability is related to the ease of compacting the RAP–WMA. Visual observation and field experience involving the compaction of both RAP and RAP–WMA indicate that RAP–WMA mixtures are easier to compact than RAP mixtures. Workable WMA enhanced the degree of RAP blending with a virgin asphalt binder and hence, produced a better performance. Previous research related to utilization of RAP–WMA is summarized in Table 2.

Based on the literature review, crumb rubber and RAP as green materials in asphalt pavement showed positive findings. The key criteria for green pavement are optimization of resources, reduction in energy consumption, and GHG emissions while improving the safety and comfort of the commuters. However, in Malaysia,

**Table 2** Summary of literature on RAP–WMA mixture performance

Author	WMA additive	RAP (%)	RAP-WMA mixture performance
Oliveira et al. (2012)	Surfactant	50	Improved rutting and fatigue resistances
Zhao et al. (2013)	Chemical	0–40	Rutting reduced at 20% RAP and slight improvement at 30% or more RAP content
Hill et al. (2013)	Organic and foamed	15–45	Improved moisture resistance
Goh (2012)	Organic	50, 75	Slightly better performance compared to control mixture
Doyle and Howard (2013)	Organic	25, 50	Equal moisture performance with control
Gou et al. (2014)	Foamed	0, 20, 30, 40	Slightly poor performance of moisture
Oner and Sengoz (2015)	Organic and chemical	10, 20, 30, 40, 50, 90	Improved moisture resistance
Gungat et al. (2016)	Organic	30, 40, 50	Improved rutting resistance
Omranian et al. (2018)	Organic	30, 50	Improved workability
Song et al. (2018)	Foamed	50	Improved resistance to moisture and rutting
Gungat et al. (2019)	Organic	30, 40, 50	Improved moisture and fatigue resistance

their usage is not maximized due to some factors. Hence, this study aims to evaluate the effects of compaction temperature in terms of resilient modulus, moisture resistance, and fatigue resistance.

## 2 Materials and Methods

### 2.1 Materials and Sample Preparation

The materials used in this study were aggregate, asphalt binder, filler, WMA additive crumb rubber, and hydrated lime (HL). Aggregates used were granite and sandstone type with AC14 gradation and follow the local standard Jabatan Kerja Raya (JKR) specification. The properties of aggregate tested in accordance with BS812-2 are as shown in Table 3. The asphalt binders were 80/100 and 60/70 penetrations. The crumb rubber supplied by a tire recycling factory is shown in Fig. 1a. For the inclusion of crumb rubber, it was added to replace 0.425 mm aggregate at 0, 10, and 20%. Three compaction temperatures were used for samples fabrication which were 120, 135, and 150 °C. The milled RAPs were obtained in 2013 from section 685 Jalan Kamunting, Perak. The road was under the jurisdiction of state and used to link towns within the state. The selected RAP content in Fig. 1b was 30, 40, and 50%. A wax-based WMA additive called RH-WMA as in Fig. 1c developed by China was used as an additive

**Table 3** Properties of aggregates

Type of aggregate	Properties	
	Specific gravity of course aggregate (%)	Specific gravity of fine aggregate (%)
Sandstone	2.71	2.72
Granite	2.60	2.62
RAP	2.66	2.61

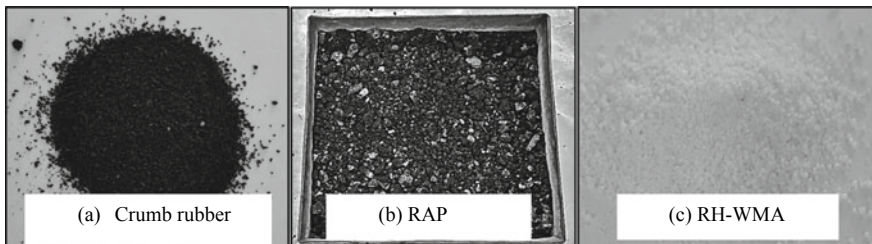


**Fig. 1** Main materials **a** RH-WMA, **b** Crumb rubber, and **c** RAP

to be blended with asphalt binder. The RH-WMA was added at 3% of the weight of the asphalt binder prior to mixing with the CR and RAP.

The experimental procedure involved in this study is illustrated in Fig. 2. It started with the materials preparation whereby RAP was processed and fractionated according to the method suggested by Gungat (2017). In this study, RAP was added as replacement of the aggregate at 30, 40, and 50%. The RH-WMA prepared by blending it into asphalt binder at 145 °C according to the method by Gungat et al. (2016) prior to addition of RAP and crumb rubber. In this study, mix design for CR and RAP was conducted separately using experimental design named response surface method. Response surface method proposed the asphalt mixture optimized design by considering the simultaneous effects of compaction temperature, binder content, and amount of recycle materials. The selection of the range of compaction temperature used as input in the response surface was based on the viscosity test and mixability. Mixability is related to the ease of mixing the aggregate, asphalt binder, and recycled materials. Compaction temperature in 15 °C increment was based on the research by Hamzah et al. (2013). After that, specimens were prepared and examined for moisture susceptibility and fatigue due to the effects of moisture and aging.

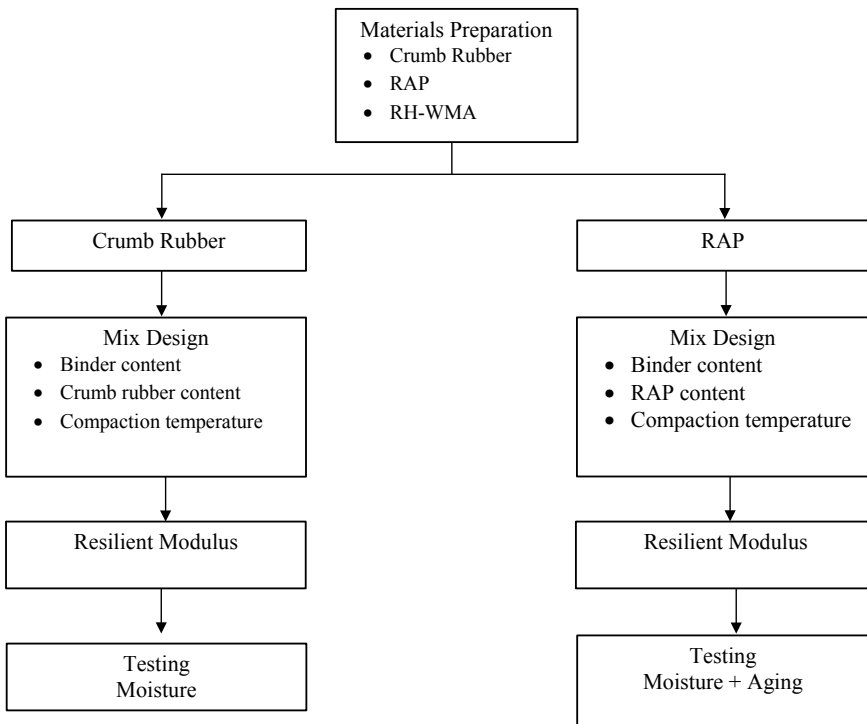


Fig. 2 Experimental procedure



**Table 4** Designation of mixtures

Mixture designation	Description
0CR	No crumb rubber
10CR	10% crumb rubber
10CRHL	10% crumb rubber with hydrated lime
0RAP	No RAP
10RAP	10% RAP
R1(MA)	RAP from R1 and subjected to moisture and aging
R1-RH(MA)	RAP from R1 added with RH-WMA and subjected to moisture and aging

For easier identification, abbreviations were used to indicate the sample. In specimen that is made of crumb rubber, the first number denotes the crumb rubber content and HL means the hydrated lime. Specimen containing RAP uses R1 to indicate the RAP, RH refers to RH-WMA, and MA refers to moisture and aging. Table 4 shows the specimen designation.

### 3 Results and Discussion

#### 3.1 Effects of Compaction Temperature During Mix Design

In this study, design mix was conducted by considering the simultaneous effects of compaction temperature, crumb rubber content, or RAP content. Compaction temperature is crucial during laying of asphalt as higher compaction contributes to environmental pollution. Tables 5 and 6 show the relationship between the compaction temperature with crumb rubber content or RAP content and binder content. In general, binder content is reduced as the compaction temperature increased due to better workability. In terms of crumb rubber content, increment of crumb rubber content slightly reduces the binder content at 20% crumb rubber. However, there is no effect of binder content at 10% crumb rubber. The changes in binder content can be related to the cost of construction. Compaction temperature is related to the effects

**Table 5** Optimum binder content of CRWMA mixture

Compaction temperature (°)	Crumb rubber content (%)		
	0	10	20
120	5.5	5.5	5.4
135	5.4	5.4	5.3
150	5.2	5.3	5.2

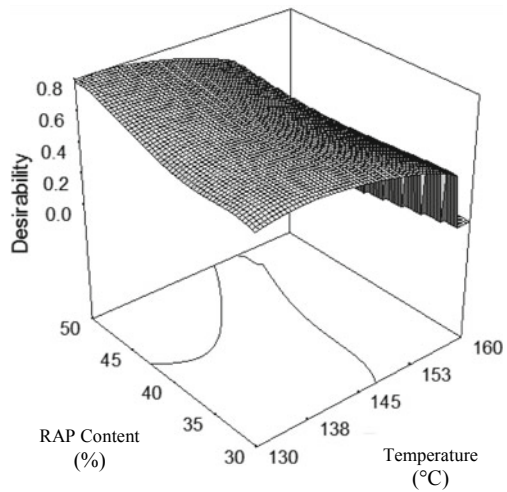
**Table 6** Optimum binder content of RAP–WMA mixture

Compaction temperature (°)	RAP content (%)			
	0	30	40	50
130	5.4	5.4	5.5	5.5
145	5.4	5.4	5.4	5.3
160	5.4	5.4	5.3	5.3

of the materials during paving. Lower compaction temperature at lower binder content is preferable because it reduces cost and better working environment due to less smoke.

Response surface method was used to model the relationship between the compaction temperature and RAP content as illustrated in Fig. 3. From Fig. 3, increment of RAP content at 130 °C compaction temperature causes slight increase in binder content when RAP content increase. The effects of RAP content on the OBC are minimal with only 0.01% variation of binder content at the same compaction temperature. This finding agrees with studies on the effects of RAP content on OBC conducted by Al-Qadi et al. (2009). However, this pattern changes as the compaction temperature increases. This means that at 130 °C compaction temperature, changes in binder content increases the cost of construction. The cost increment due to binder content can be counterbalanced with the RAP usage because RAP contains valuable aggregate and binder. If higher compaction temperature is selected, more energy consumption is required and thus produces more fumes during paving. Hence, lowest compaction temperature can be chosen due to greener environment during road construction and thus minimizes negative effects on the environment.

**Fig. 3** Relationship between compaction temperature and RAP content



### 3.2 Effects of WMA on Resilient Modulus of Crumb Rubber and RAP Mixtures

Resilient modulus is an important parameter to indicate the mixtures' quality and used as an input for the mechanistic-empirical pavement design. Figures 4 and 5 summarize the resilient modulus of various types of mixtures containing RAP and crumb rubber. Figure 4 presents the resilient modulus of various types of mixtures containing crumb rubber and hydrated lime. All graphs exhibit similar trends whereby the resilient modulus slightly increases with 10% inclusion but drops with inclusion of 20% except 10CR with HL. The average increment from 0CR to 10CR of samples prepared at various compactions is 7.7% and 4.6%, respectively, for 0HL and 2HL. Whereas, the average drop of resilient modulus for sample prepared at 135 and 145 °C is 10.0 and 7.6% for 0HL and 2HL. Hamad et al. (2014) postulated that the resilient modulus reduction is due to the loss in structural capacity of the rubberized mixture

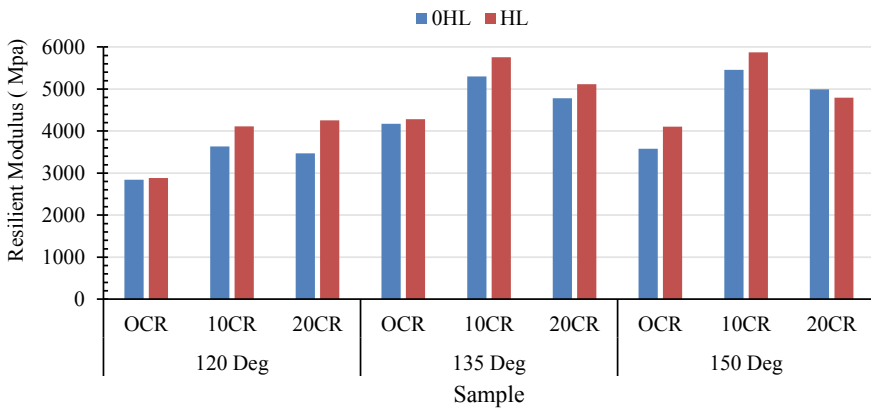


Fig. 4 Resilient modulus of CRWMA mixtures

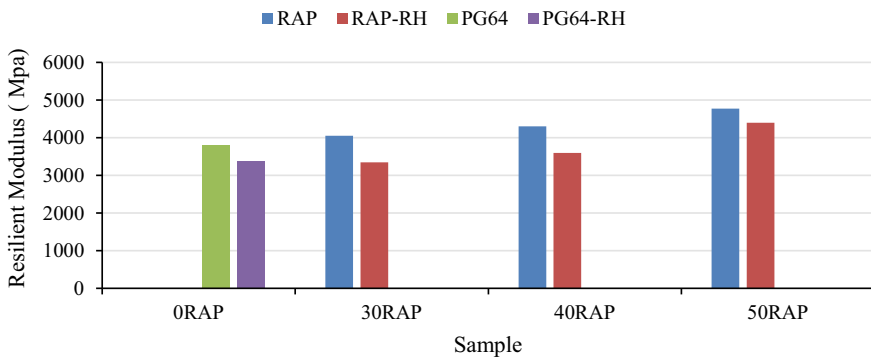


Fig. 5 Resilient modulus of RAP mixtures

which results in low cohesion of mixture that leads to poor interaction between crumb rubber and binder. This also could be possible because of increase of the rebound of the mixture due to crumb rubber inclusion. Therefore, more deformation can take place due to the compression of rubber particles (Willoughby 2001). While, other authors stated that the reduction of resilient modulus occurs because of the reduction of binder content was replaced by crumb rubber that increases in value (Ariyapijati et al. 2017). The graphs show that the compaction temperature at 135 °C has the highest resilient modulus compare to the resilient modulus at 150 °C. At higher temperature, the crumb rubber is already melted wholly and mixed with binder and thus lowering the value of resilient modulus of the asphalt mixture. Mashaan et al. (2014) stated that reduction in temperature causes increment in resilient due to mixture becomes stiffer at lower temperature, but too low temperature will cause the bonding which is not strong.

Figure 5 shows the resilient modulus of RAP sample with and without WMA. The resultant graphs exhibit increased resilient modulus with RAP content. Similar trend was reported by Arshad et al. (2015) on the RAP–WMA mixtures containing 30, 40, and 50% RAP with Sasobit. The stiffness is attributed to the aging and hardening process (Boriack et al. 2014). The increase of resilient modulus with average of 7.9% in the RAP mixtures is attributed to the aged binder in the RAP. Meanwhile, the asphalt mixture specimen containing RH-WMA additive results in slightly lowered resilient modulus with an average reduction of 13.9%.

The linear relationship between resilient modulus and types on mixture which are CRWMA and RAP is statistically analyzed based on analysis of variance (ANOVA) using general linear model (GLM). Data analysis was performed at 95% confidence level ( $\alpha = 0.05$ ) for evaluating the significant effects of each independent variables of CRWMA mixture (CR content, HL content compaction temperature) and RAP mixture (RAP content and additive) on the resilient modulus results. The results are shown in Tables 7 and 8. From Tables 7 and 8, it shows that compaction temperature, crumb rubber content, and hydrated lime are significant factors that contribute to changes in resilient modulus of mixture. For RAP mixture, it is found that RAP content and additive are significant factors that contribute to changes in resilient modulus of mixture.

**Table 7** ANOVA Results of resilient modulus of CRWMA using general linear model

Variables	DF	Adj SS	F	P	Significance
Compaction temperature	2	6,976,606	50.44	<0.00001	Yes
Crumb rubber content	2	5,909,321	42.72	<0.00001	Yes
Anti-stripping	1	483,682	6.99	0.021	Yes
Error	12	829,865			
Total	17	14,199,473			
<i>R</i> -Sq = 94.16% <i>R</i> -Sq(adj) = 91.72%					

**Table 8** ANOVA results of resilient modulus of RAP using general linear model

Variables	DF	Adj SS	F	P	Significance
RAP content	3	1,186,068	25.11	0.013	Yes
Additive	1	610,443	38.77	0.008	Yes
Error	3	47,242			
Total	7	1,843,754			
$R\text{-Sq} = 97.44\%$ $R\text{-Sq}(\text{adj}) = 94.02\%$					

### 3.3 Moisture Resistance of Crumb Rubber WMA

Moisture is one of the common causes of pavement failure. The moisture resistance of crumb rubber WMA was evaluated based on stripping. This study uses the image analysis program developed by MATLAB for determining stripping percentage. The stripping percentage was evaluated based on the exposure of aggregate. In the image analysis, the optimal luminance threshold level of 0.4 was determined to distinguish the white and black pixels. Threshold level of 4.0 is selected as it seems to be a realistic value to recognize the stripping areas. Figure 6 shows the binary image obtained for the dry and wet samples, respectively. From this figure, it can be seen that more stripping occurred on the specimen without hydrated lime. Hydrated lime as the stripping agent reduces the effects of moisture on the stripping. Qualitatively, by scrutinizing the condition of the sample in dry and wet conditions, the binary image of sample shows that conditioned samples have higher black intensity before tested. This stipulates that more asphalt binder was skimmed off from aggregate after tested due to water effect that causes loss of adhesion due to moisture effect or moisture damage (Aguiar-Moya et al. 2018).

After converted from 'Red-Green-Blue' (RGB) image to binary image, the level of stripping evaluated using MATLAB is as shown in the graph in Fig. 7. Quantitatively, from the graph in Fig. 7, it shows an increase in level of stripping for all compositions of samples when the samples were subjected to moisture. The highest stripping level is 58.04% shown by 0% CR in wet condition.

From the analysis, it shows that inclusion of crumb rubber created weak link of asphalt binder and aggregate in water which has made the asphalt binder to skim off. As stated by Shatanawi et al. (2013), crumb rubber has limited solubility in asphalt binder which is the reason why the compositions are more susceptible to water effect. Nevertheless, the difference of stripping percentage stipulates trivial difference of only  $\pm 12\%$  with the control mixture. However, upon concerning on hydrated lime content, samples with additives have better coating of aggregates by asphalt binder as the anti-stripping agent improves the adhesion and/or the debonding behavior of the binder and aggregate, because of the hydrophobic properties making it more water repellent. This implies that, modification of pavement through recycling needs proper treatment in improving moisture resistance properties.



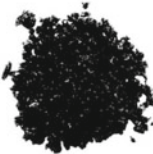






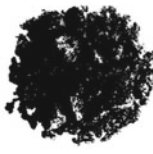


Sample	Condition of sample	
	Dry	Wet
0CR		
0CRHL		
10CR		
10CRHL		
20CR		
20CRHL		

Fig. 6 Binary image obtained for the dry and wet of CRMA mixtures

### 3.4 Moisture and Fatigue Resistance of RAP–WMA Mixture

Some concerns when utilizing RAP are the low temperature and fatigue cracking performance because the stiffness of the asphalt mixture can dramatically increase with the inclusion of RAP. Nevertheless, research indicated that addition of RAP can

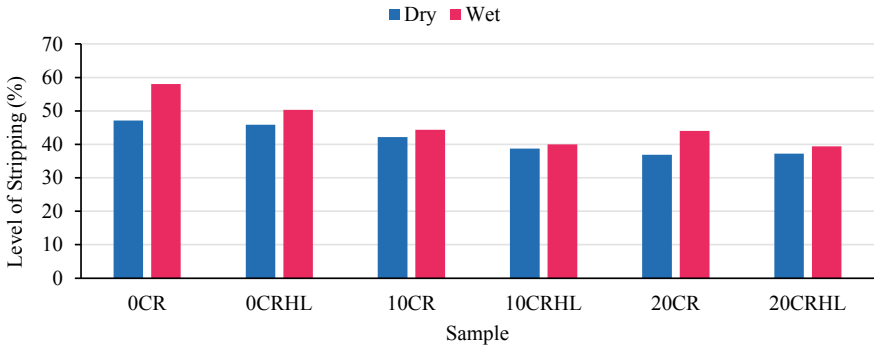


Fig. 7 Level of stripping

improve the moisture resistance. Hence, this study evaluates the combined effects of moisture and fatigue or aging. Specimen was subjected to moisture and aging prior testing. The fatigue failure is determined based on the number of cycles that cause fracture of the asphalt specimen. Prior to the determination of fatigue failure, the initial strain and maximum tensile at the center of the specimen are calculated. The initial stiffness is equivalent to the value at 100th loading cycle in accordance to the procedure in European Standard EN 12697-24 (2004). Figure 8 exhibits the fatigue curve of a specimen that subjected to the combined effects of aging and moisture. The fatigue curve was developed based on the result obtained from diametral fatigue test.

Graphical comparison between those figures shows that the fatigue curves of specimen subjected to moisture and aging exhibit a steeper slope. The gradient of the slope is indicated by the lower value of  $n$  in Table 9. The negative sign of  $n$  refers to the slope of the fatigue curve. In general, a higher value of  $n$  results in a higher fatigue life. The regression parameters obtained from the fatigue relationship with their  $R^2$  values are shown in Table 9. By using the regression parameters, the fatigue failure for each type of mixture can be determined.

Slope of the linear line is used as indicator of the fatigue resistance. The gradient of the slope is indicated by the value of  $n$  in Table 9. In general, a higher value of

Fig. 8 Fatigue curve of specimen subjected to moisture and aging

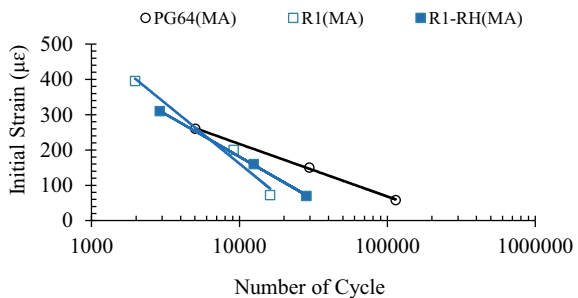


**Table 9** Fatigue curve regression parameters

Types of mixture	Regression coefficient		$R^2$
	$K$	$n$	
PG64(MA)	5.00E+08	-2.005	0.9468
R1(MA)	3.00E+06	-1.182	0.8663
R1-RH(MA)	2.00E+07	-1.513	0.9498

$n$  results in a higher fatigue life. From Table 9, PG64(MA) has higher value of  $n$  compared with the mixture that containing RAP. This means that addition of RAP reduces the fatigue life.

In general, the addition of RAP reduces the mixture resistance to fatigue. When using high RAP content, the fatigue resistance can be reduced due to the addition of aged binder that stiffened the asphalt mixtures (Sabouri et al. 2015). The incorporation of RH-WMA additive enhances the fatigue resistance. The RAP-WMA mixture is more resistance to fatigue compares to the RAP mixture only. Similar findings on the fatigue life enhancement with the use of WMA additive by using other test methods were also reported (Timm et al. 2011; Goh and You 2011; Oliveira et al. 2012). Even though the addition of RAP can improve the moisture resistance of WMA, the effects of aging had stiffened the mixture and resulted in reduced fatigue resistance. Nevertheless, the fatigue resistance of specimen containing RH-WMA additive is better than those comprising of RAP only. Aging stiffens the asphalt binder and hence hastens the cracking development. On the contrary, moisture weakens the bonding between the aggregate and binder. Several studies found that mixture containing a high amount of RAP with WMA additive improved the moisture resistance (Oliveira et al. 2012; Shu et al. 2012). In relation to RAP, Huang et al. (2005) postulated that the strong bond between the aged asphalt and the aggregate particles aids in improving the moisture resistance. However, it was also highlighted that RAP stiffness particularly when incorporating a high RAP content can lead to cracking problem and need to be monitored (Zaumanis and Mallick 2015). Therefore, the findings from this study indicate that the combination of moisture and aging reduces the fatigue resistance. At the high RAP content, the environmental and traffic loading repetition can expedite the fatigue failure.

## 4 Conclusions

Based on the study, methods and procedures were managed to scrutinize the objectives laid down earlier. From the analysis, it can be concluded that incorporation of recycled materials and WMA additive using the RH-WMA in the mixture reduces the design mix temperature of the mixture. This provides significant improvement toward the environment worth as the road construction will be more environmentally friendly and less energy consumption. Akin with this benefit, usage of RAP is also a substantial economic benefit as it will help for reducing the construction cost through



recycling the asphaltic pavement. To add, comparing with the conventional asphalt pavement mixture, CRWMA and RAP with WMA show more desirable performance in terms of resilient modulus. However, for moisture resistance, CRWMA treatment on the crumb rubber will improve the performance. For the combined effects of moisture and aging, it seems the addition of WMA additive improves the fatigue resistance. Thereby, the outcome acquired from study on the utilization of recycled materials will be able to initiate the measure line to produce more greener approach in the road construction industries globally.

## References

- Abdul Hassan, N., Airey, G. D., Putra Jaya, R., Mashros, N., & Aziz, M. A. (2014). A review of crumb rubber modification in dry mixed rubberised asphalt mixtures. *Jurnal Teknologi (Sciences & Engineering)*, 70(4), 127–134.
- Abdullah, M. E., et al. (2014). Warm mix asphalt technology: A review. *Jurnal Teknologi*, 71(3), 39–52.
- Aguiar-Moya, J. P., Baldi-Sevilla, A., Salazar-Delgado, J., Pacheco-Fallas, J. F., Loria-Salazar, L., Reyes-Lizcano, F., et al. (2018). Adhesive properties of asphalts and aggregates in tropical climates. *International Journal of Pavement Engineering*, 19(8), 738–747. <https://doi.org/10.1080/10298436.2016.1199884>.
- Al-Qadi, I. L., Carpenter, S. H., Roberts, G., Ozer, H., Aurangzeb, Q., Elseifi, M., & Trepanier, J., (2009). *Determination of usable residual asphalt binder in RAP*. Illinois Center for Transportation (ICT).
- Ariyapijati, R. H., Hadiwardoyo, S. P., & Sumabrata, R. J. (2017). Contributions crumb rubber in hot mix asphalt to the resilient modulus. *AIP Conference Proceedings*, 1855. <https://doi.org/10.1063/1.4985475>.
- Arshad, A. K., Kridan, F. A. M., Kamaluddin, N. A., & Shafie, E. (2015). Evaluation of warm mix asphalt performance with high RAP content. *Jurnal Teknologi*, 73(4).
- Asadi, S. S., Babu, T. N., Kumar, B. H., Sumanth, M., & Kumar, G. S. (2016). Crumb rubber utilization in pavements to improve the durability: An experimental study. *International Journal of Applied Engineering Research*, 11(9), 6418–6423.
- Asphalt Recycling and Reclaiming Association (ARRA). (2001). *Basic Asphalt Recycling Manual*. United States: FHWA.
- Aurangzeb, Q., Al-Qadi, I. L., Ozer, H., & Yang, R. (2014). Hybrid life cycle assessment for asphalt mixtures with high RAP content. *Resources, Conservation and Recycling*, 83, 77–86. <https://doi.org/10.1016/j.resconrec.2013.12.00>.
- Boriack, P. C., Katicha, S. W., Flintsch, G. W., & Tomlinson, C. R. (2014). *Laboratory evaluation of asphalt concrete mixtures containing high contents of reclaimed asphalt pavement (RAP) and binder* (No. FHWA/VCTIR 15-R8). Virginia Center for Transportation Innovation and Research.
- Capitao, S. D., Picado-Santos, L. G., & Matinho, F. (2012). Pavement engineering materials: Review on the use of warm-mix asphalt. *Construction and Building Materials*, 36, 1016–1024. <https://doi.org/10.1016/j.conbuildmat.2012.06.038>.
- Chiu, C. T., Hsu, T. H., & Yang, W. F. (2008). Life cycle assessment on using recycled materials for rehabilitating asphalt pavements. *Resources, Conservation and Recycling*, 52(3), 545–556.
- Copeland, A. (2011). *Reclaimed asphalt pavement in asphalt mixtures: State of the practice*. Report No. FHWA-HRT-11-021, Federal Highway Administration, McLean, Virginia.
- Copeland, A., D'Angelo, J., Dongre, R., Belagutti, S., & Sholar, G. (2010). Field evaluation of high reclaimed asphalt pavement–warm-mix asphalt project in Florida: Case study. *Transportation Research Record*, 2179(1), 93–101.

- D'Angelo, J., Harm, E., Bartoszek, J., Baumgardner, G., Corrigan, M., Cowsert, J., & Yeaton, B. (2008). *Warm-mix asphalt: European practice* (p. 68). US Department of Transportation.
- Dinis-Almeida, M., & Afonso, M. L. (2015). Warm mix recycled asphalt—A sustainable solution. *Journal of Cleaner Production*, *107*, 310–316.
- Dinis-Almeida, M., Castro-Gomes, J., & de Lurdes Antunes, M. (2012). Mix Design considerations for warm mix recycled asphalt with bitumen emulsion. *Construction and Building Materials*, *28*(1), 687–693.
- Doyle, J. D., & Howard, I. L. (2011). Laboratory assessment of skid resistance for high RAP content warm mixed asphalt. In *Geo-Frontiers 2011: Advances in geotechnical engineering* (pp. 4515–4524).
- Doyle, J. D., & Howard, I. L. (2013). Rutting and moisture damage resistance of high reclaimed asphalt pavement warm mixed asphalt: Loaded wheel tracking vs. conventional methods. *Road Materials and Pavement Design*, *14*(sup2), 148–172.
- European Standard. (2004). EN 12697-24. *Bituminous Mixtures. Test Methods for Hot Mix Asphalt. Resistance to Fatigue*.
- FHWA. (2008). *User Guidelines for By-Product and Secondary Use Materials in Pavement Construction*. Washington, D.C: FHWA Publication FHWA-RD-97-148, Federal Highway Administration.
- Fontes, L. P. T. L., Trichês, G., Pais, J. C., & Pereira, P. A. A. (2010). Evaluating permanent deformation in asphalt rubber mixtures. *Construction and Building Materials*, *24*(7), 1193–1200. <https://doi.org/10.1016/j.conbuildmat.2009.12.021>.
- Gheni, A. A., Abdelkarim, O. I., Abdulazeez, M. M., & ElGawady, M. A. (2017). Texture and design of green chip seal using recycled crumb rubber aggregate. *Journal of Cleaner Production*, *166*, 1084–1101.
- Goh, S. W. (2012). *Development and Improvement of Warm-Mix Asphalt Technology*. Ph.d. Thesis, Michigan Technological University. United States.
- Goh, S. W., & You, Z. (2011). Mechanical properties of porous asphalt pavement materials with warm mix asphalt and RAP. *Journal of Transportation Engineering*, *138*(1), 90–97.
- Gungat, L. (2017). *Effects of RH-WMA Additive on Rheological Properties of High Amount Reclaimed Asphalt Binders*. Doctoral Thesis, School of Civil Engineering, Universiti Sains Malaysia, Nibong Tebal, Penang.
- Gungat, L., Hamzah, M. O., Yusoff, N. I. M., & Goh, S. W. (2019). Design and properties of high reclaimed asphalt pavement with RH-WMA. In *IOP conference series: Materials science and engineering* (Vol. 512, No. 1, p. 012055). IOP Publishing.
- Gungat, L., Yusoff, N. I. M., & Hamzah, M. O. (2016). Effects of RH-WMA additive on rheological properties of high amount reclaimed asphalt binders. *Construction and Building Materials*, *114*, 665–672.
- Guo, N., You, Z., Zhao, Y., Tan, Y., & Diab, A. (2014). Laboratory performance of warm mix asphalt containing recycled asphalt mixtures. *Construction & Building Materials*, *64*, 141–149. <https://doi.org/10.1016/j.conbuildmat.2014.04.002>.
- Hamad, G. S., Jaya, R. P., Hassan, N. A., Aziz, M. M. A., & Mohd Yusak, M. I. (2014). *Influences of Crumb Rubber Size on Hot Mix Asphalt Mixtures*. Doctoral dissertation, Universiti Teknologi Malaysia.
- Hamzah, M. O., Golchin, B., & Tye, C. T. (2013). Determination of the optimum binder content of warm mix asphalt incorporating rediset using response surface method. *Construction and Building Materials*, *47*, 1328–1336.
- Hansen, K.R., Copeland, A., & National Asphalt Pavement Association. (2013). *Annual asphalt pavement industry survey on recycled materials and warm-mix asphalt usage: 2009–2012* (No. IS-138). National Asphalt Pavement Association.
- Hassan, N. A. (2017). Rubberized road: Turning waste into road materials. In *International Seminar on Natural Rubber in Roads*.
- Hicks, G. (2010). *Assessment of Warm Mix Technologies for Use with Asphalt Rubber Paving Applications Technical Memo Report Number: CP2C- 2010 – 103TM, 930* (530).

- Hill, B. (2011). *Performance Evaluation of Warm Mix Asphalt Mixtures Incorporating Reclaimed Asphalt Pavement*. Master Science Thesis, University of Illinois, Illinois.
- Hill, B., Behnia, B., Buttlar, W., & Reis, H. (2013). Evaluation of warm mix asphalt mixtures containing reclaimed asphalt pavement through mechanical performance tests and an acoustic emission approach. *Journal of Materials in Civil Engineering*, 25(12), 1887–1897. [https://doi.org/10.1061/\(asce\)mt.19435533.0000757](https://doi.org/10.1061/(asce)mt.19435533.0000757).
- Howard, I. L., Cooley, L. A., Dennis, C., & State, J. D. D. (2009). *Laboratory Testing and Economic Analysis of High RAP Warm Mixed Asphalt*. Report FHWA/MS-DOT-RD-09-200. Mississippi Department of Transportation.
- Huang, B., Li, G., Vukosavljevic, D., Shu, X., & Egan, B. K. (2005). Laboratory investigation of mixing hot-mix asphalt with reclaimed asphalt pavement. *Transportation Research Record*, 1929(1), 37–45.
- Ibrahim, M. R., Katman, H. Y., & Karim, M. R. (2007). Determination of target binder content for rubberised porous asphalt. *Proceedings of the Eastern Asia Society for Transportation Studies*, 6, 59–75.
- Karlsson, R., & Isacson, U. (2006). Material-related aspects of asphalt recycling-state of the art. *Journal of Materials in Civil Engineering*, 18(1), 81–92.
- Katman, H. Y., Ibrahim, M. R., Karim, M. R., & Mahrez, A. (2011). Resistance to disintegration of rubberized porous asphalt. *Asian Transport Studies*, 1(4), 445–455.
- Katman, H. Y., Karim, M. R., Mahrez, A., & Ibrahim, M. R. (2005). Performance of wet mix rubberised porous asphalt. *Proceedings of the Eastern Asia Society for Transportation Studies*, 5, 695–708.
- Lee, J. C., Edil, T. B., Tinjum, J. M., & Benson, C. H. (2010). Quantitative assessment of environmental and economic benefits of recycled materials in highway construction. *Transportation Research Record: Journal of the Transportation Research Board*, 2158(1), 138–142.
- Liu, S., Cao, W., Fang, J., & Shang, S. (2009). Variance analysis and performance evaluation of different crumb rubber modified (CRM) asphalt. *Construction and Building Materials*, 23(7), 2701–2708. <https://doi.org/10.1016/j.conbuildmat.2008.12.009>.
- Mashaan, N. S., Ali, A. H., Karim, M. R., & Abdelaziz, M. (2014). A review on using crumb rubber in reinforcement of asphalt pavement. *The Scientific World Journal*. <https://doi.org/10.1155/2014/214612>.
- Mashaan, N. S., Ali, A. H., Karim, M. R., & Abdelaziz, M. (2011). Effect of crumb rubber concentration on the physical and rheological properties of rubberised bitumen binders. *International Journal of the Physical Sciences*, 6(4), 684–690. <https://doi.org/10.5897/IJPS11.113>.
- McDaniel, R. S., & Anderson, R. M. (2001). *Recommended Use of Reclaimed Asphalt Pavement in the Superpave Mix Design Method*. Technician's Manual, NCHRP Report 452. Transportation Research Board Washington, D.C.
- Middleton, B., & Forfylow, R. W. (2009). Evaluation of warm-mix asphalt produced with the double barrel green process. *Transportation Research Record*, 2126(1), 19–26.
- Miliutenko, S., Björklund, A., & Carlsson, A. (2013). Opportunities for environmentally improved asphalt recycling: The example of Sweden. *Journal of Cleaner Production*, 43, 156–165.
- Mogawer, W. S., Austerman, A. J., Bonaquist, R., & Roussel, M. (2011). Performance characteristics of thin-lift overlay mixtures. *Transportation Research Record: Journal of the Transportation Research Board*, 2208(1), 17–25. <https://doi.org/10.3141/2208-03>.
- Mucinis, D., Sivilevicius, H., & Oginskas, R. (2009). Factors determining the inhomogeneity of reclaimed asphalt pavement and estimation of its components content variation parameters. *The Baltic Journal of Road and Bridge Engineering*, 4(2), 69–69.
- NAPA. (2013). *FHWA Seek Input from Asphalt Mix Producers for Survey*. Online Report. Accessed on December 13, 2013.
- Oliveira, J. R., Silva, H. M., Abreu, L. P., & Gonzalez-Leon, J. A. (2012). The role of a surfactant-based additive on the production of recycled warm mix asphalts—Less is more. *Construction and Building Materials*, 35, 693–700.

- Omranian, S. R., Hamzah, M. O., Gungat, L., & Teh, S. Y. (2018). Evaluation of asphalt mixture behavior incorporating warm mix additives and reclaimed asphalt pavement. *Journal of Traffic and Transportation Engineering (English Edition)*, 5(3), 181–196. <https://doi.org/10.1016/j.jtte.2017.08.003>.
- Oner, J., & Sengoz, B. (2015). Utilization of recycled asphalt concrete with warm mix asphalt and cost-benefit analysis. *PLoS ONE*, 10(1), 1–18.
- Praticò, F. G., Moro, A., & D'Agostino, P. (2015). An experimental investigation into innovative pavements for city logistics. *WIT Transactions on the Built Environment*, 146, 325–336.
- Putman, B. J., & Amirkhanian, S. N. (2006). Crumb rubber modification of binders: interaction and particle effects. In *Proceedings of the Asphalt Rubber 2006 Conference* (Vol. 3, pp. 655–677).
- Roberts, F. L., Engelbrecht, J. C., & Kennedy, T. W. (1984). Evaluation of recycled mixtures using foamed asphalt. *Transportation Research Record*, 968, 78–85.
- Sabouri, M., Bennert, T., Sias Daniel, J., & Richard Kim, Y. (2015). A comprehensive evaluation of the fatigue behaviour of plant-produced RAP mixtures. *Road Materials and Pavement Design*, 16(sup2), 29–54.
- Shatanawi, K. M., Biro, S., Naser, M., & Amirkhanian, S. N. (2013). Improving the rheological properties of crumb rubber modified binder using hydrogen peroxide. *Road Materials and Pavement Design*, 14(3), 723–734.
- Shen, J., Amirkhanian, S., & Aune Miller, J. (2007). Effects of rejuvenating agents on superpave mixtures containing reclaimed asphalt pavement. *Journal of Materials in Civil Engineering*, 19(5), 376–384.
- Shu, X., Huang, B., Shrum, E. D., & Jia, X. (2012). Laboratory evaluation of moisture susceptibility of foamed warm mix asphalt containing high percentages of RAP. *Construction and Building Materials*, 35, 125–130.
- Solaimanian, M., Milander, S., Boz, I., & Stoffels, S. (2011). *Development of guidelines for usage of high percent RAP in warm-mix asphalt pavements* (No. FHWA-PA-2011-013-PSU 032). Department of Transportation, Pennsylvania.
- Song, W., Huang, B., & Shu, X. (2018). Influence of warm-mix asphalt technology and rejuvenator on performance of asphalt mixtures containing 50% reclaimed asphalt pavement. *Journal of Cleaner Production*, 192, 191–198. <https://doi.org/10.1016/j.jclepro.2018.04.269>.
- Timm, D. H., Willis, J. R., & Kvasnak, A. (2011). Full-scale structural evaluation of fatigue characteristics in high reclaimed asphalt pavement and warm-mix asphalt. *Transportation Research Record*, 2208(1), 56–63.
- United States Environmental Protection Agency (EPA). (2000). *Hot Mix Asphalt Plants Emissions Assessment Report, Emissions Monitoring and Analysis Division*. Office of Air Quality Planning and Standards, United States Environmental Protection Agency, Research Triangle Park, NC, December 2000.
- Vidal, R., Moliner, E., Martínez, G., & Rubio, M. C. (2013). Life cycle assessment of hot mix asphalt and zeolite-based warm mix asphalt with reclaimed asphalt pavement. *Resources, Conservation and Recycling*, 74, 101–114.
- West, R., Kvasnak, A., Tran, N., Powell, B., & Turner, P. (2009). Testing of moderate and high reclaimed asphalt pavement content mixes: Laboratory and accelerated field performance testing at the national center for asphalt technology test track. *Transportation Research Record*, 2126(1), 100–108.
- West, R. C., Willis, J. R., & Marasteanu, M. O. (2013). *Improved mix design, evaluation, and materials management practices for hot mix asphalt with high reclaimed asphalt pavement content* (Vol. 752). Transportation Research Board.
- Willoughby, K. A., et al. (2001). *Construction-Related Asphalt Concrete Pavement Temperature Differentials and The Corresponding Density Differentials*. Research Project Agreement T9903, Task A3 Pavement Consultants Inc., Seattle, WA.
- Xiao, F., Putman, B. J., & Amirkhanian, S. N. (2006). Laboratory investigation of dimensional changes of crumb rubber reacting with asphalt binder. In *Proceeding asphalt rubber 2006 conference* (Vol. 82, No. 76.4, p. 71).

- Xiao, F., Zhao, W., Gandhi, T., & Amirkhanian, S. N. (2010). Influence of antistripping additives on moisture susceptibility of warm mix asphalt mixtures. *Journal of Materials in Civil Engineering*, 22(10), 1047–1055.
- Zaumanis, M., & Mallick, R. B. (2015). Review of very high-content reclaimed asphalt use in plant-produced pavements: state of the art. *International Journal of Pavement Engineering*, 16(1), 39–55.
- Zaumanis, M., & State, L. (2015). *Warm mix asphalt*. <https://doi.org/10.1007/978-3-662-44719-2>.
- Zhao, S., Huang, B., Shu, X., & Woods, M. (2013). Comparative evaluation of warm mix asphalt containing high percentages of reclaimed asphalt pavement. *Construction and Building Materials*, 44, 92–100. <https://doi.org/10.1016/j.conbuildmat.2013.03.010>.